
The importance of endogenous cannabinoids in stress-related disorders and depression

Dissertation

zur

Erlangung des Doktorgrades (Dr. rer. nat.)

der

Mathematisch-Naturwissenschaftlichen Fakultät

der

Rheinischen Friedrich-Wilhelms-Universität Bonn

vorgelegt von

Imke Jenniches

aus

Neuss

Bonn, April 2016

Angefertigt mit Genehmigung der Mathematisch-Naturwissenschaftlichen Fakultät der
Rheinischen Friedrich-Wilhelms-Universität Bonn

1. Gutachter: Prof. Dr. A. Zimmer
2. Gutachter: Prof. Dr. M. Hoch

Tag der Promotion: 19.12.2016

Erscheinungsjahr: 2017

*“Man merkt nie, was schon getan wurde, man sieht immer nur, was
noch zu tun bleibt.”*

Marie Curie

Abbreviations

AA	Arachidonic acid
ACTH	Adrenocorticotropin hormone
2-AG	2-arachidonoylglycerol
AEA	Arachidonylethanolamine (Anandamide)
ATP	Adenosine triphosphate
BCA	Bicinchoninic acid assay
BCP	1-bromo-3-chloropropane
BDNF	Brain-derived neurotrophic factor
BLA	Basolateral amygdala
BMM	Bone marrow-derived macrophages
bp	Base pair
BSA	Bovine serum albumine
BrdU	5-Bromo-2-Deoxyuridine
CamKII α	Calcium/calmodulin dependent protein kinase II α
CB1	Cannabinoid receptor 1
cm	Centimeter
CMV	Human cytomegalovirus (CMV) promoter
CNS	Central nervous system
CRH	Corticotropin-releasing hormone
CRHR1	Corticotropin-releasing hormone receptor 1
CSDS	Chronic social defeat stress
dB	Decibel
DAG	Diacylglycerol
DAGL	Diacylglycerol lipase
DAPI	4',6-diamidino-2-phenylindole
dH ₂ O	Deionized H ₂ O
DIG	Digoxigenin
DMEM	Dulbecco's Modified Eagl Medium
DMSO	Dimethylsulfoxid
DNA	Desoxyribonucleic acid
DTT	Dithiothreitol
eCB	Endocannabinoid
ECS	Endocannabinoid system
EDTA	Ethylene glycol tetraacetic acid
ELISA	Enzyme-linked immunosorbent assay
EtOH	Ethanol
FAAH	Fatty acid amid hydrolase
FAM	6-carboxyfluorescein
FCS	Fetal calf serum
FGF	Fibroblast growth factor

Abbreviations

FITC	Fluorescein isothiocyanate
fl	Floxed (flanked by loxP sites)
G418	Geneticin
GABA	γ -aminobutyric acid
<i>g</i>	Gravitational force
g	Gram
GPR	G-protein coupled receptor
GR	Glucocorticoid receptor
h	Hour
HBSS	Hank's buffered salt solution
HCl	Hydrochloric acid
HEK293T	Human Embryonic Kidney 293T cells
HPA axis	Hypothalamic–pituitary–adrenal axis
HRP	Horseradish peroxidase
i.p.	intraperitoneal
JNK1	c-Jun N-terminal kinase 1
kb	Kilobase
kDa	Kilodalton
kg	Kilogram
kHz	Kilohertz
loxP	“locus of X-ing over” in Phage P1
M	Molar
m	Meter
mM	Millimolar
mA	Miliampere
MAGL	Monoacylglycerol lipase
MALDI	Matrix-assisted laser desorption/ionization
MAPK8	Mitogen-activated protein kinase 8
M-CSF	Macrophage colony-stimulating factor
MeOH	Methanol
MGB	Minor groove binder
min	Minutes
MR	Mineralocorticoid receptor
mRNA	Messenger RNA
ms	Milliseconds
MS	Mass spectrometry
n	Number (sample size)
NAc	Nucleus accumbens
NAPE	N-acyl-phosphatidylethanolamine
NAPE-PLD	NAPE-phospholipase D
NCAM	Neural cell adhesion molecule
NeuN	Neuronal nuclear antigen

Abbreviations

nm	Nanomolar
ns	Not significant
ng	Nanogram
PBS	Phosphate buffered saline
PCR	Polymerase chain reaction
PE	Phosphatidylethanolamine
PFA	Paraformaldehyd
PFC	Prefrontal cortex
Pgk-1	Phosphoglycerate kinase-1 promotor
PI3K	Phosphatidylinositide 3-kinase
PKA	Protein kinase A
PKC	Protein kinase C
PLC	Phospholipase C
PVN	Periventricular nucleus
RNA	Ribonucleic acid
RT	Room temperature
RT-PCR	Reverse transcription-PCR
s	Second
SDS	Sodium dodecyl sulfate
SEM	Standard error of the mean
SSC	Saline sodium citrate
TAP	Tandem affinity purification
TE	Tris EDTA
THC	Δ^9 -tetrahydrocannabinol
TLC	Thin layer chromatography
TOF	Time of flight
Tris	Tris (hydroxymethyl) aminomethane
TRPV1	Transient receptor potential vanilloid type-1
U	Unit
UV	Ultraviolet
VTA	Ventral tegmental area
WHO	World Health Organization
WT	Wild type
μ l	Microliter
μ M	Micromolar

Summary

The endogenous cannabinoid system (ECS) is a unique neuromodulatory system, essentially involved in a variety of physiological processes. It consists of the two major endogenous cannabinoids (eCBs), anandamide and 2-AG, and a set of cannabinoid receptors. The signaling mechanism especially in the central nervous system (CNS) is well characterized. In the CNS, both endocannabinoids inhibit the release of excitatory and inhibitory neurotransmitters through the activation of presynaptic cannabinoid receptors.

The ECS is predominantly expressed in brain regions crucially involved in the regulation of memory and emotion, such as the prefrontal cortex, hippocampus and amygdala. Disruption of the ECS through pharmacological or genetic invalidation of cannabinoid CB1 receptors has been linked to depression in humans and depression-like behaviors in mice. Thus, there is an increasing evidence to support a role for the ECS in the neurobiology of psychiatric disorders. However, the similar mode of action of both eCBs exacerbates the discrimination of distinct functions to either anandamide or 2-AG. To elucidate the impact of 2-AG on the development and manifestation of anxiety- and depression-related disorders, constitutive as well as cell-type specific knockout mice of the main 2-AG biosynthetic enzyme diacylglycerol lipase α (DAGL α) were analyzed in detail. The deletion of *Dagla* caused severe behavioral alterations leading to increased anxiety, altered fear responses and depressive-like phenotypes. In the past decade, the endocannabinoid system has also emerged as an important regulator of the stress response and as a candidate mediator of stress adaptation. In line with this, the constitutive and neuronal deletion of *Dagla* markedly increased the sensitivity to chronic stress. Despite the vastly gained knowledge concerning the ECS, the prime cellular source of 2-AG in the brain is yet unknown. Neurons, microglia as well as astrocytes hold a functional ECS and produce 2-AG *in vitro*. First promising insights regarding cellular source of 2-AG under baseline conditions and in response to chronic stress are given through this study.

The present findings evidently support the assumption that a dysregulated ECS, in particular the altered 2-AG signaling, negatively affects the emotional state of rodents.

Contents

1	Introduction	1
1.1	The endocannabinoid system.....	1
1.2	ECS signaling	3
1.3	Metabolism of 2-AG: the diacylglycerol lipases.....	4
1.4	Stress-related and depressive disorders.....	7
1.4.1	Stress and anxiety disorders	7
1.4.2	The stress-depression connection.....	9
1.4.3	ECS in emotional processes	11
1.4.4	Modeling depression in mice	13
1.5	Aim of the thesis	15
2	Material and Methods	16
2.1	Equipment.....	16
2.2	Chemicals and reagents.....	18
2.2.1	Chemicals.....	18
2.2.2	Kits.....	19
2.2.3	Buffers and solutions	19
2.2.4	Enzymes and antibodies	21
2.2.5	Antibiotics	21
2.2.6	Plasmids	22
2.3	Animals	22
2.4	Behavioral experiments.....	23
2.4.1	Sucrose preference test	23
2.4.2	Forced swim test	23
2.4.3	Social preference test.....	24
2.4.4	Social avoidance test.....	24
2.4.5	Home cage activity measurement	24
2.4.6	Open-field test	25
2.4.7	Light-dark box test.....	25
2.4.8	Zero-maze test	25
2.4.9	Fear conditioning paradigm	26
2.4.10	Hot plate test	27
2.4.11	Pup retrieval test.....	27
2.4.12	Maternal behavior.....	27
2.4.13	Tetrad test	27
2.4.14	Chronic social defeat paradigm	28
2.5	Measurement of endocannabinoids.....	29
2.6	Measurement of corticosterone.....	29
2.7	Immunohistochemistry.....	30
2.7.1	DAGL α staining	30
2.7.2	DAGL α /Iba1 co-staining	31
2.7.3	Adult neurogenesis.....	31
2.8	Cell culture.....	32
2.8.1	Isolation and cultivation of bone marrow-derived Macrophages	32
2.8.2	Cultivation and transfection of Neuro-2a cells	33
2.9	Cultivation and electroporation of <i>E. coli</i>	34
2.10	Molecular biology methods.....	35
2.10.1	DNA purification and measurement.....	35
2.10.2	Agarose gel electrophoresis	36
2.10.3	DNA amplification by PCR/ genotyping	36
2.10.4	Cloning of the DAGL α expression vector	40

2.10.5	RNA purification and measurement.....	41
2.10.6	Reverse transcription polymerase chain reaction.....	41
2.10.7	Real-time reverse transcription PCR (qRT-PCR).....	42
2.11	Protein biochemistry	43
2.11.1	Polyacrylamide gel electrophoresis	43
2.11.2	Western Blot.....	44
2.11.3	Tandem affinity purification.....	44
2.11.4	MALDI-TOF/TOF mass spectrometry	46
2.12	Click chemistry.....	47
2.12.1	<i>In vitro</i> assays.....	47
2.12.2	Lipid isolation and click reaction	48
2.12.3	Thin layer chromatographie (TLC).....	49
2.13	Statistical analysis	49
3	Results	50
3.1	Behavioral and molecular analysis of <i>Dagla</i>^{-/-} mice.....	50
3.1.1	Endocannabinoid measurements and gene expression analysis.....	50
3.1.2	Tetrad test	53
3.1.3	Maternal behavior and body weight.....	54
3.1.4	Analysis of anxiety-related behavior.....	56
3.1.5	Analysis of depression-related behavior.....	58
3.2	Behavioral and molecular analysis of neuron-specific <i>Dagla</i>^{-/-} mice.....	61
3.2.1	Endocannabinoid measurements and gene expression analysis.....	62
3.2.2	Analysis of anxiety-related behavior.....	64
3.2.3	Fear conditioning paradigm	65
3.2.4	Analysis of depression-related behavior.....	67
3.2.5	Adult neurogenesis.....	68
3.3	Behavioral and molecular analysis of microglia-specific <i>Dagla</i>^{-/-} mice	69
3.3.1	Endocannabinoid measurements and gene expression analysis.....	70
3.3.2	Analysis of anxiety-related behavior.....	72
3.3.3	Fear conditioning paradigm	73
3.3.4	Analysis of depression-related behavior.....	75
3.4	Chronic social defeat stress	77
3.4.1	Chronic social defeat stress: group-housed intruder	77
3.4.2	Chronic social defeat stress: single-housed intruder	88
3.5	Identification of potential novel interaction partners of DAGLα	101
3.5.1	Cloning of the DAGL α expression vector	101
3.5.2	Tandem affinity purification of DAGL α	104
3.5.3	Analysis of bound proteins via MALDI-TOF	107
3.5.4	<i>In vitro</i> assays using click-chemistry	110
4	Discussion	114
4.1	Behavioral and molecular characterization of mice lacking <i>Dagla</i>	114
4.2	Chronic social defeat stress	121
4.3	<i>In vitro</i> approaches to characterize DAGL α and identify potential interaction partners	130
4.4	Conclusion and Outlook.....	134
	Bibliography.....	136
A	Appendix	155
A.1	Protein list.....	155
A.2	Publications	167
A.3	Declaration	168
	Acknowledgement.....	169

Introduction

1.1 The endocannabinoid system

Since time immemorial plants are used as therapeutics against a variety of diseases. The medicinal use of *Cannabis sativa* goes back to 2000 BC and even the psychotropic properties are known since then (Murray et al. 2007). Thus, *Cannabis sativa* and its extracts are one of the oldest herbal drugs. However, only in 1964 the psychoactive ingredient Δ^9 -tetrahydrocannabinol (THC) was isolated and identified (Gaoni & Mechoulam 1964). It took another 30 years until the molecular target of THC, the endogenous cannabinoid receptors, were identified. In the late 1980s, the first cannabinoid receptor (CB1) was identified and characterized (Devane et al. 1988; Matsuda et al. 1990) followed by the cannabinoid receptor 2 (CB2) (Munro et al. 1993) and the two main endogenous cannabinoids *N*-arachidonylethanolamine (anandamide, AEA) and 2-arachidonoylglycerol (2-AG) in mid 1990s (Devane et al. 1992; Mechoulam et al. 1995) (Fig. 1).

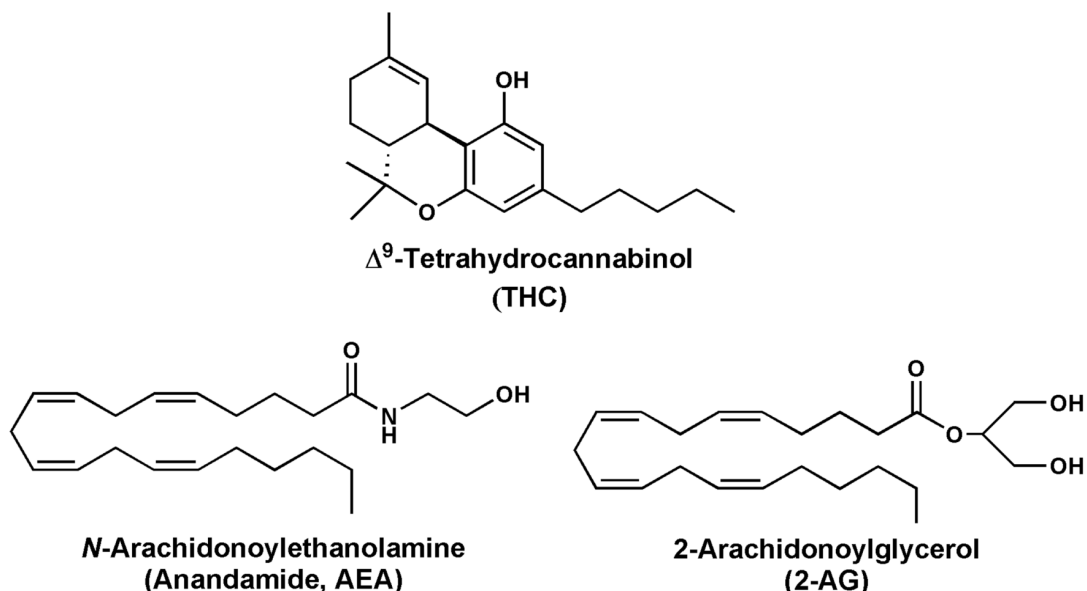


Figure 1: Structural formula of the main psychoactive compound of *Cannabis sativa*, Δ^9 -tetrahydrocannabinol (THC), and the endogenous cannabinoids anandamide and 2-AG

In the past decades the research interest in the cannabinoid field has grown tremendously and today the search term “cannabinoid” gives more than 19000 hits in “Pubmed” (<http://www.ncbi.nlm.nih.gov/pubmed/>), the worldwide most frequently used free search engine for publications on life sciences, with upward tendency. Growing research

interest elucidated the role of the endocannabinoid system (ECS) in many physiological processes and showed that the ECS plays an important role in health and disease. Its signaling mechanism especially in the central nervous system (CNS) is well characterized.

In the CNS, the endogenous cannabinoids (eCBs) act as retrograde messenger molecules on inhibitory and excitatory synapses (Katona et al. 1999; Katona et al. 2006). 2-AG and anandamide are produced in the postsynapse, released into the synaptic cleft and activate presynaptic cannabinoid receptors, thereby initiating ECS signaling. In contrast to other neurotransmitters, eCBs are mainly synthesized on demand rather than stored in vesicles. The two major cannabinoid receptors CB1 and CB2 belong to the superfamily of G protein-coupled receptors and exhibit distinct expression profiles. CB1 is highly expressed in the brain and constitutes the main neuronal cannabinoid receptor (Matsuda et al. 1990), whereas CB2 is mainly expressed on immune cells and in the periphery (Munro et al. 1993; Pacher & Mechoulam 2011). Recent publications showing the presence of CB2 on brainstem neurons and in other brain areas (Van Sickle et al. 2005; Ashton et al. 2006; Li & Kim 2015) led to an “identity crisis” of the receptor (Atwood & Mackie 2006), and until today the functional presence of CB2 on neurons remains controversial. Besides the two well-characterized cannabinoid receptors CB1 and CB2 rising evidence supports the occurrence of other eCB targets, like the transient receptor potential vanilloid type-1 (TRPV-1) receptor, the orphan G-protein coupled receptors GPR55 (Di Marzo et al. 2010; Ross 2009) and GPR18 (McHugh et al. 2012), and the peroxisome proliferator activated receptors (PPAR) α and γ (Pistis & Melis 2010).

Additionally, the ECS comprises several catabolic and metabolic enzymes. The two main endogenous cannabinoids anandamide and 2-AG are produced on demand from lipid precursors via distinct pathways. The canonical view is that anandamide is mainly synthesized by the *N*-acyltransferase (NAT) and *N*-acyl-phosphatidylethanolamines-specific phospholipase D (NAPE-PLD) and hydrolyzed by the fatty acid amino hydrolase (FAAH) (for review see Rahman et al. 2014). Instead, two *sn*2-specific diacylglycerol lipases (DAGL α and DAGL β) are responsible for the synthesis of 2-AG, a monoacylglycerol, which is mainly metabolized by monoacylglycerol lipase (MAGL) to arachidonic acid and glycerol. In addition, both eCBs can be oxidized by cyclooxygenase-2 (COX-2), distinct lipoxygenases (LOXs), or cytochromes P450 (CYPs) (Urquhart et al. 2015) leading to the production of new biological active metabolites (Rouzer & Marnett 2011; Alhouayek M & Muccioli 2014).

Overall the complex composition and intrinsic signaling pathways reveal the important contribution of the ECS in a variety of biological processes. The following sections will give a short synopsis of neuronal ECS signaling, the biosynthesis of the main eCB 2-AG and the contribution of the ECS in emotional processes.

1.2 ECS signaling

At neuronal synapses the cannabinoid neurotransmitter system acts in a retrograde fashion. Hereby, the endogenous cannabinoids reduce synaptic inputs onto the stimulated neuron in a highly selective and restricted manner. Upon depolarization of the postsynaptic neuron leading to an increase of cytoplasmatic Ca^{2+} levels, the endogenous cannabinoids are synthesized and released into the synaptic cleft. Subsequently, the eCBs bind to presynaptic cannabinoid receptors and thereby activate G_i signaling. This signaling cascade leads, among others, to a decrease of intracellular Ca^{2+} levels by inhibiting Ca^{2+} channels, thus inhibiting neurotransmitter release (Fig. 2). The described mechanism is responsible for the depolarization-induced suppression of inhibition (DSI) or depolarization-induced suppression of excitation (DSE), in GABAergic neurons (Ohno-Shosaku et al. 2001) or glutamatergic neurons, respectively (Kreitzer et al. 2001).

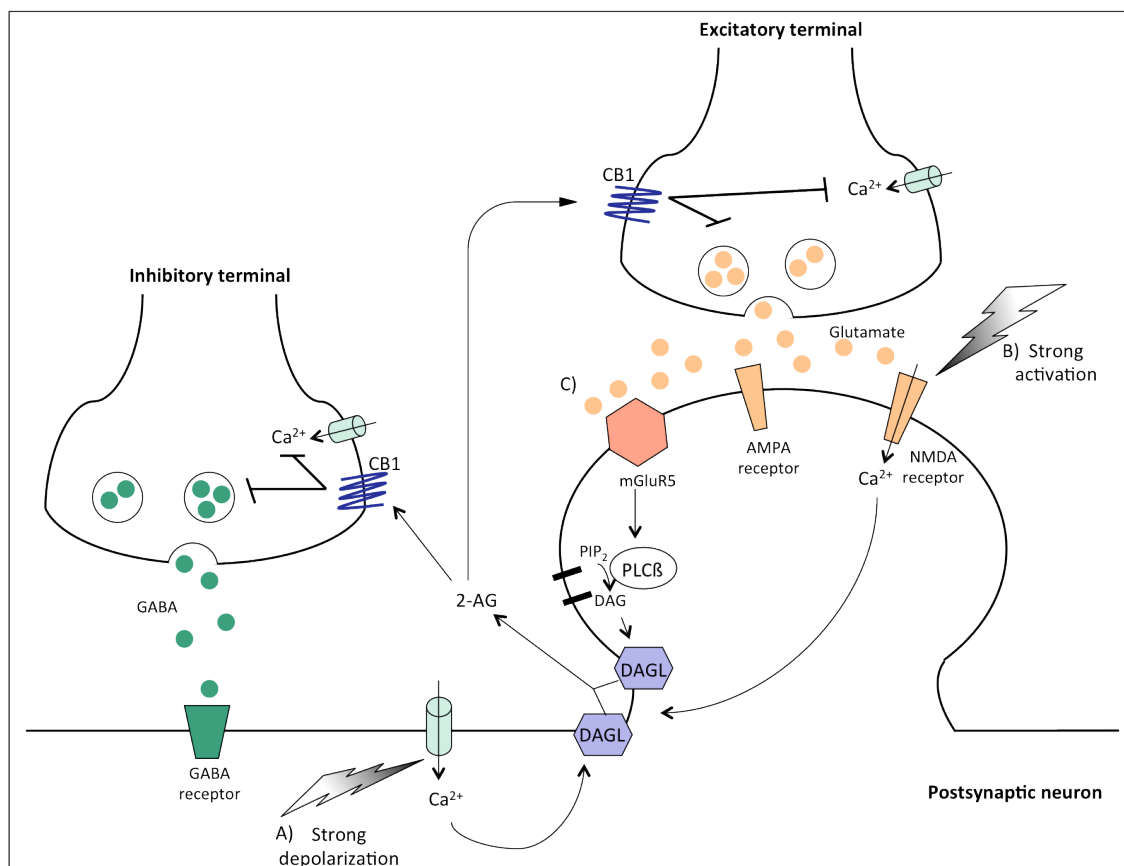


Figure 2: Retrograde signaling of the endocannabinoid system, exemplarily illustrated for the action of 2-AG: A) Strong postsynaptic depolarization causes influx of Ca^{2+} through voltage-gated Ca^{2+} channels. The increase in intracellular Ca^{2+} concentration induces the production of diacylglycerol (DAG) through unknown pathways. B) Strong glutamate signaling activates NMDA receptors, resulting in a large Ca^{2+} elevation and induction of 2-AG production and release through the same pathways. C) Massive release of glutamate activates mGluR5/1 receptors and triggers production of DAG via the activation of PLC β . Subsequent DAGL activity converts DAG into 2-AG. Abbreviations: 2-AG: 2-arachidonoyl glycerol, AMPA: α -amino-3-hydroxy-5-methyl-4-isoxazolepropionic acid receptor (ionotropic glutamate receptor), CB1: cannabinoid receptor 1, DAG: diacylglycerol, DAGL: diacylglycerol lipase, GABA: γ -aminobutyric acid (inhibitory neurotransmitter), NMDA receptor: *N*-methyl-D-aspartate receptor (ionotropic glutamate receptor), PIP₂: phosphatidylinositol-2-phosphat, PLC β : phospholipase-C β .

In addition, a further well-described mechanism triggers the release of 2-AG at glutamatergic synapses. A massive release of glutamate can lead to an activation of postsynaptic metabotropic glutamate receptors (mGluR1/mGluR5) and triggers the production of diacylglycerol (DAG) by phospholipase-C β (PLC β). Subsequent DAGL activity leads to the conversion of DAG into 2-AG (for review see: Katona & Freund 2008). Furthermore, strong activation of highly Ca²⁺-permeable N-methyl-D-aspartate (NMDA) receptors can directly lead to a Ca²⁺ influx and thereby induce endocannabinoid release via yet unknown pathways (Kano et al. 2009) (Fig. 2). For the termination of cannabinoid receptor activation the eCBs are rapidly removed from the synaptic cleft and degraded presynaptically by different hydrolytic pathways.

Besides its prevalence in the CNS, the ECS exerts key peripheral functions related to immunity, bone metabolism, gastrointestinal-, cardiovascular- and reproductive functioning (Chiurchiú et al. 2015; Idris & Ralston 2012; Izzo & Sharkey 2010; Montecucco & Di Marzo 2012; Meccariello et al. 2014). However, functions and signaling mechanisms are best described in the CNS.

1.3 Metabolism of 2-AG: the diacylglycerol lipases

2-AG and anandamide are the two best-studied endogenous cannabinoids. Nevertheless, 2-AG is the most abundant eCB in the CNS, with concentrations up to 800 fold higher than anandamide (Sugiura et al. 1995), and acts as a full agonist on both cannabinoid receptors (Gonsiorek et al. 2000; Savinainen et al. 2001). Even though anandamide binds with higher affinity to CB1, it is just a partial agonist on cannabinoid receptors (Mackie et al. 1993). Furthermore, the retrograde eCB signaling seems to be primary 2-AG dependent, since DSI is completely lost in the hippocampus of mice lacking DAGL α (Gao et al. 2010; Tanimura et al. 2010). Based on these differences, 2-AG might be the main natural cannabinoid agonist and the key endocannabinoid involved in retrograde signaling in the brain (Sugiura et al. 2006; Tanimura et al. 2010). 2-AG is mainly produced by the hydrolysis of a DAG molecule containing arachidonic acid in *sn*2 position. DAGs are important second messenger molecules, which can directly activate effector molecules or, as in this particular case, serve as a substrate to generate further signaling lipids (Ueda et al. 2014). The DAG precursor is provided by phospholipase C (PLC)-mediated hydrolysis of the membrane phospholipid phosphatidylinositol (PI). In a next step the DAG lipases hydrolyze DAG into 2-AG and a free fatty acid (Prescotts & Majerus 1983; Sugiura et al. 1995).

However, other pathways to generate 2-AG involving phospholipase-A1 and lyso-PLC have also been described (Bisogno et al. 1999).

The degradation of 2-AG is mainly mediated by MAGL. This enzyme catalyzes the hydrolysis of 2-AG into arachidonic acid and glycerol (Dinh et al. 2002). However, more recently, the α/β -hydrolases ABHD6 and ABHD12 have been reported to also hydrolyze endocannabinoids (Blankman et al. 2007; Fiskerstrand et al. 2010). Furthermore, 2-AG can be oxidized by LOX-12 and COX-2 (for review see Urquhart et al. 2015) resulting in the production of bioactive prostanoid glyceryl ester that play an important role in pain and immunomodulation (Hu et al. 2008) (Fig. 3).

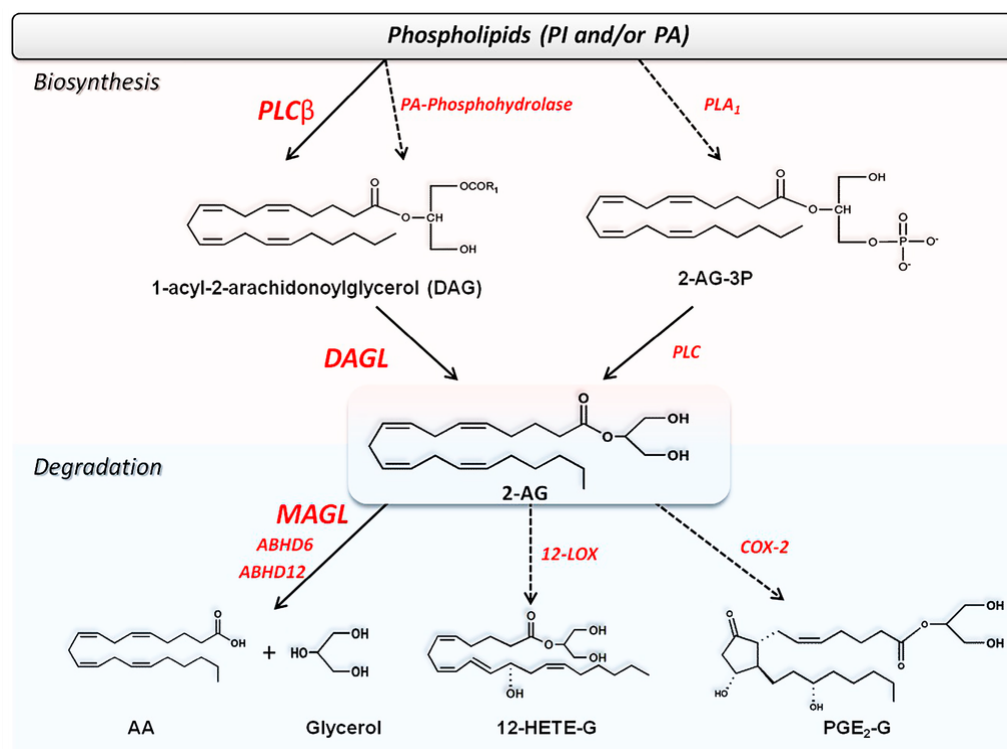


Figure 3: Alternative biosynthetic and degradative pathways of 2-AG (Fezza et al. 2014):

AA: arachidonic acid, 2-AG: 2-arachidonoylglycerol, ABHD6/12: serine hydrolases, α/β -hydrolase domain 6/12, COX-2: cyclooxygenase 2, DAGL: diacylglycerol lipase, 12-LOX: 12-lipoxygenase, MAGL: monoacylglycerol lipase, PA: phosphatidic acid, PGE₂-G: prostaglandin E₂ glycerol ester, PI: phosphatidylinositol, PLA_1 : phospholipase A₁, PLC: phospholipase C.

DAG lipases were first described and studied in the context of arachidonic acid release (Prescott & Majerus 1983; Allen et al. 1992). However, since the identification of 2-AG as an endocannabinoid (Sugiura et al. 1995) the function and regulation of DAG lipases appeared in a new light. Two isoforms of the 2-AG producing DAG lipases, DAGL α and DAGL β , have been cloned and described in detail (Bisogno et al. 2003). Both enzymes show a high similarity in men and mice (DAGL α : 97 %, DAGL β : 79 %), are closely related and exhibit an *sn1*-specificity in terms of their DAG substrates (Bisogno et al. 2003). Nevertheless, both enzymes show different distinct expression profiles in the developing brain and adult organism. While DAGL α is constantly expressed during

neuronal development and in the adult brain, DAGL β is less abundant in the adult CNS, but has a broader expression pattern in peripheral tissues (Bisogno et al. 2003). Throughout the brain development, DAGL α is located in axon growth cones shifting to postsynaptic dendritic spines in the adult CNS (Bisogno et al. 2003). Both enzymes are absent from axonal tracts in the adult mouse brain (Bisogno et al. 2003).

Knockout studies revealed an 80-90 % reduction of brain 2-AG in *Dagla*^{-/-} mice and only a 50 % reduction in *Daglb*^{-/-} mice (Gao et al. 2010; Tanimura et al. 2010). However, DAGL β seems to be the main synthesizing enzyme of 2-AG in the liver (Gao et al. 2010). Thus, the two isoforms individually contribute to the 2-AG production in a tissue-dependent manner (Gao et al. 2010). Even though recent studies showed a regulatory phosphorylation of DAGL α (Shonesy et al. 2013) and proteomic studies indicate that both isoforms can be palmitoylated (Kang et al. 2008; Martin & Cravatt 2009), still very little is known about the regulation of DAGL activity.

In the CNS, neurons are thought to be the main producer of 2-AG. However, microglia cells, as the primary immune effector cells in the central nervous system, produce large amounts of endocannabinoids, especially 2-AG. *In vitro* studies revealed that the production of eCBs in microglia is approximately 20-fold higher than in neurons (Walter et al. 2003a). In addition, astrocytes also possess a functional ECS and produce endocannabinoids (Walter et al. 2002, 2003b).

Even though the main source of 2-AG in the CNS is not yet clear, it has already been shown that altered endocannabinoid signaling greatly influences the emotional state of humans and rodents and contributes to the pathophysiology of anxiety and depression (Hill et al. 2008a; Patel & Hillard 2006; Steiner et al. 2008). Thus, the following sections will introduce stress-related and depressive disorders and the contribution of the ECS in the development of these psychiatric diseases.

1.4 Stress-related and depressive disorders

1.4.1 Stress and anxiety disorders

Prolonged stress is mostly associated with negative emotions, such as anxiety and fear. Anxiety is defined as a future-oriented mood state in anticipation of a possible, forthcoming danger, while fear is an alarm response to a present or imminent threat (Barlow 2002). In general, fear and anxiety are necessary warning adaptation in humans and animals, facilitating adaptations for survival. However, in case of anxiety disorders these emotional states become excessive and unreasonable. All anxiety disorders share the core features of excessive fear, anxiety, and avoidance, but differ in the specific object or situation of concern (American Psychiatric Association 2013). The estimated lifetime prevalence of an anxiety disorder exceeds 15 % (Kessler et al. 2009). Patients suffering from such diseases are often severely restricted in their every day life, including the inability to work and impairments in social interactions (Kessler et al. 2009). Generalized anxiety disorder (GAD) is one of the most common anxiety disorders, with a lifetime risk of about 4 %, and is among others marked by chronic worrying, nervousness, and tension (Ruscio et al. 2007). Diagnostic criteria for GAD according to “The Diagnostic and Statistical Manual of Mental Disorders - Fifth Edition“ (DSM-V) (American Psychiatric Association 2013) are exemplarily listed in table 1.

Table 1: Diagnostic criteria for generalized anxiety disorder (GAD) according to the DSM-V

DSM-V diagnostic criteria for generalized anxiety disorder
A. Excessive anxiety and worry, occurring more days than not for at least 6 month
B. The individual finds it difficult to control the worry.
C. The anxiety and worry are associated with 3 (or more) of the following symptoms:
1. Restlessness or feeling keyed up or on edge
2. Being easily fatigued
3. Difficulty concentrating or mind going blank
4. Irritability
5. Muscle tension
6. Sleep disturbances
D. The anxiety, worry, or physical symptoms cause distress or impairment in social, occupational, or other important areas of function.
E. The disturbances is not attributable to the physiological effects of a substance or another medical condition.
F. The disturbance is not better explained by another mental disorder.

Another highly prevalent stress- and fear-related disease is the post-traumatic stress disorder (PTSD). Since the fifth DSM edition, PTSDs are no longer classified as classical anxiety disorders, but are rather categorized as trauma- and stress-related diseases. PTSD is developed after an exposure to traumatic events and is accompanied by a constellation of heterogeneous symptoms including hyperarousal, sleep disturbances, difficulty concentrating and most notably re-experiencing of the traumatic event (American Psychiatric Association 2013). Therefore, this disorder shares symptoms with “distress” disorders, such as major depression, and anxiety disorders, for instance GAD or panic disorders. Lifetime PTSD prevalence ranges between 6-9 % in the general population, but among victims of severe traumatic events, such as war, genocides or rapes, the prevalence of PTSD is 20 % up to 40 % (reviewed in Sareen 2014). Consequently, PTSD represents a common mental health problem, arising from the formation of pathological fear memory (for review see Desmedt et al. 2015). The ability to learn fear allows organisms to anticipate harm and to develop appropriate defense behavior, hence fear memory facilitates adaptation and is essential for survival. However, if the memory is reactivated via a non-specific stress response, leading to a generalization of fear, it entails a pathological state. Therefore, PTSD embodies a learning paradigm in which long-term memories related to distinct events persist over time and context (Zoellner et al. 2014).

Particularly the limbic system, including the amygdala, the hippocampus and the prefrontal cortex, are responsible for emotional processing and the formation of fear memory. Anxiety disorders are often associated with a malfunction of this system (for review see Dunsmoor & Paz 2015; Baldi et al. 2015). Several signaling pathways crucial for the development of anxiety and stress-related disorders have been described. It became apparent that amygdalar and hippocampal synaptic plasticity, epigenetic changes and increased stress-hormone levels are connected with stress- and anxiety disorders (for review see Peña et al. 2014; Deppermann et al. 2014). However, the underlying mechanisms are not fully understood. Moreover, the ECS was shown to play a crucial role in the processing of mood and emotions. The connection between the ECS and emotion is specified in chapter 1.4.3.

Today's first line pharmacotherapy for several anxiety disorders consists of anxiolytic drugs, such as benzodiazepines, or antidepressants, such as selective serotonin reuptake inhibitors (Coplan et al. 2015). However, not all patients respond to the currently available treatment options and high degree of co-occurrence of depressive and anxiety disorders impede the diagnosis and subsequent pharmacological and psychological treatment (Coplan et al. 2015). Thus, the comprehensive understanding of biological mechanism involved in these mental disorders and the development of new treatment strategies is of high importance.

1.4.2 The stress-depression connection

Depression is a highly prevalent psychiatric disorder with a lifetime risk up to 20 % and is associated with high levels of mortality and morbidity (Kessler et al. 2005; Holma et al. 2010). According to the World Health Organization (WHO), depression is the leading cause of disability worldwide and is one of the most diagnosed mental disorders among adults (Fact sheet N°369, WHO, October 2015). Even though the understanding of the pathophysiology of depression including its diverse causes has evolved in the last decades, vast gaps remain in the treatment and individual therapy of depressive disorders. This is also reflected in the fact that at least 30 % of the patients do not remit after a year of multiple antidepressant therapies and treatment-resistance with up to 20 % is rather high (Warden et al. 2007; Mrazek et al. 2014). The common treatment of major depressive disorders (MDD) consists of a combined pharmacological and psychological therapy. The classical therapeutics such as monoaminoxidase inhibitors, selective reuptake inhibitors and tricyclic antidepressants are given to increase neurotransmitter levels. These treatment strategies are a consequence of the widely accepted monoamine-hypothesis, which states that the deficit of certain neurotransmitters, such as serotonin, dopamine and noradrenalin, are the main causes of depression (Schildkraut 1965; Coppen 1967). However, several other antidepressants exist, such as ketamine or lithium, which do not directly target neurotransmitter levels, but are nevertheless effective even though the exact mode of action is unknown (Scheuing et al. 2015; Can et al. 2014).

Today MDD is diagnosed based on “The Diagnostic and Statistical Manual of Mental Disorders - Fifth Edition“ (DSM-V) (American Psychiatric Association 2013). According to the DSM-V, primarily symptoms of either depressed mood or anhedonia (loss of interest, loss of pleasure) must be manifested and overall at least five criteria as seen in the DSM-V list must be present for at least two weeks (Tab. 2).

Table 2: Diagnostic criteria for MDD according to the DSM-V

DSM-V diagnostic criteria for Major Depressive Disorder
1. Depressed mood most of the day.
2. Diminished interest or pleasure in all or most activities.
3. Significant unintentional weight loss or gain.
4. Insomnia or hypersomnia.
5. Agitation or psychomotor retardation noticed by others.
6. Fatigue or loss of energy.
7. Feelings of worthlessness or excessive or inappropriate guilt.
8. Diminished ability to think or concentrate, or indecisiveness.
9. Thoughts of death or suicide.

MDD represents a major public health concern, because of the short- and long-term detrimental effects to the patients and for the various long-lasting co-morbidities, such as cardiovascular disease and metabolic syndrome (Gan et al. 2013; Rotella & Manucci 2013). However, anxiety disorders are the most common comorbidities of depression (Wittchen & Jacobi 2005).

Genetic factors play an important role in the development of MDD, as indicated by family studies showing a 2- to 3-fold increased lifetime risk of developing MDD among first- degree relatives. Twin studies even showed a heritability of 40-50 % (for review see Levison 2006). Several candidate genes have been implicated in depressive disorders such as serotonin-transporter (Lesch et al. 1996; Uher & Guffin 2010) or brain-derived neurotrophic factor (BDNF) (Eisch et al. 2003; Chen et al. 2006). However, these genes rather represent a genetic predisposition than being solely responsible for the development of MDD. Psychiatric disorders, like MDD, usually result from a complex interplay of genetic and environmental factors that act cumulatively throughout lifetime (Uher 2014). These environmental factors are mostly adverse events during childhood or ongoing and recent stress (Kendler et al. 2002; Kendler et al. 2006). Hereby, chronic stress is a main environmental risk factor for development of depressive disorders (de Kloet et al. 2005; Lupien et al. 2009). The well-described effect of chronic stress on the development of depression is also supported by the finding of a disrupted hypothalamic-pituitary-adrenal (HPA) axis in MDD patients (for review see Anacker et al. 2011).

The HPA axis, including its end-effectors the glucocorticoid hormones, is part of the body's stress response system. In order to adapt to a stressful event, which can be any internal or external stimulus perceived as a threat to the homeostasis, the organism triggers several physiological and behavioral alterations (Chrousos 2009). This stress response system is located both in the CNS and in peripheral organs. The central effector system includes parts of the HPA axis and the locus ceruleous/norepinephrine-autonomic systems with their end-products cortisol and norepinephrine and epinephrine, respectively (Chrousos 2009). Brain regions belonging to the limbic system differentially regulate the HPA axis and the release of glucocorticoids. Accordingly, the amygdala is believed to activate the HPA axis, whereas the hippocampus is crucial for the termination of the HPA axis response to stress (for review see Smith & Vale 2006).

However, this system can be maladaptive if the stress stimulus has a stronger intensity and/or duration than the individual ability to an adequate response. This dysregulation results in the development of a series of adverse effects, such as mood alteration, induction of anxiety or cognitive dysfunction (Marques et al. 2009). Under healthy conditions, the HPA axis is controlled by a negative feedback loop by which cortisol inhibits the release of upstream effector molecules, particularly the corticotropin-

releasing hormone (CRH) and the adrenocorticotrophic hormone (ACTH). However, persistent stress can disturb this glucocorticoid feedback mechanism (Fig. 4).

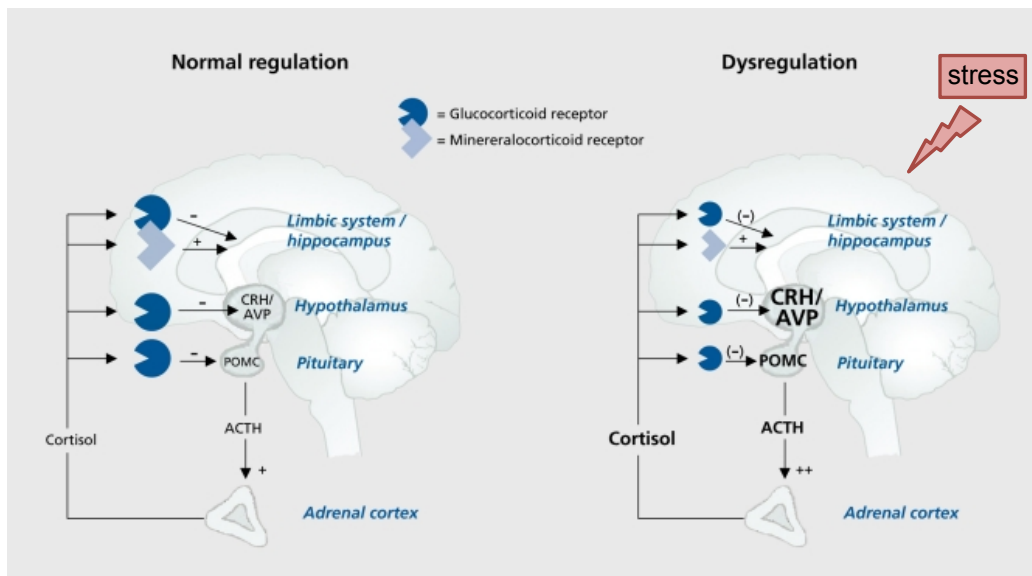


Figure 4: Normal and impaired regulation of the HPA axis (modified from Ising & Holsboer 2006): AVP: arginine vasopressin, ACTH: Adrenocorticotrophic hormone, CRH: corticotropin-releasing hormone, POMC: Pro-opiomelanocortin.

The HPA axis is further regulated on the level of the hypothalamus and by a diverse group of afferent projections not only from limbic, but also from mid-brain, and brain stem nuclei (Herman et al. 2003). Furthermore, the ECS influences the release of glucocorticoids and is an important modulator of the physiological stress responses. Thus, the next section addresses the role of the ECS in stress and emotion.

1.4.3 ECS in emotional processes

For millennia cannabis has been consumed throughout different cultures for its mood elevating and euphoric effects (Williamson & Evans 2000). Since the discovery of the psychoactive plant compound THC and its mode of action by activating the cannabinoid receptors, the ECS became of great research interest as a modulator of mood and emotion. However, adverse effects of cannabis such as panic attacks or paranoia have also been described. Furthermore, excessive cannabis use during adolescence has been associated with an increased risk of schizophrenia (Rubino & Parolaro 2008) and CB1 receptor availability is reduced in the hippocampus of schizophrenia patients (Ranganathan et al. 2015).

Dysregulation of the ECS has been implicated in several psychiatric disorders. Previous studies showed reduced serum anandamide levels and an increased CB1 receptor availability throughout the brain of patients suffering from PTSD (Neumeister et

al. 2014). Furthermore, increased CB1 receptor density was reported in the prefrontal cortex of depressed suicide victims (Hungund et al. 2004). In line with this, the CB1 receptor and the eCB synthesizing enzymes are abundantly expressed in brain areas implicated in emotional and mood regulation, such as the amygdala, hypothalamus and the hippocampus (Mackie et al. 2005; Patel et al. 2009). Furthermore, CB1 receptors and endocannabinoids participate in the control of the HPA axis, indicating an important role in stress response (Hill et al. 2010a). For instance repeated homotypic stress produces a robust elevation of amygdalar 2-AG content and thereby induces HPA axis habituation (Patel et al. 2009; Hill et al. 2010b). In addition, mice with disrupted endocannabinoid signaling are more sensitive to chronic stress (Dubreucq et al. 2012).

For a brief period from 2006 until 2008, the CB1 antagonist rimonabant was clinically used in Europe under the trade name Accomplia® to treat obesity. However, the compound caused serious adverse psychiatric side effects including anxiety and depression (Christensen et al. 2007), which led to a withdrawal of Accomplia® from the market. These clinical findings validated previous results from rodent studies showing that the genetic or pharmacological blockade of CB1 increases depression- and anxiety-like behavior (Valverde et al. 2005; Valverde & Torrens 2012). Furthermore, serum endocannabinoid levels are decreased in depressed patients (Hill et al. 2008) and the chronic treatment with antidepressants led to a significant increase in 2-AG levels in various brain areas, indicating that 2-AG could be important for the antidepressant effect of these drugs (Smaga et al. 2014). Depression is frequently associated with a reduced adult neurogenesis (Sheline et al. 2003; Lee et al. 2013), also seen in mice with reduced cannabinoid levels (Gao et al. 2010). In line with these discoveries, endocannabinoids promote adult neurogenesis (Zhang et al. 2014) and the cannabinoid receptors are highly expressed in neuronal stem cells (Galve-Roperh et al. 2013).

In conclusion, the ECS is an important modulator of emotional processes and disrupted endocannabinoid signaling contributes to the development of affective disorders. Therefore, modulation of the ECS is a promising target to treat depressive and anxiety disorders.

1.4.4 Modeling depression in mice

Animal modeling of human diseases is an essential cornerstone in the analysis of disease mechanisms and the preclinical testing of potential new therapeutic drugs. Especially rodents are routinely used to model and investigate various human diseases including diseases of the CNS for instance epilepsy, Parkinson's disease, Huntington's disease, Alzheimer's disease, traumatic brain injury and stroke (Grone & Baraban 2015; Lee et al. 2012; Lee et al. 2013; Kitazawa et al. 2012; Marklund & Hillered 2011; Fluri et al. 2015). The emphasis is apparently on diseases associated with neurodegeneration. However, in the last decades several animal models and paradigms to mimic psychiatric disorders have been established and routinely used, such as schizophrenia, depression and anxiety disorders (Samsom & Wong 2015).

Neuropsychiatric diseases are associated with a variety of heterogeneous physiological and psychological symptoms. Whereas most of the physiological alterations, such as weight gain or loss, insomnia or hypersomnia and neuroanatomical changes are easily measurable in rodents, most of the psychological aspects like depressed mood, guilt and low self-esteem cannot be convincingly ascertained (Nestler & Hyman 2010; Dedic et al. 2011).

Up to now, three criteria, including construct validity, face validity and predictive validity, are widely accepted to assess the reliability of an animal model (McKinney and Bunney 1969; Nestler & Hyman 2010). Construct validity implies that the symptoms manifested in an animal are based on the same neurobiological mechanism as in humans. Face validity is defined as a similarity of specific behavioral or physiological symptoms of the disease between the animal and affected humans. Lastly, the same treatment strategies have to be effective in the model as in the clinic (predictive validity) (McKinney and Bunney 1969). The more criteria a proposed model fulfills, the more convincing and widely accepted it will be (Dedic et al. 2011).

Neuropsychiatric disorders, like depression, are multifactorial diseases and therefore inherently difficult to mirror in rodents. Nevertheless, various symptoms of depression can be tested in rodents (Tab. 3).

Table 3: Depression-associated endphenotypes that can be modeled in mice (adopted from Dedic et al. 2011)

DSM-V symptoms	Endophenotypes in mice	Appropriate test/analysis
Depressed mood	Cannot be modeled	-
Decreased interest or loss of pleasure	Anhedonia	Sucrose preference
Weight gain or loss	Can easily be measures	Weight gain/ loss after stress
Insomnia or Hypersomnia	Abnormal sleep architecture	EEG recordings
Agitation or psychomotor retardation	Alterations in locomotion	Open-field, alterations in home-cage activity
Fatigue or loss of energy	Alterations in locomotion	Reduced home-cage activity, Nest building
Feelings of worthlessness or inappropriate guilt	Cannot be modeled	-
Diminished ability to think or concentrate	Deficits in working and spatial memory	Morris water maze, Y-maze
Thoughts of death or suicide	Cannot be modeled	-
	Additional endophenotypes	
	Anxiety-related behavior	Open-field, Light-dark box, O-maze
	Changes in social behavior	Social interaction/ avoidance
	Behavioral despair	Tail suspension test, Forced swim test
	Neuroendocrine disturbance	Corticosterone secretion, Dexamethasone suppression
	Neuroanatomical changes	Hippocampal volume

Nowadays most (non-genetic) animal models of depression mainly rely on stress-induced behavioral changes (Kato et al. 2015), since chronic stress is a main risk factor for the development of depression (de Kloet et al. 2005; Lupien et al. 2009). Accepted models are the chronic unpredictable mild stress (for review see Willner 2005), social defeat stress (Berton et al. 2006), maternal separation (for review see Nishi et al. 2014) and prenatal stress (Mueller & Bale 2008). Although none of these models perfectly reproduce the symptoms of depression observed in humans, translational rodent models combined with the analysis of postmortem tissue from depressed patients led to important discoveries in the last decades (Menard et al. 2015). To develop an appropriate rodent model of depression, advance in genetics and pharmacology must be combined with environmental challenges like chronic stress (Dedic et al. 2011).

In conclusion, modeling depression in mice is a useful and necessary tool to understand the pathophysiology of this disease and to find new therapeutic targets for a pharmacological treatment of depressive disorders.

1.5 Aim of the thesis

One aim of this study was to investigate the impact of 2-AG and its main synthesizing enzyme DAGL α on the development of depressive- and anxiety-like behaviors. Therefore, constitutive as well as different conditional *Dagla*^{-/-} mice were analyzed. Disruption of the ECS has been linked to depression in humans and depression-like behaviors in mice. Since eCBs are produced on demand, the pathways and enzymes involved in endocannabinoid biosynthesis play a major role in regulating the activity of this system. However, up to now the main cellular source of 2-AG in the CNS is still unknown. To determine the impact of DAGL α activity in neurons and microglia cells, which are the main 2-AG producing cells *in vitro*, different cell type-specific *Dagla*^{-/-} mice were analyzed. The behavioral and molecular analysis of these knockout mouse lines will give an insight into the impact of DAGL α activity in anxiety and depressive disorders.

A second aim of this thesis was to analyze the reactivity of the constitutive as well as neuronal-specific *Dagla*^{-/-} mice to chronic stress, using a model of chronic social defeat stress. Chronic stress is a main risk factor of major depressive disorder and genetic or pharmacologic blockade of the CB1 receptor leads to an increased sensitivity towards chronic stress. Thus, this study aims to determine the impact of 2-AG on this altered stress reactivity.

A further aim was to establish a suitable method to discover potential interaction partners of DAGL α . Even though several *in vitro* studies revealed certain potential regulatory mechanisms, until now very little is known about the regulation of DAGL α . Therefore, protein-protein interactions between DAGL α and potential candidate proteins were analyzed using tandem affinity purification.

Material and Methods

2.1 Equipment

Technical instrument	Identifier, Company
Analgesia Meter Hot Plate	TSE Systems
Analytical balance	BP 121 S, Sartorius
Animal tracking software	EthoVision [®] XT, Noldus
Cell culture incubator	Binder GmbH
Centrifuges	Biofuge fresco, Heraeus Instruments Biofuge pico, Heraeus Instruments Biofuge stratos, Heraeus Instruments Megafuge 1.0R, Heraeus Instruments
Cryostat	CM3050S, Leica GmbH
Digital gel documentation	ChemiDoc MP imaging systems, Bio-Rad Laboratories
Electroporation system	MicroPulser [™] Electroporator, Bio-Rad Laboratories
Electrophoresis chamber (agarose gels)	Sub-Cell GT System, Bio-Rad Laboratories
Electrophoresis chamber (polyacrylamide gels)	XCell SureLock [®] Mini-Cell, Life Technologies
EMCCD camera equipped with a 494/20 and 572/28 bandpass emission filter wheel	Rolera MGI plus EMCCD camera, Decon Science Tec
Home cage activity measurement	Mouse-E-Motion, Infra-e-motion, Henstedt-Ulzburg,
Imaging of TLC plates: LED lamp equipped with a HEBO V01 excitation filter.	10 x 1 W 420 nm LEDs, Roithner Lasertechnik HEBO V01, Hebo Spezialglas
Laminar flow hood	Herasafe, Kendro
Liquid handling platform	Janus [®] , Perkin Elmer
Magnetic stirrer	MR 3001 K, Heidolph, Fisher
Microplate analyzer	MRX TC II, Dynex Technologies
Microscope	Eclipse TS 1000, Nikon Axiovert 200 M fluorescent microscope, Zeiss
Open-field test device	Open-field ActiMot, TSE Systems
PCR cyclers	iCycler, Bio-Rad Laboratories
pH meter	inoLab, WTW

Technical instrument	Identifier, Company
Real-time PCR cyclers	LightCycler [®] 480 Instrument II, Roche
Spectrophotometer	NanoDrop 1000, Thermo scientific
SpeedVac SPD111V	Thermo Fisher
Startle response box	TSE startle response test system, TSE Systems
Sterilizing oven	Varioklav 25T, H+P Labortechnik
Tissue homogenizer	Precellys 24, Bertin Technologies
Ultrasonic bath	Ultrasonic cleaning bath USC-THD, VWR
Vortexer	Vortex-Genie 2, Scientific Industries
Western Blot System	iBlot [®] Gel Transfer Device, Life Technologies

2.2 Chemicals and reagents

2.2.1 Chemicals

Chemicals	Company
Amitriptiline hydrochloride	Sigma-Aldrich
Albumin bovine Fraction V, pH 7.0 standard grade, lyophil. (BSA)	Serva
ANTI-FLAG [®] M2 Affinity Gel	Sigma-Aldrich
Azidocoumarin (3-azido-7-hydroxycoumarin)	Carl Roth
Brilliant Blue R-250	Sigma-Aldrich
1-Bromo-3-chloropropane (BCP)	Sigma-Aldrich
BrdU (B5002-250mg)	Sigma-Aldrich
Cremophor [®] EL/ Kolliphor [®] EL	Sigma-Aldrich
Cu(I)TFB(Tetrakis(acetonitrile)copper(I) tetrafluoroborate)	Sigma-Aldrich
DAPI Fluoromount-G [®]	SouthernBiotech
N,N-diisopropylethylamine	Sigma-Aldrich
ECL Western Blotting substrate	Thermo Fisher (Pierce [™])
Ethidium bromide solution (10 mg/ml)	Sigma-Aldrich
Fluoromount-G [®]	SouthernBiotech
JZL184, MAGL Inhibitor	Sigma-Aldrich
Lipofectamin [®] 2000 Transfection Reagent	Thermo Fisher
2-Methylbutan/ Isopentan	Sigma-Aldrich
Paraformaldehyd	Sigma-Aldrich
<i>Strep-tag</i> [®] Protein Purification Buffer Set	IBA Lifescience
Sucrose, for microbiology	Sigma-Aldrich
Strep-Tactin [®] Superflow [®] high capacity 50% suspension	IBA Lifescience
THC (dronabinol)	THC Pharm GmbH
TRizol [®] Reagent	Thermo Fisher
Tween20	Sigma-Aldrich
URB594, FAAH Inhibitor	Sigma-Aldrich

2.2.2 Kits

Kits	Company
PeqGOLD Plasmid Miniprep Kit I	Peqlab
PeqGOLD Gel Extraction Kit C-Line	Peqlab
GeneElute™ HP Plasmid MidiPrep Kit	Sigma-Aldrich
GoTaq® Green Master Mix (PCR)	Promega
BCA Protein Assay Kit	Thermo Fisher (Pierce™)
Two-TAP Cloning Kit, mammalian (5-1623-001)	IBA Lifescience

2.2.3 Buffers and solutions

If not stated otherwise all buffers and solutions were prepared with dH₂O and all chemicals were purchased from Applichem, Life Technologies, Merck, Carl Roth or Sigma-Aldrich.

Buffer and solution	Composition	Application
Borate buffer	0.1 M Boric acid adjusted to pH 8.5	Immunohistochemistry
Citrate buffer	10 mM Citric acid 0.05 % (v/v) Tween 20 adjusted to pH 6.0	Immunohistochemistry
Clickmix/ Coumarin labeling solution	850 μ l Ethanol 50 μ l 10 mM Cu(I)TFB in acetonitrile 10 μ l 2 mg/ml Azidocoumarin in EtOH	Click chemistry
Hünigs base	4 % <i>N,N</i> -diisopropylethylamine in hexane	Click chemistry
Mouse tail lysis buffer	100 mM Tris/HCl pH 8.0 5 mM EDTA 200 mM NaCl 0.2 % (w/v) SDS	Mouse tail lysis
2x SSC	0.3 M NaCl 30 mM Na-citrate dihydrate adjusted to pH 7.0	Immunohistochemistry
TAE buffer	40 mM Tris-acetate 1 mM EDTA pH 8.0	Agarose gel electrophoresis
TBS (Tris-buffered saline)	50 mM Tris-HCl 150 mM NaCl adjusted to pH 7.5	Immunohistochemistry
TE buffer	10 mM Tris 1 mM EDTA, pH 8.0 adjusted to pH 7.4	DNA isolation
4 % PFA	4 % (w/v) Paraformaldehyd	Fixation of brain tissue
RIPA	5 mM EDTA 10 mM Tris pH 8.0 0.1 % SDS 150 mM NaCl 0.5 % Dexychoic acid 1 % Nonidet-P40 add 1 tablet cOmplete™ Mini per 10 ml RIPA buffer and store at 4°C	Protein isolation

2.2.4 Enzymes and antibodies

Enzyme/ antibody/ serum	Company
Proteinase K	NEB
Superscript II Reverse Transcriptase	Invitrogen
Taq Polymerase	NEB
Phusion High Fidelity DNA Polymerase	NEB
Restriction enzyme: <i>XbaI</i> , <i>HindIII</i>	NEB
Restriction buffer 2.1	NEB
Anti-DAGL α (DGL α -Rb-Af380, rabbit, polyclonal)	Frontier Institute Co.Ltd
Anti-DAGL α (ab81914, goat, polyclonal, AB_1658310)	Abcam
Anti-BrdU (ab6326, rat, monoclonal, AB_305426)	Abcam
Anti-Iba1 (019-19741, rabbit, polyclonal)	Abcam
Anti-NeuN AlexaFluor [®] 488 (MAB377X, mouse, monoclonal, AB_2149209)	Merck Milipore
Anti-FLAG [®] (F7425, rabbit, polyclonal, AB_439687)	Sigma-Aldrich
Donkey anti-goat AlexaFluor [®] 488 (A-11055, AB_10564074)	Life Technologies
Donkey anti-rabbit HRP conjugated (711-035152, AB_10015282)	Dianova
Donkey anti-rabbit AlexaFluor [®] 488 (A-21206, AB_10049650)	Life Technologies
Goat anti-rabbit AlexaFluor [®] 594 (A-11037, AB_10561549)	Life Technologies
Goat anti-rat AlexaFluor [®] 594 (A-11007, AB_10561522)	Life Technologies
Normal goat serum (ab7481)	Abcam
Normal donkey serum (ab7475)	Abcam

2.2.5 Antibiotics

Substance	Working concentration	Company
Ampicillin	100 μ g/ml	Applichem
Kanamycin	50 μ g/ml	Applichem
G418 Sulfate, Geneticin [®]	400 μ g/ml	Thermo Fisher

2.2.6 Plasmids

Plasmid	Description
pCR-BluntII-TOPO (BC148308)	MGC premier mouse cDNA clone: Dagla (BioCat GmbH)
pENTRY-IBA51	StarGate Entry Vector is required to generate Donor Vectors (IBA)
pESG-IBA168	Allows the expression of C-terminal Twin-Strep [®] -FLAG-tag-fusion-proteins, contains the CMV promotor

2.3 Animals

In this study constitutive as well as different tissue-specific Dagla deficient mice (2-4 months old) were used for molecular and behavioral analysis. To generate Dagla knockout mice two loxP sites flanking exon 1, which contains the promoter region, were inserted (Ternes 2013). This loxP sites allow Cre-mediated excision of the flanked exon. The Cre recombinase is derived from the P1 Bacteriophage and catalyses site-specific recombination between two recognition sites (loxP sites) leading to the excision of DNA fragments (Hoess et al. 1984). This Cre/loxP system is widely used to produce constitutive as well as conditional loss of gene function in specific-cell types.

Accordingly, to obtain constitutive Dagla deficient mice (Dagla^{-/-}) homozygous Dagla floxed (Dagla^{fl/fl}) mice on a C57BL/6J genetic background were bred with Pdgfra-Cre mice (Lallemand et al. 1998), a transgenic mouse line which express Cre ubiquitously (Ternes 2013; Jenniches et al. 2015). In addition, to generate cell-specific Dagla knockout mice Dagla^{fl/fl} mice were either bred with Synapsin 1-Cre transgenic mice (Zhu et al. 2001) to obtain neuron-specific Dagla deficient mice (Syn-Dagla^{-/-}) or LysM-Cre transgenic mice (Clausen et al. 1999) to generate myeloid cell-specific Dagla knockout mice (LysM-Dagla^{-/-}). Synapsin 1-Cre mice express the Cre recombinase under the neuron-specific promoter Synapsin 1, which leads to Cre/loxP recombination exclusively in neurons. Whereas in LysM-Cre mice Cre expression is driven by the Lysozyme M promoter, which leads to Cre-mediated DNA excision in myeloid cells, like microglia and macrophages.

For all experiments Dagla^{fl/fl} littermates or wild type controls (WT) on a C57BL/6J genetic background were used as control animals. WT mice were originally obtained from a commercial breeder (Janvier, France) and bred at our animal facility. Unless otherwise stated, all mice were group-housed (4-5 animals per cage) in standard laboratory cages

under a normal light-dark cycle (light phase for 12 hours, light on at 09:00 am) with *ad libitum* access to food and water under SFP conditions. Male CD1 mice (6 months old retired breeders), used as aggressor mice in the chronic social defeat stress (CSDS) paradigm, were obtained from a commercial breeder (Janvier, France) and single-caged in standard laboratory cages under a reversed light-dark cycle (light phase for 12 hours, light on at 09:00 pm) with *ad libitum* access to food and water. All experiments followed the guidelines of the German Animal Protection Law and the Local Committee for Animal Health, LANUV NRW, approved the experiments.

2.4 Behavioral experiments

2.4.1 Sucrose preference test

Anhedonic-like behavior of mice was analyzed by a sucrose preference test. Mice were housed individually and the animals could freely choose between 1 % sucrose solution and water. In general most rodents prefer sweet solutions to mere water with a preference up to 95 % for C57BL/6 mice (Pothion et al. 2004). This preference is typically decreased in various affective disorders, including depression and therefore a plausible measure of depressive-like behavior in mice (Katz et al. 1981). The consumption was measured for 48 h and the position of the bottles was changed after 24 h. The sucrose preference (%) was calculated as sucrose solution consumed divided by the total amount of solution consumed.

2.4.2 Forced swim test

Animals were tested for behavioral despair in the forced swim test. This test is based on the assumption that mice try to escape an aversive (stressful) stimulus such as water. For this test mice were placed individually into a glass cylinder (height 28 cm, diameter 20 cm) containing water (height 14 cm, 24-25°C). Immobility time was recorded during the last 4 min of the 6 min testing period and is considered a measure of helpless behavior (Porsolt et al. 1977).

For pharmacological studies mice were treated either with the antidepressant amitriptyline or with MAGL (JZL184) or FAAH (URB597) inhibitors. Therefore, mice received either 10 mg/kg amitriptyline i.p. 30 min prior to the test, or 20 mg/kg JZL184 or 0.5 mg/kg URB597 2 h before the forced swim test. JZL184, URB597 and amitriptyline hydrochloride were dissolved in Tween20 and afterwards diluted in 0.9% saline (final concentration of

Tween20 < 0.1%). Vehicle control animals were treated with Tween20 (final concentration < 0.1%) diluted in 0.9% saline.

2.4.3 Social preference test

Social interaction behavior of mice was assessed by the social preference test. Social interaction is a fundamental component of rodent behavior and disrupted in a variety of neuropsychiatric disorders (Nestler & Hyman 2010). To analyze social interaction mice were individually habituated to the transparent open-field box (44 cm x 44 cm) for 5 min on three consecutive days before the testing day. The floor was covered with bedding material. On the testing day the arenas (open-field boxes) contained two metal grid cages in opposing corners and an unfamiliar mouse of the same gender and age was placed in one of the metal grid cages. The test animals were introduced and their location recorded for 10 min using the EthoVision XT software (Noldus Information Technology Inc.). Calculated was the time spent investigating the partner mouse compared to the empty cage. A sign of social preference is a significantly higher time spent investigating (the nose of the mouse is not more than 1 cm from the wall of the grid cage) the partner mouse compared to the empty cage.

2.4.4 Social avoidance test

Social avoidance behavior was analyzed in a variant form of the social interaction test. Mice were habituated as described in 2.4.3. On the testing day one metal grid cage containing a foreign CD1 mouse (male retired breeder) was placed close to one wall of the open-field box. The movement of each test animal was recorded for 5 min using the EthoVision XT software (Noldus Information Technology Inc.). Calculated was the time spent investigating the foreign CD1 mouse. The less time the test mouse spent interacting with the CD1 the higher the social avoidance behavior. In this test CD1 mice were used for the interaction analysis, because animals of the same mouse strain were used as aggressors in the chronic social defeat paradigm (described in chapter 2.4.14). Thus, stressed (defeated) mice tend to spend less time interacting with a foreign CD1 mouse, indicative of social avoidance behavior.

2.4.5 Home cage activity measurement

Home cage activity was recorded using an infrared system (Mouse-E-Motion, Infra-e-motion GmbH), whereby an infrared sensor is attached to the mouse cage lid and records movements in the home cage every 30 s. For this test mice were housed in single-cages

and habituated to the reversed light/dark cycle (light phase for 12 hours, light on at 9:00 pm) for at least seven days. Movements were sampled and averaged over 1 h.

2.4.6 Open-field test

Anxiety behavior and locomotor activity were analyzed using the open-field test. Animals were tested in a sound-isolated, dimly illuminated room (20 lux) in an open-field box (44 cm x 44 cm). The mice were allowed to explore the box freely and their behavior was recorded for 10 or 30 min. Analysis was conducted using ActiMot (TSE Systems) or the “EthoVision XT” software (Noldus Information Technology Inc). The time spent in the center of the open-field box (25 % of the whole area) is considered a measure of anxiety. Rodents usually avoid open lit-up areas and increased anxiety is associated with decreased time spent in the center of the open-field box. In addition, spontaneous locomotor activity and exploratory behavior were determined by the total distance travelled in the arena and the number of rearings.

2.4.7 Light-dark box test

Anxiety behavior was analyzed in the light/dark box test. Animals were tested in a sound-isolated room in an open-field box (44 cm x 44 cm) divided into a light (2/3 of area) and a dark (1/3 of the area) compartment. The light compartment was brightly illuminated (800 lux). Each animal was placed in the dark compartment and allowed to explore the arena freely for 10 min, while their behavior was recorded. This test is based on the fact that rodents avoid open highly illuminated areas (Crawley et al. 1984; Bourin & Hascöet 2003) and that increased anxiety behavior further decreases the time spent in the open compartment.

2.4.8 Zero-maze test

Anxiety-related behavior was also tested in the zero-maze (height 40 cm, internal diameter 46 cm, width 5.6 cm) in a sound-isolated room. The maze was divided into four equal quadrants, with non-transparent walls enclosing the two opposite quadrants. Animals were placed in the open area of the zero-maze and their movements were recorded for 5 min with 600-700 lux illumination. Time spent in the different areas and distance travelled was analyzed using “EthoVision XT” software (Noldus Information Technology Inc.).

2.4.9 Fear conditioning paradigm

The Fear conditioning paradigm is based on the analysis of fear extinction, a process, which leads to a decline of conditioned fear response. This behavioral test is based on the process of respondent conditioning, in which a conditioned (neutral) stimulus is associated with an unconditioned stimulus. Here the neutral stimulus is a sound-cue, which is paired with an aversive stimulus (electric foot-shock) to evoke a fear response. On the extinction days following the conditioning the animals were presented only to the sound-cue and the freezing behavior was determined. Freezing is a measure of anxiety in rodents and characterized by persistent immobility of the animal.



Figure 5: Startle response test system (modified from TSE Systems)

For this test a sound-protected box equipped with a foot shock device, loud speakers and a vibration-sensitive platform to detect movements was utilized (Fig. 5; TSE-Systems GmbH). For conditioning, mice were placed in a small grid chamber and after 3 minutes a tone (80 dB, 9 kHz) was presented for 20 s, which co-terminated with a 2 s electric foot shock of 0.7 mA. To evaluate the conditioned freezing response mice were placed into a glass cylinder (diameter 8 cm) in the same box and after 3 min habituation, the same tone was presented. Vibrations caused by the movements of the animal were recorded during conditioning and on days 1, 2, 3 and 6 after conditioning (extinction trial 1, 2, 3, 6). Periods of activity were indicated by peaks exceeding twice the baseline level. Behavior was considered as freezing, if the amplitude of the peaks remained below this threshold for more than 3 s. The percentage of time that the animal spent freezing during a test session was calculated for each trial and served as an indicator for the decline from one session to the next.

2.4.10 Hot plate test

The hot plate test is used to assess acute pain sensitivity of rodents to a thermal stimulus. Animals were placed in a plastic cylinder on a 52°C hot surface (Analgesia Meter Hot Plate, TSE Systems). The latency (in seconds) to the first reaction of pain was measured. This first reaction of pain is defined as shaking the hind paw, licking the paw or jumping. The test was terminated when the animal showed the first reaction of pain or after 30 s.

2.4.11 Pup retrieval test

Maternal care was assessed by the pup retrieval test. In this test, the entire litter was removed and after 5 minutes 3 pups (day 2-7 after birth) were returned to the home cage away from the nest at an opposite end of the cage. The entire test was recorded on video. The latency (in seconds) to sniff a pup and retrieve it to the nest was measured. If a female had not retrieved all pups within 5 min the test was terminated, resulting in a latency of 300 s. In addition, the pups were checked for the presence of a milk spot as an indicator for nursing behavior.

2.4.12 Maternal behavior

To analyze maternal care the behavior of nursing female mice were recorded using a time-sampling procedure (20 sec observation every third minute for 1 h between 9 AM and 10 AM on postnatal days 2–7). This results in 21 observations of each dam per day. During the days of observation females and their litter were single-housed and the home cages were not changed, because cage cleaning can stress the nursing females and therefore may affect the maternal behavior. Frequencies of nursing and overall time spent interacting with the pups were calculated by taking the average of observations per dam of 3-4 observation days.

2.4.13 Tetrad test

The tetrad test is widely used to analyze cannabinoid receptor-mediated behavioral effects in rodents. This test consists of a series of behavioral paradigms including spontaneous activity, hypothermia, catalepsy and analgesia. Animals were treated with 8 mg/kg THC (dronabinol) or 0.9 % saline (i.p.) 30 min before the test. Rectal body temperature was measured directly before the injection and 30 min after injection. Subsequently, spontaneous activity was analyzed in a 10 min open-field test, followed by a hot plate test. THC injection solution was prepared by diluting THC stock solution (100

mg/ml in 100 % EtOH) in cremophor and saline. Vehicle solution contained equal concentrations of EtOH and cremophor diluted in saline.

2.4.14 Chronic social defeat paradigm

Chronic stress is a main cause of depression in humans (de Kloet et al. 2005; Lupien et al. 2009). Several chronic stress models have been established to investigate stress-induced depressive-like behavior and molecular adaptations in rodents, such as chronic social defeat stress (CSDS). In humans, chronic social defeat, like bullying in schools or workplaces, can lead to sociophobia, the loss of self-esteem, anxiety and depression (Björkqvist 2001). The animal model CSDS is based on a resident-intruder paradigm, in which a young male mouse (intruder) is placed into the home cage of another older, more aggressive male (resident). The defeated animal is considered to experience social stress.

2.4.14.1 Screening for aggressive CD1 mice

Reproducible and successful application of chronic social defeat stress is strongly dependent on the consistent levels of aggressive behaviors of the CD1 mice. In general single-caged retired breeders exhibit the strongest territoriality and aggressiveness against foreign males and are therefore the most recommended aggressors. Nevertheless, aggression levels vary greatly between individuals and a screening procedure is essential. In this study a screening procedure described by Golden et al. 2011 was applied.

The 3 days screening was performed in the home cage of the CD1 mouse. Each day a novel 7-9 weeks old C57BL6/J mouse was placed in the home cage of the aggressor for up to 5 min and the latency to the first aggression is recorded. Only CD1 mice that attacked in at least two of the three screening days with a latency to attack less than 60 s were selected for the social defeat paradigm.

2.4.14.2 Social defeat protocol

Chronic social defeat stress is a widely used chronic stress model for rodents to elicit depressive-like behavior. This paradigm is based on repeated social defeat sessions between a young C57BL6/J mouse and a larger and aggressive male CD1 mouse, which were screened for aggressive behavior (Point 2.4.12.1). In this paradigm a 7-9 weeks old male C57BL6/J mice was subjected to bouts of chronic social defeat by a CD1 mouse for 5-10 min daily for 10 consecutive days (Golden et al. 2011). After each social defeat the animals were separated by a perforated plastic glass wall which allows sensory but no

physical contact for the following 24 h (Fig. 6). In order to prevent any habituation the intruder C57BL6/J mice was exposed to a novel resident's home cage on each day. Subsequent to the last social defeat the animals were single-caged and tested in a battery of different anxiety- and depression-related behavioral tests.



Figure 6: Cage divided by a perforated plexiglass wall (Golden et al. 2011)

2.5 Measurement of endocannabinoids

Brains were collected and immediately frozen in liquid nitrogen. For pharmacological studies, mice were intraperitoneally injected with either 20 mg/kg JZL184 or 0.9 % saline 2 hours before tissue collection. Striatum, cortex, hippocampi, and amygdala samples were punched from the frozen brain slices (1.0 mm) with the use of a metal matrix for mouse brains (Zivic Instruments) and cylindrical brain punchers (Fine Science Tools; internal diameter, 1.0 mm). Extraction and quantification of endogenous cannabinoids (eCB) was carried out as previously described (Lomazzo et al. 2014) by Dr. Laura Bindila (Prof. Beat Lutz, Institute of Physiological Chemistry, University Medical Center, Mainz). Endogenous 2-AG levels were measured employing a 5500 QTrap[®] triple-quadrupole linear ion trap mass spectrometer (AB SCIEX). For quantification, triplicate calibration curves were run. Quantification of 2-AG was performed using Analyst 1.6.1 software. The obtained eCB values were normalized to the amount of protein.

2.6 Measurement of corticosterone

Fecal corticosterone levels were measured using the DetectX[®] Corticosterone Enzyme Immunoassay Kit (Arbor Assays). To extract steroids from collected feces (stored at -80°C) samples were firstly dried for 2 h at 37°C. Subsequently, 200 – 300 mg of dried feces were transferred into a 5 ml microcentrifuge tube and 1 ml 100 % EtOH per 100 mg

of solid was added. For extraction samples were incubated for 30 min at RT in a shaking incubator. Subsequently, samples were centrifuged at 4500 rpm for 15 min. Six hundred μ l of the supernatant was transferred into a 1.5 ml microcentrifuge tube and the samples were evaporated to dryness in a SpeedVac for 1 h at 35°C. Extracted samples were kept at -20°C overnight.

On the next day samples were dissolved in 100 μ l EtOH, followed by 400 μ l Assay buffer, and vortexed and incubated for 5 min at RT. The vortexing and incubation steps were repeated for three times. Afterwards the samples were diluted 1:2 with assay buffer, since the ethanol concentration must be less than 5 % for the following immunoassay. The immunoassay was performed according to the manufacturer's protocol. After incubation of all kit reagents for 30 min at RT, the corticosterone standards were prepared according to the manufacturer's protocol (concentration range: 78.128 pg/ml to 10000 pg/ml). Subsequently, 50 μ l of diluted samples or standards (in duplicates) were pipetted into the wells of a clear microtiter plate coated with an antibody to capture sheep antibodies followed by 25 μ l DetectX[®] Corticosterone (Peroxidase-) Conjugate and 25 μ l DetectX[®] Corticosterone Antibody. After 1h shaking at RT, wells were aspirated and washed 4 times with 300 μ l wash buffer following 100 μ l TMB substrate per well. Towards 30 min incubation at RT 50 μ l stop solution were added to each well. The samples were analyzed at 450 nm in a microplate reader.

2.7 Immunohistochemistry

2.7.1 DAGL α staining

The loss of DAGL α protein was confirmed by immunohistochemistry staining of cryofixed brain slices. Brains were perfused with 4 % paraformaldehyde (PFA) in phosphate-buffer saline (PBS), overnight cryoprotected with 20 % sucrose in PBS at 4°C, frozen in dry ice cooled isopentane and stored at -80°C. Brains slices (thickness: 18 μ m) were permeabilized with TBS (Tris-buffered saline) containing 0.3 % Tween-20 for 10 min at RT and subsequently washed 3 times for 5 min in TBS. Antigen retrieval was conducted by 20 min incubation with citrate buffer at 65°C, followed by 3 washing steps (5 min, RT) in TBS. Afterwards, slices were blocked with TBS plus (TBS containing 0.3 % Triton X-100, 10 % donkey serum and 2 % BSA) for 1 h at RT followed by the staining with anti-DAGL α antibody (DGL α -Rb-Af380) overnight at 4°C (final concentration 0.5 μ g/ml in TBS plus). On the next day, slices were washed with TBS (3 times 5 min at RT) and again blocked with TBS plus for 1 h at RT. Subsequently, the AF488 labeled rabbit-specific secondary antibody was added for 1 h at RT (dilution 1:500 in TBS plus, Donkey anti-rabbit

AlexaFluor®488). After a washing step in TBS (3 times 5 min at RT) stained brain slices were embedded in DAPI Fluoromount-G® media (Southern Biotechnology Associates, Inc.). Fluorescence images were obtained with a Zeiss Axiovert 200 M fluorescent microscope with 20x and 10x objective lenses.

2.7.2 DAGL α /Iba1 co-staining

To verify the Dagla LysM-Cre mouse line, brain slices of LysM-Dagla^{-/-} and Dagla^{fl/fl} mice were co-stained with anti-DAGL α (ab81914, goat, Abcam) and Iba1 (019-19741, rabbit, Abcam) antibodies. Stainings were performed and kindly provided by PD Dr. Andras Bilkei-Gorzo (Institute of Molecular Psychiatry, University of Bonn). Iba1 (ionized calcium binding adaptor molecule 1) is a microglia/macrophage-specific protein, which is widely used as a marker for microglia cells. Brains were perfused with 4 % paraformaldehyde (PFA) in phosphate-buffer saline (PBS) and subsequently embedded in paraffin (paraffin embedding was performed in cooperation with the Institute of Pathology, University Hospital Bonn, Bonn). Brains slices (thickness: 4 μ M) were permeabilized and blocked with 3 % BSA in PBS (phosphate-buffered saline) containing 0.5 % Triton X-100 for 60 min at RT and subsequently washed twice for 5 min in PBS. Subsequently, slices were co-stained with anti-DAGL α (1:300) and anti-Iba1 (1:200) antibodies diluted in 3 % BSA in PBS for 48 h at 4°C, followed by 20 min incubation at RT. Afterwards, slices were washed with PBS (3 times 10 min at RT) and incubated with the secondary antibodies donkey anti-goat AlexaFluor®488 (1:1000; Life Technologies) and goat anti-rabbit AlexaFluor®594 (1:1000; Life Technologies) diluted in 3 % BSA in PBS. After a washing step in PBS (3 times 10 min at RT), stained brain slices were embedded in Fluoromount-G® media (Southern Biotechnology Associates, Inc.). Fluorescence images were obtained with a Zeiss Axiovert 200 M fluorescent microscope with 20x objective lenses.

2.7.3 Adult neurogenesis

To label dividing cells, 5-bromo-2'-deoxyuridine (BrdU, 50 mg/kg dissolved in sterile PBS; Sigma Aldrich) was i.p. injected once daily on 3 consecutive days. The thymidine analog BrdU is incorporated into replicating DNA in dividing cells and can be subsequently detected by anti-BrdU antibodies. Mice were sacrificed with isopentane either 24 h or 21 days after the last BrdU injection and transcardially perfused with 4 % PFA in PBS. Brains were cryoprotected with 20 % sucrose for 24 h and frozen in dry ice-cooled isopentane. Subsequently, brains were embedded in Tissue Tek and serial coronal free-floating cryosections (40 μ M) were cut through the rostrocaudal axis of the hippocampus from bregma -0.94 to -3.34 mm. All steps of the staining protocol were conducted on free-

floating section in 24-well plates and if not stated otherwise all steps were performed at RT. First slices were washed 3 times with TBS and permeabilized for 10 min in TBS containing 0.3 % Tween-20. Subsequently, after 3 washing steps in TBS (5 min) slices were incubated in 2xSSC for 20 min at 65°C. Afterwards, slices were shortly washed in dH₂O and incubated in 2 M HCl for 30 min at 37°C followed by 10 min incubation in Borate buffer. Then, slices were 3 times washed with TBS for 5 min and blocked in TBS plus II (TBS containing 0.3 % Triton X-100, 5 % goat serum, 2 % BSA) for 1h. In a next step, slices were stained with anti-BrdU antibody (dilution 1:500 in TBS plus II) and AF488-conjugated anti-NeuN antibody (dilution 1:250 in TBS plus II) overnight at 4°C. On the next day slices were washed 3 times for 5 min with TBS and again blocked with TBS plus II for 1 h. Subsequently, the AF594-labeled rat-specific secondary antibody was added for 2 h at RT (dilution 1:500 in TBS plus II). After a washing step in TBS (3 times 5 min at RT) stained brain slices were transferred to glass coverslips and embedded in DAPI Fluoromount-G[®] media (Southern Biotechnology Associates, Inc.). Fluorescence images were obtained with a Zeiss Axiovert 200 M fluorescent microscope with 20x objective lens. BrdU-positive cells were counted in the subgranular zone of the hippocampus. The total number of cells was calculated as follows:

$$N = \text{total cells counted} \times (1/\text{ssf}) \times (1/\text{asf}) \times (1/\text{tsf})$$

The selected sampling fraction (ssf) is 0.125 (6/48) for the 24 h time point after BrdU injection and 0.167 (8/48) for 21 days after BrdU injection, because 6 or 8 slides out of 48 were used for analysis. Since the whole dentate gyrus was used as the counting frame, the value for the area sampling fraction (asf) equals 1. Furthermore the thickness sampling fraction (tsf = the height of the dissector/ the mean thickness of the section) is 0.25 (10/40). The calculated number of BrdU positive cells was multiplied by the factor of 2, because only one hemisphere was used for the analysis.

2.8 Cell culture

2.8.1 Isolation and cultivation of bone marrow-derived Macrophages

Bone marrow-derived macrophages (BMM) were isolated from femur and tibia of adult (2-4 months) wild type and *Dagla*^{-/-} mice, respectively. BMM are primary macrophages derived from bone marrow cells *in vitro* in the presence of the macrophage colony-stimulating factor (M-CSF). The growth factor M-CSF is responsible for the proliferation

and differentiation of myeloid progenitor cells into cells of the macrophage/monocyte lineage. In this study the culture medium of L929 cells, a cell line that secretes M-CSF, was used a source of this growth factor. Therefore L929 cells were cultured and the medium of confluent cells was collected and stored at -20°C until further usage. For the differentiation of bone marrow cells into a homogenous population of mature BMMs L929-conditioned medium was added to the growth medium (15 % (v/v)). In the following the isolation of BMM is described in detail:

After baring the hind legs from skin and muscle tissue without bruising the bone, bones were stored in ice-cold PBS and all following steps were performed under sterile conditions. Bones were cut with a scissor at both ends to expose the medullary canal and the bone marrow was rinsed with a 27-gauge needle and 10 ml ice-cold PBS into a 10 cm cell culture dish. By pipetting the bone marrow cells up and down a single-cells suspension was revealed and transferred through a 0.2 µm cell strainer into a 50 ml falcon tube. Subsequently, 20 ml of PBS were added and the isolated cells were centrifuged for 10 min (1200 g, 4°C). Meanwhile cells were counted using a hemacytometer. The cell pellet was resuspended in an adequate amount of growth medium (described below) to obtain a density of 1.5×10^6 cells/ ml. Subsequently, 1 ml cell suspension diluted in 10 ml growth medium was plated on a 10 cm petri dish and cultivated at 5 % CO₂ and 37°C. On the third day 5 ml of fresh growth medium were added to each petri dish and cells were further cultivated as described previously. Fully differentiated macrophages were harvested with a cell scraper at day 7 and plated for further experiments in standard cell culture dishes.

Macrophage growth medium

RPMI 1640

+ Heat-inactivated FCS	10	% (v/v)
+ Penicillin/Streptomycin mix	1	% (v/v)
+ β-Mercaptoethanol	0.1	% (v/v)
+ L292-conditioned medium/ M-CSF	15	% (v/v)

Sterile-filtered with an 0.2 µm filter

All chemicals were purchased from Life Technologies and Gibco.

2.8.2 Cultivation and transfection of Neuro-2a cells

In this study Neuro-2a (N2a) cells, a mouse neuroblastoma cell line, were used for the expression of c-terminal tagged DAGLα. N2a cells were cultivated in DMEM (4.5 g/l glucose) containing 10 % (v/v) heat-inactivated FCS (fetal calf serum), 1 % (v/v)

Penicillin/streptomycin mix and 1 % (v/v) Sodium-pyruvate. All chemicals were purchased from Life Technologies and Gibco. For maintenance sub-confluent cultures (70-80%) were split twice weekly 1:5 or 1:10 and cultivated at 5 % CO₂ and 37°C. Therefore adherent cells were washed with PBS and incubated with trypsin (1 ml 0.25 % trypsin-EDTA per T75 flask) for 5 min at 37°C. Subsequently, cells were detached by gently tapping against the cell culture flask and 9 ml growth medium (per ml trypsin) was added to inactivate trypsin. Afterwards detached cells were transferred into a 15 ml falcon and centrifuged (800 g, 5 min, 4°C). The cell pellet was resuspended in 10 ml growth medium and distributed on fresh culture flasks.

For transfection 3×10^5 cells per well were seeded in a 6-well plate (10 cm² surface area/well) and cultivated for 24 h until all cells adhered to the surface. On the next day 1.5 ml fresh growth medium was added to each well and the cells were transfected with the help of Lipofectamin[®]2000 transfection reagent (Life Technologies). Lipofectamin is a cationic liposome based transfection reagent that interacts with negatively charged nucleic acids, allowing them to easily pass the cell membrane. It provides high transfection efficiency, high transgene expression in numerous mammalian cell types and at the same time low cytotoxicity.

The following transfection mixture was applied:

Transfection mixture per well:	Incubation
2.5 µg Vector DNA in 150 µl DMEM	5 min, RT
12 µl Lipofectamine [®] 2000 in 150 µl DMEM	5 min, RT
Mix both solutions	10 min, RT

The described transfection mixture was added to each well and after 24 h at 5 % CO₂ and 37°C the medium was replaced by fresh growth medium. Selection of transfected cells by adding the appropriate antibiotic (400 µg/ml G418) to the medium started 48 h after transfection. The vector contained cDNA of DAGL α and a neomycin (G418) resistance cassette.

For long-term storage N2a cells were frozen at -80°C in growth medium containing 10 % DMSO. Therefore a cell pellet from a 70-80 % confluent T75 culture flasks was resuspended in 1 ml freezing medium, slowly frozen (1°C/ min) using Mr.Frosty[™] Freezing Container (Nalgene) at -80°C and stored at -80°C.

2.9 Cultivation and electroporation of *E. coli*

The *E.coli* TOP10 strain was used for molecular cloning experiments. For plasmid isolation bacterial cells were cultured in LB medium (5 ml or 100 ml) containing the

appropriate antibiotic (kanamycin or ampicillin) at 37°C and 180 rpm overnight. In general bacterial cultures were either inoculated with a single-clone picked from an LB agar plate or 1:100 with a pre-culture.

LB medium

H ₂ O		
Tryptone	1	% (w/v)
Yeast extract	0.5	% (w/v)
NaCl	1	% (w/v)
Autoclaved at 121°C, 20 min		
for LB agar add agarose	1.5	% (w/v)

For electroporation electrocompetent *E.coli* TOP10 cells (50 µl) were either incubated with 10 µl ligation reaction, or 1 µl plasmid DNA 5 min on ice and transferred into a pre-cooled electroporation cuvette (GenePulser[®]Cuvette 0.2 cm, Bio-Rad). Subsequently, the cells were electroporated using an electropulser (MicroPulser[™]; program EC2: 2.5 kV, 1 Pulse). Immediately 800 µl antibiotic-free LB medium was added and the cells were transferred into a 2 ml microcentrifuge tube and incubated for 1 h at 37°C. Afterwards 100 µl of the electroporated cells were plated on a LB agar plate containing 100 µg/ml ampicillin or 50 µg/ml kanamycin and incubated overnight at 37°C. On the next day single colonies were picked for further investigations. For long-term storage 500 µl of an overnight culture were added to 500 µl sterile glycerol, gently mixed and stored at -80°C.

2.10 Molecular biology methods

2.10.1 DNA purification and measurement

Plasmid DNA was amplified in *E. coli* TOP10. In order to isolate plasmid DNA, commercially available Mini and Midi kits for plasmid purification were used. For Mini preparation the plasmid DNA isolation protocol provided in the PeqGOLD Plasmid Miniprep Kit I (Peqlab) was used. For Midi preparation, the GeneElute[™] HP Plasmid MidiPrep Kit (Sigma) was utilized according to the manufacturer's instructions.

For mouse genotyping DNA from mice tail biopsies were isolated. Tissue samples were incubated overnight in mouse tail lysis buffer and proteinase K (1 mg/ml) at 45°C on an agitating shaker (550 rpm). Subsequently, the samples were centrifuged (12000 g, 10 min) and the supernatant was transferred into a fresh tube. Adding an equal volume of

isopropanol precipitated the DNA. Afterwards the DNA pellet was twice washed with 70 % ethanol, dried for approximately 10 min at 50°C and dissolved in 100 µl TE buffer.

The concentration of DNA was determined using a spectrophotometer. DNA absorbs ultraviolet light at a wavelength of 260 nm (A_{260}). The absorbance of 1 unit at A_{260} is equivalent to a DNA concentration of 50 µg/ml. The purity of a DNA preparation is assessed by the ratio of absorbance at 260 and 280 nm. A pure DNA preparation exhibits an A_{260}/A_{280} ratio of approximately ≈ 1.8 .

2.10.2 Agarose gel electrophoresis

For separation of DNA fragments from PCR reactions or plasmid restriction digests agarose gel electrophoresis was performed. Therefore 1 % or 1.5 % agarose gels in TAE buffer were poured and run in a TAE buffer containing electrophoresis chamber at 120 V for 50 min. 1 Kb Plus DNA Ladder (Life Technologies) was used for estimating the size of the DNA fragments. For all reactions not performed with the GoTaq® Green Master Mix, the following 6x loading dye was used: 30 % (v/v) glycerol, 0.4 % (w/v) Orange G (Sigma-Aldrich).

DNA fragments in agarose gels were stained with ethidium bromide. Therefore gels were incubated in a 1.5 µg/ml ethidium bromide bath for 10-20 min and stained DNA fragments were detected with a ChemiDoc MP imaging systems at 300 nm.

2.10.3 DNA amplification by PCR/ genotyping

For sequence specific amplification of DNA fragments for molecular cloning and mouse genotyping, polymerase-chain reaction (PCR) was applied. Each PCR reaction was specifically adapted to the temperature requirements of the oligonucleotides and the length of the desired PCR product. GoTaq® Green Master Mix (Promega) was used for all genotyping PCR reactions. The Master Mix contains Taq Polymerase, dNTPs, MgCl₂ and reaction buffer. Established PCR conditions and a list of oligonucleotides are listed below:

1) The amplified mouse Dagla cDNA led to a 3135 bp PCR fragment (Tab. 4):

Table 4: PCR reaction and corresponding program for Dagla cDNA amplification

PCR reaction for the amplification of Dagla cDNA		
Sterile water	34.5 μ l	
pESG-forward Primer: 5'-AGCG GCTCTT CAATGCCCGGGATCGTGGTG -3'	0.5 μ l	
pESG-reverse Primer: 5'-AGCG GCTCTT CTCCCGCGTGCCGAGATGACC -3'	0.5 μ l	
Phusion High Fidelity DNA Polymerase	1 μ l	
Buffer HF (NEB)	10 μ l	
Deoxynucleotide Mix (10 mM, Sigma Aldrich)	1 μ l	
DMSO	1.5 μ l	
pCR-BluntII-TOPO (Dagla cDNA clone) (100-150 ng/ μ l)	1 μ l	
Program		
1 x Initial denaturation	98°C	2 min
30 x Denaturation	98°C	30 s
Annealing	68°C	45 s
Elongation	72°C	2 min
1 x Final elongation	72°C	5 min
Cooling	4°C	∞

2) For the genotyping of the constitutive *Dagla*^{-/-} mice the following PCR strategy was used (Tab. 5):

Table 5: PCR reaction and corresponding program for the genotyping of *Dagla*^{-/-} mice

PCR reaction (20 µl) for <i>Dagla</i> ^{-/-} mice genotyping		
Sterile water		7.5 µl
P1: KO_PCRA_fwd: 5'-TAGCTTAGCCCCCATGTGAC-3'		0.5 µl
P2: KO_PCRA_rev: 5'-CCCAGTAGCCACAGAACCAT-3'		0.5 µl
P3: KO_PCRA_WT_Allel: 5'-GAGATGGGTCCACCTCCTT-3'		0.5 µl
GoTaq® Green Master Mix		10 µl
Mouse tail DNA (100-150 ng/µl)		1 µl
Program		
1 x Initial denaturation	95°C	30 s
30 x Denaturation	95°C	30 s
Annealing	56°C	60 s
Elongation	68°C	60 s
1 x Final elongation	68°C	5 min
Cooling	4°C	∞

The wild type allele led to a PCR product of 404 bp, whereas the knockout allele yielded a 204 bp fragment (Fig. 7).

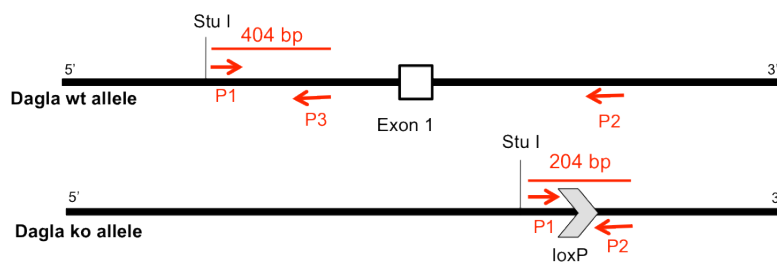


Figure 7: PCR strategy for genotyping of constitutive *Dagla*^{-/-} mice

3) For genotyping of the Syn- and LysM-Dagla^{-/-} mouse lines two PCR reactions were conducted, in which both the loxP sites (Tab. 6) and the presence of the Cre recombinase (Tab. 7) were verified. PCR setups and programs are listed below:

Table 6: PCR reaction and corresponding program for the genotyping of Dagla^{fl/fl} mice

PCR reaction (20 µl) for Dagla ^{fl/fl} (Syn- and LysM-Dagla ^{-/-}) mice genotyping: loxP			
Sterile water		8 µl	
P4: LoxPa_fwd: 5'-CCTCCAGGCCTACAGAA-3'		0.5 µl	
P5: LoxPa_rev: 5'-CACCGGAGAACTGGTTTG-3'		0.5 µl	
GoTaq® Green Master Mix		10 µl	
Mouse tail DNA (100-150 ng/µl)		1 µl	
Program			
1 x Initial denaturation		95°C	30 s
30 x Denaturation		95°C	30 s
Annealing		60°C	60 s
Elongation		68°C	60 s
1 x Final elongation		68°C	5 min
Cooling		4°C	∞

Expected fragment size for the wild type allele was 630 bp. Integration of the loxP sites resulted in a 680 bp DNA-fragment (Fig. 8).

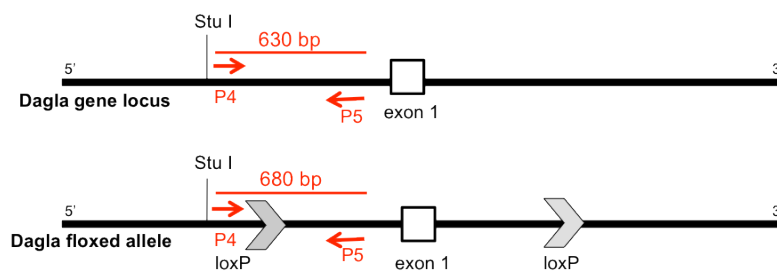


Figure 8: PCR strategy for the genotyping of Dagla^{fl/fl} mice

Table 7: PCR reaction and corresponding program for the genotyping of Syn- and LysM-Dagla^{-/-} mice

PCR reaction (20 µl) for Syn- and LysM-Dagla^{-/-} genotyping: Cre recombinase		
Sterile water	8 µl	
Cre_fwd: 5'-CATTGGGCCAGCTAAACAT-3'	0.5 µl	
Cre_rev: 5'-CCCGGCAAACAGGTAGTTA-3'	0.5 µl	
GoTaq [®] Green Master Mix	10 µl	
Mouse tail DNA (100-150 ng/µl)	1 µl	
Program		
1 x Initial denaturation	94°C	3 min
30 x Denaturation	94°C	30 s
Annealing	62°C	60 s
Elongation	72°C	60 s
1 x Final elongation	72°C	7 min
Cooling	4°C	∞

The presence of Cre led to a 454 bp fragment. The PCR strategy for the verification of the Cre recombinase was similar for both Cre-lines (LysM-Cre and Synapsin1-Cre).

2.10.4 Cloning of the DAGL α expression vector

The Two-TAP Cloning Kit (Iba Lifescience) was used to generate a DAGL α expression vector. This two-step cloning approach allows easy and fast subcloning of the gene of interest into different expression vectors, which provide different promoters and tags. All cloning steps were performed according to the manufacturer's protocol. Initially Dagla cDNA was amplified from mouse cDNA clone (pCR-BluntII-TOPO) using primers containing the *LguI* StarCombinase1[™] recognition site (GCTCTTC) (Chapter 2.10.3) for efficient insertion of the DNA fragment into the pENTRY-IBA51 donor vector. After verifying the integration by a restriction digest with *XbaI* and *HindIII* and sequence analysis (GATC Biotech AG), the Dagla cDNA was subcloned into the final expression vector pESG-IBA-168 containing a c-terminal tandem Strep-tag II and Flag-tag. Subcloning was conducted in a simultaneous restriction and ligation reaction using *Esp3I* endonuclease and T4-DNA ligase (step 2). All cloning steps were performed in *E.coli* TOP cells. The sequence-specific cleavage of DNA was performed with restriction endonucleases in their recommended buffer systems. DNA digestion for analytical purposes was performed with 1 µg DNA for 3 h at 37°C. Detailed cloning steps are listed below:

Step 1: Cloning of Dagla cDNA into pENTRY-IBA51

pENTRY-IBA51 (ca. 5 ng, 1860 bp)	10 μ l
PCR product (0.7 ng/ μ l pro 0.5 kb)	12 μ l
StarSolution M1 (<i>LguI</i> restriction enzyme (5 U/ μ l))	1 μ l
StarSolution M2 (T4-DNA-Ligase (1 U/ μ l))	1 μ l
StarSolution M3 (buffer)	1 μ l

Incubate for 1 h at 30°C

Step 2: Subcloning of Dagla cDNA into pESG-IBA168

pESG-IBA168 (ca. 5 ng, 5497 bp)	10 μ l
pENTRY-IBA51-Dagla (2 ng/ μ l)	12 μ l
StarSolution A1 (<i>Esp3I</i> restriction enzyme (10 U/ μ l))	1 μ l
StarSolution A2 (T4-DNA-Ligase (1 U/ μ l))	1 μ l
StarSolution A3 (buffer + 250 mM DTT + 12.5 mM ATP)	1 μ l

Incubate for 1h at 30°C

2.10.5 RNA purification and measurement

Total RNA from frozen brain tissue was extracted using Trizol[®] Reagent (Life Technologies). Brain tissue was transferred into 2 ml tubes containing 1.4 mm zirconium oxide beads and homogenized in TRizol[®] (100 mg tissue/1 ml TRizol[®]) by vigorous shaking in a tissue homogenizer. After centrifugation (12000 *g*, 10 min 4°C) the homogenate was transferred into a fresh tube and 1-bromo-3-chloropropane (BCP) (1:5) was added. After sustained vortexing for 30 s and 3 min incubation at RT, samples were centrifuged (12000 *g*, 10 min, 4°C) and the RNA containing upper phase was transferred into a fresh tube. Subsequently, the RNA was precipitated with isopropanol (1:1) and washed two times with 75 % EtOH. Finally the RNA was dried for 10 min at 50°C and then dissolved in 20 μ l RNase-free water and stored at -80°C. Purity and RNA concentration were evaluated by optical density measurements at 260 and 280 nm. The absorbance of 1 unit at 260 nm is equivalent to a RNA concentration of 40 μ g/ml.

2.10.6 Reverse transcription polymerase chain reaction

Isolated RNA was transcribed into cDNA by reverse transcription using SuperScript[®] II Reverse Transcriptase and Oligo(dT)₁₂₋₁₈ primers (Life Technologies). As a first step the absolute amount of RNA per sample (1000 ng) was adjusted to a volume of 10 μ l.

Subsequently, 1 μl (0.5 $\mu\text{g}/\mu\text{l}$) of the Oligo(dt)₁₂₋₁₈ primer were added to each reaction. The cDNA synthesis was performed with the following master mix and the described cycling program:

Master Mix per reaction	
Sterile water	1 μl
5 x first strand buffer (Life Technologies)	4 μl
DTT (0.1 M, Life Technologies)	2 μl
Deoxynucleotide Mix (10mM, Sigma-Aldrich)	1 μl

Cycling parameters	
10 μl RNA (200-1000 ng, dissolved in RNase-free water) + 1 μl Oligo(dt) ₁₂₋₁₈ primer	
70°C	10 min
4°C	3 min
Add 8 μl master mix per sample	
42°C	2 min
4°C	3 min
Add 1 μl SuperScript® II Reverse Transcriptase per sample	
42°C	60 min
70°C	15 min
4°C	10 min

The obtained cDNA was adjusted to a concentration of 15 ng/ μl and stored at -20°C.

2.10.7 Real-time reverse transcription PCR (qRT-PCR)

Differences in mRNA expression were determined in triplicate by custom TaqMan® Gene Expression Assays (Applied Biosystems). The TaqMan gene expression analysis is one option for real-time RT-PCR using the FRET (fluorescence resonance energy transfer) technology. FRET is based on an energy transfer between two chromophores. For RT-PCR a short gene-specific oligonucleotide probe, fluorescently labeled at the 5' end (FAM = 6-carboxyfluorescein) and quenched by a non-fluorescent tag (MGB = minor groove binder) at the 3' end, is added to the cDNA sample together with an unlabeled pair of primers. Due to the complementarity the probe hybridizes with the target sequence and is cleaved during the PCR reaction through the 5'→3' exonuclease activity of the polymerase. Thereby the fluorescent signal is no longer quenched and increases with

each PCR cycle proportionally to the amount of available cDNA template. For relative quantification, the expression level of the gene of interest is compared to the expression level of a constitutively expressed housekeeping gene. In this study GAPDH was used as a housekeeping control. Each 10 μ l reaction consisted of 1x TaqMan[®] universal PCR Master Mix (Applied Biosystems, Darmstadt, Germany), 4 μ l cDNA and 1x Custom TaqMan[®] Gene Expression Assay (Tab. 8). Samples were processed in a LightCycler[®] 480 (Roche, Germany) with the following cycling parameters: 95°C for 10 min, 40 cycles at 95°C for 15 s and 60°C for 1 min. Analysis was performed using the LightCycler[®] 480SW Software version 1.5.1 (Roche, Germany) and analyzed with the 2- $\Delta\Delta$ CT method (Livak & Schmittgen 2001).

Table 8: TaqMan[®] Gene Expression Assay ID's and corresponding genes used for gene expression analysis

Target mRNA	Assay ID
BDNF	Mm01334042_m1
CB1 receptor (Cnr1)	Mm00432621_s1
CRH	Mm01293920_s1
CRHR1	Mm00432670_m1
Dagla	Mm00813830_m1
Daglb	Mm00523381_m1
FAAH	Mm00515684_m1
c-FOS (FOS)	Mm00487425_m1
GAPDH	Mm99999915_g1
GR (Nr3c1)	Mm00433832_m1
MAGL (Mgll)	Mm00432621_s1
NAPE-PLD	Mm00724596_m1

2.11 Protein biochemistry

2.11.1 Polyacrylamide gel electrophoresis

Isolated and purified proteins were separated and analyzed via SDS-Polyacrylamide gel electrophoresis (SDS-PAGE). Therefore, 13 μ l of each protein purification step were added to 5 μ l 4x NuPAGE[®] LDS sample buffer and 2 μ l 10x NuPAGE[®] Sample Reducing (500 mM DTT) agent and heated for 10 min at 70°C. Samples were separated on precast NuPAGE[™] Novex[™] 4-12 % Bis-Tris Protein Gels using a protein electrophoresis chamber (200 V, 45 min). NuPAGE[™] MES SDS Running buffer (1x: 50 mM MES, 50 mM

Tris Base, 0.1 % SDS, 1 mM EDTA, pH 7.3) complemented with 0.1 % NuPAGE™ Antioxidants was used as running buffer. All chemicals were purchased from Life Technologies.

In a next step protein gels were either stained with Coomassie Brilliant Blue to visualize all proteins or used for western blotting. Coomassie Brilliant Blue is a commonly used dye to stain proteins. For this staining protein gels were first incubated in the Coomassie staining solution (0.5 g Brilliant Blue R-250, 45 % methanol, 45 % dH₂O, 10 % acetic acid) for 30 min at RT and afterwards destained by changing the destain solution (20 % methanol, 70 % dH₂O, 10 % acetic acid) several times, until the background disappeared and only the protein bands were visible.

2.11.2 Western Blot

Western blotting was used to identify specific proteins. Therefore, proteins were first separated via polyacrylamide gel electrophoresis (Chapter 2.11.1) and were transferred to a PVDF (polyvinylidene difluoride) membrane (iBlot® 2 Transfer Stacks, PVDF; Life Technologies) using the iBlot® Gel Transfer Device. Subsequently, the membrane was blocked with 5 % BSA or skim milk powder in TBS-T (TBS containing 0.1 % Tween-20) for 1 h at RT and overnight incubated at 4°C with anti-DAGL α (1:500, DGL α -Rb-Af380) or anti-FLAG (1:500, F7425) antibody diluted in 5 % BSA in TBS. On the next day, the membrane was washed three times in TBS-T and incubated with a horseradish peroxidase-conjugated secondary antibody diluted in 5 % BSA in TBS-T (1:10000, donkey anti-rabbit-HRP, Dianova) for 2 h at RT. After washing the membrane 3 times with TBS-T for 5 min at RT, 1 ml ECL substrate (Pierce) was added to the blot and proteins were directly detected with the ChemiDoc MP imaging systems. Enhanced chemiluminescence (ECL) is a method that provides highly precise detection of proteins. In this chemiluminescent reaction the horseradish peroxidase catalyzes the oxidation of luminol into a light-emitting reagent.

2.11.3 Tandem affinity purification

Tandem affinity purification (TAP) is a purification strategy for the efficient isolation of native protein complexes. In this study a Strep-Flag-TAP (SF-TAP) was conducted. Therefore, the DAGL α protein was C-terminal tagged with a tandem Strep-tag II followed by a single Flag-tag using the pESG-IBA168 expression vector. Both protein-tags have a medium affinity and avidity to their immobilized binding partners, allowing an elution of the

SF-tagged protein under native conditions. The Strep-tag consists of 8 amino acids (Trp-Ser-His-Pro-Gln-Phe-Glu-Lys) and is capable of binding into the biotin-pocket of streptavidin. Bound proteins were eluted with desthiobiotin having a strikingly greater affinity to streptavidin than the Strep-tag. Biotin and streptavidin form one of the strongest non-covalent interactions in nature. In addition, previous studies showed that a tandem Strep-tag unlike a single Strep-tag increases the purification yield (Junttila et al. 2005). The Flag-tag consists of 8 amino acids (Asp-Tyr-Lys-Asp-Asp-Asp-Asp-Lys) and binds to the anti-FLAG antibody, which is covalently attached to agarose. The FLAG octapeptide was used to elute bound proteins (Fig. 9). The detailed purification protocol is described below.

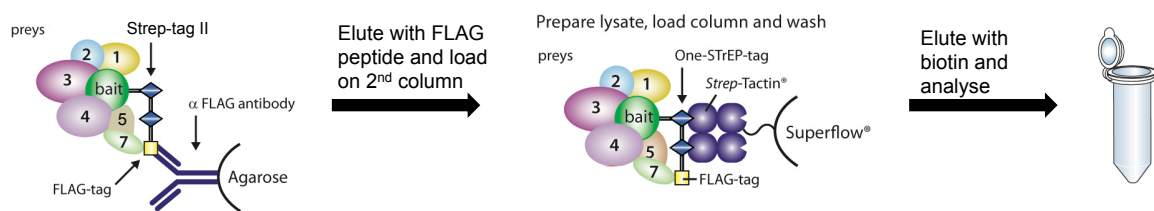


Figure 9: Principal of tandem affinity purification using Strep-tag II and Flag-tag (adopted from IBA Lifescience)

Tagged DAGL α protein was overexpressed in Neuro-2a cells. To purify DAGL α and bound proteins a cell pellet from two T175 cell culture flasks of 80-90 % confluent N2a cells (approximately 5×10^7 cells) was dissolved in 500 μ l RIPA buffer containing one cComplete™ Mini protease inhibitor cocktail tablet (Roche) per 10 ml RIPA buffer and incubated for 30 min on ice. Subsequently, disrupted cells were centrifuged (10000 g, 10 min, 4°C) and the supernatant was used for TAP. The order of the two purification steps was essential for the amount of purified protein and the highest yields were obtained if the FLAG purification step was followed by the Strep purification. First 90 μ l Anti-FLAG®M2 affinity gel (Sigma-Aldrich) together with 100 μ l TBS were added to a Spin Column with a polyethylene filter (~30 μ m pore size, Pierce) and equilibrated 2 x 250 μ l with RIPA buffer and shortly centrifuged (100 g, 5 s). Subsequently, the cell lysate was added to the column and incubated in an overhead-tumbler for 1h at 4°C to guarantee optimal binding of the tagged protein to the matrix. All following steps were conducted at RT and via gravity-flow instead of centrifugation. In a next step, the affinity gel was washed once with 500 μ l TBS containing 0.2 % Nonidet-P40 and twice with 500 μ l TBS. To elute the bound proteins 2 x 200 μ l elution buffer (TBS + 200 μ g/ml FLAG®Peptide, Sigma-Aldrich) was added to the column and each time incubated for 10 min at RT. During incubation the column was properly closed and inverted several times. The eluates (E1, E2) were collected, combined and further used for the Strep-tag purification system.

Therefore, 100 μ l Strep-Tactin[®]Superflow[®] suspension was added to a Spin Column (described above) and 3 times washed with 500 μ l TBS (100 g, 5 s). Subsequently, the eluate from the Flag purification was added to the column and incubated in an overhead-tumbler for 1 h at 4°C. Afterwards the column was washed 3 times with buffer W (100 mM Tris-HCl pH 8.0, 150 mM NaCl, 1 mM EDTA; Iba Lifescience). All following steps were again conducted at RT and via gravity-flow instead of centrifugation. To elute all bound proteins 2 x 200 μ l elution buffer E (100 mM Tris-HCl pH 8.0, 150 mM NaCl, 1 mM EDTA, 2.5 mM desthiobiotin; Iba Lifescience) was added to the column and each time incubated for 10 min at RT. During the incubation time the column was frequently inverted. The eluates were collected, combined and 4x concentrated with 3K centrifugal filters (Amicon Ultra-0.5 ml; Merck Millipore) to a volume of 100 μ l. Concentrated purified proteins were stored in 50 % glycerol at -20°C. Samples (10-20 μ l) were taken from all purification steps and used for polyacrylamide gel electrophoresis and western blot analysis.

2.11.4 MALDI-TOF/TOF mass spectrometry

Matrix Associated Laser Desorption Ionization (MALDI) coupled to time of flight (TOF) analyzers have been successfully applied to determine the mass of proteins, peptides and polymers. In addition, TOF/TOF is a tandem mass spectrometry method where two time-of-flight mass spectrometers are used consecutively. MALDI-TOF/TOF mass spectrometry gives a specific peptide map when proteins are digested with specific enzymes like trypsin. This peptide maps can be used to identify proteins via existing databases. In this study MALDI-TOF/TOF was used to identify potential interaction partners of DAGL α . Therefore, TAP- and Flag-purified proteins (see 1.11.3) were first electrophoretic separated on precast NuPAGE[™] Novex[™] 4-12% Bis-Tris Protein Gels. Precast gels were run for approximately 2.5 cm and stained with Coomassie Brilliant Blue to label all proteins. Subsequently, gels were destained until the background was completely gone and the protein bands were only stained faintly. All following steps, MALDI analysis and protein identification, were conducted in cooperation with Dr. Marc Sylvester at the Institute of Biochemistry and Molecular Biology (AG Prof. Dr. Volkmar Gieselmann, University of Bonn). Polyacrylamide gels were cut in 6 pieces per lane followed by a complex procedure in which proteins were reduced, alkylated and digested. These samples are mixed with a suitable matrix solution and spotted onto a metal plate. During MALDI analysis a pulsed laser irradiates the sample, leading to ionization of the sample molecules. These ions are analyzed in a TOF/TOF tandem mass spectrometer. The time of ion flight through the electromagnetic fields differs according to the mass-to-charge ratio (m/z) value of the ion. Finally, mass spectra from major peptide ions are obtained and compared to databases to identify all proteins in the sample.

2.12 Click chemistry

2.12.1 *In vitro* assays

Analysis of DAGL α activity was assessed by *in vitro* assays using a labeled substrate (synthesized and kindly provided by Prof. C. Thiele, LIMES Life and Medical Sciences Institute, University of Bonn). The two applied substrates are diacylglycerols (DAGs) with a labeled palmitic acid in the *sn*-1 position (1-palmitoyl-2-linoyl-*sn*-glycerol and 1-palmitoyl-2-arachidonoyl-*sn*-glycerol; Fig. 10). The labeling consists of a terminal c-c triple bond, which is not present in any natural occurring fatty acid. After the extraction of lipids the terminal alkyne could be easily labeled via the so-called click-reaction with a fluorogenic dye and separated via thin layer chromatography (TLC). Subsequently, clicked fatty acids were detected by fluorescence imaging (described in detail in Chapter 2.12.2 and 2.12.3).

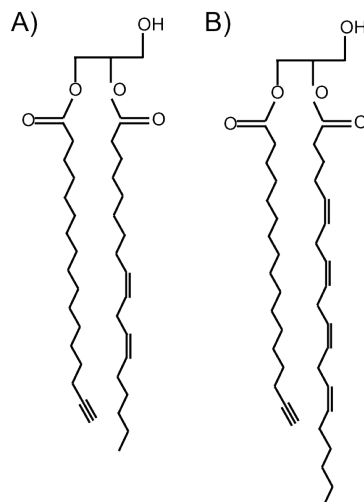


Figure 10: The labeled DAGL α substrates: A) 1-palmitoyl-2-linoyl-*sn*-glycerol and B) 1-palmitoyl-2-arachidonoyl-*sn*-glycerol

In vitro assays were performed with cell cultures or lysates of WT and Dagla^{-/-} macrophages (BMM) and SF-TAP purified DAGL α . For the experiments in cell culture 25 μ M or 50 μ M of the substrate (1-palmitoyl-2-linoyl-*sn*-glycerol, stock: 4.9 mM in trifluoroacetic acid) were added to the growth medium of WT and Dagla^{-/-} BMM (5×10^5 cells/ well in a 6-well plate) and after 24 h lipids were extracted. Therefore cells were washed twice with 1 ml PBS followed by lipid extraction with 500 μ l MeOH/CHCl₃ (5/1) per well by vigorously shaking for 30 s. Subsequently, the MeOH/CHCl₃ mix was transferred into a microcentrifuge tube and 100 μ l CHCl₃ were added. The lipid fraction was used directly for TLC analysis (Chapter 2.12.2) or stored at -20°C.

The *in vitro* assays with cell lysates were performed as follows: First macrophages were seeded 24 h before the experiment in a density of 5×10^5 cells/ well in a 6-well plate.

On the following day, cells were harvested by trypsination and subsequent centrifugation (1200 g, 10 min, 4°C). Cells were washed in sterile PBS and centrifuged again. Afterwards, cell pellets (each 5×10^5 cells) were resuspended in 100 µl assay buffer (50mM Tris/HCl pH 7.0, 0.1 % Triton X-100) and disrupted by repeated (10x) pipetting through a 27-gauge needle. Cell Lysates were centrifuged (800 g, 5 min, 4°C) again and the supernatant was transferred into a new microcentrifuge tube. For the *in vitro* assay cell lysates were incubated with 50 µM substrate for 0 min, 10 min, 30 min, 120 min or 180 min at 37°C. Subsequently, lipids were extracted by adding 2 x 2 volumes (200 µl each) of MeOH/CHCl₃ (1/1). The lower MeOH/CHCl₃ phase containing the lipid fraction was stored at -20°C until further analysis.

For *in vitro* assays with tagged DAGLα 10 µl concentrated TAP or Flag purified DAGLα (in 50 % glycerol) was added to 90 µl assay buffer (50mM Tris/HCl pH 7.0, 0.1 % Triton X-100) and incubated with 50 µM substrate for 0 min, 10 min, 30 min or 120 min at 37°C. Lipid extraction and storage was performed as described above.

2.12.2 Lipid isolation and click reaction

Lipids from *in vitro* assays or cell cultures were isolated with MeOH/CHCl₃ (5/1 or 1/1) and stored at -20°C. Before TLC analysis was performed, the fatty acids were further extracted and clicked. Therefore the lipid fraction (400 µl for *in vitro* assays and 600 µl for cell culture experiments) was first centrifuged (12000 g, 30 s) and the supernatant was transferred into a fresh 2 ml microcentrifuge tube. To acetify the solution 400 µl H₂O containing 1 % acetic acid was added, vigorously shaken and centrifuged as above. The lower phase from the two phase mixture containing the fatty acids was collected and evaporated in a speed vac for 10 min at 45°C. Subsequently, 7 µl CHCl₃ were added per sample and samples were 3 times vortexed for 2 min and in between centrifuged as above. Afterwards 30 µl coumarin labeling solution (clickmix: 850 µl Ethanol, 50 µl 10 mM Cu(I)TFB in acetonitrile 10 µl 2 mg/ml Azidocoumarin in EtOH) was added and samples were incubated for 3 h at 43°C. In parallel 7 µl of each standard (50 µM CHCl₃) were also mixed with 30 µl clickmix, incubated as above and hereafter treated as the other samples. Following the click-reaction, 30 µl CHCl₃ was added and samples/standards were vortexed for 2 min, sonicated for 5 min in an ultrasonic bath and again 3 times vortexed for 2 min and centrifuged as above. Ten µl of each sample and standard were applied onto silica gel TLC plates (Chapter 2.12.3).

2.12.3 Thin layer chromatographie (TLC)

Thin layer chromatographie (TLC) is a method used to separate the components of a mixture using a thin stationary phase. In this study, silica gel 60 plates (Merck) with silica gel, a granular, porous form of silicon oxide, as the stationary phase were used. First, 10 μ l of each sample or standard were carefully applied onto the TLC-plates with a small glass capillary. After the samples were completely dried the TLC plates were run in a saturated chamber containing $\text{CHCl}_3/\text{MeOH}/\text{H}_2\text{O}/\text{acetic acid}$ (65/25/4/1) for 10 cm (above the start zone). Subsequently, the plates were dried and run in isohexane/ethyl acetate (1/1) to the upper edge of the plate and again dried. To ensure that all coumarin dye molecules are in the strongly fluorescent deprotonated form, the plates were shortly soaked in *N,N*-diisopropylethylamine (Hünigs base). Immediately the coumarin signal was detected using a high sensitivity Electron-Multiplying CCD (EMCCD) camera, equipped with a 494/20 and 572/28 bandpass emission filter wheel, which is part of the imaging system. Labeled fatty acids were detected using a series of exposures (420 nm, LED lamp) with detection at 494 and 572 nm. In the described makro (provided by Prof. C.Thiele, LIMES Life and Medical Sciences Institute, University of Bonn; Thiele et al., 2012) 8 pictures with each of the two filters with exposure times between 20 ms and 5 s were taken resulting in a total of 16 images. Intensities of individual bands of labeled fatty acid were quantified using ImageJ densitometry software, and expressed relative to the substrate signal, as a measure of fatty acid relative abundance in the different samples.

2.13 Statistical analysis

Data are presented as means \pm SEM and the numbers of samples are indicated in the individual figures. Statistical significance was assessed by Students t-Test, Mann-Whitney U test or two-way ANOVA with Bonferroni's post-hoc test. Significance level was set at $p < 0.05$. GraphPad Prism software (Version 5.0d, GraphPad Software Inc.) was used for the analysis of behavioral data.

Results

3.1 Behavioral and molecular analysis of $Dagla^{-/-}$ mice

The following section outlines the behavioral and molecular analysis of constitutive $Dagla$ deficient mice. $Dagla^{-/-}$ mice were tested in different anxiety- and depression-related behavioral tests to reveal the impact of DAGL α in the regulation of mood and emotion. All anxiety- and depression-related behavioral experiments (Chapter 3.1.3, 3.1.4) were performed at least twice with different cohorts of animals. All animals were tested in a battery of behavioral tests always starting with the least stressful one. In all cases, first a sucrose preference test, followed by an open-field, social preference, light-dark test and forced swim test were performed, or alternatively open-field, zero-maze and forced swim test. The tests were performed in weekly intervals. Another cohort of animals was housed in a room with an inverse light-dark cycle and tested for home cage activity. If not stated otherwise, all behavioral experiments were performed with mixed-gender groups.

3.1.1 Endocannabinoid measurements and gene expression analysis

Constitutive $Dagla^{-/-}$ mice were generated by crossing homozygous $Dagla$ floxed ($Dagla^{fl/fl}$) mice on a C57BL/6J genetic background with P $gk1$ -Cre mice (Ternes 2013; Jenniches et al. 2015), a transgenic mouse line expressing Cre ubiquitously (Lallemand et al. 1998). Therefore, either wild type C57BL/6J (WT) or $Dagla^{fl/fl}$ mice are adequate control animals. In the following part of the results WT mice were used as controls. However, to exclude that loxP sites might influence gene expression, mRNA levels of ECS related genes of $Dagla^{-/-}$, WT and $Dagla^{fl/fl}$ mice were compared.

Gene expression analysis showed similar expression levels of $Dagla$ and other ECS related genes in $Dagla^{fl/fl}$ mice and WT controls (Fig. 11A). In addition, relative quantification of whole mRNA revealed a complete loss of $Dagla$ transcript in brain tissue of $Dagla^{-/-}$ mice ($t = 11.75$, $p < 0.0001$; Fig. 11A) using a probe which spans the exon junction between exon 8 and 9, as already shown in previous studies (Ternes 2013). The deletion of DAGL α protein was validated by immunohistochemistry staining of cryofixed brain slices. Staining was completely lost in $Dagla^{-/-}$ tissue (Fig. 11B).

Since DAGL α is the main synthesizing enzyme of 2-AG in the adult brain, the measurements of endocannabinoids (eCB) is an important indicator for the knockout of

Dagla and the analysis of possible compensatory mechanisms. Measurements were performed by Dr. Laura Bindila (Work group of Prof. Dr. Beat Lutz, Institute of Physiological Chemistry, Johannes Gutenberg University Medical Center, Mainz). Results showed a 80-90 % reduction of 2-AG levels in cortex, hippocampus, striatum (genotype: $F_{(1,23)} = 124.4$, $p < 0.0001$) and amygdala ($t = 17.69$, $p < 0.0001$) of $Dagla^{-/-}$ mice (Fig. 11C). 2-AG content was unchanged in $Dagla^{fl/fl}$ compared to WT controls ($t = 1.558$, $p = ns$; Fig. 11D), showing that the insertion of the loxP sites did not influence the activity of DAGL α . Furthermore, a significantly reduced level of anandamide in cortex, hippocampus (genotype: $F_{(1,23)} = 23.63$, $p < 0.0001$) and amygdala ($t = 3.308$, $p < 0.01$) of $Dagla^{-/-}$ mice (Fig. 11E) was discovered. This reduction seemed to be brain region-dependent, because anandamide levels in the striatum did not differ between genotypes ($t = 0.6376$, $p = ns$). In contrast, arachidonic acid (AA) content, the main metabolite of 2-AG, was unaffected in most of the analyzed brain areas. Only amygdalar AA was significantly reduced in $Dagla^{-/-}$ mice ($t = 11.20$, $p < 0.0001$; Fig. 11F).

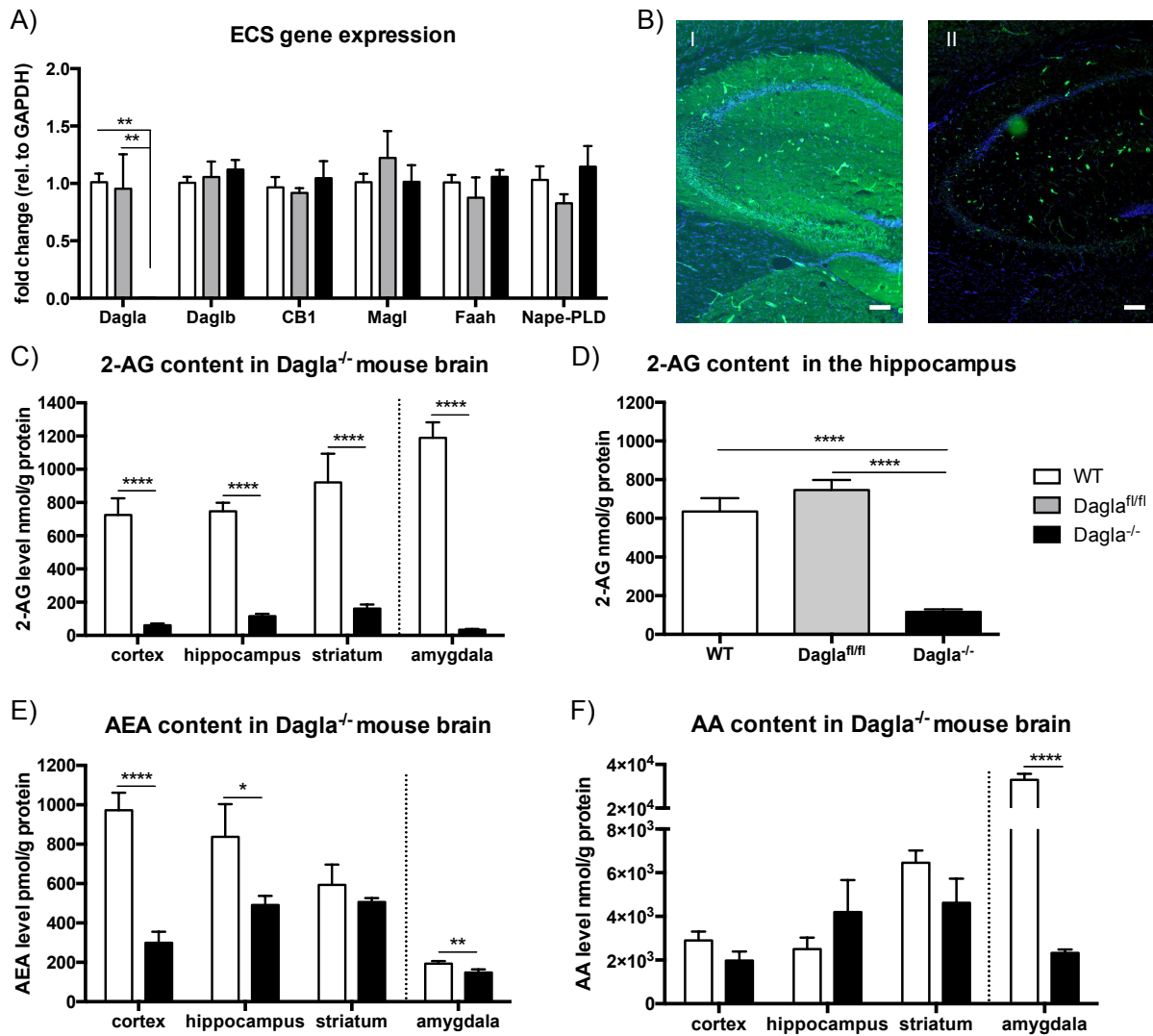


Figure 11: Validation of *Dagla*^{-/-} mice and endocannabinoid (eCB) measurement. (A) Shown are mRNA levels normalized to GAPDH. Real-time RT-PCR results show a complete loss of *Dagla* mRNA transcript in *Dagla*^{-/-} mice (two-way ANOVA, Bonferroni's post-hoc test, values represent mean \pm SEM: $n = 5$ animals/group, **** $p < 0.0001$). (B) Representative DAGL α immunostainings of (I) wild type and (II) *Dagla*^{-/-} mice hippocampi. Staining is completely absent in *Dagla*^{-/-} (scale: 100 μ m) (C) 2-AG levels are significantly decreased (by 80-90%) in cortex, hippocampus, striatum and amygdala of *Dagla*^{-/-} mice. (D) Similar 2-AG levels were observed in *Dagla*^{fl/fl} mice and WT controls. (E) Anandamide (AEA) levels were decreased in cortex by 60%, hippocampus by 30% and amygdala by 25%, but not in the striatum of *Dagla*^{-/-} mice. (F) Arachidonic acid (AA) content was significantly reduced in the amygdala, but not changed in cortex, hippocampus and striatum of *Dagla*^{-/-} mice. Please note that the amount of 2-AG, AEA and AA in the amygdala was measured in a separate experiment. Statistical analysis for eCB measurement in cortex, hippocampus and striatum: two-way ANOVA, Bonferroni's post-hoc test, values represent mean \pm SEM: $n = 5$ animals/group, * $p < 0.05$, ** $p < 0.01$, **** $p < 0.0001$. Statistical analysis for eCB measurement in amygdala samples: Student's t-test, values represent mean \pm SEM: $n = 10$ animals/group, ** $p < 0.01$, **** $p < 0.0001$ (modified from Jenniches et al. 2015).

Subsequent to the molecular analysis of *Dagla*^{-/-} mice, the animals were subjected to a variety of different behavioral tests. Initially, the animals were analyzed in a tetrad test to assess CB1 receptor-mediated effects.

3.1.2 Tetrad test

The tetrad test is widely used to analyze cannabinoid receptor (CB1)-mediated behavioral effects in rodents. Treatment with THC leads to decreased locomotor activity, decreased body temperature and analgesia in WT animals (Little et al. 1988). The tetrad test was conducted once with 4-5 animals per group to analyze CB1 mediated-effects and reveal potential changes of CB1 signaling in *Dagla*^{-/-} mice.

THC treatment (8 mg/kg) led to a similar reduction of body temperature in WT and *Dagla*^{-/-} mice (treatment effect: $F_{(1,15)} = 22.77$, $p < 0.001$; genotype effect: $F_{(1,15)} = 0.4895$, $p = \text{ns}$; Fig. 12A). Furthermore, *Dagla*^{-/-} mice and WT showed a delayed pain response in the hot plate test after THC treatment ($F_{(1,16)} = 15.62$; $p < 0.01$; Fig. 12B). This analgesic effect of THC did not differ between genotypes ($F_{(1,16)} = 2.917$; $p = \text{ns}$; Fig. 12B). In addition, THC treatment led to a reduced locomotor activity in the open-field test, as seen in a significantly reduced distance travelled ($F_{(1,16)} = 46.83$, $p < 0.0001$; Fig. 12C), and reduced rearings in both genotypes ($F_{(1,15)} = 171.5$, $p < 0.0001$; Fig. 12D). However, vehicle treated *Dagla*^{-/-} mice had a overall reduced locomotor activity including reductions in distance travelled ($F_{(1,16)} = 4.850$, $p < 0.05$; Fig. 12C) and rearings ($F_{(1,15)} = 11.34$, $p < 0.01$; Fig. 12D).

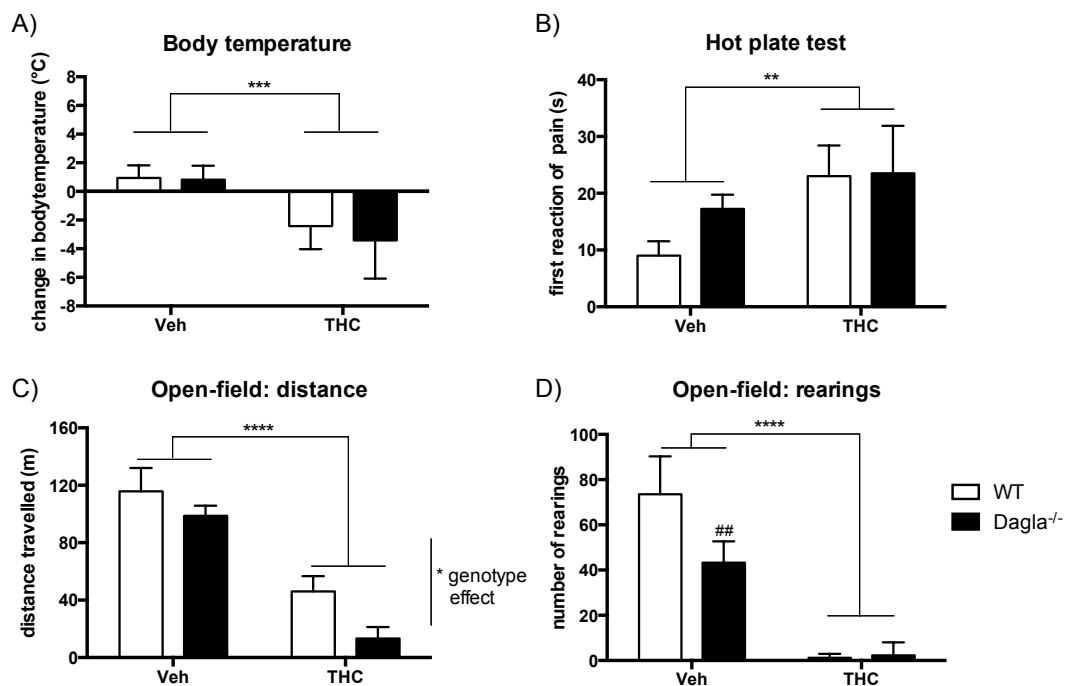


Figure 12: Tetrad test of *Dagla*^{-/-} mice. (A) THC treatment (8 mg/kg) significantly reduced body temperature of *Dagla*^{-/-} mice and WT controls. (B) Furthermore, THC had a similar analgesic effect in both genotypes, leading to a delayed pain response in the hot plate test. (C) THC treatment led to a significantly reduced distance travelled in *Dagla*^{-/-} mice and WT controls. However, *Dagla*^{-/-} mice had a generally reduced locomotor activity (genotype effect: * $p < 0.05$). (D) Treatment with THC also reduced rearings in both genotypes. In addition, significantly decreased number of rearings was found in vehicle treated *Dagla*^{-/-} mice (## $p < 0.01$). Statistical analysis: two-way ANOVA, Bonferroni's post-hoc test, values represent mean \pm SEM: $n = 4-5$ animals/group, * $p < 0.05$, ** $p < 0.01$, *** $p < 0.001$, **** $p < 0.0001$, ## $p < 0.01$.

In conclusion, THC treatment resulted in similar behavioral changes in *Dagla*^{-/-} and WT mice. Thus, lack of *Dagla* did not influence CB1 receptor-mediated effects of THC.

3.1.3 Maternal behavior and body weight

Mice lacking *Dagla* are viable and fertile, but if nests were disturbed, for instance after cage changes, *Dagla*^{-/-} mice often neglected their offspring. It is considered to be highly characteristic for rodents to retrieve pups, if they are absent from the nest. Therefore, maternal behavior was analyzed in the pup retrieval test. Indeed, *Dagla*^{-/-} mice needed significantly more time to recollect the pups from the opposite corner of the home cage into the nest compared to WT controls, indicating a decreased maternal care behavior ($U = 8.00$, $p < 0.05$; Fig. 13A). In addition, one of the tested *Dagla*^{-/-} dams did not retrieve their pups at all and two dams only retrieved one or two out of three pups during the test period of 300 s. On the other hand, the percentage of pups from each litter of tested dams with visible milk spots did not differ between genotypes ($t = 0.8044$, $p = \text{ns}$; Fig. 13B).

In line with these results, nursing behavior ($t = 1.21$, $p = \text{ns}$; Fig. 13C) and interaction time with the offspring ($t = 1.259$, $p = \text{ns}$; Fig. 13D) were not affected in *Dagla*^{-/-} mice. For the analysis of maternal care, the behavior of nursing female mice was recorded using a time-sampling procedure (20 sec observation every third minute for 1 h between 9 AM and 10 AM on postnatal days 2–7), resulting in 21 observations of each dam per day. Pup retrieval and maternal care behavior was assessed in different cohorts. Compatible with the described results, no significant differences in the body weight of *Dagla*^{-/-} pups compared to age matched control mice were observed ($F_{(1,12)} = 0.9201$, $p = \text{ns}$; Fig. 13E), which strongly supports that nursing behavior was unchanged. However, after weaning (at the age of 3 weeks) the body weight of *Dagla*^{-/-} mice was significantly reduced compared to WT controls (male mice: $F_{(1,26)} = 20.9$, $p < 0.001$; female mice: $F_{(1,22)} = 128.6$, $p < 0.0001$; Fig. 13F,G).

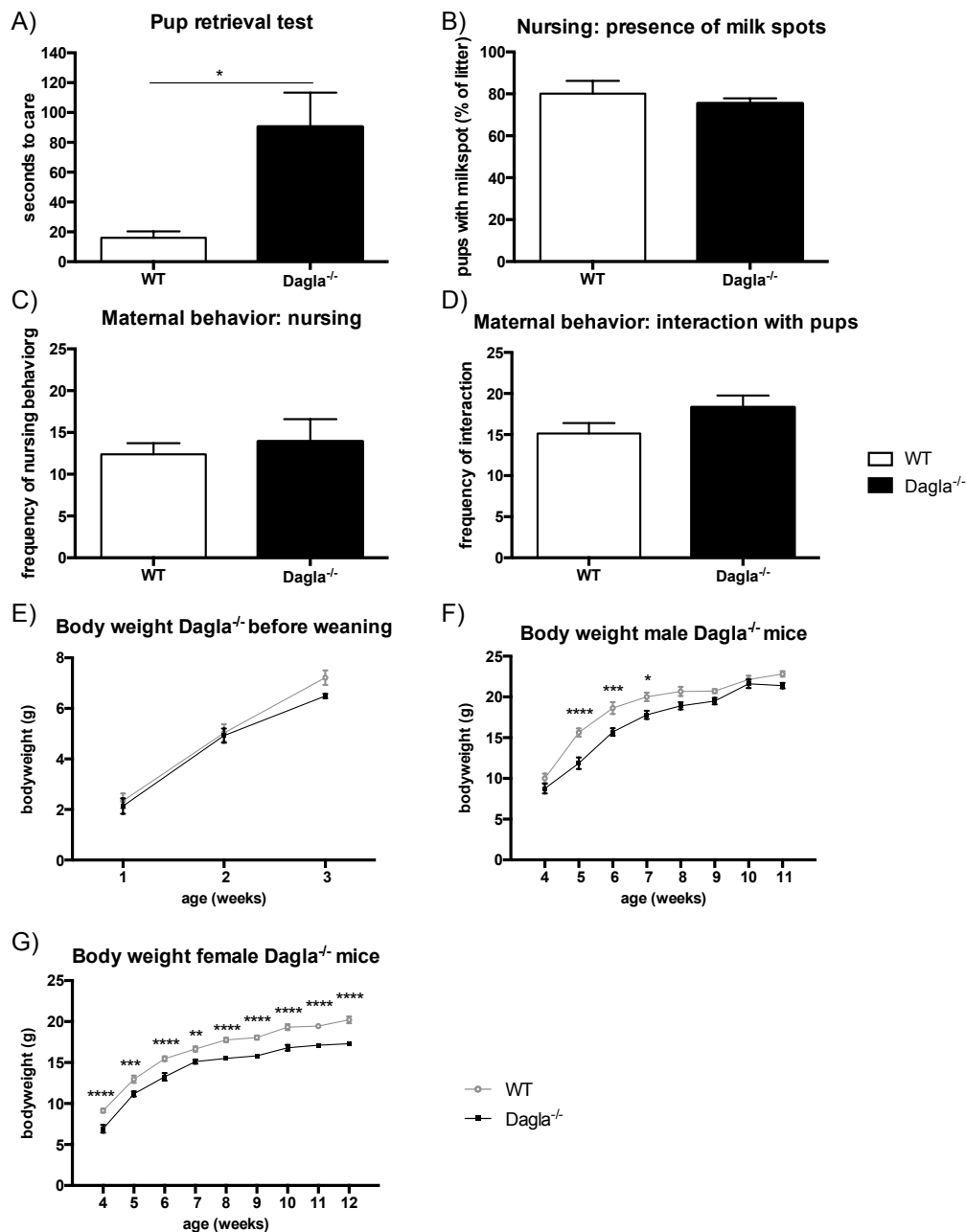


Figure 13: Dagla^{-/-} mice showed a deficit in maternal care and reduced body weight. (A) Dagla^{-/-} mice showed decreased maternal care compared to WT controls in the pup retrieval test. The latency in seconds was recorded to sniff the pups and retrieve them to the nest (Mann-Whitney U test, values represent mean \pm SEM: n = 7 mice/group, *p < 0.05). (B) However, percentage of pups with milk spots per litter did not differ between genotypes (Student's t-test, values represent mean \pm SEM: n = 5-7 litter, p = ns). (C) Nursing behavior as a measure of maternal care did not differ between Dagla^{-/-} and WT control mice. Shown is the mean number of observations of nursing behavior during observation period (Student's t-test, values represent mean \pm SEM: n = 4-7 dams, p = ns). (D) Interaction of moms with pups was similar for both genotypes. Shown is the mean number of observations of interaction with pups during observation period (Student's t-test, values represent mean \pm SEM: n = 4-7 dams, p = ns). (E) Body weights of Dagla^{-/-} and WT controls before weaning did not differ between the genotypes (two-way ANOVA with repeated measurements, Bonferroni's post-hoc test, values represent mean \pm SEM: n = 7 animals/group). (F, G) However, body weights of adolescent and adult male (F: n = 12 animals/group) and female (G: n = 14 animals/group) Dagla^{-/-} mice were significantly reduced. Please note that the SEM was very small for some data points, thus resulting in very small error bars (two-way ANOVA with repeated measurements, Bonferroni's post-hoc test, values represent mean \pm SEM: **p < 0.01, ***p < 0.001, ****p < 0.0001) (modified from Jenniches et al. 2015).

To determine if the deficit in maternal care reflects a general disturbance of social behavior, a social preference test was performed (Fig. 14A,B). WT and Dagla^{-/-} mice

displayed a similar ratio of the time spent with the partner mouse was compared to the empty cage ($t = 0.4321$, $p = \text{ns}$; Fig. 14A). The time spent with the gender-matched partner mouse was significantly higher compared to the empty cage in both genotypes ($F_{(1,36)} = 51.27$, $p < 0.0001$; Fig. 14B), indicative of a normal sociability in both genotypes.

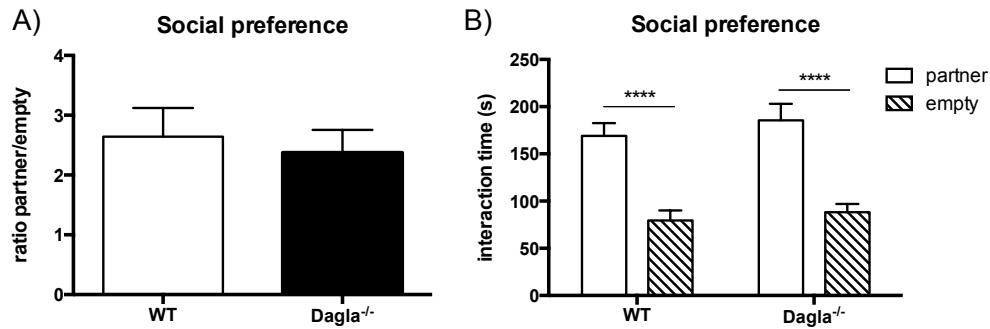


Figure 14: Dagla^{-/-} mice displayed normal sociability. (A) Dagla^{-/-} mice showed the same social preference like WT controls. The ratio between the time spent with a partner to time spent with an empty cage did not differ between genotypes (Student's t-test, values represent mean ± SEM: $n = 10$ animals/group, $p = \text{ns}$). (B) Preference for the partner mouse was significantly higher in both genotypes (two-way ANOVA, Bonferroni's post-hoc test, values represent mean ± SEM: $n = 10$ animals/group, **** $p < 0.0001$) (modified from Jenniches et al. 2015).

3.1.4 Analysis of anxiety-related behavior

To reveal potential effects of Dagla knockout on anxiety-related behavior, several tests were performed. First, anxiety-like behavior and locomotion was analyzed in the open-field test, where the time spent in the center of the open-field box is inversely correlated to the state of anxiety (Gould et al. 2009). Data are presented as distance travelled (Fig. 15A) and time spent in the center (Fig. 15B) over time in 10-min bouts. The total distance travelled was similar in Dagla^{-/-} and WT mice ($F_{(1,23)} = 1.986$, $p = \text{ns}$; Fig. 15A). In addition, the distance travelled decreased during the test session (between the 10-min bouts) in both genotypes due to habituation to the novel environment, revealing a significant main effect for time ($F_{(2,46)} = 35.93$, $p < 0.0001$; Fig. 15A). However, Dagla^{-/-} mice spent less time exploring the center of the open-field compared to WT controls (genotype effect: $F_{(1,20)} = 5.751$, $p < 0.05$; Fig. 15B). These results indicate that exploratory behavior and locomotor activity was not affected by the deletion of Dagla, whereas anxiety levels were slightly elevated in Dagla^{-/-} mice.

Anxiety-like behavior was further analyzed in the light/dark box test (Fig. 15C-G). In this test the time spent in the dark area is correlated to the state of anxiety. Furthermore, delayed first entries into the light area and less transitions between the two areas are measures of anxiety. The time spent in the dark area ($F_{(1,36)} = 0.0000005$, $p = \text{ns}$; Fig. 15C), distance travelled in both compartments ($F_{(1,36)} = 2.830$, $p = \text{ns}$; Fig. 15D) and the first entry into the light area did not differ between genotypes ($t = 0.4582$, $p = \text{ns}$; Fig. 15E). However, the

number of transitions between the two areas was significantly decreased for $Dagla^{-/-}$ mice ($t = 2.708$, $p < 0.05$; Fig. 15F), indicating a slightly increased anxiety-like behavior in $Dagla^{-/-}$ mice. Furthermore, $Dagla^{-/-}$ mice showed a decreased number of rearings in both areas (genotype: $F_{(1,36)} = 21.18$, $p < 0.0001$; Fig. 15G). Reduced frequencies of rearing are correlated with reduced exploratory behavior and increased anxiety.

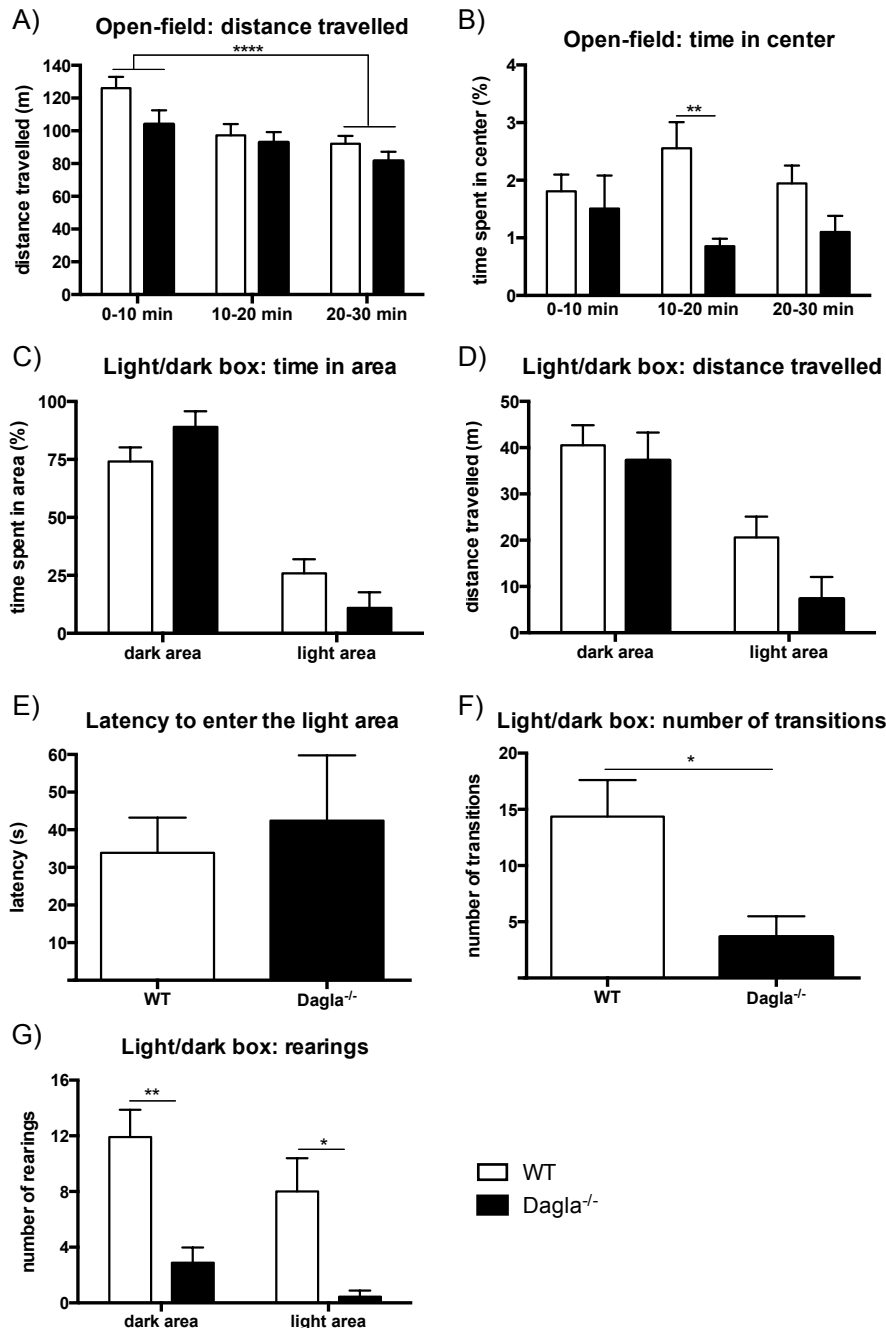


Figure 15: $Dagla^{-/-}$ mice showed slightly increased anxiety-like behavior. (A,B) Exploratory and anxiety-related behavior was analyzed in the open-field test. (A) No significant genotype differences in total distance travelled were observed (two-way ANOVA, Bonferroni's post-hoc test, values represent mean \pm SEM: $n = 11$ animals/group, $p = ns$). (B) $Dagla^{-/-}$ spent less time exploring the center and therefore displayed an anxiety-like phenotype (two-way ANOVA, Bonferroni's post-hoc test, values represent mean \pm SEM: $n = 11$ animals/group, * $p < 0.05$, ** $p < 0.01$). (C-G) Anxiety-behavior was further analyzed in the light/dark box test. (C) Time spent in the dark area did not differ between genotypes (two-way ANOVA, Bonferroni's post-hoc test, values represent mean \pm SEM: $n = 9-11$ animals/group, $p = ns$). (D) $Dagla^{-/-}$ and WT mice showed a similar distance travelled in both

areas (two-way ANOVA, Bonferroni's post-hoc test, values represent mean \pm SEM: $n = 9-11$ animals/group, $p = ns$). (E) The latency to first enter the light area was similar in both genotypes (Student's t -test, values represent mean \pm SEM: $n = 9-11$ animals/group, $p = ns$). (F) However, number of transitions between both areas was significantly decreased for $Dagla^{-/-}$ mice compared to WT controls (Student's t -test, values represent mean \pm SEM: $n = 9-11$ animals/group, $*p < 0.05$). (G) The number of rearings in both areas was significantly decreased in $Dagla^{-/-}$ mice compared to WT controls (two-way ANOVA, Bonferroni's post-hoc test, values represent mean \pm SEM: $n = 9-11$ animals/group, $*p < 0.05$, $**p < 0.01$) (modified from Jenniches et al. 2015).

Anxiety-like behavior was further analyzed in the zero-maze test, where time spent in the open areas is negatively correlated with the state of anxiety (Shepherd et al. 1994). A similar time spent in the open area was observed for $Dagla^{-/-}$ and WT mice ($F_{(1,40)} = -12.80$, $p = ns$; Fig. 16A), indicative of a unaltered anxiety-state of mice lacking *Dagla*. Two-way ANOVA of the distance travelled revealed a significant genotype effect ($F_{(1,40)} = 4.739$, $p < 0.05$; Fig. 16B). Distance travelled in the open area was significantly increased in $Dagla^{-/-}$ mice ($t = 2.939$, $p < 0.01$; Fig. 16B).

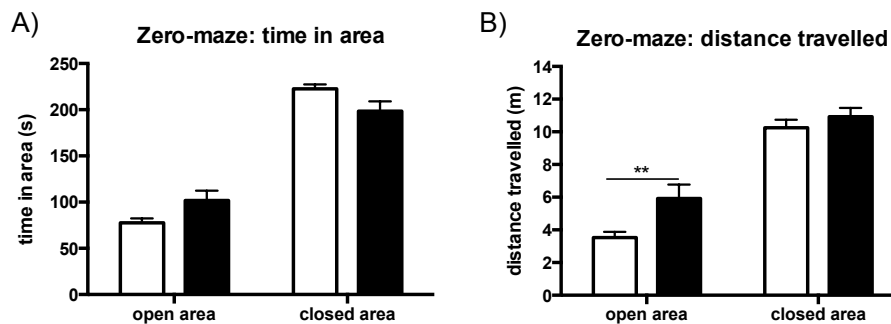


Figure 16: $Dagla^{-/-}$ mice showed an altered behavior in the zero-maze test. (A,B) Anxiety-like behavior was analyzed in the zero-maze test. (A) Time spent in the open or dark area was not significantly changed in $Dagla^{-/-}$ mice (two-way ANOVA, Bonferroni's post-hoc test, values represent mean \pm SEM: $n = 20-22$ animals/group, $p = ns$). (B) However, distance travelled in the open arms was significantly increased in $Dagla^{-/-}$ mice (two-way ANOVA, Bonferroni's post-hoc test, values represent mean \pm SEM: $n = 20-22$ animals/group, $**p < 0.01$) (modified from Jenniches et al. 2015).

Overall the results of the conducted tests revealed a slightly increased anxiety-like behavior of mice lacking *Dagla*.

3.1.5 Analysis of depression-related behavior

Disturbed cannabinoid signaling has been correlated with depressive-like behavior in rodents (Martin et al. 2002; Valverde & Torrens 2012). To analyze the impact of *DAGL* α and 2-AG on this depression-related phenotype, $Dagla^{-/-}$ mice were subjected to several behavioral tests.

First, home cage activity was analyzed. Changes in the general activity and disturbances in the light/dark cycle are related to depression. Similar time-dependent alterations in the home cage activity were observed in $Dagla^{-/-}$ and WT mice. Both mouse lines displayed an increased activity during the dark phase and a normal circadian rhythm

($F_{(95, 1235)} = 0.9226$, $p = \text{ns}$; Fig. 17A). Additionally, locomotor activity during the light and the dark phase did not differ between genotypes ($F_{(1,13)} = 0.05578$, $p = \text{ns}$; Fig. 17A).

Next, despair behavior, which is often considered as a symptom of depression, was evaluated in the forced swim test. In this test the immobility time of the animals is a measure of depressive-like behavior (Porsolt et al. 1977) and antidepressant drugs decrease the immobility time. The deletion of *Dagla* led to an increased immobility time in both male and female mice. The forced swim test revealed a significant genotype effect ($F_{(1,37)} = 31.07$, $p < 0.0001$; Fig. 17B), but no gender effect ($F_{(1,37)} = 1.085$, $p = \text{ns}$; Fig. 17B).

Another symptom of depression, anhedonia (reduced responsiveness to pleasurable stimuli), was investigated in the sucrose preference test. *Dagla*^{-/-} mice had a reduced preference for sucrose revealing a genotype effect ($F_{(1,33)} = 7.397$, $p < 0.05$; Fig. 17C), which was significant in males ($t = 3.296$, $p < 0.01$; Fig. 17C), but not in females ($t = 0.5783$, $p = \text{ns}$; Fig. 17C).

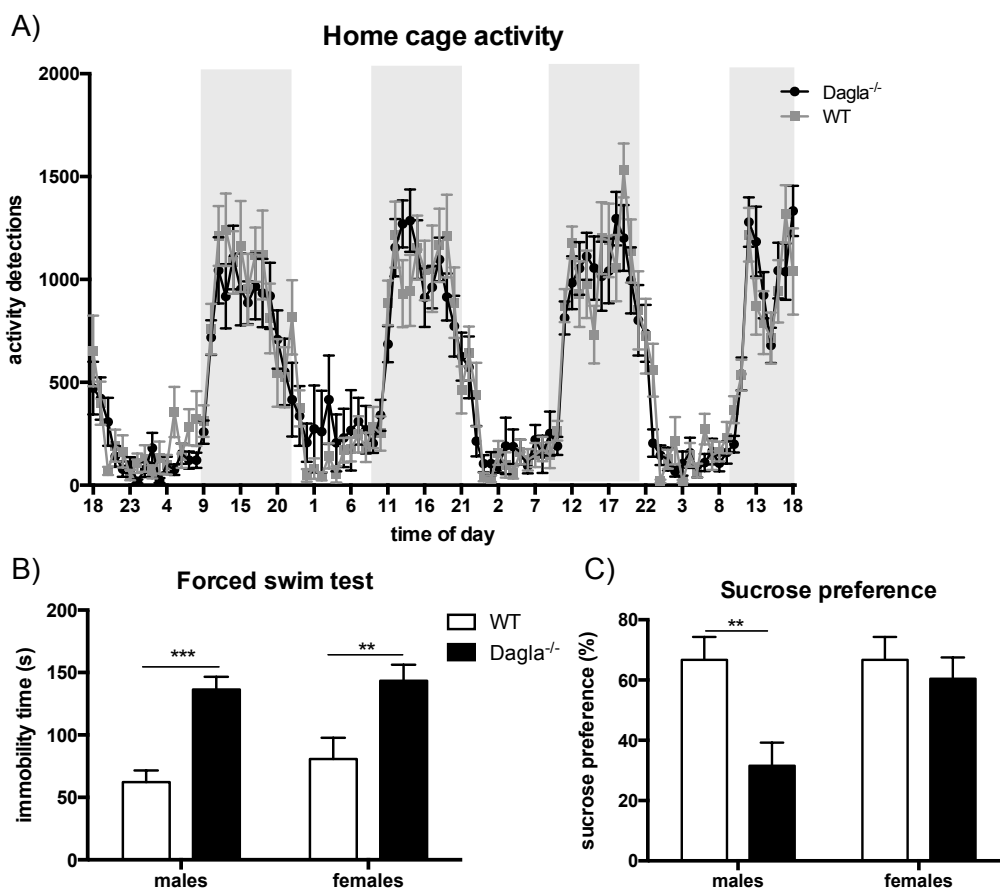


Figure 17: *Dagla*^{-/-} mice displayed a depressive-like phenotype. (A) Locomotor activity and circadian rhythm was analyzed by home cage activity measurement. *Dagla*^{-/-} mice did not show any changes in circadian rhythm and overall activity (two-way ANOVA repeated measurements, Bonferroni's post-hoc test, values represent mean \pm SEM: $n = 14$ animals/group, $p = \text{ns}$). (B) Male and female *Dagla*^{-/-} mice displayed depression-like behavior in the forced swim test. The immobility time of *Dagla*^{-/-} animals was significantly increased compared to WT controls (two-way ANOVA, Bonferroni's post-hoc test, values represent mean \pm SEM: $n = 8-12$ animals/group, ** $p < 0.01$, *** $p < 0.001$). (C) Anhedonia was assessed by sucrose preference. Sucrose preference of male but not female *Dagla*^{-/-} mice was significantly decreased compared to WT controls (two-way ANOVA, Bonferroni's post-hoc test, values represent mean \pm SEM: $n = 8-11$ animals/group, ** $p < 0.01$) (modified from Jenniches & Zimmer 2015).

Treatment with the antidepressant amitriptyline (10 mg/kg) significantly decreased the immobility time of *Dagla*^{-/-} (vehicle vs. amitriptyline: $t = 5.386$, $p < 0.0001$; Fig. 18A) and control mice in the forced swim test (vehicle vs. amitriptyline: $t = 2.963$, $p < 0.05$) and could therefore reverse the depressive-like phenotype of *Dagla*^{-/-} mice. In addition, after treatment with amitriptyline there was no longer a significant difference detectable between the genotypes ($t = 0.2239$, $p = \text{ns}$). Furthermore, to analyze the impact of 2-AG and anandamide on the depressive-like phenotype, *Dagla*^{-/-} mice were treated either with the MAGL inhibitor JZL184 or the FAAH inhibitor URB597 2 h before the forced swim test. Neither JZL184 nor URB597 significantly changed the immobility time of *Dagla*^{-/-} (JZL184: $t = 1.122$, $p = \text{ns}$; URB597: $t = 0.3351$, $p = \text{ns}$; Fig. 18A) or WT mice (JZL184: $t = 1.468$, $p = \text{ns}$; URB597: $t = 1.560$, $p = \text{ns}$; Fig. 18A) compared to vehicle controls. However, subsequent to both treatments no significant difference between the genotypes was observed (JZL184: $t = 2.022$, $p = \text{ns}$; URB597: $t = 0.6697$, $p = \text{ns}$). In contrast, the comparison of the vehicle treated animals revealed a significant genotype effect ($t = 3.205$, $p < 0.01$; Fig. 18A). Measurements of 2-AG and anandamide levels in the amygdala after JZL184 treatment showed an increase of 2-AG in WT ($t = 5.812$, $P < 0.0001$; Fig. 18C) and *Dagla*^{-/-} mice ($t = 9.398$, $p < 0.0001$; Fig. 18B,C). However, even after the treatment with JZL184, *Dagla*^{-/-} mice still showed a much lower 2-AG level than vehicle treated WT mice ($t = 12.14$, $p < 0.0001$; Fig. 18C). Thus, MAGL inhibition could not restore the 2-AG level in the amygdala of *Dagla*^{-/-} mice. Furthermore, after treatment with JZL184 no differences in anandamide levels between the genotypes were detected ($t = 0.5918$, $p = \text{ns}$; Fig. 18D), which was observed in the vehicle control group ($t = 3.414$, $p < 0.01$; Fig. 18D). Therefore, MAGL inhibition seemingly normalized anandamide levels in the amygdala of *Dagla*^{-/-} mice.

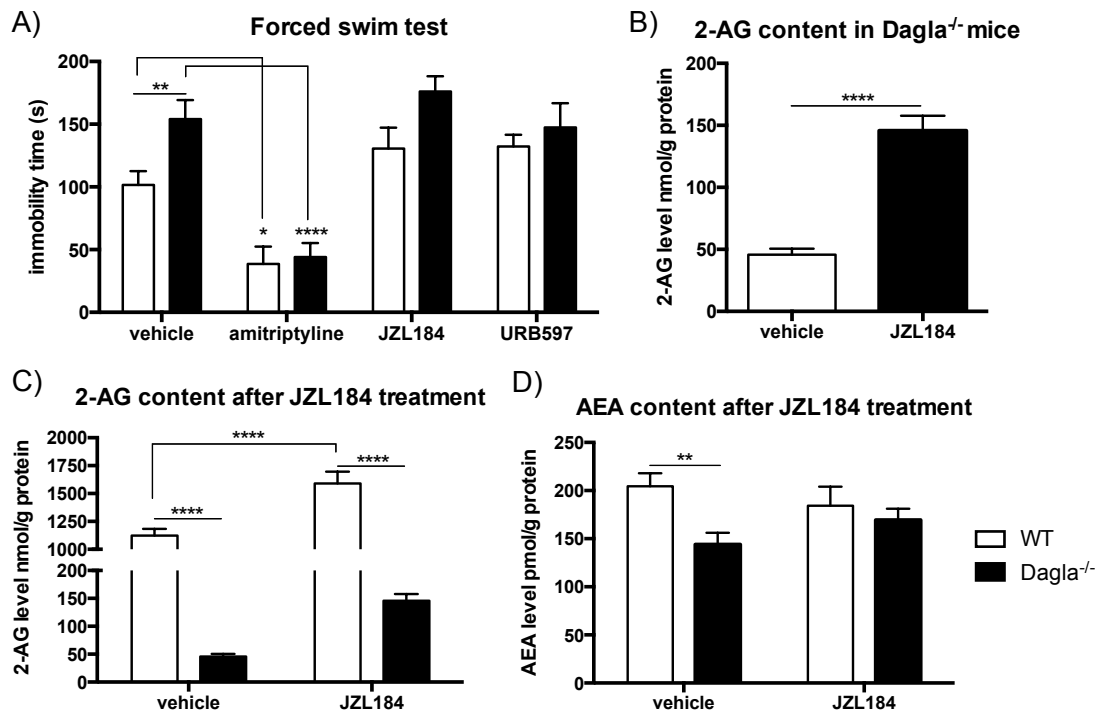


Figure 18: Effects of MAGL and FAAH inhibition and antidepressant treatment in the forced swim test. (A) Antidepressant treatment with 10 mg/kg amitriptyline significantly decreased immobility time of WT and Dagla^{-/-} mice. In contrast, neither treatment with 20 mg/kg JZL184 nor with 0.5 mg/kg URB597 significantly changed the immobility of WT or Dagla^{-/-} mice. However, after treatment with MAGL and FAAH inhibitor we could no longer observe a difference between the genotypes (two-way ANOVA, Bonferroni's post-hoc test, values represent mean \pm SEM: n = 10-19 animals/group, #p < 0.0001, **p < 0.0001, #####p < 0.0001). (B,C) Treatment with 20 mg/kg JZL184 significantly increased 2-AG levels in the amygdala of WT (C: two-way ANOVA, Bonferroni's post-hoc test, values represent mean \pm SEM: n = 5-10 animals/group, #####p < 0.0001) and Dagla^{-/-} mice (B: Student's t-test, values represent mean \pm SEM: n = 5-10 animals/group, ****p < 0.0001). However, MAGL inhibition could not restore the 2-AG level in Dagla^{-/-} mice (C: two-way ANOVA, Bonferroni's post-hoc test, values represent mean \pm SEM: n = 5-10 animals/group, ****p < 0.0001). (D) Treatment with JZL184 did not significantly change AEA levels in the amygdala in WT or Dagla^{-/-} mice. However, after MAGL inhibition no difference between the genotypes was observed (two-way ANOVA, Bonferroni's post-hoc test, values represent mean \pm SEM: n = 5-10 animals/group, p = ns) (modified from Jenniches et al. 2015).

The results show that mice lacking Dagla display several symptoms related to depression. In conclusion, the deletion of Dagla, thus the lack of 2-AG, caused a severe disturbance in the emotional state of rodents.

3.2 Behavioral and molecular analysis of neuron-specific Dagla^{-/-} mice

As described in chapter 3.1, constitutive lack of Dagla led to increased anxiety and a depressive-like phenotype in mice. However, which cell type might be responsible for this phenotype is still unknown. Therefore, this part of the results summarizes the molecular and behavioral analysis of neuron-specific Dagla^{-/-} mice (Syn-Dagla^{-/-}). All anxiety- and depression-related behavioral experiments were performed once with male or mixed-gender

cohorts. The animals were tested in several behavioral tests, always starting with the least stressful one.

3.2.1 Endocannabinoid measurements and gene expression analysis

To obtain Syn-Dagla^{-/-} mice, homozygous Dagla^{fl/fl} mice were bred with Synapsin1-Cre mice (Zhu et al. 2001). In all following experiments Dagla^{fl/fl} littermates were used as control animals. Knockout of Dagla was verified by TaqMan gene expression analysis, which revealed a 60-70 % reduction of Dagla mRNA in cortex ($t = 6.01$, $p < 0.0001$; Fig. 19A) and hippocampus ($t = 3.352$, $p < 0.05$; Fig. 19B) of Syn-Dagla^{-/-}. Reductions of Dagla mRNA in the amygdala failed to reach the level of significance ($t = 2.525$, $p = ns$; Fig. 19B). In addition, mRNA levels of other genes related to the ECS were not affected (Fig. 19A). Syn-Dagla^{-/-} mice were further verified by staining of cryofixed brain slices. Immunostainings showed an almost complete loss of DAGL α protein (Fig. 19C).

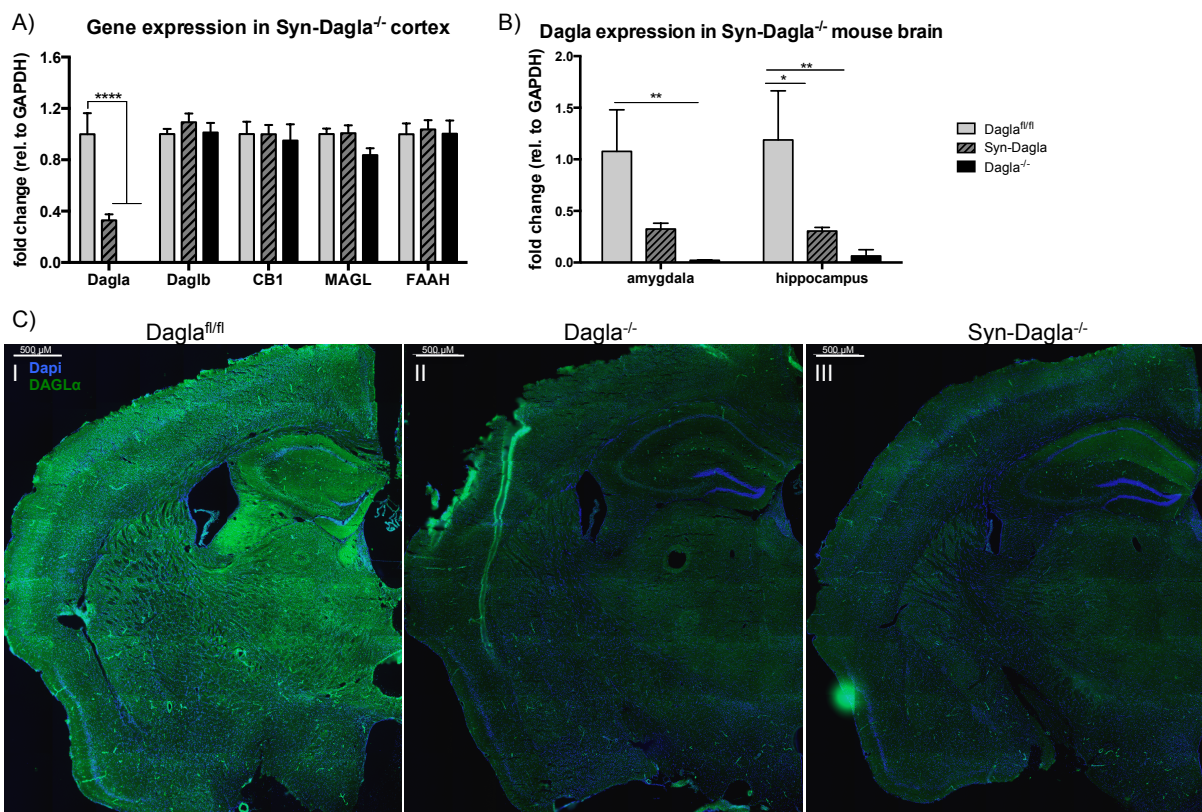


Figure 19: Validation of Syn-Dagla^{-/-} mice and endocannabinoid (eCB) measurement. (A) Shown are mRNA levels normalized to GAPDH. Real-time RT-PCR results show a 60 % reduction of Dagla mRNA transcript in Syn-Dagla^{-/-} mice compared to Dagla^{fl/fl} controls. However, other genes related to the endocannabinoid system did not differ between genotypes ($n = 4-6$ animals/group). (B) In addition, Dagla mRNA levels were significantly reduced (60-70 %) in amygdala and hippocampus of Syn-Dagla^{-/-} mice compared to Dagla^{fl/fl} controls (two-way ANOVA, Bonferroni's post-hoc test, values represent mean \pm SEM; $n = 3-4$ animals/group, * $p < 0.05$, ** $p < 0.01$, **** $p < 0.0001$). (C) Representative DAGL α immunostainings of (I) Dagla^{fl/fl}, (II) Dagla^{-/-} and (III) Syn-Dagla^{-/-} mice brain slices. Staining is completely absent in Dagla^{-/-} brain and almost lost in Syn-Dagla^{-/-} brain (scale: 500 μ m; blue: Dapi; green: DAGL α staining).

The main cellular source of 2-AG in the brain is still unknown. Neurons, microglia and astrocytes have been shown to produce 2-AG *in vitro* (Walter et al. 2003a). Therefore, endocannabinoid levels were measured in different brain parts of Syn-Dagla^{-/-} mice. This analysis was performed by Dr. Laura Bindila (University of Mainz). 2-AG levels were unchanged in hippocampus ($t = 0.02273$, $p = \text{ns}$; Fig. 20A) and prefrontal cortex (PFC) ($t = 0.6304$, $p = \text{ns}$; Fig. 20A) of Syn-Dagla^{-/-} mice compared to Dagla^{fl/fl} control mice. Furthermore, anandamide (hippocampus: $t = 1.357$, $p = \text{ns}$; PFC: $t = 0.7648$, $p = \text{ns}$; Fig. 20B) and AA (hippocampus: $t = 1.207$, $p = \text{ns}$; PFC: $t = 2.247$, $p = \text{ns}$; Fig. 20C) levels were not affected in Syn-Dagla^{-/-} mice compared to controls. However, this eCB measurement showed a significant reduction of AA in the hippocampus and PFC of constitutive Dagla^{-/-} mice (Fig. 20C), which was not present in previous experiments (Fig. 11F).

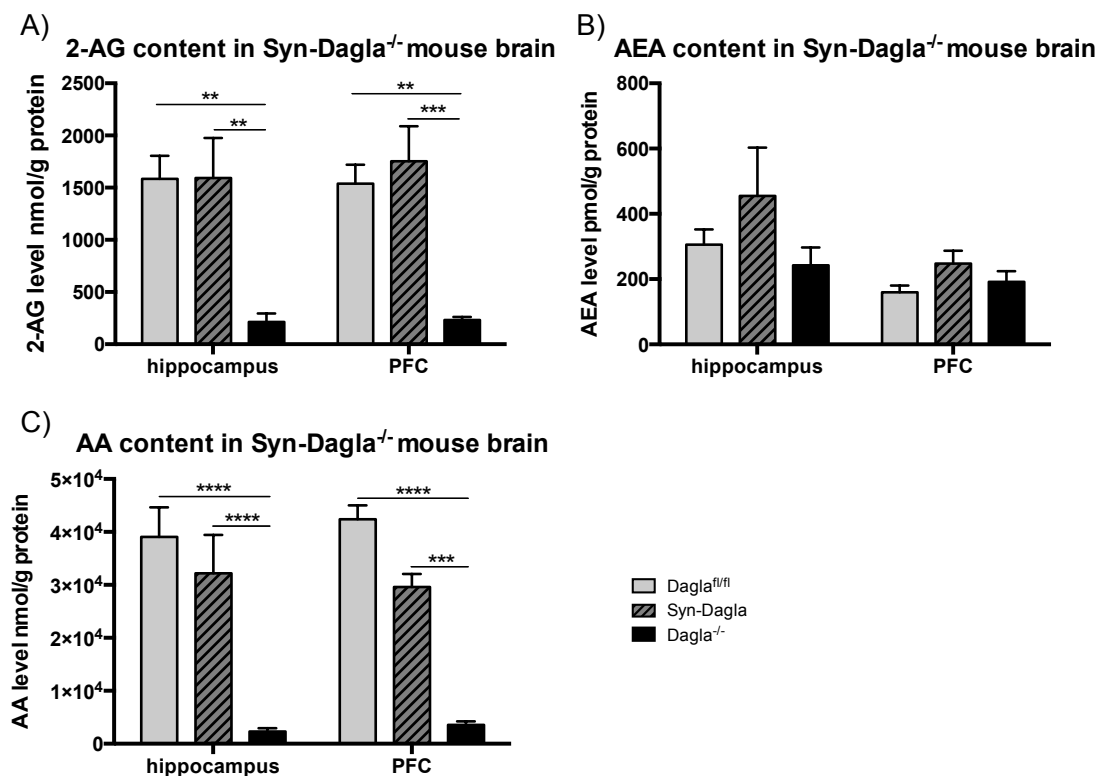


Figure 20: 2-AG and anandamide levels were not affected by the neuron-specific knockout of Dagla. (A-C) Shown are the amounts of 2-AG and anandamide (AEA) relative to the amount of total protein per sample. (A) 2-AG levels were not decreased in cortex or hippocampus of Syn-Dagla^{-/-} mice compared to Dagla^{fl/fl} control mice. (B) Furthermore, anandamide (AEA) levels were not changed in Syn-Dagla^{-/-} mice compared to controls. (C) Arachidonic acid (AA) content was also not altered in Syn-Dagla^{-/-} mice. For direct comparison values of constitutive Dagla^{-/-} mice are also represented. Statistical analysis for eCB measurement: two-way ANOVA, Bonferroni's post-hoc test, values represent mean \pm SEM; $n = 5-6$ animals/group, *** $p < 0.001$, **** $p < 0.0001$.

In addition, male adult 2-3 month old Syn-Dagla^{-/-} mice have an approximately 10 % reduced body weight compared to controls ($t = 2.523$, $p < 0.05$; Fig. 21). The reduction was less pronounced compared to constitutive Dagla^{-/-} mice.

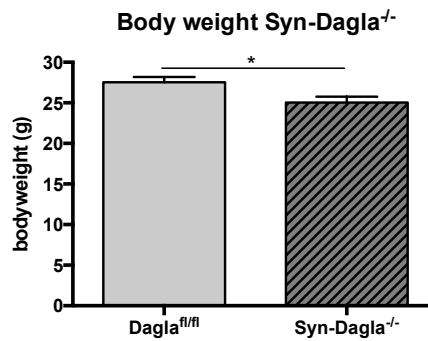


Figure 21: Syn-Dagla^{-/-} mice had a reduced body weight. Adult (2-3 month old) male Syn-Dagla^{-/-} mice have a significantly reduced body weight compared to age-matched Dagla^{fl/fl} control mice (Students t-test, values represent mean \pm SEM: n = 10 animals/group, *p < 0.05).

Following the molecular analysis and body weight measurements, Syn-Dagla^{-/-} mice were analyzed in different anxiety- and depression-related behavioral tests.

3.2.2 Analysis of anxiety-related behavior

Locomotor activity and anxiety-related behavior of male Syn-Dagla^{-/-} mice was assessed in the open-field test. Data are presented as distance travelled (Fig. 22A) and time spent in the center (Fig. 22B) over time in 10-min bouts. Distance travelled ($F_{(1,18)} = 0.9124$, p = ns; Fig. 22A) and the time spent in the center ($F_{(1,18)} = 1.128$, p = ns; Fig. 22B) did not differ significantly between Syn-Dagla^{-/-} and Dagla^{fl/fl} control mice. Distance travelled (between the 10-min bouts) decreased over time in both genotypes, leading to a significant time effect ($F_{(2,36)} = 73.61$, p < 0.0001; Fig. 22A).

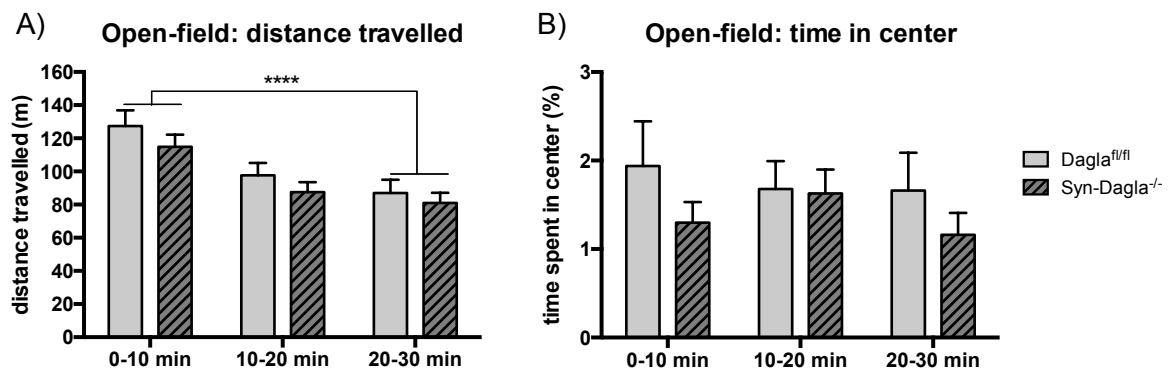


Figure 22: Syn-Dagla^{-/-} mice displayed no anxiety-like behavior. (A,B) Exploratory and anxiety-related behavior of male Syn-Dagla^{-/-} was analyzed in the open-field test. (A) No significant genotype differences in total distance travelled were observed (two-way ANOVA, Bonferroni's post-hoc test, values represent mean \pm SEM: n = 11 animals/group, p = ns). (B) In addition, time spent exploring the center did not differ between genotypes. (two-way ANOVA, Bonferroni's post-hoc test, values represent mean \pm SEM: n = 10 animals/group, *p < 0.05, **p < 0.01).

Thus, in contrast to constitutive Dagla^{-/-} mice, Syn-Dagla^{-/-} mice exhibited no anxiety-like phenotype in the open-field test.

3.2.3 Fear conditioning paradigm

Previous studies showed that the constitutive lack of CB1 or *Dagla* leads to a deficit in fear extinction (Marsicano et al. 2002; Ternes 2013; Jenniches et al. 2015). To analyze the impact of neuronal DAGL α to this phenotype, a mixed-gender group of Syn-*Dagla*^{-/-} mice was subjected to the same paradigm.

Extinction of fear is characterized by a decreasing freezing response over time. Two types of fear extinction can be distinguished: between-session extinction considers the decline in freezing behavior between extinction trials. Within-session extinction describes the decline in freezing that occurs within a single extinction trial. Behavioral data were analyzed for between- and within-session extinction

A decline of fear responses between the extinction trials E1 to E3 was observed for *Dagla*^{fl/fl} control mice, whereas freezing times of Syn-*Dagla*^{-/-} animals increased over time (Fig. 23A). The knockout line sustained an elevated freezing level, whereas *Dagla*^{fl/fl} controls returned progressively to base-line levels. Two-way ANOVA revealed a significant main effect for genotype ($F_{(1,62)} = 25.81$, $p < 0.0001$; Fig. 23A) and time x genotype interaction ($F_{(3,62)} = 3.858$, $p < 0.05$; Fig. 23A). Syn-*Dagla*^{-/-} animals reacted with increased fear responses on extinction days E2 ($p < 0.05$), E3 ($p < 0.01$) and E6 ($p < 0.001$) compared to *Dagla*^{fl/fl} controls. In addition, a significantly increased freezing time on extinction trial E6 compared to E1 was observed in Syn-*Dagla*^{-/-} mice ($t = 3.755$, $p < 0.01$; Fig. 23A). Thus, Syn-*Dagla*^{-/-} mice displayed disrupted between-session fear extinction.

Next, within-session extinction was determined. For the first extinction session E1, no decline in the freezing response was detected in any of the genotypes. Freezing behaviors of Syn-*Dagla*^{-/-} mice were comparable to *Dagla*^{fl/fl} animals (genotype effect: $F_{(1,48)} = 0.1068$, $p = \text{ns}$; Fig. 23B). In contrast, significant main effects for genotype were observed for the following extinction trials E2 ($F_{(1,48)} = 6.988$, $p < 0.05$; Fig. 23C), E3 ($F_{(1,48)} = 19.01$, $p < 0.0001$; Fig. 23D) and E6 ($F_{(1,48)} = 26.44$, $p < 0.0001$; Fig. 23E). Syn-*Dagla*^{-/-} animals showed continuously increased fear responses on extinction trials E2, E3 and E6 (Fig. 23C-E). At extinction trial E2, a decline of the freezing response was detected for *Dagla*^{fl/fl} mice, whereas the freezing time of Syn-*Dagla*^{-/-} mice remained constant during the whole test session (Fig. 23C). In addition, a sustained freezing behavior was detected upon persisting tone presentation on extinction trial E3 ($p < 0.05$ after 60 s until the end of the session; Fig. 23D) and E6 ($p < 0.01$ after 60 s until 120s, $p < 0.001$ after 120 s until 180 s; Fig. 23E). However, no significant interactions between genotype and freezing behavior were observed (E2: $F_{(2,48)} = 0.9859$, $p = \text{ns}$; E3: $F_{(2,48)} = 0.1449$, $p = \text{ns}$; E6: $F_{(2,48)} = 2.008$, $p = \text{ns}$; Fig. 23C-E). The analysis of within-session extinction revealed that Syn-*Dagla*^{-/-} mice showed a tendency towards an impaired fear extinction during prolonged tone presentation.

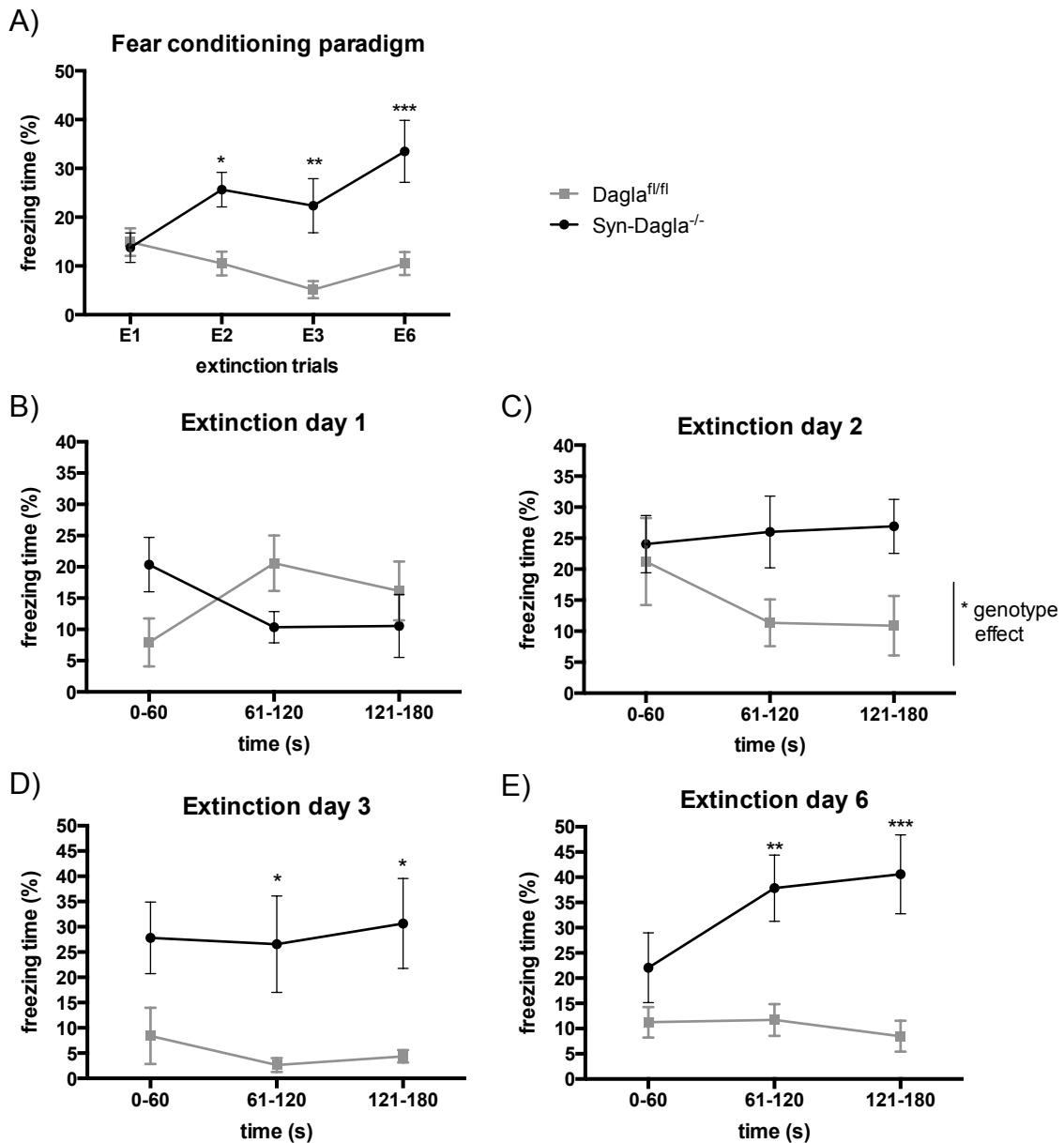


Figure 23: Syn-Dagla^{-/-} mice displayed an increased fear response and impaired fear extinction. (A-E) Syn-Dagla^{-/-} and Dagla^{fl/fl} controls were conditioned with a tone-foot shock pairing in the conditioning chamber. All animals were exposed to a 180 s tone in a neutral environment 1, 2, 3 and 6 days after the conditioning procedure. (A) Syn-Dagla^{-/-} mice showed an increased freezing behavior (two-way ANOVA, Bonferroni's post-hoc test, values represent mean \pm SEM: $n = 9$ animals/group, * $p < 0.05$, ** $p < 0.01$, *** $p < 0.001$) and an impaired between-session extinction of conditioned fear (two-way ANOVA, Bonferroni's post-hoc test, values represent mean \pm SEM: $n = 9$ animals/group, genotype effect **** $p < 0.0001$, interaction * $p < 0.05$). (B) On extinction day E1, Syn-Dagla^{-/-} and Dagla^{fl/fl} mice showed similar freezing behavior. (C-E) However, Syn-Dagla^{-/-} mice showed increased freezing behavior on extinction day 2, 3 and 6 (two-way ANOVA, Bonferroni's post-hoc test, values represent mean \pm SEM: $n = 8-9$ animals/group, * $p < 0.05$, ** $p < 0.01$, *** $p < 0.001$).

In conclusion, lack of Dagla in neurons led to an increased fear response and a deficit in between-session extinction in a cued fear conditioning paradigm. A comparable phenotype was detected in constitutive Dagla^{-/-} mice (Ternes 2013; Jenniches et al. 2015).

3.2.4 Analysis of depression-related behavior

A constitutive lack of *Dagla* led to the development of a depressive-like phenotype in mice. Therefore, *Syn-Dagla*^{-/-} mice (mixed-gender group) were subjected to different behavioral tests related to depression. First, activity in the home cage was analyzed. Home cage activity measurements revealed time-dependent alterations in both *Syn-Dagla*^{-/-} and *Dagla*^{fl/fl} animals, resulting in similar circadian rhythm in both genotypes ($F_{(46,828)} = 1.131$, $p = \text{ns}$; Fig. 24A). However, a reduced locomotor activity in *Syn-Dagla*^{-/-} mice was observed (genotype effect: $F_{(1,18)} = 5.936$, $p < 0.05$; Fig. 24A). Overall activity was significantly reduced in the dark, active phase of the animals ($t = 2.968$, $p < 0.05$; Fig. 24B), but not in the light phase ($t = 1.223$, $p = \text{ns}$; Fig. 24B).

Furthermore, despair behavior was analyzed in the forced swim test. Immobility time was significantly increased in *Syn-Dagla*^{-/-} mice ($t = 2.257$, $p < 0.05$; Fig. 24C), indicative of a depressive-like phenotype. Another symptom of depression, anhedonia, was evaluated in the sucrose preference test. *Syn-Dagla*^{-/-} had a significantly reduced preference for sucrose ($t = 4.377$, $p < 0.001$; Fig. 24D).

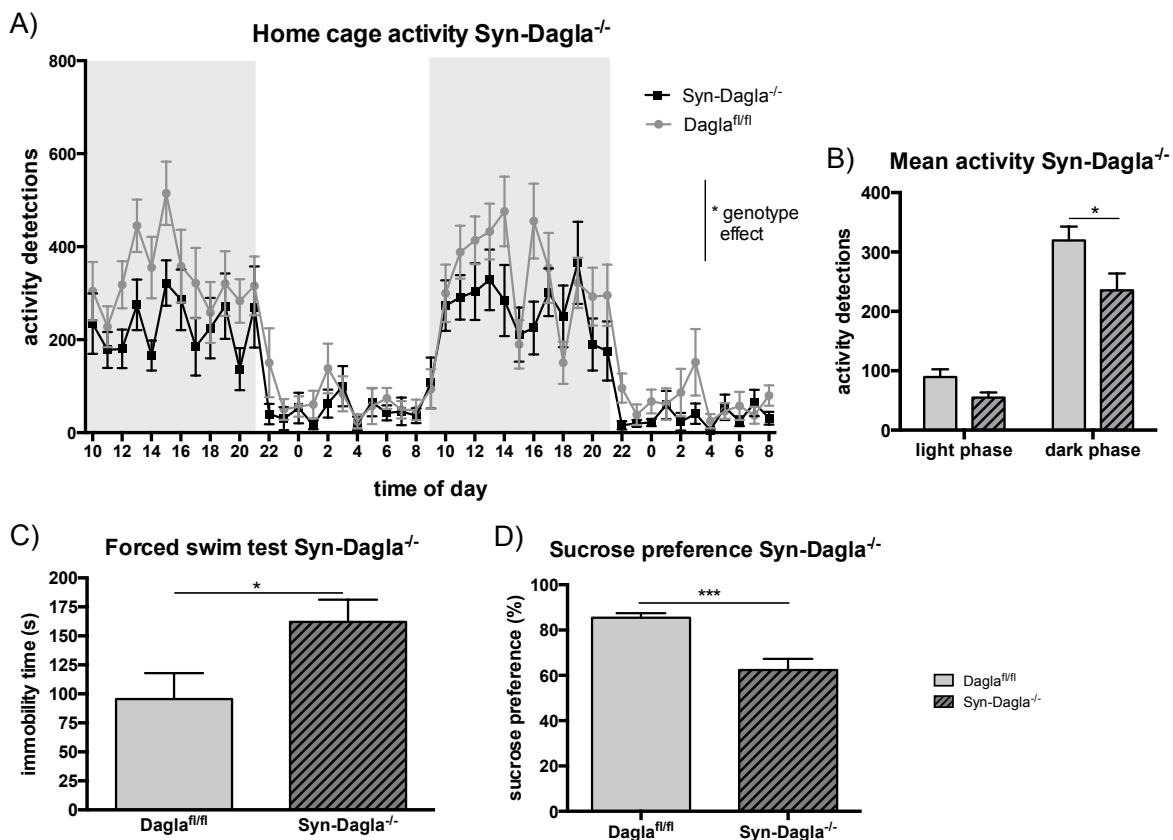


Figure 24: *Syn-Dagla*^{-/-} mice displayed a depressive-like phenotype. (A) Locomotor activity and circadian rhythm was analyzed by home cage activity measurements. *Syn-Dagla*^{-/-} mice displayed a similar circadian rhythm as *Dagla*^{fl/fl} controls, but reduced locomotor activity (two-way ANOVA repeated measurements, Bonferroni's post-hoc test, values represent mean \pm SEM: $n = 10$ animals/group, interaction: $p = \text{ns}$, genotype: $p < 0.05$). (B) Overall activity was significantly reduced in the the dark, but not in the light phase (two-way ANOVA, Bonferroni's post-hoc test, values represent mean \pm SEM: $n = 10$ animals/group, * $p < 0.05$). (C) *Syn-Dagla*^{-/-} mice displayed a depression-like behavior in the forced swim test. The immobility time of *Syn-Dagla*^{-/-} animals was

significantly increased compared to $Dagla^{fl/fl}$ controls (Students t-test, values represent mean \pm SEM: n = 10 animals/group, *p < 0.05). (C) Anhedonia was assessed by sucrose preference. Sucrose preference of $Syn-Dagla^{-/-}$ mice were significantly reduced compared to $Dagla^{fl/fl}$ controls (Students t-test, values represent mean \pm SEM: n = 10 animals/group, ***p < 0.001).

In summary, $Syn-Dagla^{-/-}$ mice displayed a depressive-like phenotype in the forced swim and sucrose preference test, similar to that seen in mice ubiquitously lacking $Dagla$.

3.2.5 Adult neurogenesis

Previous studies showed a reduced adult neurogenesis in mice lacking $Dagla$, leading to a reduced number of BrdU (5-bromo-2'-deoxyuridine) positive cells in the dentate gyrus of the hippocampus (Jenniches et al. 2015). Reduced adult neurogenesis and a reduction of hippocampal volume are related to depression. To elucidate the participation of neuronal DAGL α to the observed phenotype, adult neurogenesis of $Syn-Dagla^{-/-}$ mice was analyzed. Neuronal proliferation and survival were analyzed in the dentate gyrus of the hippocampus, one of the two neurogenic niches in the adult brain.

The number of BrdU labeled cells was similar in $Syn-Dagla^{-/-}$ and $Dagla^{fl/fl}$ mice on day 1 (t = 1.651, p = ns; Fig. 25) and day 21 (t = 1.371, p = ns; Fig. 25) after BrdU injection. Thus, neuronal proliferation (day 1) and survival (day 21) were not altered in the hippocampus of $Syn-Dagla^{-/-}$ mice.

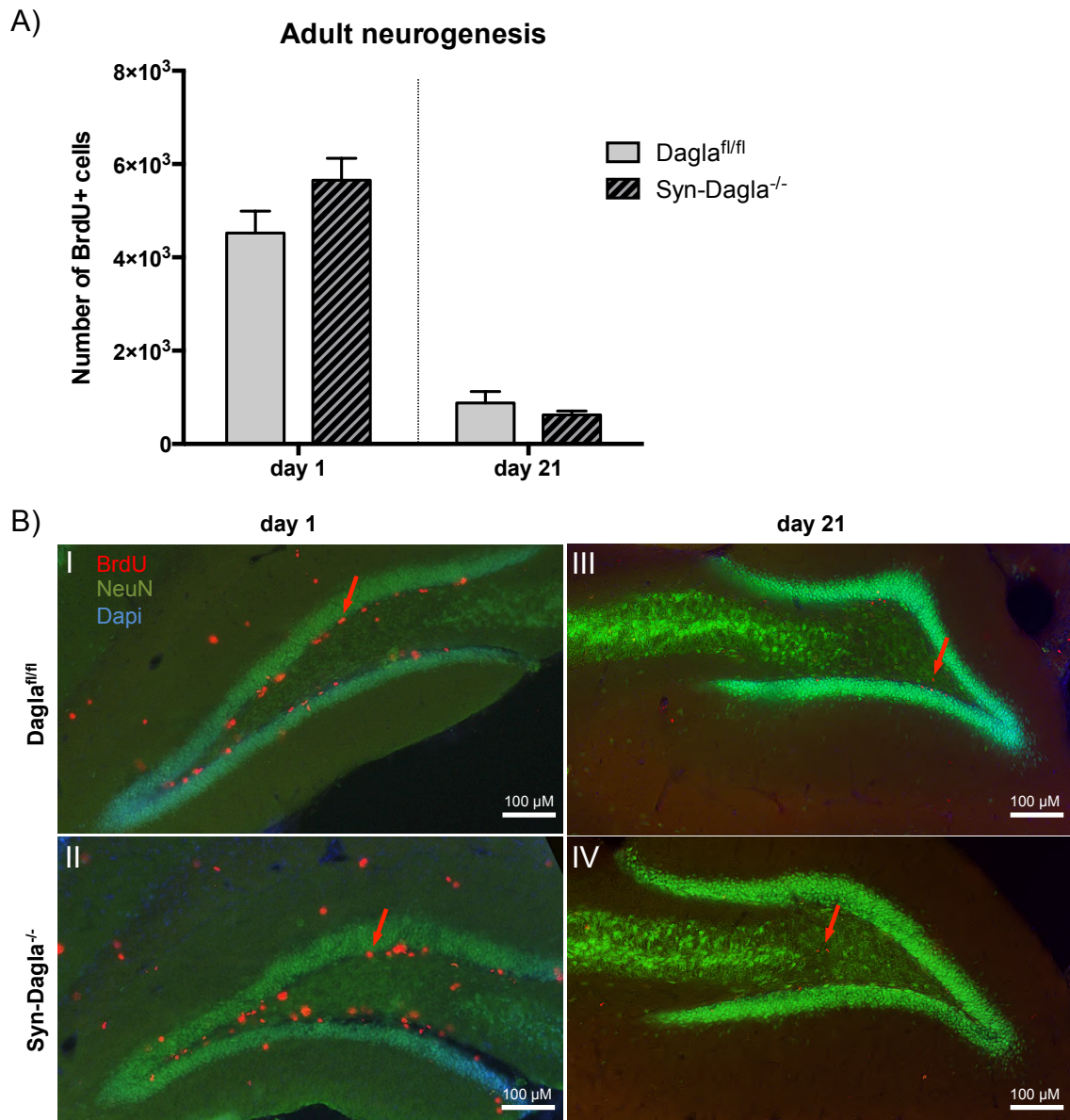


Figure 25: Adult neurogenesis was similar in both Syn-Dagla^{-/-} and Dagla^{fl/fl} mice. (A) Proliferation and neuronal survival in the subgranular zone of the hippocampus was similar in Syn-Dagla^{-/-} mice and Dagla^{fl/fl} controls (Students t-test, values represent mean \pm SEM: $n = 3-4$ animals/group, $p = ns$). (B) Representative microphotograph of BrdU labeled (red fluorescent), NeuN (green fluorescent) and Dapi (blue fluorescent) stained cells in the dentate gyrus of the hippocampus of Syn-Dagla^{-/-} mice (BII, IV) and Dagla^{fl/fl} controls (BI, III) 24 h and 21 days after BrdU injection.

3.3 Behavioral and molecular analysis of microglia-specific Dagla^{-/-} mice

Microglia produce high amounts of 2-AG *in vitro* and exhibit a functional endocannabinoid system. Thus, the deletion of Dagla in these cells might contribute to the observed anxiety and depression-like phenotype of constitutive Dagla^{-/-} mice. To elucidate the role of DAGL α in microglia, LysM-Dagla^{-/-} mice were analyzed in the same behavioral paradigms as Dagla^{-/-} mice. All anxiety- and depression-related behavioral experiments were performed at least

twice with independent cohorts of animals (male or mixed-gender groups). Animals were tested in several behavioral tests always starting with the least stressful one.

3.3.1 Endocannabinoid measurements and gene expression analysis

To obtain LysM-Dagla^{-/-} mice, homozygous Dagla^{fl/fl} mice were bred with LysM-Cre mice (Clausen et al. 1999). In all following experiments Dagla^{fl/fl} littermates were used as control animals. Gene expression analysis revealed similar Dagla ($t = 1.022$, $p = \text{ns}$; Fig. 26A) and Daglb mRNA levels ($t = 0.6480$, $p = \text{ns}$; Fig. 26B) in whole brain tissue samples of LysM-Dagla^{-/-} mice and Dagla^{fl/fl} controls.

LysM-Cre leads to a specific deletion of Dagla in cells of the monocyte-lineage, representing a minor part of the CNS cell populations. Thus, a specific deletion in microglia and macrophages is difficult to detect in whole brain samples. Therefore, LysM-Dagla^{-/-} mice were further verified by immunohistochemistry stainings of cryofixed brain slices. Brain Slices of LysM-Dagla^{-/-} and Dagla^{fl/fl} control mice were co-stained with anti-Dagla and anti-Iba1 antibodies. Immunostainings showed a significantly reduced number of Dagla/Iba1 double-positive cells in LysM-Dagla^{-/-} animals compared to controls ($t = 3.915$, $p < 0.001$; Fig. 26B,C), resulting in a 30 % knockout of Dagla in microglia of LysM-Dagla^{-/-} mice. In addition, previous studies showed an 80 % reduction of Dagla mRNA in primary macrophages of this very LysM-Dagla^{-/-} mouse line (Jehle et al. 2016).

Next, endocannabinoid levels were determined. For direct comparison, eCB levels were also measured in constitutive Dagla^{-/-} mice. Similar 2-AG contents in the cortex ($t = 1.063$, $p = \text{ns}$), striatum ($t = 0.3642$, $p = \text{ns}$) and hippocampus ($t = 1.083$, $p = \text{ns}$; Fig. 26D) were detected in LysM-Dagla^{-/-} and Dagla^{fl/fl} mice. As expected, 2-AG levels were dramatically reduced in different brain areas of Dagla^{-/-} mice (Fig. 26D). In addition, anandamide levels (referred as AEA) were significantly reduced in the cortex of LysM-Dagla^{-/-} mice compared to Dagla^{fl/fl} controls ($t = 4.146$, $p < 0.001$; Fig. 26E). A similar tendency was seen in the hippocampus (Fig. 26E). Interestingly, anandamide levels were equally reduced in brain samples of LysM-Dagla^{-/-} and Dagla^{-/-} mice (cortex: $t = 0.6877$, $p = \text{ns}$; hippocampus: $t = 0.5878$, $p = \text{ns}$; Fig. 26E). However, no differences in arachidonic acid (AA) contents between LysM-Dagla^{-/-} mice, Dagla^{-/-} mice and Dagla^{fl/fl} controls were detected ($F_{(2,32)} = 2.065$, $p = \text{ns}$; Fig. 26F).

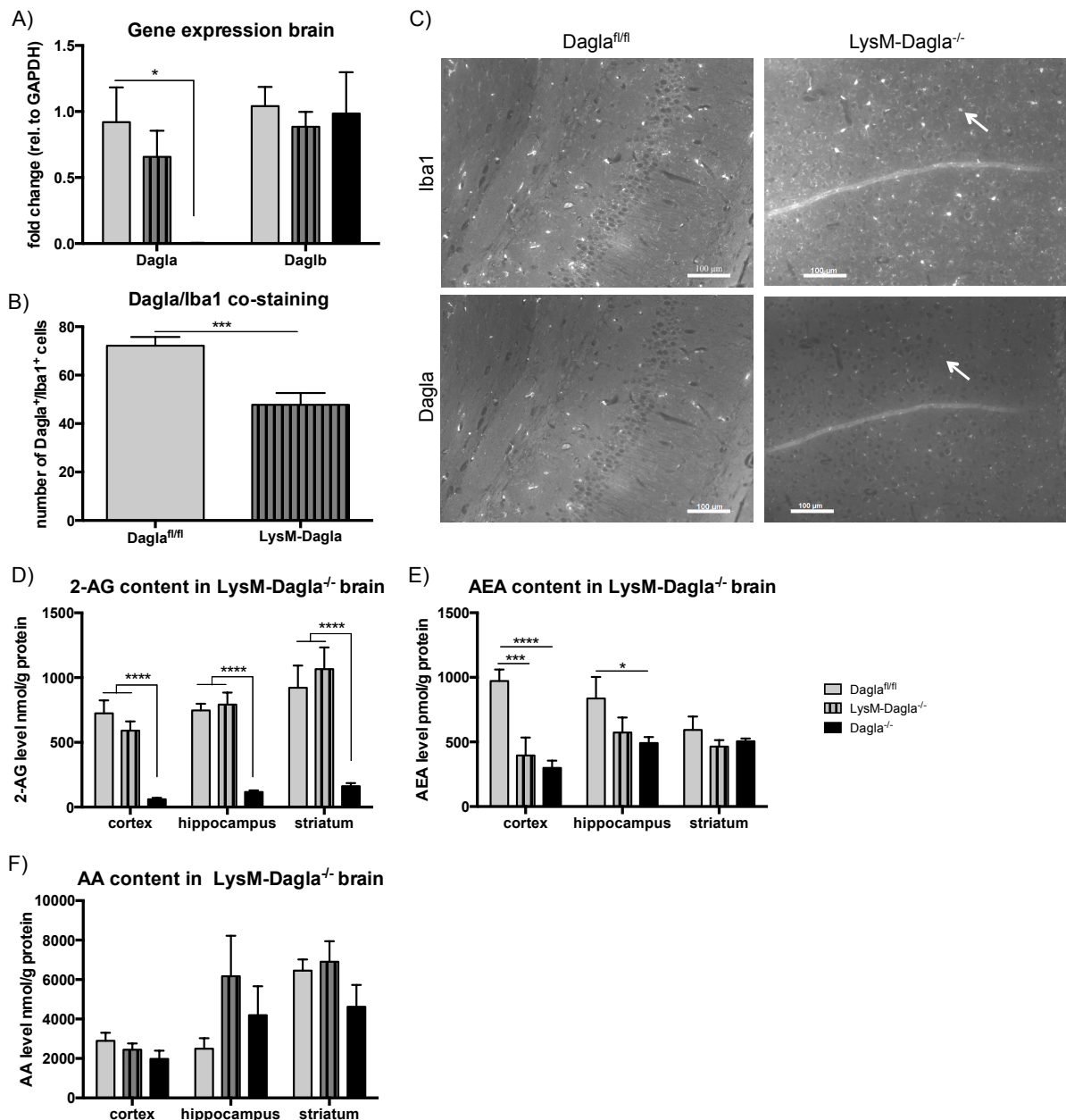


Figure 26: Verification of LysM-Dagla^{-/-} mice and eCB measurements. (A) Shown are mRNA levels normalized to GAPDH. Real-time RT-PCR showed similar expression levels of Dagla and Daglb in LysM-Dagla^{-/-} and Dagla^{fl/fl} mice (two-way ANOVA, Bonferroni's post-hoc test, values represent mean \pm SEM: n = 4-5 animals/group (Dagla^{fl/fl} and LysM-Dagla^{-/-}), n = 2 animals/group (Dagla^{-/-}), *p < 0.05). (B) Number of Dagla/Iba1 double-positive cells was significantly reduced in LysM-Dagla^{-/-} mice (Students t-test, values represent mean \pm SEM: n = 17-20 analyzed slides/group of 3 animals/group, ****p < 0.001). (C) Shown are representative microphotographs of Iba1 and Dagla labeled brain slices of 2-3 month old LysM-Dagla^{-/-} mice and Dagla^{fl/fl} controls. Arrows mark an Iba1-positive and Dagla-negative microglia cell (scale: 100 μ m). (D) Similar 2-AG levels were measured in the cortex, hippocampus or striatum of LysM-Dagla^{-/-} mice and Dagla^{fl/fl} controls. (E) However, anandamide (AEA) levels were significantly reduced in cortex of LysM-Dagla^{-/-} mice compared to controls. (F) In addition, arachidonic acid (AA) content was not altered in LysM-Dagla^{-/-} mice. For direct comparison values of constitutive Dagla^{-/-} mice are also presented. Statistical analysis: two-way ANOVA, Bonferroni's post-hoc test, values represent mean \pm SEM: n = 4-5 animals/group, *p < 0.05, ***p < 0.001, ****p < 0.0001.

In contrast to the constitutive as well as neuronal deletion of Dagla, microglia-specific deletion did not influence the body weight. Body weights of adult (2-3 months old) male and

female LysM-Dagla^{-/-} mice were similar to age- and gender-matched Dagla^{fl/fl} controls ($F_{(1,17)} = 0.0009384$, $p = \text{ns}$; Fig. 27).

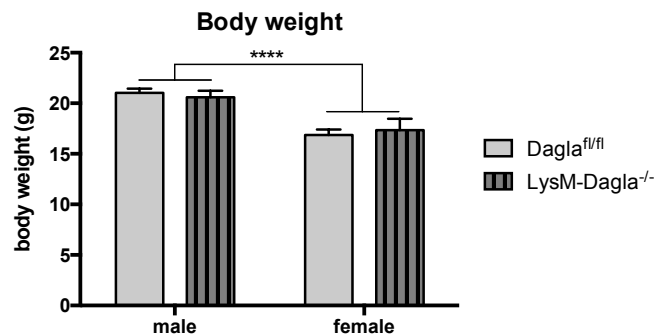


Figure 27: Body weights were similar for both LysM-Dagla^{-/-} mice and Dagla^{fl/fl} controls. Body weight of adult (2-3 month old) male and female LysM-Dagla^{-/-} mice did not differ from Dagla^{fl/fl} control mice. However, female mice have a generally reduced body weight compared to age-matched males regardless of genotype. Statistical analysis: two-way ANOVA, Bonferroni's post-hoc test, values represent mean \pm SEM: $n = 5-6$ animals/group, **** $p < 0.0001$.

In summary, it can be stated that the specific deletion of Dagla in microglia and macrophages did not influence 2-AG levels in the brain, but caused a significant reduction in cortical anandamide levels. Following the molecular analysis, LysM-Dagla^{-/-} mice were analyzed in different anxiety- and depression-related behavioral tests.

3.3.2 Analysis of anxiety-related behavior

To investigate locomotor activity and anxiety-related behavior, male LysM-Dagla^{-/-} mice were analyzed in the open-field test (Fig. 28A,B). Data are presented as distance travelled (Fig. 28A) and time spent in the center (Fig. 28B) over time in 10-min bouts. Distance travelled ($F_{(1,51)} = 0.8485$, $p = \text{ns}$; Fig. 28A) and time spent in the center ($F_{(1,50)} = 0.1322$, $p = \text{ns}$; Fig. 28B) were similar for both genotypes. LysM-Dagla^{-/-} mice displayed normal locomotor activity and similar anxiety-related behavior when compared to Dagla^{fl/fl} controls. In addition, a decreased distance travelled over time (between the 10-min bouts) was observed in both genotypes (time effect: $F_{(2,51)} = 21.03$, $p < 0.0001$; Fig. 28A), indicative of a habituation to the novel environment.

Anxiety-like behavior was further analyzed in the zero-maze test (Fig. 28C,D). Time spent in the open area ($F_{(1,44)} = -1.007 \times 10^{-13}$, $p = \text{ns}$; Fig. 28B) and distance travelled in the open area ($F_{(1,44)} = 0.3474$, $p = \text{ns}$; Fig. 28B) revealed no genotype effects.

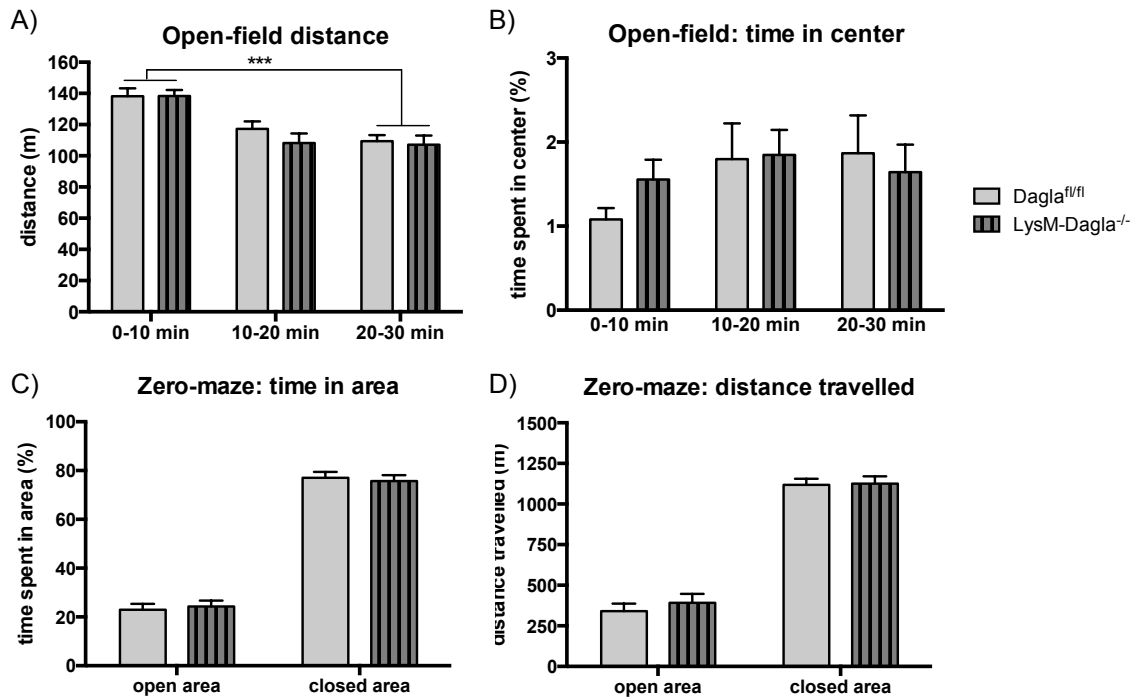


Figure 28: LysM-Dagla^{-/-} mice displayed normal locomotor activity and no anxiety-like behavior. (A,B) Exploratory and anxiety-related behavior of male LysM-Dagla^{-/-} was analyzed in the open-field test. (A,B) Distance travelled (A) and the time spent exploring the center (B) were similar for both genotypes (two-way ANOVA, Bonferroni's post-hoc test, values represent mean \pm SEM: $n = 10$ animals/group, $***p < 0.001$). (C-D) Anxiety-like behavior was further analyzed in the zero-maze test. (C) Time spent in the open and dark area was similar for LysM-Dagla^{-/-} mice and Dagla^{fl/fl} controls. (D) Distance travelled did not differ between genotypes (two-way ANOVA, Bonferroni's post-hoc test, values represent mean \pm SEM: $n = 10-14$ animals/group).

In conclusion, LysM-Dagla^{-/-} mice showed no kind of anxiety-like behavior in the open-field and zero-maze test.

3.3.3 Fear conditioning paradigm

As already shown in previous studies and the present study, mice lacking Dagla either ubiquitously (Ternes 2013, Jenniches et al. 2015) or specifically in neuronal tissue (Chapter 3.2.3) displayed a distinct deficit in fear extinction and increased fear responses in a cue-dependent conditioning paradigm. However, 2-AG produced by other cell types might also influence the extinction of conditioned fear. Accordingly, LysM-Dagla^{-/-} mice were analyzed in the same cued fear conditioning paradigm as Syn-Dagla^{-/-} mice (Chapter 3.2.3).

A distinct decline in the freezing response over time (from extinction trial E1 to E6) was observed in LysM-Dagla^{-/-} and Dagla^{fl/fl} mice (time effect: $F_{(3,76)} = 2.828$, $p < 0.05$; Fig. 29A). Both genotypes displayed similar freezing times (genotype effect: $F_{(1,76)} = 2.451$, $p = \text{ns}$; Fig. 29A). Thus, LysM-Dagla^{-/-} mice and Dagla^{fl/fl} controls exhibited between-session fear extinction.

Next, within-session fear extinction was determined. For all extinction trials, LysM-Dagla^{-/-} mice displayed similar extinction patterns as Dagla^{fl/fl} control animals (time x genotype interaction: E1: $F_{(2,57)} = 0.5966$, $p = \text{ns}$; E2: $F_{(2,57)} = 0.2068$, $p = \text{ns}$; E3: $F_{(2,57)} = 0.01195$, $p = \text{ns}$; E6: $F_{(2,60)} = 0.09858$, $p = \text{ns}$; Fig. 29B-E). The observed freezing times on extinction days E1, E2 and E3 did not differ between the genotypes (E1: $F_{(1,57)} = 0.02575$, $p = \text{ns}$; E2: $F_{(1,57)} = 2.267$, $p = \text{ns}$; E3: $F_{(1,57)} = 1.055$, $p = \text{ns}$; Fig. 29B-D). However, on extinction day E6 freezing levels of LysM-Dagla^{-/-} were significantly increased compared to controls (genotype effect: $F_{(1,60)} = 4.357$, $p < 0.05$; Fig. 29E).

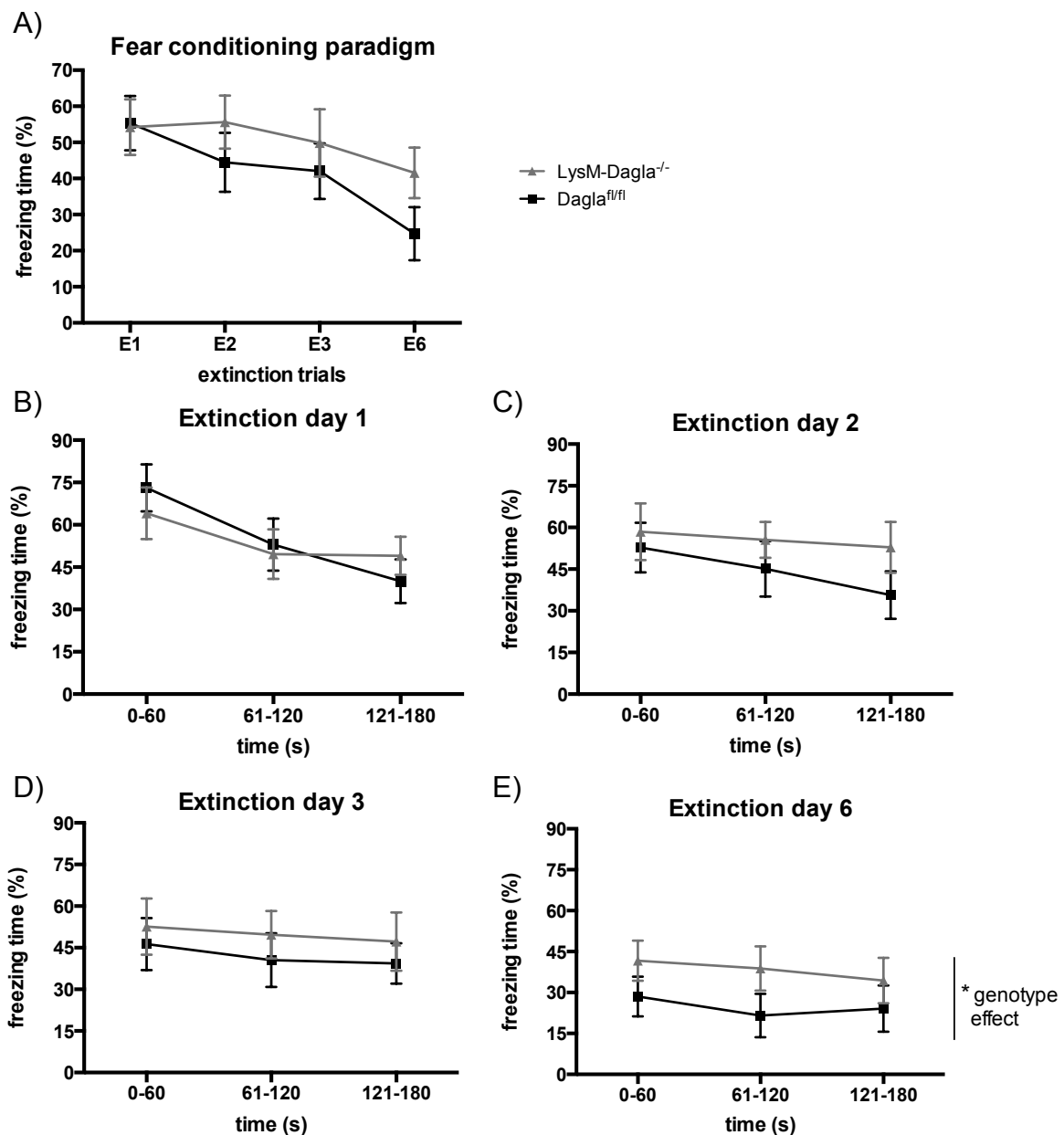


Figure 29: LysM-Dagla^{-/-} mice displayed normal fear extinction, but mildly increased fear response. (A-E) LysM-Dagla^{-/-} and Dagla^{fl/fl} controls were conditioned with a tone-foot shock pairing in the conditioned chamber. All animals were exposed to a 180 s tone in a neutral environment 1, 2, 3 and 6 days after the conditioning procedure. (A-E) Similar between- and within-session extinction was observed for LysM-Dagla^{-/-} mice and Dagla^{fl/fl} controls. (E) However, LysM-Dagla^{-/-} mice showed an increased freezing response on extinction day E6. Statistical analysis: two-way ANOVA, Bonferroni's post-hoc test, values represent mean \pm SEM: $n = 10-11$ animals/group, * $p < 0.05$.

The results show that *Dagla* in microglia does not modulate the extinction of conditioned fear, but influences the intensity of the fear response.

3.3.4 Analysis of depression-related behavior

Depression-like behavior of *LysM-Dagla*^{-/-} mice (mixed-gender cohort) was analyzed in the forced swim, sucrose preference and social preference tests. Initially, locomotor activity and circadian rhythm of *LysM-Dagla*^{-/-} mice were analyzed by home cage activity measurements. Overall activity and circadian rhythm of *LysM-Dagla*^{-/-} animals were similar to *Dagla*^{fl/fl} controls (genotype effect: $F_{(1,17)} = 0.4481$, $p = \text{ns}$; time x genotype interaction: $F_{(49,833)} = 0.7016$, $p = \text{ns}$; Fig. 30A).

Next, despair behavior was evaluated in the forced swim test. Immobility time of *LysM-Dagla*^{-/-} mice did not differ from controls ($t = 0.1110$, $p = \text{ns}$; Fig. 30B). However, sucrose preference was significantly reduced in *LysM-Dagla*^{-/-} animals compared to *Dagla*^{fl/fl} mice ($U = 28.00$, $p < 0.05$; Fig. 30C), indicative of a depressive-like phenotype.

Furthermore, social preference was determined in an independent mixed-gender cohort of animals. Reduced social preference is a further indicator of a depressive-like phenotype. *Dagla*^{fl/fl} and *LysM-Dagla*^{-/-} mice displayed a similar ratio of the time spent with the partner mouse compared to the empty cage ($t = 0.0$, $p = \text{ns}$; Fig. 30D). The time spent with the gender-matched partner mouse was significantly higher compared to the empty cage in both genotypes ($F_{(1,20)} = 28.35$, $p < 0.0001$; Fig. 30E). Thus, *LysM-Dagla*^{-/-} animals displayed a normal sociability.

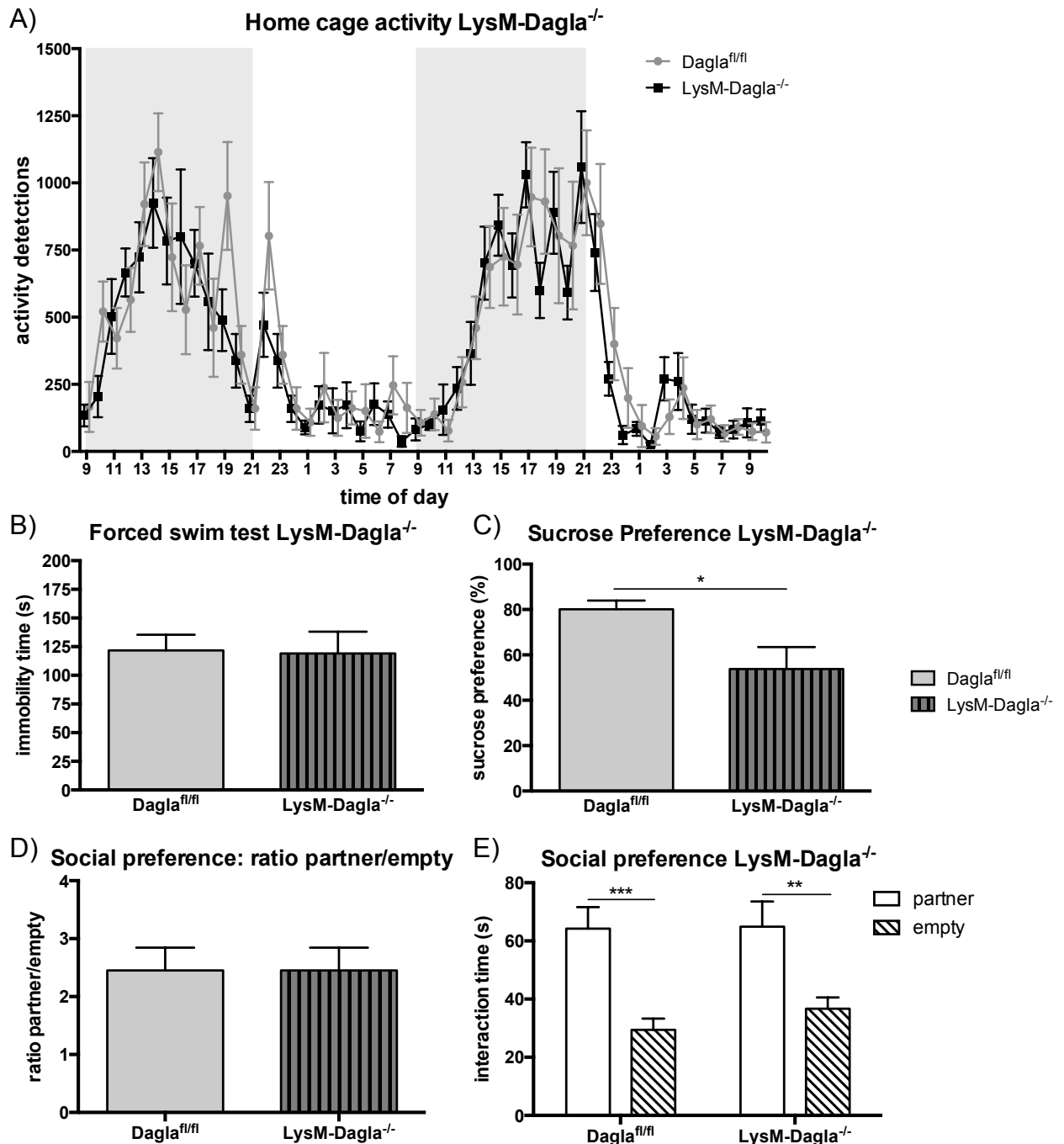


Figure 30: LysM-Dagla^{-/-} mice showed no depressive-like behavior in the forced swim and social preference test, but displayed a reduced sucrose preference. (A) Locomotor activity and circadian rhythm was analyzed by home cage activity measurements. Circadian rhythm and overall activity of LysM-Dagla^{-/-} mice was similar to Dagla^{fl/fl} controls (two-way ANOVA repeated measurements, Bonferroni's post-hoc test, values represent mean \pm SEM: n = 10 animals/group). (B) LysM-Dagla^{-/-} mice showed no depression-like behavior in the forced swim test. The immobility time did not differ between genotypes (Students t-test, values represent mean \pm SEM: n = 10 animals/group, p = ns). (C) However, LysM-Dagla^{-/-} showed a reduced preference for sucrose compared to control animals (Mann-Whitney U test, values represent mean \pm SEM: n = 10-12 animals/group, p < 0.05). (D) LysM-Dagla^{-/-} animals displayed a normal sociability. The ratio of time spent with a partner mouse to time spent with an empty cage was similar for both genotypes (Student's t-test, values represent mean \pm SEM: n = 10-12 animals/group, p = ns). (E) Preference for the partner mouse was significantly higher in LysM-Dagla^{-/-} and Dagla^{fl/fl} animals (two-way ANOVA, Bonferroni's post-hoc test, values represent mean \pm SEM: n = 10-12 animals/group, **p < 0.01, ***p < 0.001).

The specific deletion of *Dagla* in microglia did not cause a depressive-like behavior in the forced swim and social preference test. However, *LysM-Dagla^{-/-}* showed a significantly reduced sucrose preference.

3.4 Chronic social defeat stress

Several chronic stress models have been established and are widely used to investigate stress-induced depressive-like behavior and molecular adaptations in rodents. Chronic social defeat stress (CSDS) is one of the most commonly applied stress models. Previous studies showed that the lack of CB1 receptors increase the sensitivity to chronic stress in rodents (Martin et al. 2002; Urgüen et al. 2004; Valverde & Torrens 2012). To determine whether the constitutive and neuronal-specific deletion of *Dagla* also leads to an altered stress response, both mouse lines were exposed to chronic social defeat stress. Furthermore, housing conditions prior to the stress paradigm were compared. Intruder mice were either group-housed or single-caged in the two weeks prior to the first social defeat.

3.4.1 Chronic social defeat stress: group-housed intruder

The chronic social defeat paradigm (CSDS) with group-housed intruders was conducted twice with independent cohorts of animals and 10 animals per group. *Dagla^{-/-}* mice and *Dagla^{fl/fl}* mice were exposed to social defeat for 10 days. Subsequently, feces were collected for corticosterone analysis and animals were subjected to different behavioral tests. All behavioral experiments were conducted with intervals of at least two days to prevent any interactions between the tests. Three days after the last behavioral test, brains were collected for molecular analysis and adrenal weights were determined. The exact timeline is depicted in figure 31.

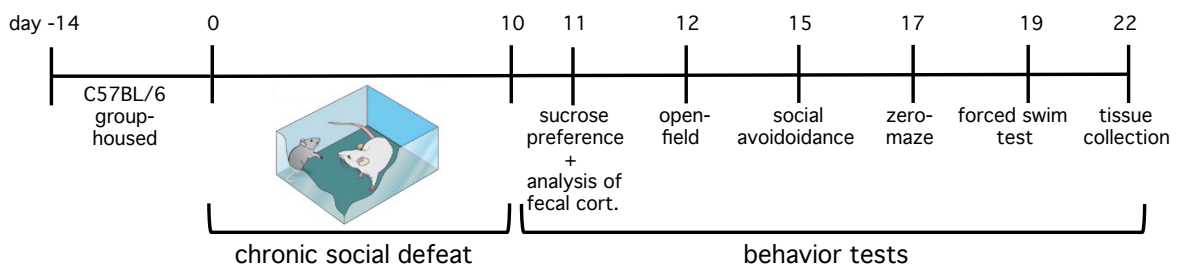


Figure 31: Timeline for the chronic social defeat stress paradigm and following behavioral tests (modified from Krishnan & Nestler 2008).

Approximately 30 % of the *Dagla^{-/-}* animals (3 out of 10 mice in each of the two paradigms) died in the first three days of chronic stress exposure. In contrast, only one out of overall 20 tested *Dagla^{fl/fl}* mice died. The underlying cause of death was uncertain. However,

due to the absence of severe wounds, injuries from fighting can be excluded. In addition, mice never died during the stress exposure (interaction time), but rather died subsequently to the social defeat. This considerable loss of animals led to a final group-size of 14 stressed $Dagla^{-/-}$ mice and 19 stressed $Dagla^{fl/fl}$ animals for molecular and behavioral analysis.

Body weight of $Dagla^{-/-}$ mice and $Dagla^{fl/fl}$ controls was not affected by chronic stress (Fig. 32A). The change in body weight was similar in both genotypes ($F_{(1,65)} = 0.06318$, $p = ns$; Fig. 32A) regardless of the stress paradigm ($F_{(1,65)} = 0.1951$, $p = ns$; Fig. 32A). Furthermore, the adrenal glands were examined. The adrenal glands secrete a variety of hormones and steroids, including the stress hormone cortisol, and therefore represent an important part of the HPA axis. Adrenal weights of $Dagla^{-/-}$ mice were significantly increased after CSDS compared to unstressed knockout mice ($t = 2.644$, $p < 0.05$; Fig. 32B). Significant effects of stress ($F_{(1,65)} = 8.493$, $p < 0.01$) and genotype ($F_{(1,65)} = 10.82$, $p < 0.01$) were detected (Fig. 32B), implying a higher reactivity of $Dagla^{-/-}$ mice to chronic stress. In addition, two-way ANOVA of fecal corticosterone levels revealed a significant stress ($F_{(1,63)} = 20.85$, $p < 0.0001$; Fig. 32C), but no genotype effect ($F_{(1,63)} = 0.02338$, $p = ns$; Fig. 32C). Thus, CSDS increased the release of corticosterone in both $Dagla^{-/-}$ and $Dagla^{fl/fl}$ animals.

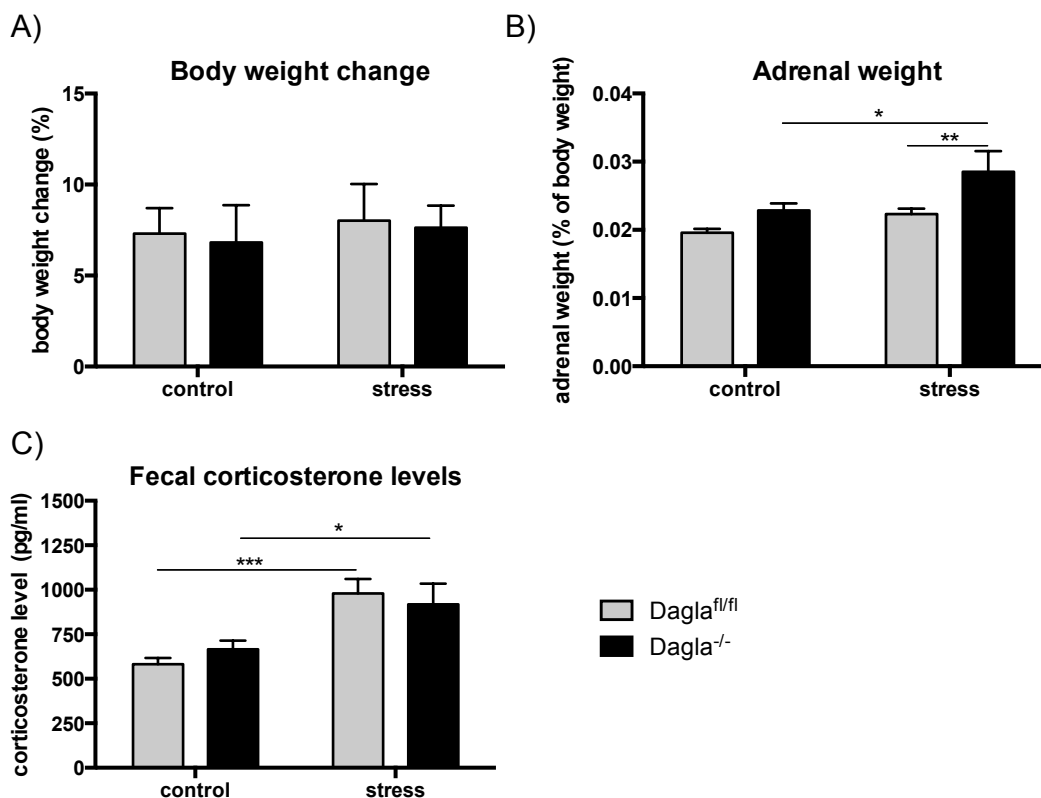


Figure 32: CSDS increased fecal corticosterone levels and adrenal weights, but did not affect the body weight. (A) Body weights were not affected by chronic stress. Change in body weight was similar in both genotypes and groups (two-way ANOVA, Bonferroni's post-hoc test, values represent mean \pm SEM: $n = 14-20$ animals/group, $p = ns$). (B) However, adrenal weights of $Dagla^{-/-}$ mice were significantly increased compared to unstressed animals and stressed $Dagla^{fl/fl}$ mice (two-way ANOVA, Bonferroni's post-hoc test, values represent mean \pm SEM: $n = 12-19$ animals/group, $*p < 0.05$, $**p < 0.01$). (C) In addition, CSDS led to a similar increase of fecal corticosterone levels in $Dagla^{-/-}$ and $Dagla^{fl/fl}$ controls (two-way ANOVA, Bonferroni's post-hoc test, values represent mean \pm SEM: $n = 14-20$ animals/group, $*p < 0.05$, $***p < 0.001$).

Subsequently to the chronic stress paradigm, anxiety- and depression-related behaviors of stressed and control *Dagla^{-/-}* and *Dagla^{fl/fl}* mice were analyzed.

First, anxiety-related behavior was assessed with the open-field and zero-maze tests. Representative results of the first group-housed CSDS experiment are shown (Fig. 33). Since the Open-field ActiMot system (TSE Systems) was not available during the performance of the behavior tests of the second CSDS experiment, the animal tracking software EthoVision[®] XT (Noldus) was utilized. Due to analysis with different software systems the data of both CSDS paradigms could not be pooled. Two-way ANOVA of distance travelled revealed a significant stress ($F_{(1,30)} = 30.80$, $p < 0.0001$; Fig. 33A), but no genotype effect ($F_{(1,30)} = 2.407$, $p = \text{ns}$; Fig. 33A). Chronic stress significantly reduced locomotor activity in *Dagla^{-/-}* mice and *Dagla^{fl/fl}* controls. In addition, time spent in the center of the open-field box was equally reduced in stressed *Dagla^{-/-}* and *Dagla^{fl/fl}* mice (stress effect: $F_{(1,30)} = 5.343$, $p < 0.05$; genotype effect: $F_{(1,30)} = 0.1260$, $p = \text{ns}$; Fig. 33B), indicating increased anxiety. To exclude that altered locomotor activity caused the reduced time in the center of the open-field box, the ratio of time in the center to total time moved was analyzed. Two-way ANOVA revealed neither a main effect of stress nor an genotype effect (stress effect: $F_{(1,30)} = 2.474$, $p = \text{ns}$; genotype effect: $F_{(1,30)} = 0.1355$, $p = \text{ns}$; Fig. 33C).

Anxiety-related behavior was further analyzed in the zero-maze test. Two-way ANOVA of the time spent in the open area revealed a significant effect for genotype ($F_{(1,30)} = 5.043$, $p < 0.05$; Fig. 33D) and genotype x stress interaction ($F_{(1,30)} = 4.190$, $p < 0.05$; Fig. 33D). Chronic stress decreased the time spent in the open area in *Dagla^{-/-}*, but not in *Dagla^{fl/fl}* animals (interaction effect). In addition, unstressed *Dagla^{-/-}* spent more time in the open area compared to *Dagla^{fl/fl}* controls ($t = 3.173$, $p < 0.01$; Fig. 33D). This altered behavior in the zero-maze test was also detected in previous studies (Jenniches et al. 2015; Fig. 16).

Distance travelled in the open area ($F_{(1,30)} = 0.3816$, $p = \text{ns}$; Fig. 33E) and overall distance travelled ($F_{(1,64)} = 0.08651$, $p = \text{ns}$; Fig. 33E) of stressed mice was comparable to unstressed controls. However, *Dagla^{-/-}* mice displayed an increased locomotor activity in this test. Significant genotype effects for distance travelled in the open area ($F_{(1,30)} = 7.741$, $p < 0.01$; Fig. 33E) and overall distance moved ($F_{(1,64)} = 7.924$, $p < 0.01$; Fig. 33F) were observed.

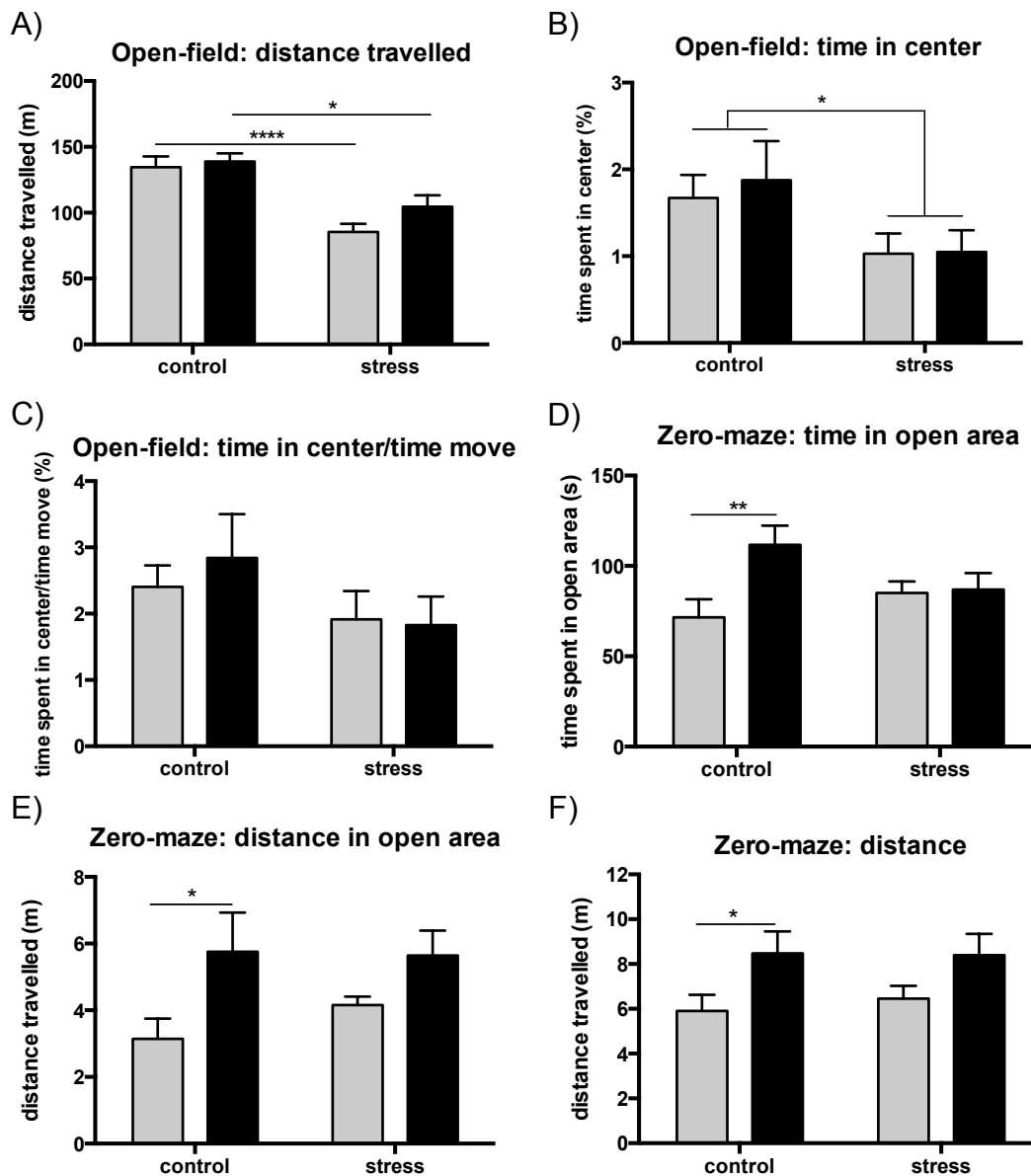


Figure 33: CSDS decreased locomotor activity and led to a mildly increased anxiety-like behavior. (A,B,C) Exploratory and anxiety-related behavior of stressed and unstressed *Dagla*^{-/-} and *Dagla*^{fl/fl} mice was analyzed in the open-field test. (A) Distance travelled was significantly decreased in stressed *Dagla*^{-/-} and *Dagla*^{fl/fl} mice. (B) In addition, time spent exploring the center was markedly reduced in stressed animals. (C) Ratio of time spent in the center to total distance travelled revealed no stress effect, but showed a similar tendency to decreased time spent in the center. (D-F) Anxiety-like behavior was further analyzed in the zero-maze test. (D) Time spent in the open area was not significantly changed by CSDS in *Dagla*^{fl/fl} mice. However, unstressed *Dagla*^{-/-} spent more time in the open area. An interaction between genotype and stress was detected ($F_{(1,30)} = 4.190$, $p < 0.05$), indicating a higher sensitivity of *Dagla*^{-/-} to chronic stress compared to *Dagla*^{fl/fl} controls. (E) Distance travelled in the open area of stressed mice was comparable to unstressed animals. However, distance travelled in the open area was significantly increased in *Dagla*^{-/-} mice compared to controls. This effect was significant in the unstressed, but not in the stressed group. (F) In addition, overall distance travelled was not affected by the stress paradigm. However, *Dagla*^{-/-} mice displayed increased overall distance travelled compared to *Dagla*^{fl/fl} controls. This trend was significant in the unstressed, but not in the stressed group of animals. Statistical analysis: two-way ANOVA, Bonferroni's post-hoc test, values represent mean \pm SEM: $n = 6-10$ animals/group, * $p < 0.05$, ** $p < 0.01$; **** $p < 0.0001$.

CSDS decreased the locomotor activity and caused a mild anxiety-like phenotype in the open-field test in *Dagla*^{-/-} and *Dagla*^{fl/fl} animals. In contrast, the zero-maze test revealed no stress-related changes in locomotion, but an increased anxiety-like behavior in *Dagla*^{-/-}

mice. A significant interaction between genotype and stress was detected, indicating a higher stress-sensitivity of *Dagla*^{-/-} mice.

Next, general activity and circadian rhythm were analyzed by home cage activity measurements. Both mouse lines displayed normal time-dependent changes in locomotor activity (circadian rhythm) after chronic stress. No significant stress effects were detected for *Dagla*^{-/-} mice (stress effect: $F_{(1,26)} = 0.1257$, $p = \text{ns}$; Fig. 34A) and *Dagla*^{fl/fl} animals (stress effect: $F_{(1,28)} = 0.8572$, $p = \text{ns}$; Fig. 34B). For the *Dagla*^{-/-} group, a significant stress x time interaction was observed ($F_{(67, 1742)} = 1.437$, $p < 0.05$; Fig. 34A), indicative of an altered activity distribution after CSDS. *Dagla*^{-/-} mice displayed a slightly shifted day/night cycle after chronic stress.

Furthermore, *Dagla*^{-/-} mice had an increased activity in the dark and a decreased activity in the light phase compared to *Dagla*^{fl/fl} controls. Significant genotype effects for mean activity during the dark ($F_{(1,56)} = 4.332$, $p < 0.05$; Fig. 34C) and the light phase ($F_{(1,26)} = 4.119$, $p < 0.05$; Fig. 34D) were observed. However, no stress effects were detected (dark: $F_{(1,56)} = 0.1850$, $p = \text{ns}$; Fig. 34C; light: $F_{(1,56)} = 1.942$, $p = \text{ns}$; Fig. 34D).

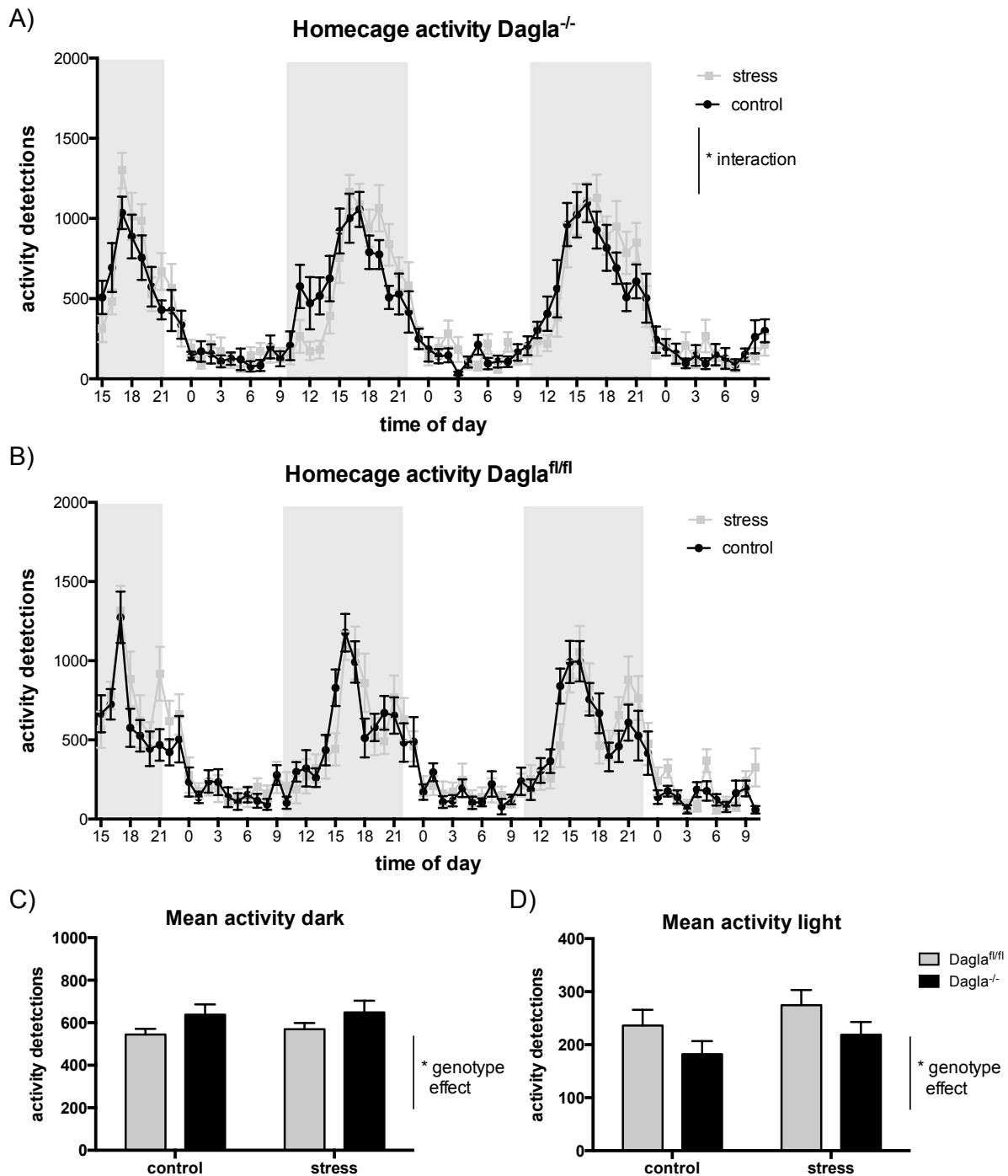


Figure 34: CSDS altered the home cage activity of $Dagla^{-/-}$, but not $Dagla^{fl/fl}$ mice. (A,B) Locomotor activity and circadian rhythm was analyzed by home cage activity measurements. (A) Circadian rhythm and overall activity of stressed $Dagla^{-/-}$ mice was similar to unstressed controls. However, a significant interaction between stress and time of day was detected (two-way ANOVA repeated measurements, Bonferroni's post-hoc test, values represent mean \pm SEM: $n = 14-15$ animals/group, $*p < 0.05$). (B) CSDS did not alter the home cage activity of $Dagla^{fl/fl}$ mice (two-way ANOVA repeated measurements, Bonferroni's post-hoc test, values represent mean \pm SEM: $n = 14-15$ animals/group). (C) $Dagla^{-/-}$ had a generally increased activity during the dark phase and (D) light phase compared to $Dagla^{fl/fl}$ controls regardless of the stress paradigm (two-way ANOVA, Bonferroni's post-hoc test, values represent mean \pm SEM: $n = 14-15$ animals/group, $*p < 0.05$).

Finally depression-related behavior was analyzed in the social avoidance, forced swim and social preference tests. Social avoidance was determined by analyzing the time spent interacting with a foreign CD1 mouse. This test was conducted with one cohort of animals.

Chronic stress significantly reduced the time spent with the CD1 mouse in *Dagla^{-/-}* and *Dagla^{fl/fl}* mice ($F_{(1,31)} = 20.31$, $p < 0.0001$; Fig. 35A), indicative of social avoidance behavior. Consequently, CSDS induced social avoidance in defeated mice. In addition, *Dagla^{-/-}* animals spent less time interacting with the CD1 mice regardless of the stress paradigm (genotype effect: $F_{(1,31)} = 8.382$, $p < 0.01$; Fig. 35A). This result support the notion that untreated (unstressed) *Dagla^{-/-}* mice displayed an anxiety-like phenotype. Furthermore, two-way ANOVA of distance travelled revealed a significant stress effect ($F_{(1,32)} = 8.917$, $p < 0.01$; Fig. 35B), but no genotype effect ($F_{(1,32)} = 0.5620$, $p = \text{ns}$; Fig. 35B). Chronic stress reduced the locomotor activity in both genotypes. To exclude that the generally decreased distance travelled influenced the outcome of the social avoidance test, the ratio of time spent interacting with the CD1 mouse to distance travelled was determined (Fig. 35C). This analysis also revealed a significant genotype effect ($F_{(1,32)} = 4.381$, $p < 0.05$; Fig. 35C). However, the stress effect missed significance ($F_{(1,32)} = 3.305$, $p = 0.0784/\text{ns}$; Fig. 35C). Thus, the detected social avoidance behavior is not solely arising from the decreased locomotor activity.

Next, anhedonia was analyzed in the sucrose preference test. Sucrose preference of stressed mice was comparable to unstressed controls. No significant stress effect was detected, using two-way ANOVA ($F_{(1,64)} = 0.01105$, $p = \text{ns}$; Fig. 35C). However, in line with the results shown in chapter 3.1.5, *Dagla^{-/-}* mice had a reduced sucrose preference compared to *Dagla^{fl/fl}* controls regardless of the treatment (genotype effect: $F_{(1,64)} = 10.66$, $p < 0.001$; Fig. 35D).

Finally, depressive-like behavior was determined in the forced swim test. Immobility time was alike for stressed and unstressed animals (stress effect: $F_{(1,66)} = 0.7841$, $p = \text{ns}$; Fig. 35E). However, *Dagla^{-/-}* animals spent significantly more time immobile regardless of the stress paradigm. Two-way ANOVA revealed a significant genotype effect ($F_{(1,66)} = 30.08$, $p = \text{ns}$; Fig. 35E), but no stress x genotype interaction ($F_{(1,66)} = 0.02214$, $p = \text{ns}$; Fig. 35E). On the one hand these results show that *Dagla^{-/-}* mice displayed a depressive-like behavior in this test, and on the other hand that CSDS did not induce depression-related phenotypes.

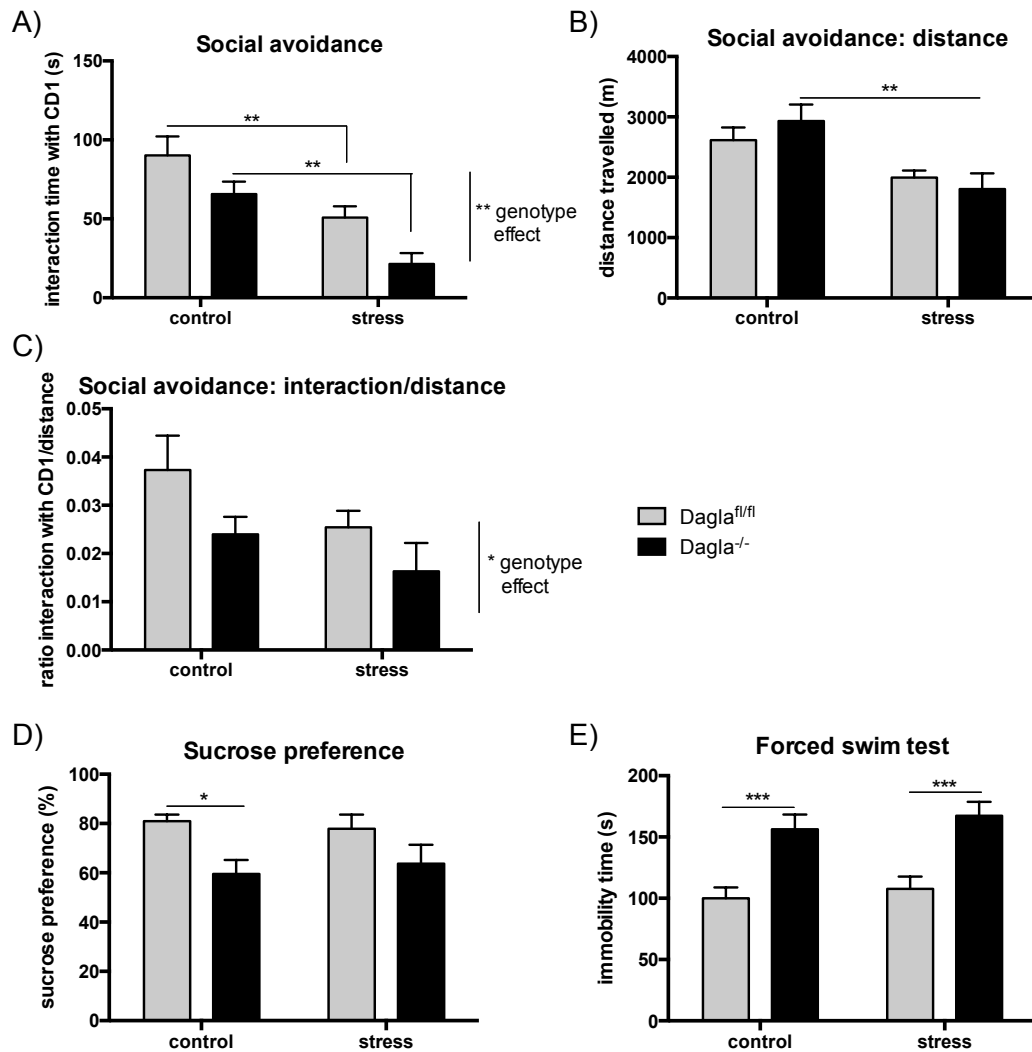


Figure 35: CSDS induced social avoidance, but no depressive-like phenotype. (A) CSDS induced social avoidance behavior in *Dagla^{-/-}* mice and *Dagla^{fl/fl}* controls. In addition, *Dagla^{-/-}* mice spent generally less time interacting with the CD1 mouse, indicating an increased anxiety-like behavior. (B) Overall distance travelled was similarly reduced in both genotypes after chronic stress. (C) Ratio of time spent interacting with the CD1 mouse to distance travelled was not altered after chronic stress. However, the trend was similar to 33A. Again a significant genotype effect was detected showing an overall decreased time of interaction in *Dagla^{-/-}* mice compared to *Dagla^{fl/fl}* controls. Statistical analysis of the social avoidance test: two-way ANOVA, Bonferroni's post-hoc test, values represent mean \pm SEM: $n = 8-10$ animals/group, * $p < 0.05$, ** $p < 0.01$. (D) Anhedonia was assessed by sucrose preference. Sucrose preference of stressed *Dagla^{-/-}* and *Dagla^{fl/fl}* animals was similar to unstressed mice. However, sucrose preference of unstressed *Dagla^{-/-}* mice was significantly decreased compared to *Dagla^{fl/fl}* controls (two-way ANOVA, Bonferroni's post-hoc test, values represent mean \pm SEM: $n = 14-20$ animals/group, * $p < 0.05$). (E) Immobility times of stressed *Dagla^{-/-}* and *Dagla^{fl/fl}* mice were comparable to unstressed animals. However, immobility time of *Dagla^{-/-}* animals was significantly increased compared to *Dagla^{fl/fl}* controls regardless of the stress paradigm (two-way ANOVA, Bonferroni's post-hoc test, values represent mean \pm SEM: $n = 14-20$ animals/group, *** $p < 0.001$).

Analysis of stressed *Dagla^{-/-}* and *Dagla^{fl/fl}* mice revealed that CSDS caused considerable behavioral alterations, especially increased anxiety and social avoidance. In addition, fecal corticosterone levels and adrenal weights were markedly increased after chronic stress. To determine the underlying molecular mechanisms, gene expression was analyzed.

Expression of genes related to the ECS and the HPA axis, were analyzed in amygdala, hippocampus and paraventricular nucleus of the hypothalamus (PVN). All of these brain regions are involved in emotional processing and stress response.

Quantification of amygdalar mRNA levels revealed no stress-dependent regulation of *Dagla* in *Dagla^{fl/fl}* animals ($t = 1.746$, $p = 0.1113$; Fig. 36A). Furthermore, gene expression of *Daglb* ($F_{(1,18)} = 3.236$, $p = \text{ns}$; Fig. 36B) and *CB1* ($F_{(1,17)} = 0.01174$, $p = \text{ns}$; Fig. 36C) in the amygdala of stressed *Dagla^{-/-}* and *Dagla^{fl/fl}* mice was comparable to unstressed animals.

Preceding analysis of glucocorticoids showed a stress-induced increase of fecal corticosterone levels in *Dagla^{-/-}* and *Dagla^{fl/fl}* mice, indicative of a dysregulated HPA axis. Therefore, gene expression of the glucocorticoid receptor (GR) was determined. The GR is an important regulator of the HPA axis, mediating the negative feedback mechanism of corticosterone. In addition, GR is often dysregulated in depression. GR expression was not affected by the stress paradigm ($F_{(1,17)} = 0.001051$, $p = \text{ns}$; Fig. 36D), but was significantly reduced in the amygdala of *Dagla^{-/-}* animals compared to *Dagla^{fl/fl}* controls ($F_{(1,17)} = 13.79$, $p < 0.01$; Fig. 36D).

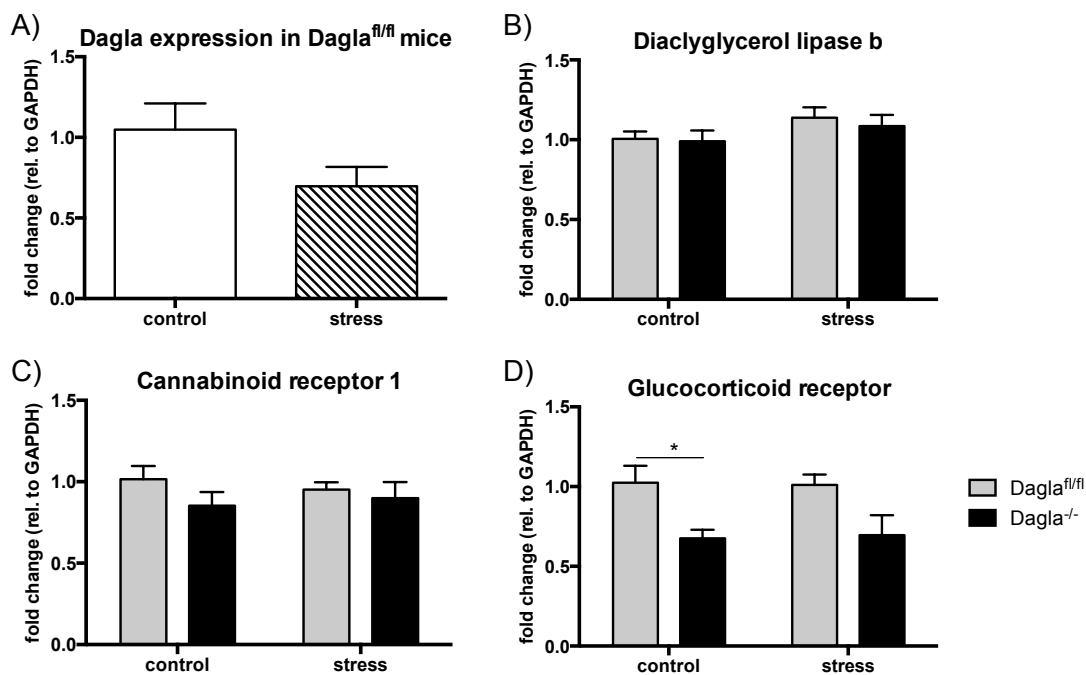


Figure 36: Gene expression analysis of the amygdala. (A-D) Shown are mRNA levels normalized to GAPDH. (A) Real-time RT-PCR results showed no significant stress-dependent regulation of *Dagla* in *Dagla^{fl/fl}* animals. However, results showed a trend towards downregulation of *Dagla* (Students t-test, values represent mean \pm SEM: $n = 4-6$ animals/group, $p = 0.1113/ \text{ns}$). (B) *Daglb* mRNA levels did not differ between stressed and unstressed animals. (C) Similar *CB1* receptor gene expression levels were detected in the amygdala of stressed and unstressed *Dagla^{-/-}* and *Dagla^{fl/fl}* mice. (D) However, glucocorticoid receptor mRNA was significantly reduced in *Dagla^{-/-}* mice compared to controls regardless of the stress paradigm. In addition, CSDS did not influence GR expression. Statistical analysis: two-way ANOVA, Bonferroni's post-hoc test, values represent mean \pm SEM: $n = 4-6$ animals/group, $*p < 0.05$.

Next, hippocampal gene expression was determined. Real-time RT-PCR results showed no stress-dependent changes of *Dagla* expression in the hippocampus of *Dagla^{fl/fl}*

mice ($t = 0.3722$, $p = \text{ns}$; Fig. 37A). The stress paradigm did also not affect CB1 receptor mRNA levels in none of the genotypes (stress effect: $F_{(1,18)} = 1.959$, $p = \text{ns}$; genotype effect: $F_{(1,18)} = 0.09311$, $p = \text{ns}$ Fig. 37B). To further analyze the HPA axis, GR gene expression was determined. Two-way ANOVA of hippocampal GR mRNA revealed no stress effect ($F_{(1,16)} = 0.1546$, $p = \text{ns}$; Fig. 37C). However, GR expression was significantly reduced in $Dagla^{-/-}$ mice compared to $Dagla^{fl/fl}$ animals ($F_{(1,16)} = 4.813$, $p < 0.05$; Fig. 37C). This result is in line with the reduced GR mRNA levels in the amygdala of $Dagla^{-/-}$ mice (Fig. 36D). Furthermore, gene expression of the brain-derived neurotrophic factor (BDNF) was analyzed. BDNF is a member of the nerve growth factor family, and is widely expressed in the adult mammalian brain. It plays a critical role in the regulation of survival, differentiation, and maintenance of different neuronal populations and has neuroprotective functions (for review see Park & Poo 2013). In addition, BDNF signaling is important for the development of molecular and behavioral manifestations of chronic social defeat stress (Berton et al. 2006). However, BDNF gene expression was not differentially regulated by the stress paradigm. Two-way ANOVA revealed no stress and no genotype effects (stress effect: $F_{(1,17)} = 0.8742$, $p = \text{ns}$; genotype effect: $F_{(1,17)} = 0.1990$, $p = \text{ns}$ Fig. 37D).

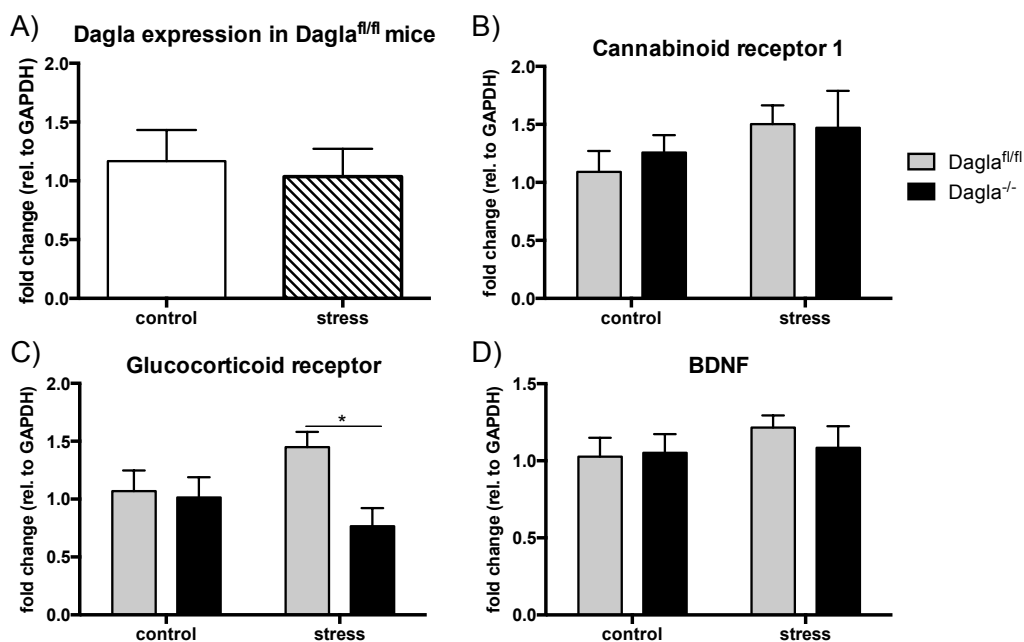


Figure 37: Gene expression analysis of the hippocampus. (A-E) Shown are mRNA levels normalized to GAPDH. (A) Real-time RT-PCR results showed no significant regulation of *Dagla* in $Dagla^{fl/fl}$ animals after CSDS (Students t-test, values represent mean \pm SEM: $n = 5$ animals/group, $p = \text{ns}$). (B) CB1 receptor gene expression of stressed $Dagla^{-/-}$ and $Dagla^{fl/fl}$ mice did not differ from unstressed animals. (C) Glucocorticoid receptor mRNA was significantly reduced in $Dagla^{-/-}$ mice compared to $Dagla^{fl/fl}$ controls regardless of the stress paradigm. In addition, CSDS did not influence GR expression. (D) mRNA levels of BDNF were similar for all four groups. (B-D) Statistical analysis: two-way ANOVA, Bonferroni's post-hoc test, values represent mean \pm SEM: $n = 5-6$ animals/group, * $p < 0.05$.

Finally, gene expression analysis of whole mRNA of the PVN of stressed and unstressed $Dagla^{-/-}$ and $Dagla^{fl/fl}$ mice were conducted. The PVN of the hypothalamus

controls a large part of stress responses and is an important regulator of the HPA axis. Thus, several genes related to the HPA axis were analyzed in detail. GR mRNA levels were significantly reduced in the PVN of *Dagla*^{-/-} mice compared to *Dagla*^{fl/fl} animals ($F_{(1,14)} = 5.029$, $p < 0.05$; Fig. 38A). However, no main effect for stress was detected ($F_{(1,14)} = 4.029$, $p = 0.0626$; Fig. 38A).

To further characterize the HPA axis activity, gene expression of the corticotropin-releasing hormone (CRH) and the corticotropin-releasing hormone receptor 1 (CRHR1) were determined. CRH is synthesized and released by the PVN of the hypothalamus and represents the first activator of the HPA axis. By binding to CRHR1, which is mainly expressed in the anterior pituitary, PVN, amygdala and hippocampus, CRH induces the production of adrenocorticotrophic hormone (ACTH). Gene expression analysis of CRH revealed no significant stress ($F_{(1,13)} = 0.006632$, $p = \text{ns}$; Fig. 38B) and genotype effects ($F_{(1,13)} = 0.3961$, $p = \text{ns}$; Fig. 38B). However, variances between animals were rather high and further experiments are necessary to draw a final conclusion. Additionally, mRNA levels of CRHR1 were similar in *Dagla*^{-/-} and *Dagla*^{fl/fl} animals ($F_{(1,13)} = 0.2248$, $p = \text{ns}$; Fig. 38C) and CRHR1 was not differentially expressed after chronic stress ($F_{(1,13)} = 1.812$, $p = \text{ns}$; Fig. 38C).

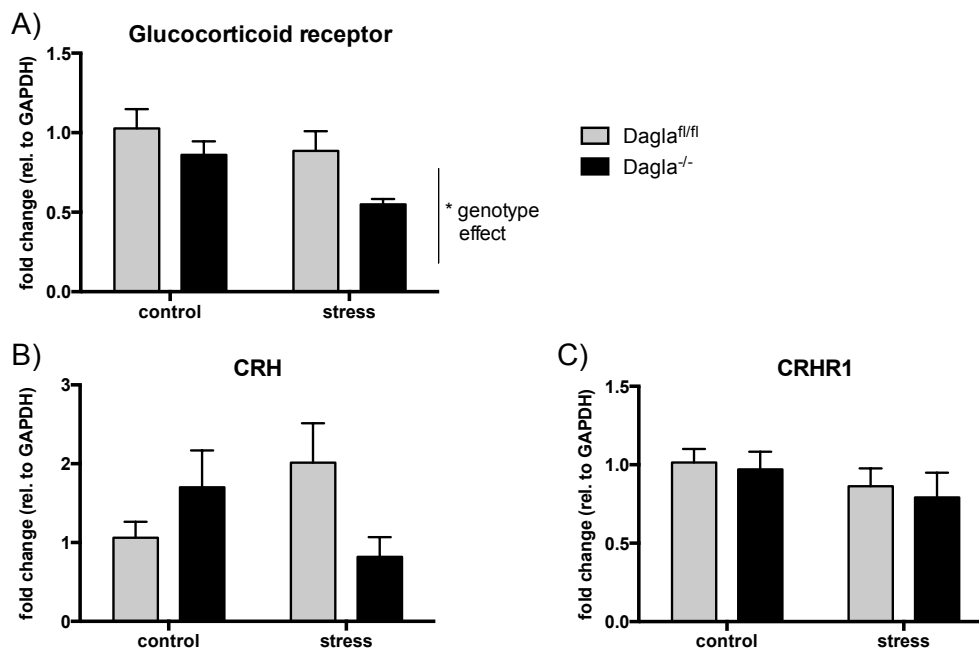


Figure 38: Gene expression analysis of the PVN. (A-D) Shown are mRNA levels normalized to GAPDH. (A) Glucocorticoid receptor mRNA was significantly reduced in *Dagla*^{-/-} mice compared to *Dagla*^{fl/fl} controls. In addition, a clear tendency towards stress-dependent decrease of GR expression was detected in both genotypes. (B) mRNA levels of CRH were similar in both genotypes and not affected by the stress paradigm. (C) CRHR1 gene expression levels of stressed mice were similar to unstressed animals. Statistical analysis: two-way ANOVA, Bonferroni's post-hoc test, values represent mean \pm SEM; $n = 3-5$ animals/group, * $p < 0.05$.

Molecular and behavioral analysis of chronically stressed *Dagla*^{-/-} and *Dagla*^{fl/fl} animals revealed increased anxiety-like behaviors, social avoidance and increased fecal

corticosterone levels in both genotypes. Nevertheless, CSDS did not result in depressive-like behaviors. In addition, GR gene expression was significantly decreased in different brain areas of control and stressed *Dagla*^{-/-} mice. Other genes typically regulated by chronic stress, such as BDNF, were not affected.

To increase the sensitivity to chronic stress, animals were single-caged for two weeks before the CSDS paradigm. Results of this experiment are described in the following part of the result section.

3.4.2 Chronic social defeat stress: single-housed intruder

The chronic social defeat paradigm with single-housed intruder mice was conducted once with *Dagla*^{fl/fl}, *Syn-Dagla*^{-/-} and constitutive *Dagla*^{-/-} animals (9-10 animals per group). The stress paradigm, all behavioral tests and tissue collection were performed as described in chapter 3.4.1 (see Fig. 31). C57BL/6 intruder mice were single-caged for two weeks before the first social defeat. As in the group-housed CSDS paradigm (Chapter 3.4.1), several stressed animals died during the first days of stress. Three *Dagla*^{-/-} mice, one *Syn-Dagla*^{-/-} and one *Dagla*^{fl/fl} animal did not survive the 10 days of CSDS. Yet again, none of the deceased animals had severe wounds. Thus, cause of death is uncertain. This considerable loss of animals led to final group sizes of 6 to 10 animals per group.

First, body weights were determined. Chronically stressed mice lost approximately 2 % of their body weight, whereas unstressed mice gained an average of 1-2 %. Two-way ANOVA of changes in body weight revealed a significant stress effect ($F_{(1,41)} = 7.231$, $p < 0.05$; Fig. 39A), but no genotype effect ($F_{(2,41)} = 0.09111$, $p = \text{ns}$; Fig. 39A). Furthermore, adrenal weights were analyzed. Adrenal weights of stressed animals were comparable to unstressed mice ($F_{(1,40)} = 0.001852$, $p = \text{ns}$; Fig. 39B). However, a significant genotype effect was observed ($F_{(2,40)} = 6.455$, $p < 0.01$; Fig. 39B). Adrenal weights of unstressed *Dagla*^{-/-} mice were significantly higher compared to *Dagla*^{fl/fl} ($t = 3.473$, $p < 0.01$) and *Syn-Dagla*^{-/-} animals ($t = 3.965$, $p < 0.001$), indicative of an imbalanced HPA axis and increased stress hormone release. Analysis of fecal corticosterone levels revealed an increased corticosterone content in *Dagla*^{-/-} animals, but not in *Syn-Dagla*^{-/-} and *Dagla*^{fl/fl} mice after CSDS. A significant stress effect ($F_{(1,33)} = 5.584$, $p < 0.05$; Fig. 39C) and stress x genotype interaction ($F_{(2,33)} = 3.566$, $p < 0.05$; Fig. 39C) was detected. Fecal corticosterone levels of stressed *Dagla*^{-/-} mice were increased compared to both unstressed *Dagla*^{-/-} mice ($t = 3.355$, $p < 0.01$) and stressed *Syn-Dagla*^{-/-} ($t = 2.685$, $p < 0.05$) animals. These results indicate an elevated stress-sensitivity of *Dagla*^{-/-} mice.

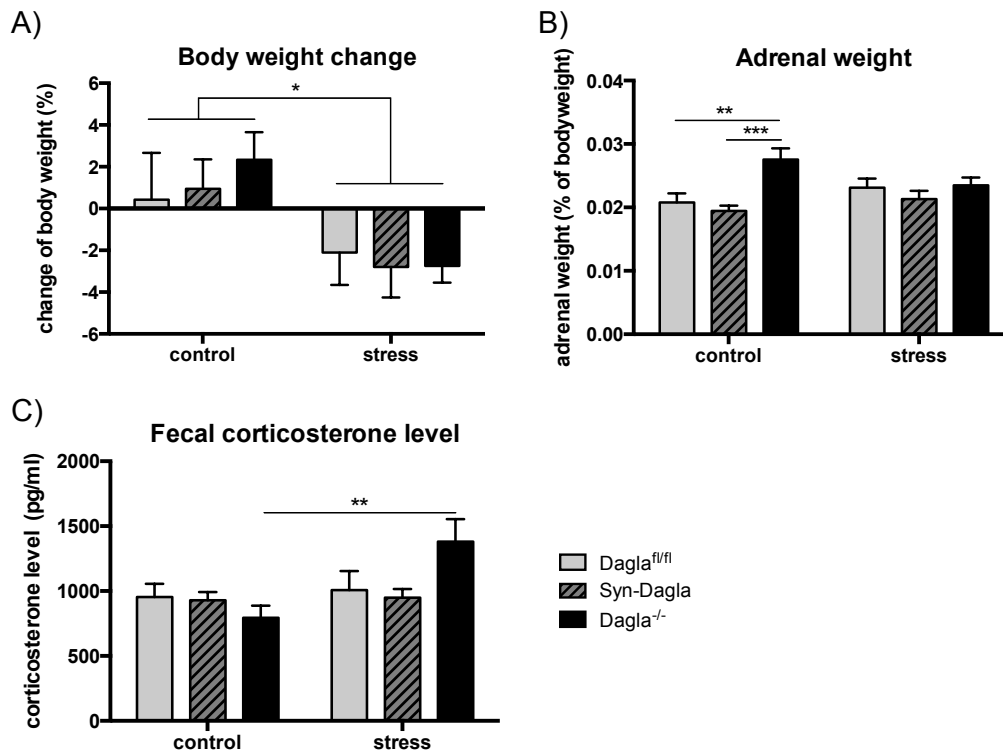


Figure 39: CSDS decreased body weight and increased fecal corticosterone levels in Dagla^{-/-} mice. (A) Body weight was significantly decreased after CSDS regardless of the genotype, leading to a significant stress effect (two-way ANOVA, Bonferroni's post-hoc test, values represent mean ± SEM: n = 6-10 animals/group, *p < 0.05). (B) Adrenal weight was not affected by the stress paradigm. However, adrenal weights of unstressed Dagla^{-/-} mice were significantly increased compared to unstressed Dagla^{fl/fl} and Syn-Dagla^{-/-} mice (two-way ANOVA, Bonferroni's post-hoc test, values represent mean ± SEM: n = 6-10 animals/group, **p < 0.01, ***p < 0.001). (C) In addition, CSDS led to increased of fecal corticosterone levels in Dagla^{-/-}, but not in Dagla^{fl/fl} and Syn-Dagla^{-/-} mice (two-way ANOVA, Bonferroni's post-hoc test, values represent mean ± SEM: n = 5-7 animals/group, **p < 0.01).

Subsequent to the chronic stress, animals were analyzed in different anxiety- and depression-related behavioral tests. First, locomotor activity and anxiety-like behaviors were analyzed in the open-field test. In this run, instead of Open-field ActiMot system (TSE Systems), the animal tracking software EthoVision[®] XT (Noldus) was utilized. Therefore, the direct comparison to previously performed open-field tests is not feasible.

Distance travelled and time spent in the center of stressed animals was comparable to unstressed controls. No stress effects for distance travelled ($F_{(1,41)} = 0.01160$, $p = \text{ns}$; Fig. 40A) and time spent in the center ($F_{(1,41)} = 1.439$, $p = \text{ns}$; Fig. 40B) were detected, using two-way ANOVA. Locomotor activities and anxiety-related behaviors were not affected by the chronic stress paradigm. Though, Syn-Dagla^{-/-} mice spent generally less time exploring the center of the open-field box (genotype effect: $F_{(2,41)} = 3.463$, $p < 0.05$; Fig. 40B), indicative of an anxiety-like phenotype.

Anxiety-like behavior was further analyzed in the zero-maze test. Two-way ANOVA revealed no stress effects for the time in the open area ($F_{(1,41)} = 2.502$, $p = \text{ns}$; Fig. 40C), distance travelled in the open area ($F_{(1,41)} = 0.7489$, $p = \text{ns}$; Fig. 40C) and overall distance travelled ($F_{(1,41)} = 1.116$, $p = \text{ns}$; Fig. 40C). However, unstressed Dagla^{-/-} mice spent more

time in the open area compared to unstressed $Dagla^{fl/fl}$ ($t = 3.012$, $p < 0.05$; Fig. 40C) and unstressed $Syn-Dagla^{-/-}$ ($t = 2.866$, $p < 0.05$; Fig. 40C) mice. This indicates a decreased anxiety-like phenotype of mice constitutively lacking $Dagla$. In addition, CSDS significantly reduced the time spent in the open area of $Dagla^{-/-}$ animals compared to unstressed $Dagla^{-/-}$ mice ($t = 2.54$, $p < 0.05$; Fig. 40C), indicating a stress-induced anxiety-like behavior. Overall distance travelled was not changed in stressed $Dagla^{-/-}$ mice compared to unstressed $Dagla^{-/-}$ animals ($t = 0.8716$, $p = ns$; Fig. 40E). In contrast, all three measures were unaffected in $Dagla^{fl/fl}$ and $Syn-Dagla^{-/-}$ mice.

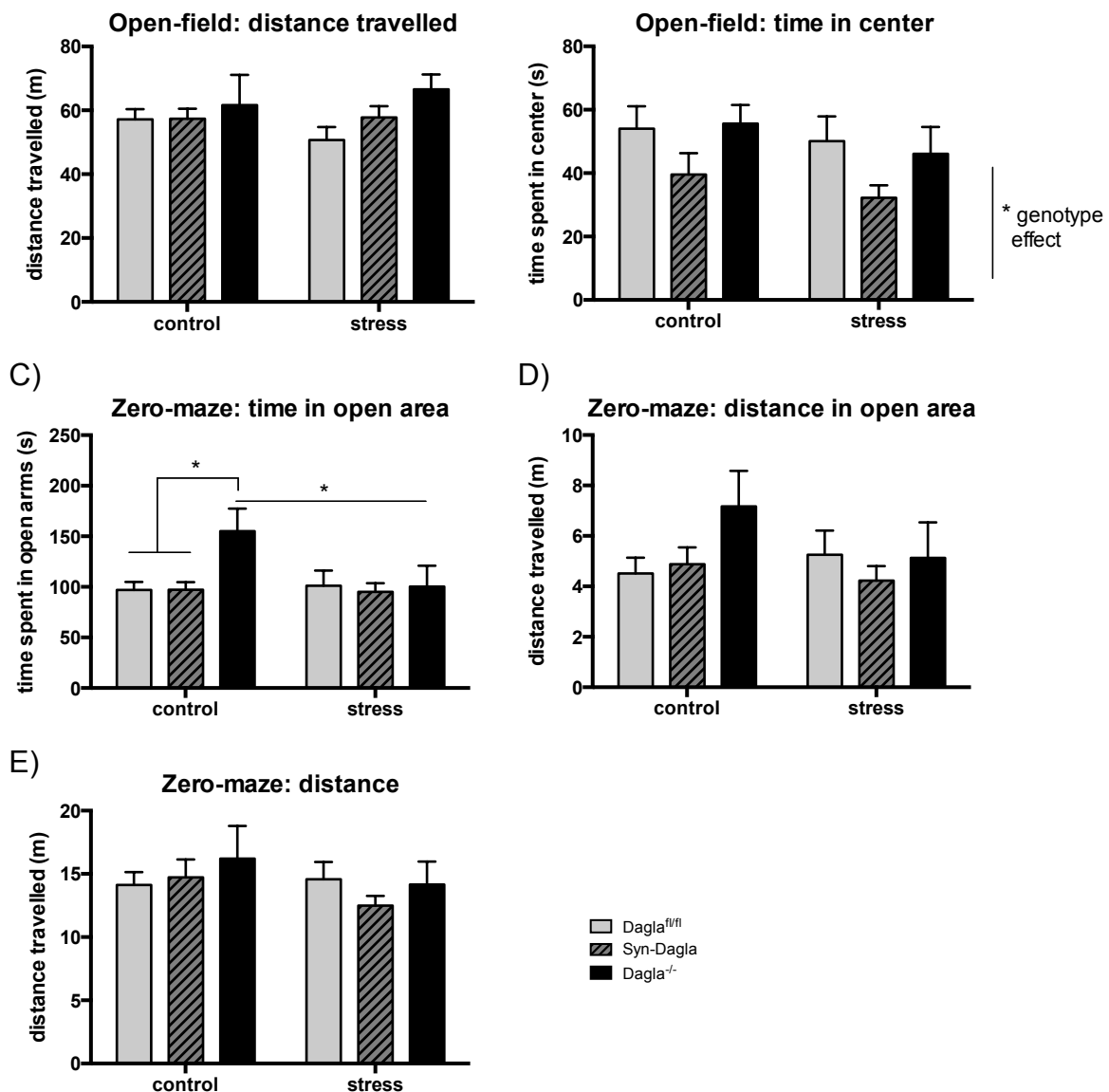


Figure 40: CSDS did not alter locomotor activity, but induced anxiety-like behavior in $Dagla^{-/-}$ mice. (A,B) Exploratory and anxiety-related behaviors of stressed and unstressed $Dagla^{-/-}$, $Syn-Dagla^{-/-}$ and $Dagla^{fl/fl}$ mice were analyzed in the open-field test. (A) Distance travelled of stressed animals was similar to unstressed controls regardless of the genotype. (B) In addition, time spent exploring the center was not altered in stressed animals. However, $Syn-Dagla^{-/-}$ spent generally less time exploring the center of the open-field. (C-E) Anxiety-like behavior was further analyzed in the zero-maze test. (C) Time spent in the open area was not significantly changed by CSDS in $Dagla^{fl/fl}$ and $Syn-Dagla^{-/-}$ mice. However, unstressed $Dagla^{-/-}$ spent more time in the open area and CSDS significantly reduced the time spent in the open area in stressed $Dagla^{-/-}$ mice. (D) Distance travelled in the open area was not altered in stressed $Dagla^{-/-}$, $Syn-Dagla^{-/-}$ and $Dagla^{fl/fl}$ mice compared to unstressed animals.

(E) In addition, overall distance travelled was similar for stressed and unstressed mice. Statistical analysis: two-way ANOVA, Bonferroni's post-hoc test, values represent mean \pm SEM: n = 6-10 animals/group, *p < 0.05.

Moreover, locomotor activity and circadian rhythm were analyzed via home cage activity measurements. For *Dagla^{fl/fl}* animals, similar time-dependent alterations in home cage activity were observed in stressed and unstressed animals. Neither a stress effect ($F_{(1,8)} = 4.069$, $p = \text{ns}$) nor a stress x time interaction ($F_{(88,704)} = 1.289$, $p = \text{ns}$; Fig. 41A) was distinguished. Thus, CSDS did not alter the overall home cage activity and the circadian rhythm of these mice. In contrast, chronic stress significantly increased the activity of *Dagla^{-/-}* (stress effect: $F_{(1,5)} = 15.28$, $p < 0.05$; Fig. 41B) and *Syn-Dagla^{-/-}* mice (stress effect: $F_{(1,5)} = 5.943$, $p < 0.05$; Fig. 41C) compared to unstressed animals of the same genotype. A significant stress x time interaction was detected for *Dagla^{-/-}* mice ($F_{(88,440)} = 3.149$, $p < 0.0001$; Fig. 41B), but not for *Syn-Dagla^{-/-}* ($F_{(88,704)} = 3.149$, $p = \text{ns}$; Fig. 41C). Thus, CSDS not only increased the locomotor activity, but also altered the distribution of motor activity in *Dagla^{-/-}* mice.

Two-way ANOVA of mean activity during dark and light phase revealed significant stress effects (dark: $F_{(1,21)} = 16.16$, $p < 0.001$; Fig. 41D; light: $F_{(1,21)} = 19.93$, $p < 0.001$ Fig. 41E), but no genotype effects (dark: $F_{(2,21)} = 0.08755$, $p = \text{ns}$; Fig. 41D; light: $F_{(2,21)} = 2.511$, $p = \text{ns}$; Fig. 41E). Thus, chronic stress increased the overall activity both during the active and inactive phase of the animals. This effect was significant for *Dagla^{-/-}* mice in the dark phase ($t = 4.148$, $p < 0.01$; Fig. 41D) and for *Dagla^{fl/fl}* ($t = 3.122$, $p < 0.05$; Fig. 41E) and *Syn-Dagla^{-/-}* mice ($t = 2.808$, $p < 0.05$; Fig. 41E) in the light phase compared to unstressed animals of the same genotype.

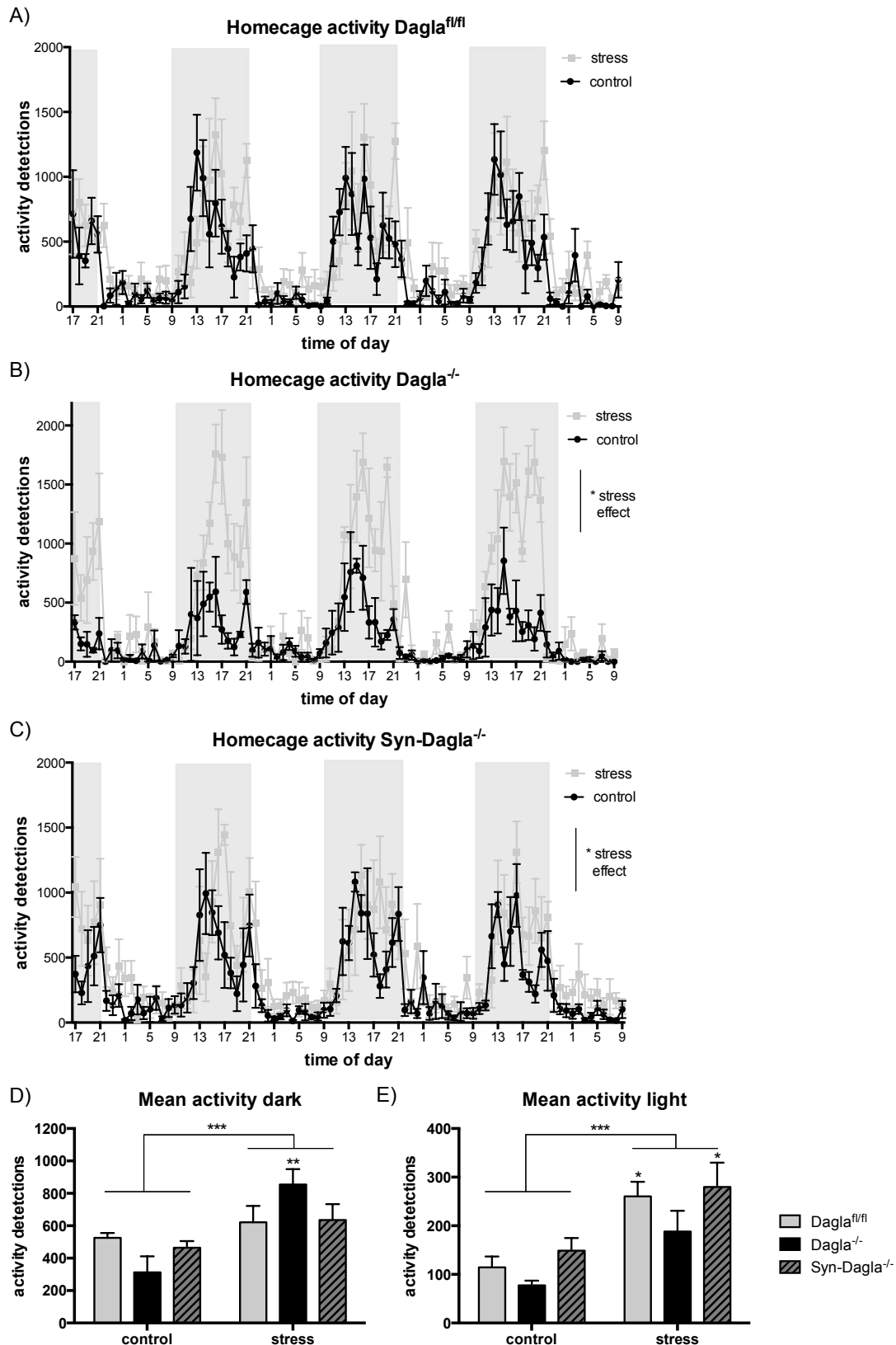


Figure 41: Chronic stress significantly increased overall activity in the home cage, but did not affect the circadian rhythm. (A-E) Locomotor activity and circadian rhythm were analyzed by home cage activity measurements. (A) Circadian rhythm and overall activity of stressed *Dagla^{fl/fl}* mice was similar to unstressed controls. (B,C) Chronic stress significantly increased the activity of *Dagla^{-/-}* and *Syn-Dagla^{-/-}* mice compared to unstressed animals of the same genotype (A-C: Statistical analysis: two-way ANOVA repeated measurements, Bonferroni's post-hoc test, values represent mean \pm SEM; n = 4-5 animals/group, *p < 0.05). (D,E) Mean activities during dark and light phase were significantly increased after stress in *Syn-Dagla^{-/-}* and *Dagla^{-/-}* mice. Statistical analysis: two-way ANOVA, Bonferroni's post-hoc test, values represent mean \pm SEM; n = 4-5 animals/group, *p < 0.05, **p < 0.01, ***p < 0.001).

Depression-related behavior was analyzed in the social avoidance, sucrose preference and forced swim tests. At first, animals were subjected to the social avoidance test, in which the interaction time with a foreign CD1 mouse is negatively correlated to social avoidance behavior. CSDS decreased the interaction time with the CD1 mice in all tested genotypes (stress effect: $F_{(1,41)} = 8.221$, $p < 0.001$; genotype effect: $F_{(2,41)} = 1.396$, $p = \text{ns}$; Fig. 42A), indicative of social avoidance and increased anxiety. In addition, the distance travelled of $Dagla^{-/-}$, $\text{Syn-Dagla}^{-/-}$ and $Dagla^{\text{fl/fl}}$ mice was not altered after chronic stress (stress effect: $F_{(1,41)} = 0.4619$, $p = \text{ns}$; Fig. 42B).

Furthermore, a sucrose preference test was conducted to analyze anhedonic-behavior. Two-way ANOVA revealed no stress effect ($F_{(1,41)} = 0.6038$, $p = \text{ns}$; Fig. 42C). CSDS did not decrease the preference for sucrose solution in neither of the $Dagla$ knockout mouse lines ($Dagla^{-/-}$, $\text{Syn-Dagla}^{-/-}$) nor in $Dagla^{\text{fl/fl}}$ controls.

Depression-related behavior was further determined in the forced swim test. Immobility times of stressed $\text{Syn-Dagla}^{-/-}$ and $Dagla^{-/-}$ mice were comparable to unstressed animals. In contrast, $Dagla^{\text{fl/fl}}$ mice showed an increased immobility time after CSDS, but the stress effect barely missed significance ($F_{(1,39)} = 3.368$, $p = 0.0741$; Fig. 42D). However, a direct comparison of unstressed and stressed $Dagla^{\text{fl/fl}}$ animals revealed a significantly increased immobility time in stressed animals ($t = 2.649$, $p < 0.05$; Fig. 42E). Thus, CSDS caused a depressive-like behavior of $Dagla^{\text{fl/fl}}$ mice. As previously described (Chapter 3.1.5, 3.2.4), $Dagla^{-/-}$ and $\text{Syn-Dagla}^{-/-}$ mice displayed an increased immobility time compared to $Dagla^{\text{fl/fl}}$ controls. This baseline depressive-like phenotype impedes the detection of stress-dependent effects in both $Dagla$ knockout mouse lines.

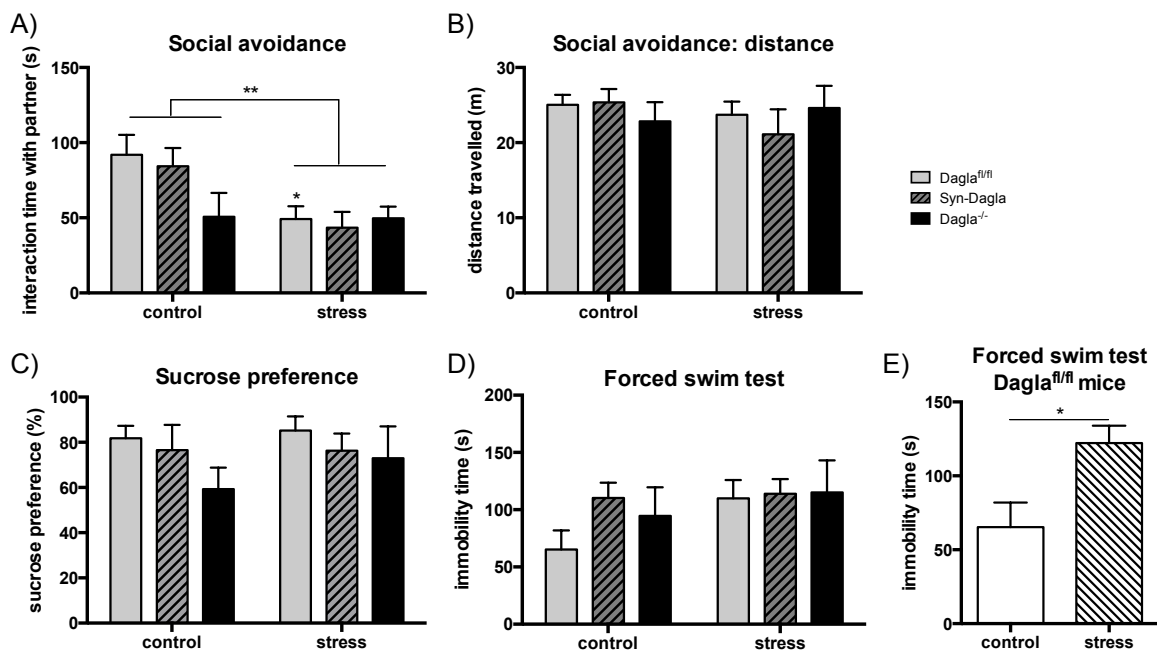


Figure 42: CSDS induced social avoidance and caused a depressive-like phenotype in $Dagla^{\text{fl/fl}}$ mice. (A) CSDS induced social avoidance behavior in $Dagla^{-/-}$ mice, $\text{Syn-Dagla}^{-/-}$ mice and $Dagla^{\text{fl/fl}}$ controls. (B) Overall

distance travelled was not altered after chronic stress in either genotype. (C) Anhedonia was assessed by sucrose preference. Sucrose preference of stressed *Dagla*^{-/-}, *Syn-Dagla*^{-/-} and *Dagla*^{fl/fl} animals was comparable to unstressed animals. However, sucrose preference of unstressed *Dagla*^{-/-} mice was slightly decreased (not significantly) compared to *Dagla*^{fl/fl} controls. (E) Immobility times of stressed and unstressed animals did not differ significantly (stress-effect: $p = 0.0741$) (two-way ANOVA, Bonferroni's post-hoc test, values represent mean \pm SEM: $n = 6-10$ animals/group, * $p < 0.05$, ** $p < 0.01$). (E) Immobility time of *Dagla*^{fl/fl} mice was significantly increased after chronic stress compared to unstressed *Dagla*^{fl/fl} controls (Student's t-test, values represent mean \pm SEM: $n = 8-10$ animals/group, * $p < 0.05$).

Behavioral analysis of chronically stressed mice revealed an increased social avoidance behavior and increased activity in the home cage in all genotypes. Furthermore, chronic stress induced a depressive-like phenotype in *Dagla*^{fl/fl} mice. To determine which pathways may be responsible for these behavioral changes, expression levels of several genes related to the ECS and the stress response system were ascertained. Gene expression was analyzed in brain areas related to mood, emotion and stress processing.

Gene expression analysis of amygdalar *Dagla* mRNA revealed significant main effects for stress ($F_{(1,9)} = 20.54$, $p < 0.01$; Fig. 43A) and genotype ($F_{(1,9)} = 26.92$, $p < 0.001$; Fig. 43A). *Dagla* expression was significantly downregulated in *Syn-Dagla*^{-/-} and *Dagla*^{fl/fl} mice after chronic stress. In addition, *Dagla* mRNA levels were significantly reduced in the amygdala of *Syn-Dagla*^{-/-} mice. Furthermore, *Mag1* mRNA levels, coding for the main degrading enzyme of 2-AG, were mildly decreased in the amygdala of *Dagla*^{-/-}, *Syn-Dagla*^{-/-} and *Dagla*^{fl/fl} mice after chronic stress ($F_{(1,16)} = 4.709$, $p < 0.05$; Fig. 43B). Gene expression of the anandamide synthesizing enzyme NAPE-PLD was not affected by the stress paradigm in either genotype (stress effect: $F_{(1,16)} = 4.709$, $p = ns$; Fig. 43C). In contrast, *Faah* mRNA levels, coding for the main degrading enzyme of anandamide, were significantly decreased in the amygdala of stressed *Dagla*^{-/-}, *Syn-Dagla*^{-/-} and *Dagla*^{fl/fl} mice (stress effect: $F_{(1,16)} = 5.892$, $p < 0.05$; genotype effect: $F_{(2,16)} =$, $p = ns$; Fig. 43D). Gene expression analysis revealed a significant downregulation of several genes related to the ECS in the amygdala of chronically stressed mice.

Next, genes related to the HPA axis were analyzed. Two-way ANOVA revealed a significant stress-dependent reduction of GR mRNA levels in the amygdala of *Dagla*^{-/-}, *Syn-Dagla*^{-/-} and *Dagla*^{fl/fl} mice (stress effect: $F_{(1,16)} = 23.01$, $p < 0.001$; Fig. 43E). This result supports that CSDS caused a disruption of the HPA axis. In addition, a significant genotype effect was detected ($F_{(2,16)} = 4.175$, $p < 0.05$; Fig. 43E), indicative of generally reduced GR expression in the amygdala of mice lacking *Dagla*. Two-way ANOVA of the CRHR1 gene expression, a receptor mediating HPA axis signaling, also revealed a significant stress ($F_{(1,16)} = 5.596$, $p < 0.05$; Fig. 43F) and genotype effect ($F_{(2,16)} = 3.691$, $p < 0.05$; Fig. 43F). Chronic stress significantly reduced CRHR1 mRNA levels in the amygdala, an effect being most pronounced in *Dagla*^{-/-} mice.

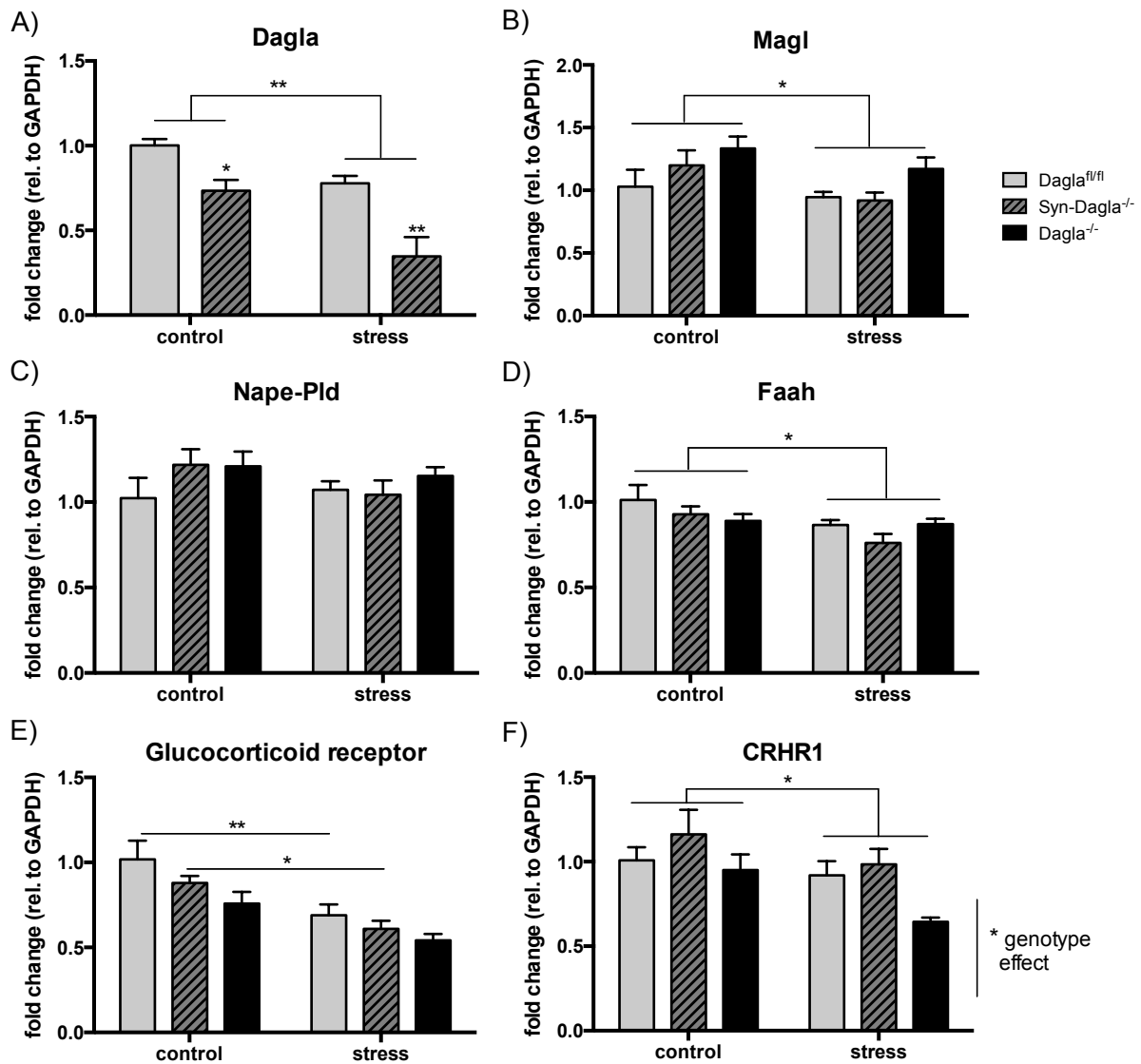


Figure 43: Gene expression analysis of the amygdala. (A-G) Shown are mRNA levels normalized to GAPDH. (A) Real-time RT-PCR results showed a significant downregulation of *Dagla* in *Syn-Dagla^{-/-}* and *Dagla^{fl/fl}* animals after CSDS. In addition, *Dagla* mRNA levels were markedly reduced in *Syn-Dagla^{-/-}* mice compared to *Dagla^{fl/fl}* controls. (B) *Magl* expression was significantly reduced after CSDS in all genotypes. (C) CSDS did not affect *Nape-Pid* expression. (D) However, *Faah* mRNA levels were significantly reduced in stressed animals. (E) *Glucocorticoid receptor* mRNA levels were significantly reduced in *Dagla^{-/-}* mice compared to *Dagla^{fl/fl}* controls regardless of the stress paradigm. In addition, CSDS caused a significant downregulation of GR expression. (F) *CRHR1* gene expression was reduced in the amygdala of stressed animals. This effect was most pronounced in *Dagla^{-/-}* mice (genotype effect: $p < 0.05$). Statistical analysis: two-way ANOVA, Bonferroni's post-hoc test, values represent mean \pm SEM; $n = 3-5$ animals/group, * $p < 0.05$, ** $p < 0.01$.

Next, hippocampal gene expression was determined. Gene expression analysis revealed similar mRNA levels of *Dagla* in stressed *Syn-Dagla^{-/-}* and *Dagla^{fl/fl}* mice compared to unstressed animals of the same genotype ($F_{(1,10)} = 0.001116$, $p = \text{ns}$; Fig. 44A). However, a significant genotype effect was detected ($F_{(1,10)} = 5.440$, $p < 0.05$; Fig. 44A), indicative of a distinct reduction of *Dagla* mRNA levels in the hippocampus of *Syn-Dagla^{-/-}* mice. *CB1* expression was not differentially regulated by CSDS in none of the genotypes (stress effect: $F_{(1,17)} = 0.07383$, $p = \text{ns}$; genotype effect: $F_{(2,17)} = 0.2438$, $p = \text{ns}$ Fig. 44B). Moreover, chronic stress caused a substantial downregulation of GR mRNA ($F_{(1,16)} = 6.4000$ $p < 0.05$; Fig. 44C).

This effect was most pronounced in Syn-Dagla^{-/-} mice ($t = 2.964$, $p < 0.05$; Fig. 44C). Furthermore, gene expression of BDNF was determined. Chronic stress did not alter hippocampal mRNA levels of BDNF in Dagla^{-/-}, Syn-Dagla^{-/-} and Dagla^{fl/fl} animals (stress effect: $F_{(1,15)} = 0.01983$, $p = \text{ns}$; genotype effect: $F_{(2,15)} = 0.4472$, $p = \text{ns}$; Fig. 44D).

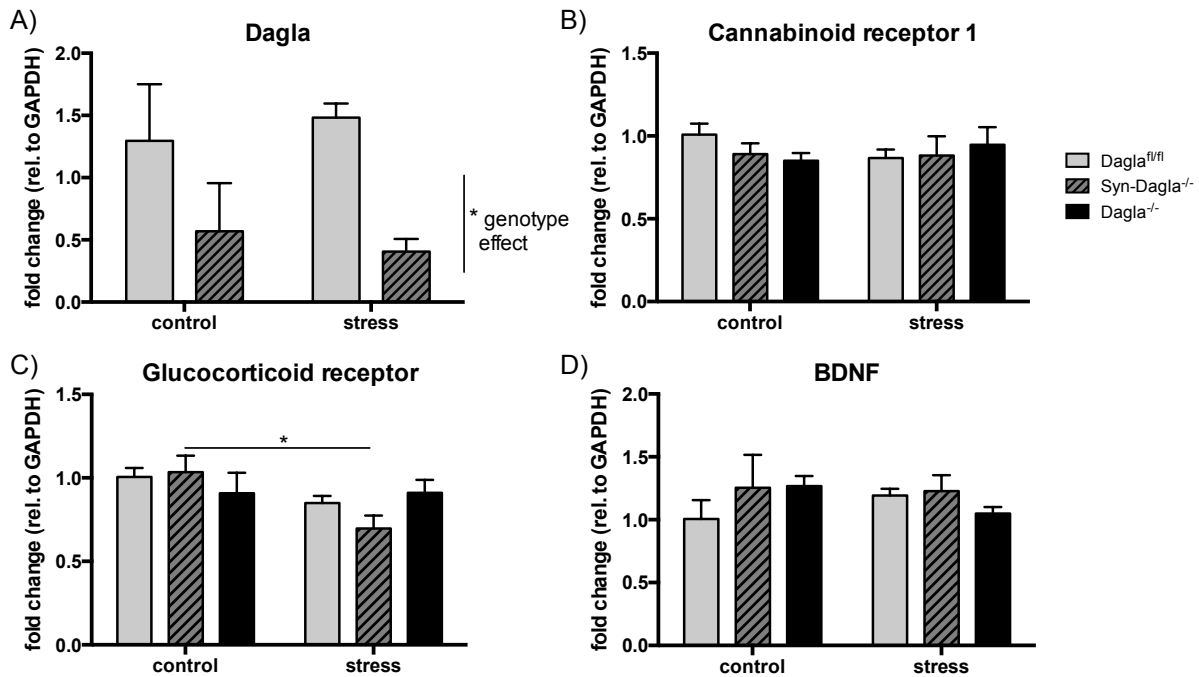


Figure 44: Gene expression analysis of the hippocampus. (A-E) Shown are mRNA levels normalized to GAPDH. (A) Real-time RT-PCR results showed similar Dagla mRNA levels in stressed and unstressed animals. However, Dagla mRNA levels were significantly reduced in Syn-Dagla^{-/-} mice compared to Dagla^{fl/fl} controls ($n = 4-5$). (B) CB1 receptor gene expression was not altered in the hippocampus of Dagla^{-/-}, Syn-Dagla^{-/-} or in Dagla^{fl/fl} mice after chronic stress. (C) However, CSDS caused a significant downregulation of glucocorticoid receptor (GR) expression (stress effect: $p < 0.05$). This effect was significant for Syn-Dagla^{-/-} mice. (D) mRNA levels of BDNF were similar for all groups. Statistical analysis: two-way ANOVA, Bonferroni's post-hoc test, values represent mean \pm SEM; $n = 3-5$ animals/group, * $p < 0.05$.

To confirm possible alterations of the HPA axis, gene expression in the PVN was analyzed. Two-way ANOVA of GR mRNA levels revealed neither a stress ($F_{(1,17)} = 0.1793$, $p = \text{ns}$) nor a genotype effect ($F_{(2,17)} = 0.7793$, $p = \text{ns}$ Fig. 45A). However, stress-dependent decrease (not significant) of GR expression in the PVN of Dagla^{fl/fl} animals was detected ($t = 2.204$, $p = \text{ns}$; Fig. 45A). Expression of CRH, the first activator of the HPA axis synthesized in the PVN, was not regulated by the stress paradigm in either genotype (stress effect: $F_{(1,16)} = 0.3605$, $p = \text{ns}$; genotype effect: $F_{(2,16)} = 2.520$, $p = \text{ns}$; Fig. 45B). However, real-time RT-PCR results of CRH gene expression displayed high variances, which complicate a conclusive statistical evaluation. Gene expression analysis of CRHR1, a CRH receptor, revealed similar mRNA levels in the PVN of Dagla^{-/-}, Syn-Dagla^{-/-} and Dagla^{fl/fl} mice regardless of the stress paradigm (stress effect: $F_{(1,17)} = 1.844$, $p = \text{ns}$; genotype effect: $F_{(2,17)} = 1.368$, $p = \text{ns}$; Fig. 45C).

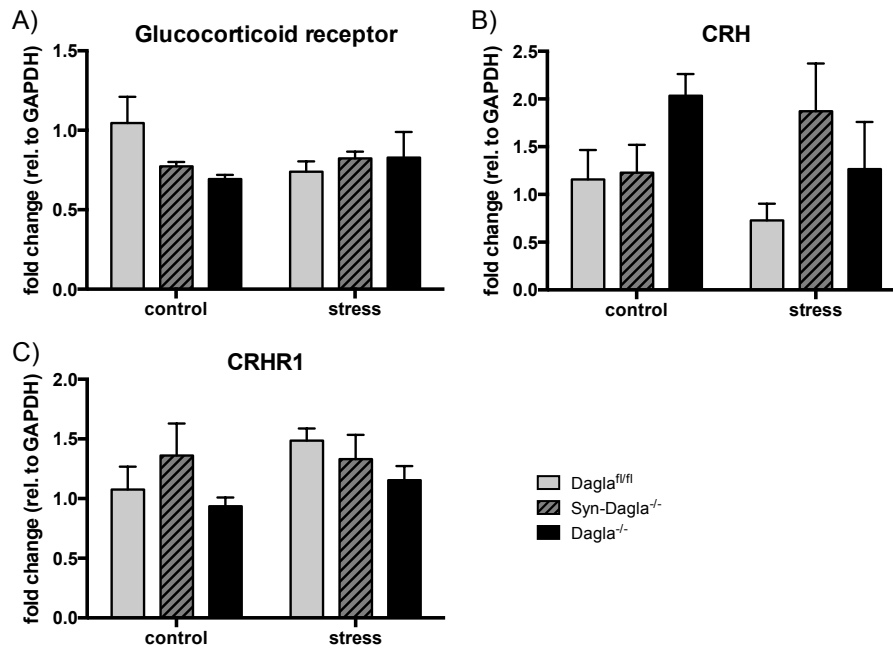


Figure 45: Gene expression analysis of the PVN. (A-C) Shown are mRNA levels normalized to GAPDH. (A) Glucocorticoid receptor mRNA levels were similar in all groups regardless of genotype and treatment. However, a clear tendency towards stress-dependent decrease of GR expression was detected in Dagla^{fl/fl} mice. (B) Analysis of CRH mRNA levels revealed no stress- and genotype-dependent regulation. (C) CSDS did not alter CRHR1 gene expression in Dagla^{-/-}, Syn-Dagla^{-/-} and Dagla^{fl/fl} animals. Statistical analysis: two-way ANOVA, Bonferroni's post-hoc test, values represent mean \pm SEM; n = 3-5 animals/group.

In summary it can be stated that the CSDS paradigm caused not only behavioral, but also gene expression changes in single-caged intruder mice. GR was downregulated in several brain areas of stressed Dagla^{fl/fl} mice, indicative of a stress-dependent dysregulation of the HPA axis. In addition, GR expression was reduced in Dagla^{-/-} and Syn-Dagla^{-/-} mice compared to Dagla^{fl/fl} controls. Interestingly, CSDS caused a downregulation of several genes related to the ECS in the amygdala of Dagla^{-/-}, Syn-Dagla^{-/-} and Dagla^{fl/fl} animals. To determine the effects of these gene expression changes on 2-AG and anandamide levels, endogenous cannabinoids were measured (Fig. 46).

Endocannabinoid measurements revealed that 2-AG levels in the amygdala and PFC of Dagla^{fl/fl} mice increased after chronic stress, whereas 2-AG contents of Syn-Dagla^{-/-} and Dagla^{-/-} mice remained constant. Two-way ANOVA of 2-AG levels in the amygdala and PFC revealed no main effects for stress (amygdala: $F_{(1,15)} = 1.601$, $p = \text{ns}$; PFC: $F_{(1,15)} = 0.6248$, $p = \text{ns}$; Fig. 46A,B), but for genotype (amygdala: $F_{(2,15)} = 43.54$, $p < 0.0001$; PFC: $F_{(2,15)} = 11.93$, $p < 0.001$; Fig. 46A,B). 2-AG levels in the amygdala ($t = 5.537$, $p < 0.001$; Fig. 46A) and PFC ($t = 2.820$, $p < 0.05$; Fig. 46B) of Dagla^{-/-} mice were significantly reduced compared to Dagla^{fl/fl} controls, but not influenced by the stress paradigm. Bonferroni's post-hoc analysis revealed significantly increased 2-AG levels in the amygdala of stressed Dagla^{fl/fl} mice ($t = 2.870$, $p < 0.05$; Fig. 46A). Same tendency was also seen in the PFC (Fig. 46B). In contrast, chronic stress did not affect 2-AG contents in the amygdala and PFC of Syn-Dagla^{-/-} mice. Furthermore, similar hippocampal 2-AG levels were detected in stressed mice and

unstressed animals of the same genotype ($F_{(1,15)} = 0.3367$, $p = \text{ns}$). Nevertheless, a significant genotype effect was observed ($F_{(2,15)} = 36.98$, $p < 0.0001$; Fig. 46C) due to the tremendously reduced 2-AG levels in $\text{Dagla}^{-/-}$ animals. In line with previous results (Chapter 3.2.1), baseline 2-AG levels were similar for $\text{Syn-Dagla}^{-/-}$ and $\text{Dagla}^{\text{fl/fl}}$ mice in all analyzed brain areas (Fig. 46A,B,C).

Next, the amount of the other main endogenous cannabinoid anandamide (Fig. 46D-F) was determined. Two-way ANOVA of anandamide levels in the amygdala and hippocampus revealed no main effects for stress (amygdala: $F_{(1,15)} = 5.620$, $p = \text{ns}$; hippocampus: $F_{(1,15)} = 0.8430$, $p = \text{ns}$; Fig. 46D,F), but for genotype (amygdala: $F_{(2,15)} = 18.60$, $p < 0.0001$; hippocampus: $F_{(2,15)} = 8.688$, $p < 0.01$; Fig. 46D,F). Anandamide contents were significantly decreased in both brain areas of $\text{Dagla}^{-/-}$ mice compared to $\text{Dagla}^{\text{fl/fl}}$ controls (amygdala: $t = 3.351$, $p < 0.05$; hippocampus: $t = 3.578$, $p < 0.01$; Fig. 46D,F). However, no stress-dependent changes in anandamide levels of $\text{Dagla}^{-/-}$ and $\text{Dagla}^{\text{fl/fl}}$ mice were observed. In contrast, a clear tendency to increased anandamide levels after CSDS was detected in the amygdala of $\text{Syn-Dagla}^{-/-}$ mice ($t = 2654$, $p = \text{ns}$; Fig. 46D), whereas hippocampal anandamide remained constant ($t = 0.6325$, $p = \text{ns}$; Fig. 46F). For the PFC, a significant stress ($F_{(1,15)} = 6.792$, $p < 0.05$; Fig. 46E) and genotype effect ($F_{(2,15)} = 24.44$, $p < 0.0001$; Fig. 46E) was detected. Anandamide contents in the PFC of $\text{Syn-Dagla}^{-/-}$ mice significantly increased in response to chronic stress ($t = 3.299$, $p < 0.05$; Fig. 46E). In addition, anandamide levels of $\text{Dagla}^{-/-}$ mice were significantly reduced compared to $\text{Dagla}^{\text{fl/fl}}$ controls ($t = 4.794$, $p < 0.001$; Fig. 46E).

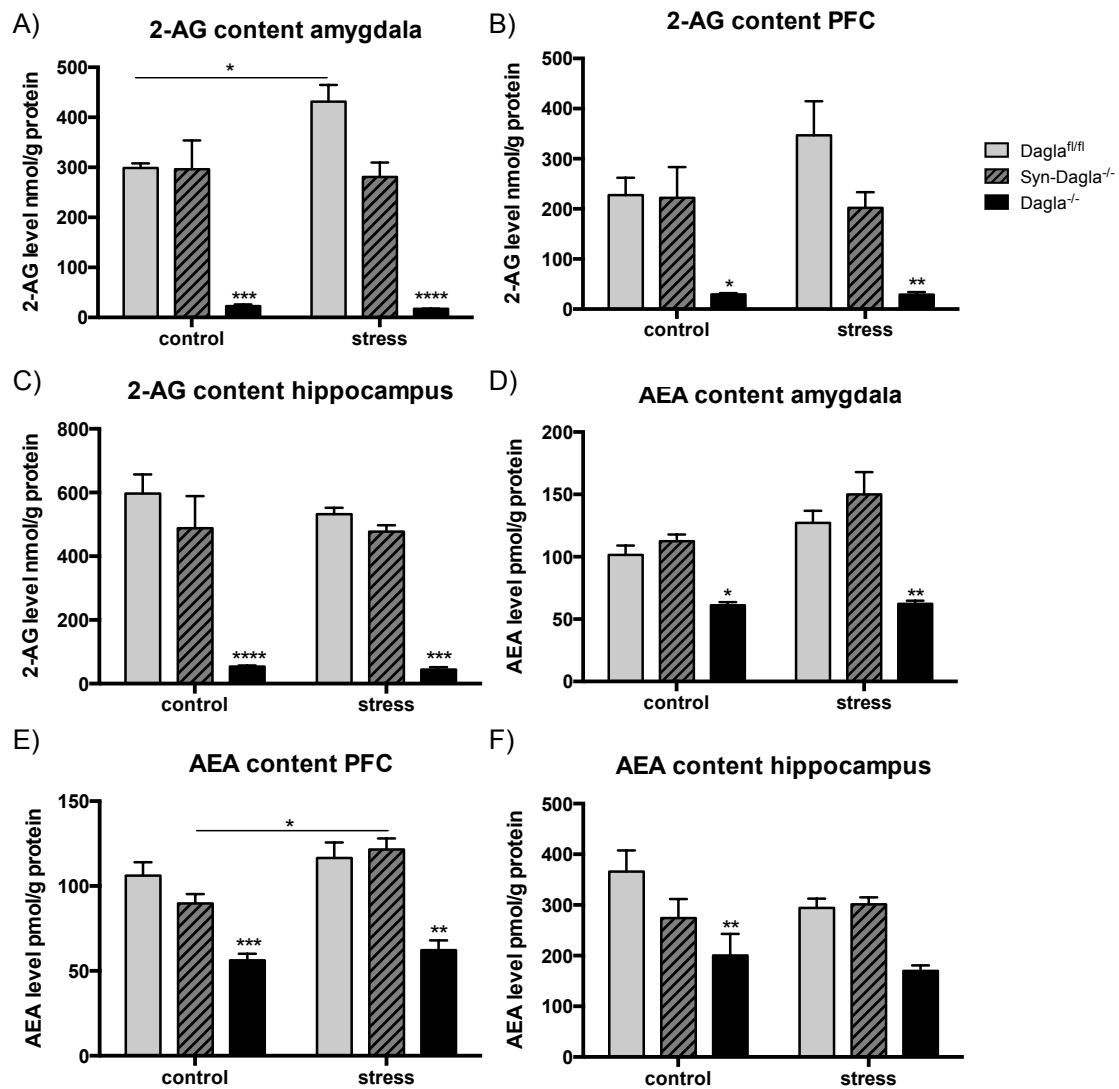


Figure 46: CSDS altered 2-AG or anandamide levels in the amygdala and PFC of *Dagla^{fl/fl}* and *Syn-Dagla^{-/-}* mice. (A-F) Shown are the amounts of 2-AG and anandamide (AEA) relative to the amount of total protein per sample. (A) 2-AG levels were significantly increased in the amygdala of stressed *Dagla^{fl/fl}* mice compared to unstressed mice. (B) 2-AG content was increased in the prefrontal cortex (PFC) of *Dagla^{fl/fl}* after CSDS. However, this trend did not reach significance. (C) In addition, chronic stress did not affect 2-AG levels in the hippocampus of *Dagla^{-/-}*, *Syn-Dagla^{-/-}* or *Dagla^{fl/fl}* mice. (D) A trend to increased anandamide levels in the amygdala of stressed *Syn-Dagla^{-/-}* mice compared to unstressed *Syn-Dagla^{-/-}* mice was detected. (E) Chronic stress significantly increased anandamide levels in the PFC of *Syn-Dagla^{-/-}* mice compared to unstressed *Syn-Dagla^{-/-}* animals. (F) Anandamide levels in the hippocampus of stressed mice were similar to unstressed animals of the same genotype. Statistical analysis for eCB measurement: two-way ANOVA, Bonferroni's post-hoc test, values represent mean \pm SEM: $n = 3-4$ animals/group, * $p < 0.05$, ** $p < 0.01$, *** $p < 0.001$, **** $p < 0.0001$.

Lastly, arachidonic acid contents were determined. A significant main effect for stress was observed in the PFC ($F_{(1,15)} = 5.367$, $p < 0.05$; Fig. 47B). CSDS increased arachidonic acid levels in the PFC of *Syn-Dagla^{-/-}* and *Dagla^{fl/fl}* animals. In contrast, amygdalar and hippocampal quantities of arachidonic acid of stressed *Dagla^{-/-}*, *Syn-Dagla^{-/-}* and *Dagla^{fl/fl}* mice were comparable to unstressed controls (amygdala: $F_{(1,15)} = 3.309$, $p = \text{ns}$; Fig. 47A; hippocampus: $F_{(1,15)} = 1.185$, $p = \text{ns}$; Fig. 47C).

In addition, two-way ANOVA revealed significant genotype effects in all brain areas (amygdala: $F_{(2,15)} = 69.60$, $p < 0.0001$; PFC: $F_{(2,15)} = 40.84$, $p < 0.0001$; hippocampus: $F_{(2,15)} = 39.65$, $p < 0.0001$; Fig. 47A-C). Arachidonic acid values were significantly reduced in the amygdala ($t = 7.294$, $p < 0.0001$; Fig. 47A), PFC ($t = 5.243$, $p < 0.001$; Fig. 47B) and hippocampus ($t = 7.317$, $p < 0.0001$; Fig. 47C) of $Dagla^{-/-}$ mice compared to $Dagla^{fl/fl}$ animals regardless of the stress paradigm.

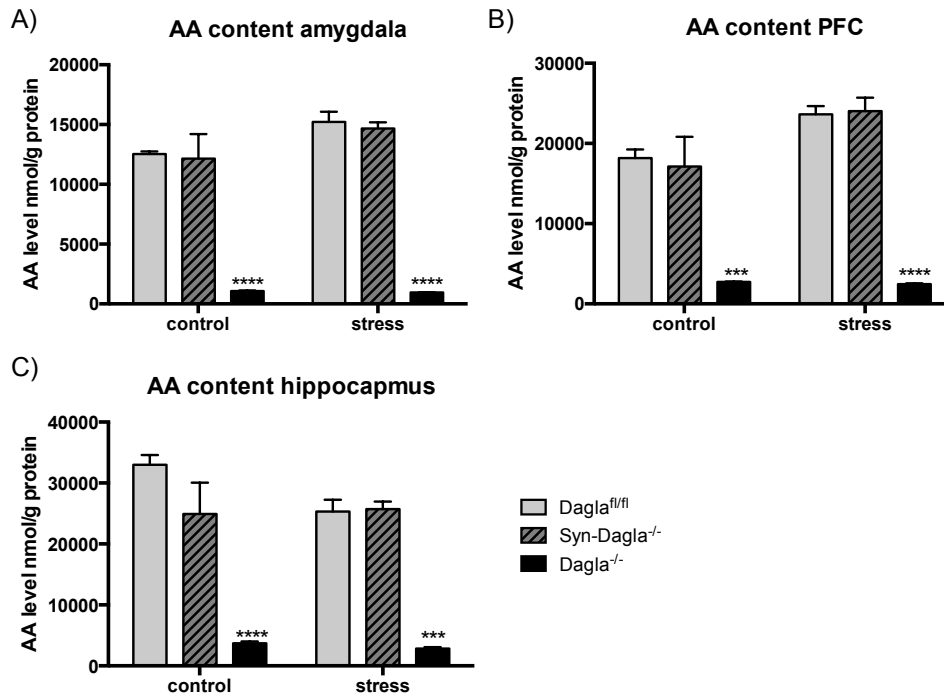


Figure 47: Chronic stress caused increased arachidonic acid levels in the PFC of $Syn-Dagla^{-/-}$ and $Dagla^{fl/fl}$ mice. (A-C) Shown are the amounts of arachidonic acid (AA) relative to the amount of total protein per sample. (A) Amygdalar arachidonic acid levels did not differ between stressed and unstressed animals of the same genotype. (B) In contrast, CSDS significantly increased arachidonic acid contents in the prefrontal cortex (PFC) of $Syn-Dagla^{-/-}$ and $Dagla^{fl/fl}$ mice. (C) Hippocampal levels of arachidonic acid were not affected by chronic stress in either genotype. (A-C) In addition, arachidonic acid content was significantly decreased in $Dagla^{-/-}$ mice compared to $Dagla^{fl/fl}$ animals in all brain areas. Statistical analysis for eCB measurement: two-way ANOVA, Bonferroni's post-hoc test, values represent mean \pm SEM: $n = 3-4$ animals/group, *** $p < 0.001$, **** $p < 0.0001$.

These results illustrate that CSDS caused substantial changes in the endocannabinoid composition in the amygdala and PFC of $Syn-Dagla^{-/-}$ and $Dagla^{fl/fl}$ mice.

3.5 Identification of potential novel interaction partners of DAGL α

Up to now very little is known about the regulation of DAGL α and its potential interaction partners. Thus, this thesis focused on the detailed characterization of DAGL α using knockout mouse models and different *in vitro* approaches. The last part of the result section outlines the cloning, expression and purification of the double-tagged DAGL α and subsequent identification of co-purified proteins, which potentially interact with the protein of interest.

3.5.1 Cloning of the DAGL α expression vector

To purify DAGL α via tandem affinity purification, an expression vector for the overexpression of the double-tagged protein was generated using a site-directed two-TAP cloning Kit from IBA Lifescience. First, Dagla cDNA was cloned into the entry vector pENTRY-IBA51. Therefore, Dagla cDNA was amplified using a forward and a reverse primer containing *Lgul* StarCombinase1™ recognition sites (GCTCTTC) for efficient integration into the entry vector, leading to a 3135 bp DNA fragment. Importantly, the coding sequence was amplified without the stop codon to ensure a continuous transcription leading to a c-terminal double-tagged DAGL α protein. In addition, the stop codon was replaced by glycine, one of the linker amino acids between the protein of interest and the c-terminal protein tag in the final expression vector pESG-IBA168.

Integration of Dagla cDNA into the vector was verified by restriction digest using the endonucleases *Xba*I and *Hind*III. Correct integration revealed two DNA fragments of 3175 bp and 1860 bp. The 5035 bp DNA fragment corresponds to the linearized or uncut vector (Fig. 48C). Orientation and sequence was verified for accuracy by sequence analysis (GATC Biotech AG).

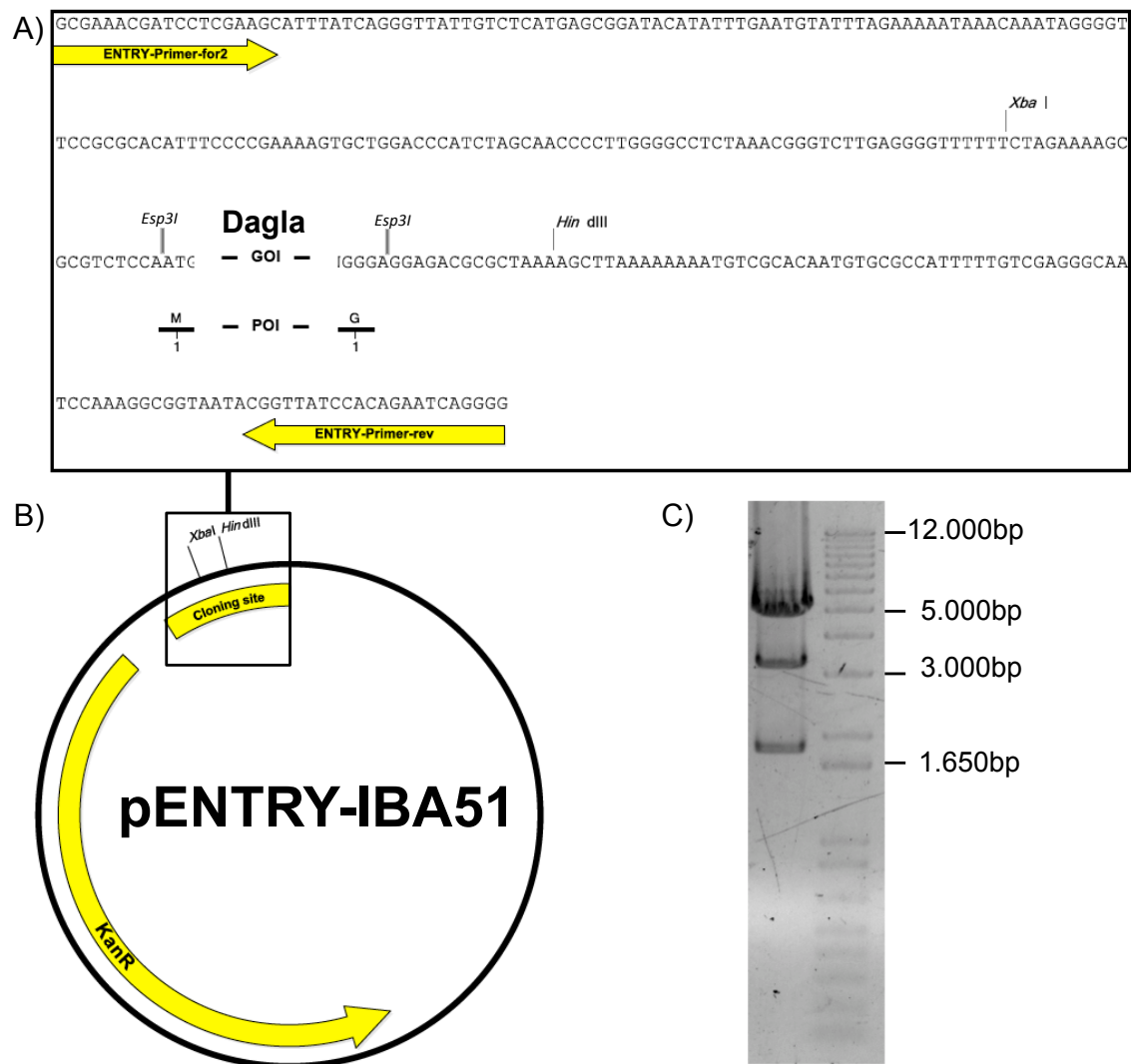


Figure 48: Cloning of the entry vector pENTRY-IBA51-Dagla. (A) Detailed sequence of the pENTRY-IBA51 cloning site. Gene of interest is inserted in the GOI marked region flanked by the amino acids methionine (M) and glycine (G). *Xba*I and *Hind*III restriction sites were used for restriction digest. In addition, ENTRY-Primer-for2 and ENTRY-primer-rev were used for sequence analysis. (B) Vector map of pENTRY-IBA51. Marked are the kanamycin resistance gene (KanR) and the cloning site, including the restriction sites of *Xba*I and *Hind*III. (C) Verification of Dagla cDNA integration into pENTRY-IBA51 via double restriction digest with *Xho*I and *Hind*III, resulting in two DNA fragments of 3175 bp and 1860 bp. GOI: gene of interest = Dagla, POI: protein of interest = DAGL α , KanR: kanamycin resistance gene (A/B: adopted from IBA Lifescience).

After verification of the first cloning step, Dagla cDNA was subcloned into the final expression vector pESG-IBA168. Subcloning was performed in a simultaneous restriction and ligation reaction using *Esp*3I endonuclease (restriction site: CGTCTC, see Fig. 49A) and T4-DNA ligase. The final vector pESG-IBA168 contained a C-terminal Strep-Flag-tag, a neomycin resistance cassette for selection in mammalian cells and the CMV (cytomegalovirus) promoter for high-level protein expression in mammalian cells (Fig. 49A,B). A short linker of 5 amino acids, enabling a better accessibility of both tags, separated the double Strep-tag II and the Flag-tag. The integration of Dagla was once more verified by restriction digest with *Xba*I and *Hind*III. Correctly inserted cDNA revealed

a 5497 bp and a 3294 bp DNA fragment. The final vector had total size of 8791 bp (Fig. 49C).

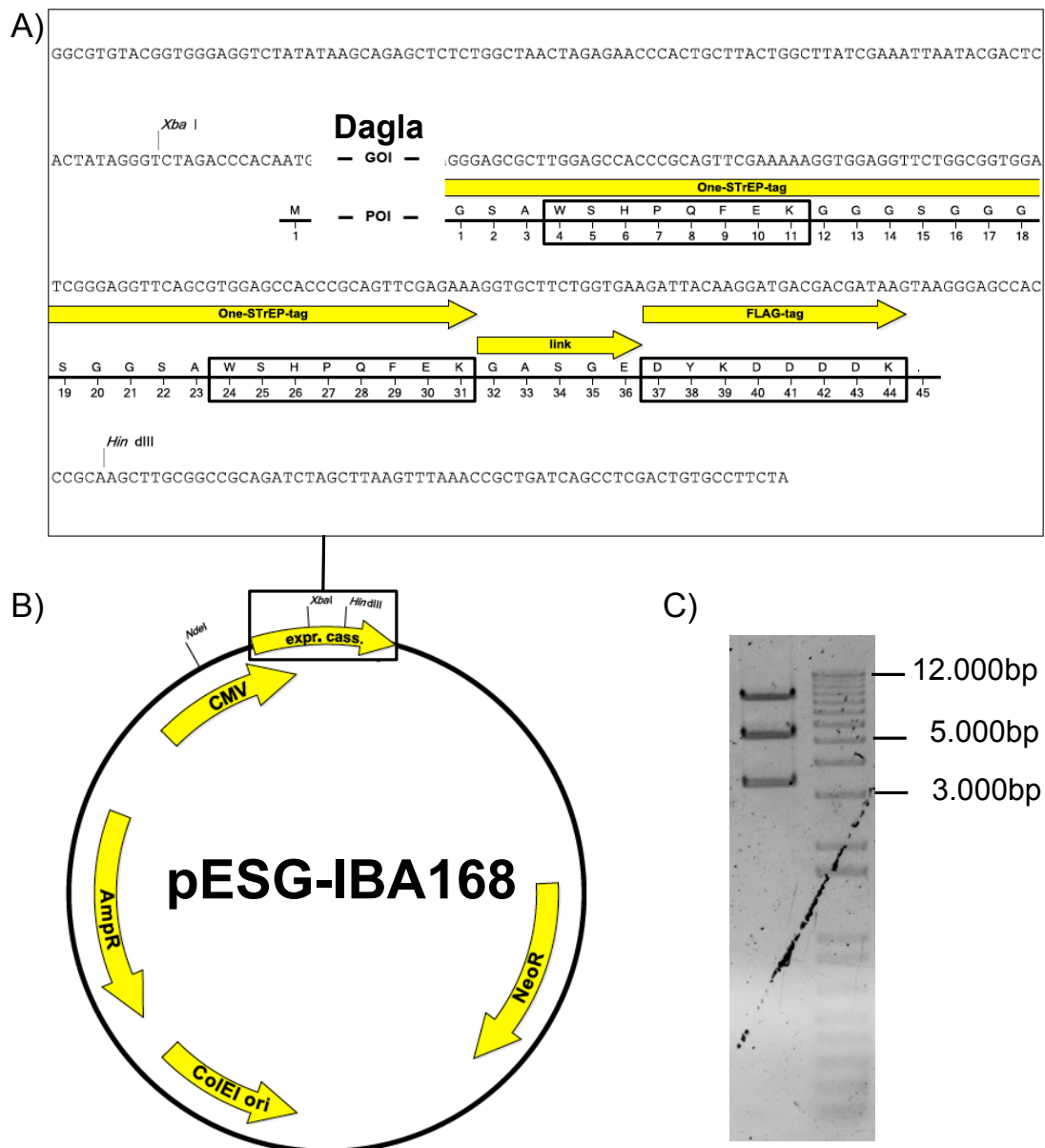


Figure 49: Cloning of the final expression vector pESG-IBA168-Dagla. (A) Detailed sequence of the expression cassette of pESG-IBA168 showing the c-terminal Strep-Flag-tag. Gene of interest, Dagla, is inserted in the GOI marked region. C-terminal Strep-Flag-tag and the five linker amino acids are marked by yellow arrows. DNA bases and corresponding amino acids forming the two tags are encircled in black. (B) Vector map of pESG-IBA168. Ampicillin resistance gene (Amp^R), neomycin resistance gene (Neo^R), cytomegalovirus (CMV) promoter, origin of replication (ColEI ori) and the expression cassette are marked by yellow arrows. (C) Verification of Dagla cDNA integration into the vector pESG-IBA168 via double restriction digest with *Xba*I and *Hind*III resulting in two DNA fragments of 5497 bp and 3294 bp. (A/B: adopted from IBA Lifescience).

The final expression vector pESG-IBA168-Dagla was used to overexpress the C-terminal tagged DAGL α in a mouse neuroblastoma cell line (Neuro-2a) for subsequent tandem purification or *in vitro* assays using click-chemistry. A neuronal cell line allows a detailed investigation of the function and regulation of DAGL α in neuronal tissue. This is of

special interest, because previous studies showed that DAGL α is the main producing enzyme of 2-AG in the brain (Gao et al. 2010). In addition, Neuro-2a cells are widely and extensively used to study neuronal signaling pathways, axonal growth and differentiation.

3.5.2 Tandem affinity purification of DAGL α

Double-tagged DAGL α was purified from Neuro-2a cells. Therefore, Neuro-2a cells were transfected with the pESG-IBA168-Dagla expression vector using Lipofectamine[®]2000 transfection reagent (Life Technologies), providing a high transfection efficiency and high transgene expression in numerous mammalian cell types.

Subsequent to the transfection, positive Neuro-2a cell clones were selected via neomycine (G418) resistance. Untransfected Neuro-2a cells with the same passage number were used as controls. Transfected and control cells were applied for tandem affinity purification (TAP) and treated equally throughout all experiments. Tandem affinity purification allows efficient isolation of native protein complexes and thereby the identification of protein-protein interactions. This method was applied to identify potential interaction partners of DAGL α and detect possible regulatory mechanisms. In this study, a C-terminal tandem Strep-tag II was combined with a Flag-tag, which led to a quite small TAP-tag (SF-TAP) of just 4.6 kDa. Due to its small size, this TAP-tag rarely interferes with protein folding and activity. In the first step, transfected Neuro-2a and control cell homogenates were purified using a modified streptavidin affinity chromatography system. In a second step, the eluted proteins were purified using an anti-Flag agarose. Subsequently, samples of the different purification steps were analyzed via SDS-PAGE and western blot to determine the purification efficiency.

Coomassie staining of SDS-PAGE gels revealed a great number of purified proteins in the flag purification eluate (first purification step) and the flow-through of the streptavidin-affinity purification in transfected as well as control Neuro-2a cells (Fig. 50A). However, no proteins were detected in the eluate of the streptavidin-affinity purification, the second and final purification step (eluate S Fig. 50A). In addition, neither the TAP purification (eluate S) from transfected Neuro-2a nor from the control cells revealed a Coomassie stained band in the expected size of 116 kDa corresponding to DAGL α (eluate S; Fig. 50A).

To increase the sensitivity of detection and to specifically identify recombinant DAGL α , the same samples were analyzed via western blot using anti-Flag and anti-DAGL α antibodies (Fig. 50B,C). Western Blot analysis, utilizing the anti-Flag antibody, showed a strong and distinct band with a molecular weight of approximately 110 kDa in the transfected Neuro-2a cells, resembling recombinant DAGL α (Fig. 50B). DAGL α was detected in all purification steps. These results show that antibody detection had a distinctly higher

sensitivity than classical Coomassie staining. The detection of recombinant DAGL α proofed a successful transfection and sufficient expression of the bait protein in Neuro-2a cells.

However, the efficiency of the streptavidin-affinity purification was rather low, leading to significant losses of the bait protein (Fig. 50B). In addition, western blot analysis with the anti-FLAG antibody revealed several other bands in the flag purification eluate of transfected and control cells. These protein bands most likely originated from unspecific antibody binding to non-target structures (Fig. 50B). Western blot analysis, utilizing the anti-DAGL α antibody, only revealed one distinct band at a molecular size of around 110 kDa in the flag purification eluate of the transfected cells, corresponding to DAGL α (Fig. 50C). Thus, western blot analysis enabled a clear detection of DAGL α after flag purification of transfected Neuro-2a cells. However, even after fourfold concentration of the streptavidin-affinity eluate, DAGL α quantity was below the detection limit of the anti-DAGL α antibody (Fig. 50C).

Since the streptavidin-affinity purification was too inefficient, the TAP purification protocol was modified to increase the quantity of the bait protein. However, neither changing the order of the two purification steps, doubling the amount of Strep-Tactin® agarose (column material: 100 to 200 μ l), increasing the time of column binding (1 h up to 3 h) nor changing the binding temperature (RT or 4°C) revealed markedly higher amounts of recombinant DAGL α (data not shown). Most likely the Strep-tag was not fully accessible due to steric hindrance and protein folding, based on its location very close to the N-terminus of the protein.

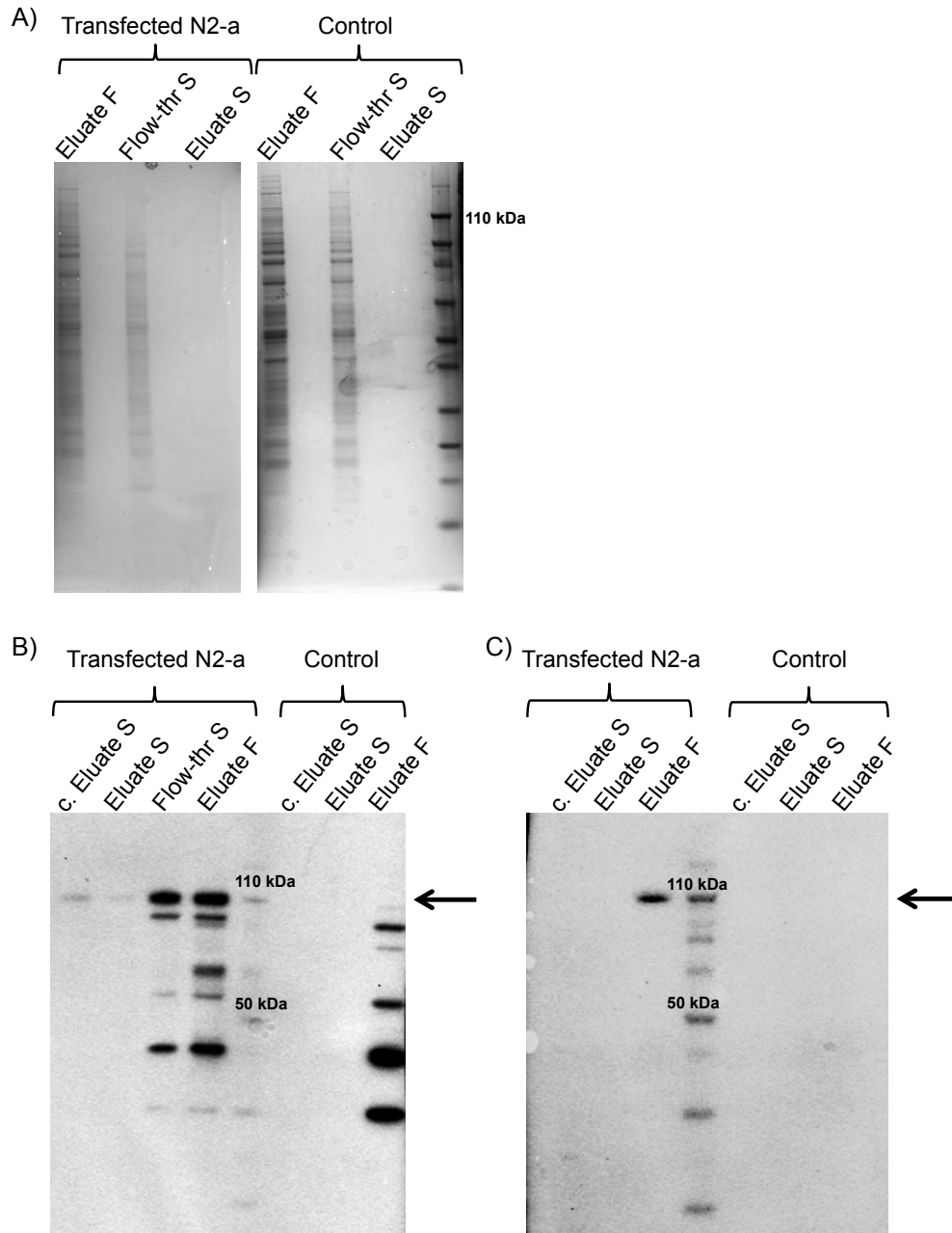


Figure 50: Tandem affinity purification of recombinant DAGL α . Eluates from different purification steps with the bait DAGL α were loaded onto SDS-PAGE followed by Coomassie staining (A) or western blotting using anti-Flag (B) or anti-DAGL α antibodies (C). Black arrows indicate the band size corresponding to DAGL α . Eluate F: Eluate flag purification; Flow-thr S: Flow-through streptavidin-affinity purification; Eluate S: Eluate streptavidin-affinity purification; c. Eluate S: 4x concentrated eluate streptavidin-affinity purification; N-2a: Neuro-2a cells.

In a next step, the TAP- and flag-purified proteins were analyzed by MALDI-TOF/TOF mass spectrometry to identify potential interaction partner of DAGL α . Due to the high sensitivity and specificity of this method even low amounts of recombinant DAGL α and co-purified proteins can be detected and identified. In fact, lower amounts of the overexpressed protein minimize the chance of random protein-protein interactions.

3.5.3 Analysis of bound proteins via MALDI-TOF

Concentrated samples of TAP-purified proteins from transfected and control Neuro-2a cells (c. Eluate S, Fig. 50B) were analyzed by MALDI-TOF/TOF-MS to identify potential interaction partners of DAGL α . Even though MALDI-TOF/TOF-MS is a very sensitive technique with low detection limits, DAGL α could not be detected in none of the two samples (data not shown). Antibody detection of recombinant DAGL α in the same samples elucidates the high sensitivity of certain antibodies compared to MALDI-TOF/TOF-MS (Fig. 50B).

As mentioned in chapter 3.5.2, the streptavidin-affinity purification led to significant losses of the bait protein (Fig. 50B). The Strep-tag was most likely not fully accessible and therefore could not unrestrictedly bind to the column resin. To strongly increase the yield of the bait protein, recombinant DAGL α was only purified using the flag affinity purification (Fig. 50B,C). MALDI-TOF/TOF-MS analysis of flag-purified proteins from transfected and control Neuro-2a cells (for representative western blot see Fig. 50B,C: Eluate F) enabled a certain identification of the bait protein DAGL α in the sample of transfected cells. Three unique peptides were identified leading to sequence coverage of around 4 % between the detected peptides and DAGL α (Fig. 51). This result allowed the reliable identification of DAGL α . In addition, DAGL α was solely detected in the sample of transfected cells, indicating a very specific purification of the recombinant protein.

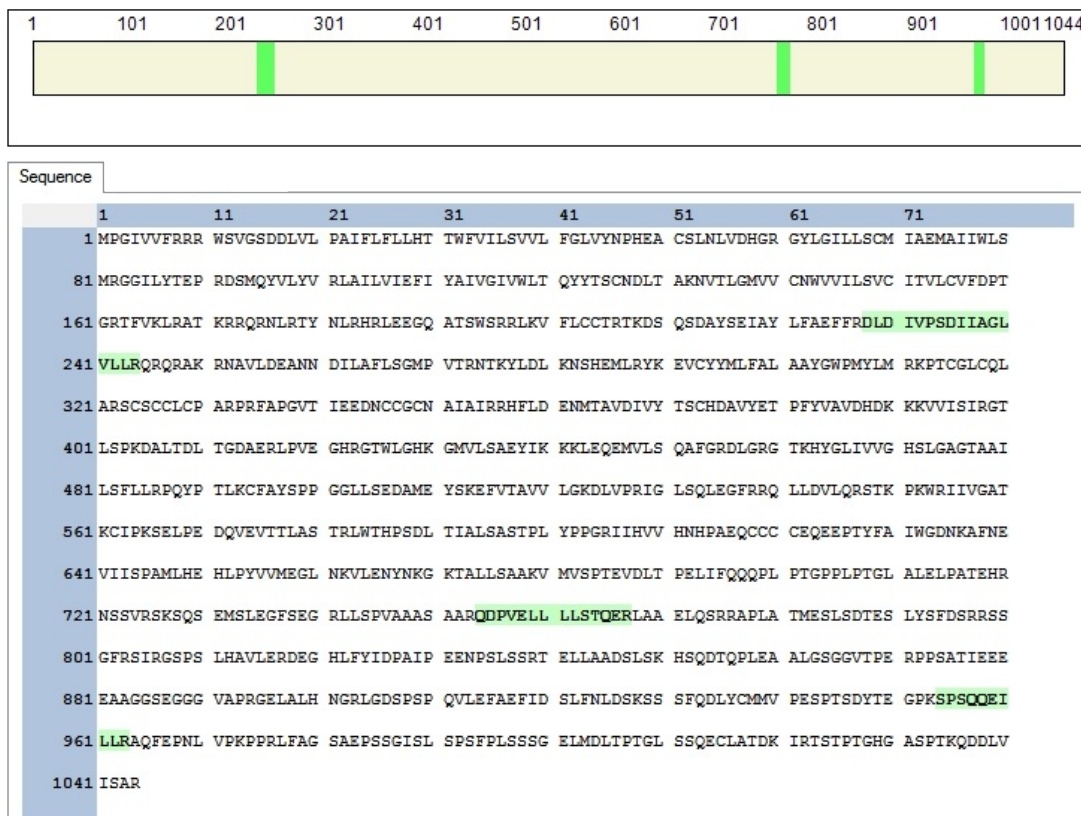


Figure 51: Sequence coverage of DAGL α . Three different peptides (marked in green) belonging to DAGL α were identified via MALDI-TOF/TOF-MS in the sample of transfected Neuro-2a cells, leading to sequence coverage of 3.93 % (Figure kindly provided by Dr. Marc Sylvester).

Overall approximately 1400 additional proteins were clearly identified, using MALDI-TOF/TOF-MS. Most of these proteins were present in both transfected and control samples and are therefore most likely to have no specific interactions with DAGL α . However, 142 of the 1400 identified proteins were exclusively present in the purification of transfected Neuro-2a cells. These proteins are mainly involved in RNA processing, energy and lipid metabolism and vesicular trafficking (Fig. 52, see Appendix A.1 for the protein list).

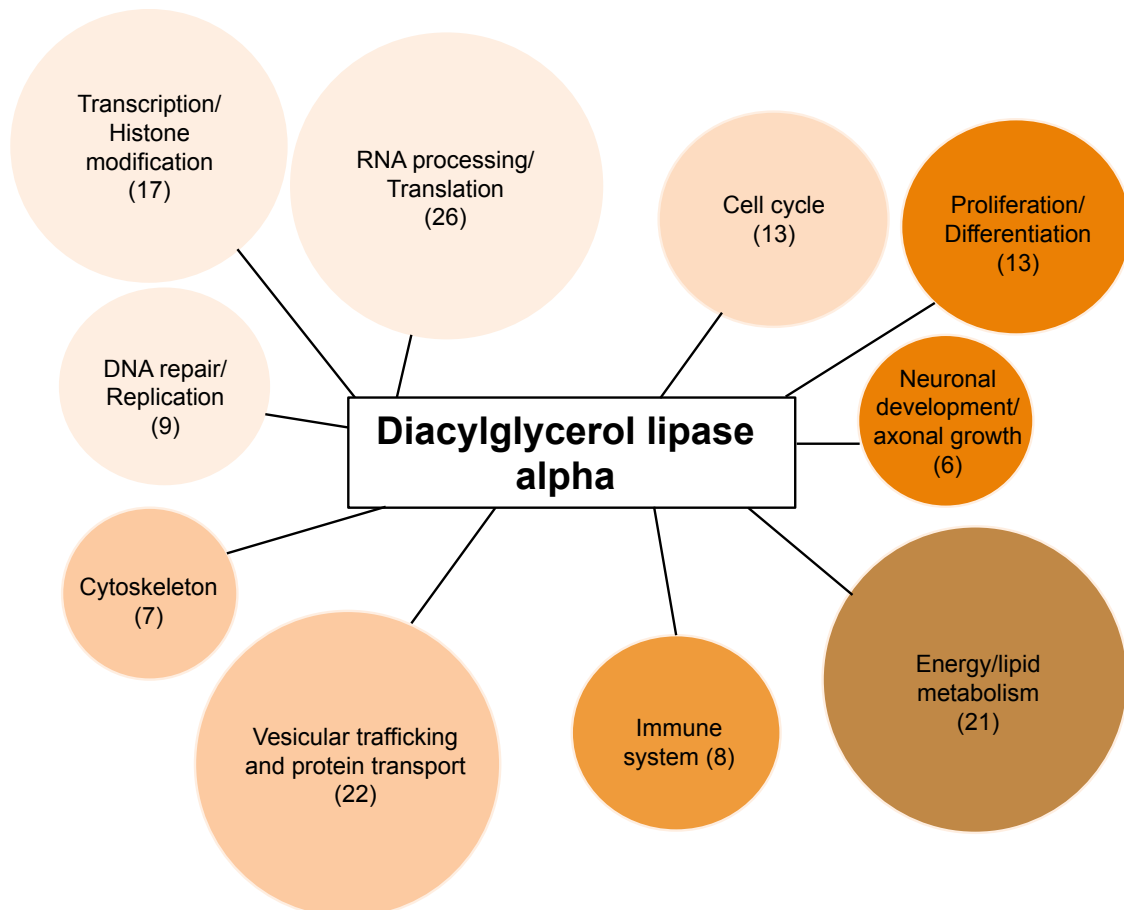


Figure 52: Potential interaction partners of DAGL α classified into groups according to their function and possible involvement in different signaling cascades. Numbers of assigned proteins are enclosed in brackets.

Interaction partners of the protein of interest are usually co-purified in similar quantities. In the following, 3 out of the 142 identified proteins, which fulfill these criteria and might be of special interest, are described in more detail and summarized in table 9.

Table 9 shows the direct comparison of MALDI-TOF/TOF-MS results from control Neuro-2a cells, sample A, and DAGL α overexpressing (transfected) Neuro-2a cells, sample B. The 3 selected proteins are of special interest due to their possible contribution to signaling pathways, in which DAGL α is or may be involved. These include NCAM, dynamin-1 and Mitogen-activated protein kinase 8 (MAPK8). All proteins were exclusively detected and identified in sample B (transfected Neuro-2a cells) by the identification of two peptides for each protein leading to sequence coverage of approximately 2 to 6 %. The amount of

peptides indicated protein quantities with a similarity to DAGL α (Tab. 9). The protein quantities were estimated based on the amount of peptides and peptide spectrum matches (PSM) resulting from the mass spectrometry analysis (Tab. 9). Peptides (Tab. 9) quote the amount of different identified peptides of one protein and therefore determine the sequence coverage. In this case, more protein leads to more identified peptides. The PSM represents the amount of MS spectra assigned to one peptide of a protein, used as an indicator for the protein quantity. A further measured value is the area, referring the added area of the chromatographic peaks belonging to the 3 strongest peptides of one protein, allowing a rough estimation of the protein amount within one sample.

Proteins were identified based on matches to their sequences resulting from comparing of observed peptide MS/MS spectra to theoretical spectra. For MAPK8, also known as c-Jun N-terminal kinase 1 (JNK1), 3 proteins were identified (Tab. 9). Thus, the identified peptides matched with more than one protein sequence related to MAPK8. In this case, 3 out of the 4 different isoforms coded by the Jnk1 gene were identified. Importance of the described proteins and their potential relation to DAGL α will be discussed in the last section of the discussion.

Table 9: MALDI-TOF/TOF mass spectrometry analysis of recombinant DAGL α and co-purified proteins

Accession	Description	Σ Coverage	Σ # Proteins	A: Area	B: Area	Coverage A	Coverage B	# Peptides A	# PSM A	# Peptides B	# PSM B
	ALBUMIN-BOVIN	82,54	62	5,674E9	8.019E8	82,54	72,49	65	1734	51	764
Q6WQJ1	Sn1-specific DAGLα	3,93	1	0	1,138E6	0,00	3,93	0,00	0,00	3	4
P13595	Neural cell adhesion molecule 1	3,32	1	1,774E6	1,238E6	0,00	3,32	0,00	0,00	2	2
P39053	Dynamamin-1	1,96	1	0	4,471E5	0,00	1,96	0,00	0,00	2	2
Q91Y86	Mitogen-activated protein kinase 8	5,73	3	1,911E6	9,947E4	0,00	5,73	0,00	0,00	2	2

High amounts of other unspecific purified proteins like albumin, most likely artifacts from cell culture or sample preparation, were detected in both samples (Tab. 9). These contaminants exacerbate the identification of low occurring proteins, because large peptide peaks of these proteins can overlap or completely overwhelm small chromatographic peaks.

In conclusion, DAGL α was successfully overexpressed and purified from Neuro-2a cells followed by identification via MALDI-TOF/TOF-MS. In addition, first results show the identification of potential interaction partners of DAGL α .

3.5.4 *In vitro* assays using click-chemistry

To analyze possible regulatory mechanisms and potential protein-protein interactions of DAGL α in detail, a new easy to perform *in vitro* assay for the analysis of DAGL α activity was tested. This *in vitro* assay is based on the so-called click-chemistry, in which a labeled biomolecule is detected via copper-catalyzed azide-alkyne cycloaddition. In this study, one fatty acid of a diacylglycerol (DAG) was labeled with a c-c triple bound (alkyne). These alkynes are not appearing naturally in fatty acids. Nevertheless, they do not affect the natural metabolism (Thiele et al. 2012). The labeled DAGs were used as DAGL α substrates in different *in vitro* activity assays.

Two different labeled DAGs were utilized as substrates for DAGL α , on the one hand 1-click-palmitoyl-2-arachidonoyl-*sn*-glycerol (Fig. 10; Fig. 53) and on the other hand 1-click-palmitoyl-2-linoyl-*sn*-glycerol (Fig. 10). DAGLs generally metabolize DAGs into monoacylglycerols (MAGs) and free fatty acids. Previous studies showed that DAGL α equally metabolizes DAGs with either linoleic or arachidonic acid on the sn2 position. In contrast, the β isoform prefers linoleic to arachidonic acid (Bisogno et al. 2010). Furthermore, DAGL α also accepts DAGs with different fatty acids in position 1, such as oleic (Bisogno et al. 2010) or stearic acid (Pedicord et al. 2011; Johnston et al. 2012). However, until now mainly radiolabeled substrates (Bisogno et al. 2010; Johnston et al. 2012) were used to determine DAGL α activity *in vitro*.

Figure 53 exemplarily depicts the metabolism of 1-click-palmitoyl-2-arachidonoyl-*sn*-glycerol (in the following referred as substrate S) by DAGL α and subsequent labeling of the resulting product. Metabolism of the second substrate 1-click-palmitoyl-2-linoyl-*sn*-glycerol (in the following referred as substrate S2) proceeds exactly similar.

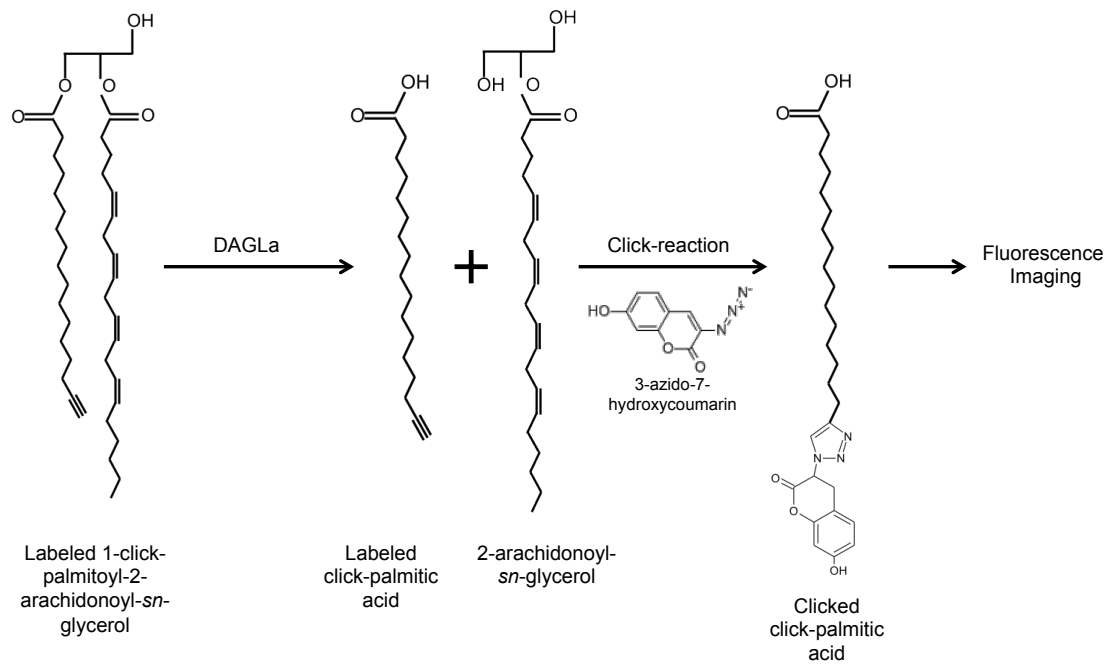


Figure 53: Metabolism of labeled DAGs by DAGL α . DAGL α activity is exemplarily shown for the metabolism of 1-click-palmitoyl-2-arachidonoyl-*sn*-glycerol. DAGL α converts the DAG into a labeled free fatty acid (click-palmitic acid) and an unlabeled monoacylglycerol, in this case 2-arachidonoyl-*sn*-glycerol (2-AG). In a next step, the labeled fatty acid reacts with the fluorogenic dye 3-azido-7-hydroxycoumarin. The resulting molecule can be detected by fluorescence imaging.

Both substrates were tested in different *in vitro* assays, utilizing cultured cells or cell lysates of bone marrow-derived macrophages (BMM) from WT and constitutive *Dagla*^{-/-} mice (Fig. 54A,B,D). Assays with WT and *Dagla*^{-/-} cells were performed to analyze the substrate specificity. Isolation of primary BMM is simple, quick and always yields in high amount of cells. In addition, the activity of flag- or TAP-purified DAGL α (from transfected Neuro-2a cells) was analyzed (Fig. 54C). The metabolic activity of DAGL α was determined by quantification of the band intensity of free click-palmitic acid relative to the applied substrate (S or S2).

Analysis of the *in vitro* assays with substrate S (1-click-palmitoyl-2-arachidonoyl-*sn*-glycerol) revealed similar band intensities of click-palmitic acid after 30 min and 3 h incubation for *Dagla*^{-/-} and WT cell lysates (genotype effect: $F_{(1,4)} = 0.05412$, $p = \text{ns}$, Fig. 54A,E), indicating that enzymes other than DAGL α metabolized substrate S. However, the produced palmitic acid clearly showed a functional metabolism of substrate S (Fig. 54A).

Addition of 10 μM orlistat, a lipase inhibitor often used to inhibit DAGLs (also known as tetrahydrolipstatin (THL)), almost completely blocked the metabolism of substrate S in WT and *Dagla*^{-/-} cell lysates. Relative band intensities of palmitic acid were strongly reduced for *in vitro* assays containing orlistat (lane 1-4; Fig. 54B) compared to untreated assays (lane 7-11; Fig. 54B). Thus, the enzymes metabolizing substrate S belong to the family of lipases, which could be inhibited by orlistat. One of these lipases might be the second DAGL isoform, DAGL β , which is still functional in *Dagla*^{-/-} mice. However, other lipases can convert DAGs

into free fatty acids and MAGs and might therefore be responsible for the detected metabolic activity in *Dagla*^{-/-} cell lysates (Fig. 54A).

Next, the activity of flag- and TAP-purified DAGL α enzymes (see Chapter 3.5.2; Fig. 50B) was analyzed. Purified proteins were incubated for up to 3 h with substrate S. Fluorescence imaging of isolated lipids revealed no band size corresponding to free click-palmitic acid in samples of flag- and TAP-purified DAGL α (Fig. 54C). Thus, no metabolic activities of the purified enzymes were detectable (Fig. 54C). This might be due to the vigorous purification steps or the missing of yet unknown co-factors.

To test the substrate specificity of the second substrate 1-click-palmitoyl-2-linoyl-*sn*-glycerol (S2) different *in vitro* assays were performed, using *Dagla*^{-/-} and WT cells and cell lysates (Fig. 54D). First, the substrate S2 was added to the culture medium of *Dagla*^{-/-} and WT cells for 24 h. No differences in the formation of free click-palmitic were detected in *Dagla*^{-/-} cells compared to WT controls (Fig. 54D, lane 1-4). In addition, various further bands were detected in both samples (Fig. 54). These signals correspond to different lipid molecules, such as MAGs (marked by a grey arrow) and phospholipids, containing the labeled click-palmitic acid (Fig. 54D, lane 1-4). These results suggest that the alkyne label did not generally interfere with the metabolism of the substrates and allowed a tracing of the lipid metabolism. However, no definite conclusion about the lipid metabolism of *Dagla*^{-/-} cells compared to WT cells can be drawn.

Finally, substrate S2 was used for *in vitro* assays with *Dagla*^{-/-} and WT BMM cell lysates (lane 5-15; Fig. 54D). Formation of click-palmitic acid was observed for *Dagla*^{-/-} and WT cell lysates (Fig. 54D). However, two-way ANOVA of the relative band intensities of click-palmitic acid revealed no genotype effect ($F_{(1,6)} = 0.004366$, $p = \text{ns}$; Fig. 54F), but a significant time effect ($F_{(2,6)} = 7.744$, $p < 0.05$; Fig. 54F). Thus, the formation of free palmitic acid increased over time, but the metabolic activity was not dependent on DAGL α .

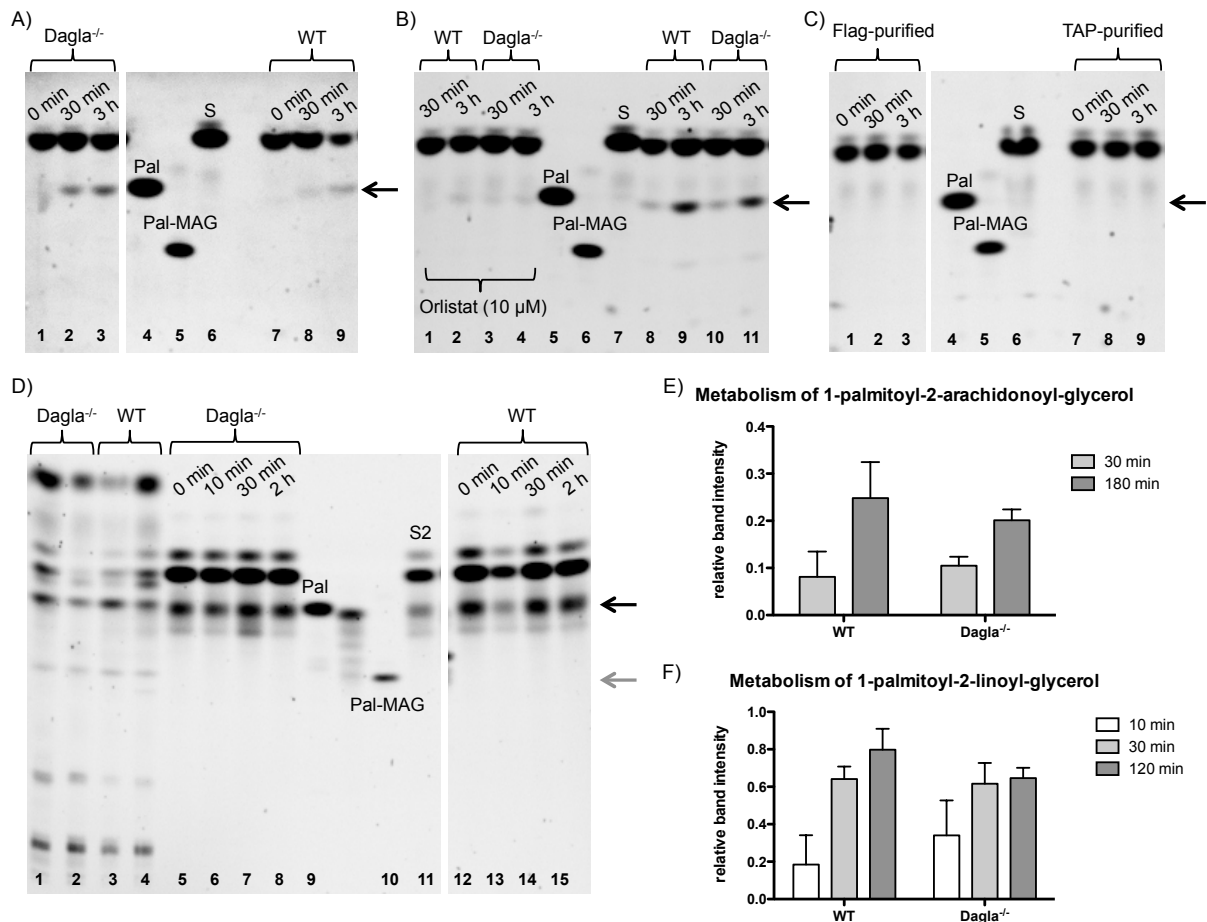


Figure 54: *In vitro* assays to determine DAGL α activity using click-chemistry. (A-D) Shown are representative pictures of DAGL α *in vitro* assays separated on TLC plates. Black arrows indicate the band size of free click-palmitic acid. Grey arrows indicate the band size of the monoacylglycerols (A-C,E) *In vitro* assays with substrate S (1-click-palmitoyl-2-arachidonoyl-*sn*-glycerol) (A) Lane 1-3: *Dagla*^{-/-} BMM lysates incubated for 0 min, 30 min and 3 h; lane 4: click-palmitic-acid; lane 5: click-palmitoyl-*sn*-glycerol; lane 6: substrate S; lane 7-9: WT BMM lysates incubated for 0 min, 30 min and 3 h. (B) lane 1-2: WT BMM lysates incubated for 30 min and 3 h with 10 μ M Orlistat; lane 3-4: *Dagla*^{-/-} BMM lysates incubated for 30 min and 3 h with 10 μ M Orlistat; lane 5-7: standards; lane 8-9: WT BMM lysates incubated for 30 min and 3 h; lane 10-11: *Dagla*^{-/-} BMM lysates incubated for 30 min and 3 h. (C) Lane 1-3: Flag-purified DAGL α incubated for 0 min, 30 min, and 3h; lane 4-6: standards; lane 7-9: flag-purified DAGL α incubated for 0 min, 30 min, and 3h. (D) *In vitro* assays with substrate S2 (1-click-palmitoyl-2-linoyl-*sn*-glycerol): lane 1-2: *Dagla*^{-/-} BMM cells overnight incubated, lane 3-4: WT BMM overnight incubated; lane 5-8: *Dagla*^{-/-} BMM lysates incubated for 0 min, 10 min, 30 min and 3 h; lane 9-10: standards; lane 11: substrate S2; lane 12-15: WT BMM lysates incubated for 0 min, 10 min, 30 min and 3 h. (E,F) Intensities of individual bands of free click-palmitic acid were quantified using ImageJ densitometry software, and expressed relative to the substrate signal. (E) Formation of free palmitic acid did not differ between *Dagla*^{-/-} and WT cells. (F) Metabolism of substrate S2 was similar in both genotypes (two-way ANOVA, Bonferroni's post-hoc test, values represent mean \pm SEM; n = 2).

In conclusion, both substrates were metabolized in *Dagla*^{-/-} and WT BMM cell lysates and could easily be detected by click-chemistry and subsequent fluorescence imaging. Click-chemistry is a promising approach to analyze enzyme activity *in vitro*. However, the applied substrates were not specific for DAGL α . DAGL β or other lipases might have metabolized the labeled DAGs. Further studies are required to confirm whether other labeled DAGs are more specific for DAGL α or not.

Discussion

One aim of this thesis was to determine the impact of DAGL α , the main synthesizing enzyme of 2-AG in the CNS, on the development and manifestation of mood disorders, such as anxiety and depression. Therefore, constitutive as well as neuronal- and microglia-specific Dagla knockout mice were comprehensively analyzed in a variety of behavioral paradigms related to anxiety and depressive disorders. To further characterize the different knockout mouse lines, molecular analysis, including endocannabinoid measurements and gene expression analysis, were performed. Mice lacking Dagla displayed substantial modifications of the composition of endogenous cannabinoids and severe behavioral changes.

A second aim was to analyze the sensitivity of Dagla^{-/-} and Syn-Dagla^{-/-} mice to chronic stress. The widely applied model of chronic social defeat stress was used to challenge knockout and control mice. Subsequently, behavioral and molecular stress responses were determined.

Lastly, this thesis aimed to establish a method disclosing interaction partners of DAGL α . Tandem affinity purification and subsequent MALDI-TOF/TOF mass spectrometry analysis revealed several candidate proteins, presenting an advantageous approach to discover potential interaction partners of DAGL α . Furthermore, novel *in vitro* DAGL α activity assays using the non-radioactive click-chemistry method were performed. Results of this part will be discussed in the finishing section of the discussion.

4.1 Behavioral and molecular characterization of mice lacking Dagla

The present study demonstrates that mice with a constitutive deletion of Dagla showed a phenotype of increased emotional and stress-related behaviors. This was characterized by a reduced exploration of the central area of the open-field, a maternal neglect behavior, a fear extinction deficit, increased behavioral despair and increased anxiety-related behaviors in the light/dark box test. Some of these behavioral changes resemble those observed in animals lacking the main neuronal cannabinoid receptor CB1. Together, these findings strongly support the notion that a disruption of endocannabinoid signaling adversely affects the emotional state of animals and results in enhanced anxiety-, stress- and fear-responses.

Dagla^{-/-} animals showed an extensive reduction (80-90%) in hippocampal, cortical, amygdalar and striatal 2-AG levels, confirming that DAGL α is the main 2-AG synthesizing

enzyme in the brain. This finding is also supported by previous studies showing that 2-AG in the CNS is predominantly produced by DAGL α , while DAGL β is the main synthesizing enzyme of 2-AG in peripheral tissues (Gao et al. 2010). Gao and colleagues found that constitutive deletion of *Daglb* caused a 50 % reduction of 2-AG in the brain and 90 % reduction in the liver (Gao et al. 2010). Consequently, DAGL β cannot compensate the loss of function of DAGL α . Nevertheless, DAGL β is expressed in neurons and non-neuronal cells in the CNS and is certainly responsible for the remaining 10-20 % 2-AG content.

Expression analysis of other ECS-related genes revealed no changes. In addition, CB1 signaling was not changed in *Dagla*^{-/-} mice. THC treatment induced similar behavioral changes in the tetrad test in *Dagla*^{-/-} and WT mice, indicative of an unaltered CB1 signaling. Consequently, the behavioral and molecular changes detected in *Dagla*^{-/-} mice can be directly linked to the lack of *Dagla* and not to modified CB1 signaling.

Interestingly, the levels of anandamide were also significantly decreased in the hippocampus, amygdala and cortex, but not in the striatum, of *Dagla*^{-/-} mice. This finding is in agreement with previous studies that have indicated a correlation of 2-AG and anandamide production in the brain (Gao et al. 2010). It seems that the activity of DAGL α and thus the level of 2-AG influenced anandamide levels in a brain region-specific manner. Although the underlying mechanism is unknown, it is noteworthy that the administration of the MAGL inhibitor JZL184 to *Dagla*^{-/-} mice increased not only 2-AG levels, but also normalized the level of anandamide (Fig. 18). It is unlikely that MAGL contributes directly to the degradation of anandamide, because MAGL deficient mice have normal anandamide levels and acute JZL184 treatment does not affect anandamide concentrations in WT mice (Schlosburg et al. 2010; Nomura et al. 2011). It is more likely that the vastly reduced production of 2-AG in *Dagla*^{-/-} mice leads to a decrease in anandamide synthesis, or an increase in anandamide degradation through an indirect mechanism.

Furthermore, 2-AG levels in the brain of neuronal- and microglia-specific *Dagla* knockout mice were not altered, most likely indicating that neither neurons nor microglia are the main 2-AG producing cells in the adult brain. In addition, anandamide levels were significantly reduced in the cortex, but not the hippocampus and striatum of *LysM-Dagla*^{-/-} mice. These findings together with the reduced anandamide levels in *Dagla*^{-/-} mouse brain suggest that the lack of *Dagla* in microglia influences the production of anandamide either released by microglia itself or other cell-types in a brain region-dependent manner. However, it should be considered that using the *LysM-Cre* line only led to a 30-40 % deletion of *Dagla*. Hence, other microglia-specific mouse lines with higher deletion efficiencies need to be analyzed to confirm this result. The present study is the first to analyze 2-AG production in different cell types *in vivo*, using conditional *Dagla* knockout mouse lines. In addition, the findings show for the first time that the main amount of 2-AG in the brain is not only released

by neurons. It is very unlikely that compensatory mechanisms, such as an upregulation of neuronal DAGL β or increased 2-AG production by other cell-types, are solely responsible for the entirely unchanged 2-AG content. Nevertheless, to further verify these results, 2-AG levels of cultured Syn-Dagla $^{-/-}$ neurons and LysM-Dagla $^{-/-}$ microglia should be determined.

In line with previous studies (Gao et al. 2010), a significantly reduced body weight was observed in Dagla $^{-/-}$ mice. This effect seems to be due to decreased food intake and shifts in energy metabolism. Treatment with a DAGL α inhibitor significantly decreased the intake of high-fat diet in mice (Bisogno et al. 2013). In addition, a recent study showed that Dagla $^{-/-}$ mice and CB1 $^{-/-}$ mice had similar lean phenotypes and reduced body fat when raised on chow or high fat diet. Body fat was decreased up to 50 % in comparison to wild type littermates (Powell et al. 2015). Pair-fed studies showed that hypophagia was the reason for this lean phenotype (Powell et al. 2015), as also reported for CB1 $^{-/-}$ animals (Cota et al. 2003). In addition, high fat diet-fed Dagla $^{-/-}$ mice had significantly lower insulin and total cholesterol levels after glucose challenge (Powell et al. 2015). These reductions in body weight and body fat were not detected in Daglb $^{-/-}$ animals (Powell et al. 2015), which have a markedly higher 2-AG level in the brain than mice lacking Dagla (Gao et al. 2010). Thus, the lean phenotype is most likely due to 2-AG-CB1 signaling in the CNS rather than in peripheral tissues. This hypothesis is consistent with the finding that mice with a neuronal-specific deletion of Dagla also displayed a reduced body weight. Even though the effect occurred to a lower extent, the present study implies that neuronal DAGL α at least partially contributes to the lean phenotype. Microglia-specific knockout of Dagla did not affect the body weight. However, as mentioned above, the LysM-Cre mouse line only displayed a deletion-efficiency of 30-40 % in microglia and 80 % in bone marrow-derived macrophages (Jehle et al. 2016). Previous studies indicated that hormones and dietary signals control microglia activity during obesity (Gao et al. 2014) and that microglia might play an important role in the physiological control of metabolism (for review see Argente-Arizón et al. 2015). To determine to which extent microglia and neurons contribute to the metabolic changes seen in HFD-fed Dagla $^{-/-}$ mice, conditional knockout mouse lines are still to be analyzed in HFD pair-feeding studies.

Behavioral studies performed with CB1 $^{-/-}$ mice indicated that a disrupted CB1 signaling promotes anxiety-related behaviors in various paradigms, such as the light-dark box or the plus maze test (Martin et al. 2002; Haller et al. 2004; Urigüen et al. 2004). Thus, a disrupted CB1 signaling seemed to promote anxious behavior. The opposite was reported when endocannabinoid levels were increased. Inhibition of the 2-AG degrading enzyme MAGL (Busquets-Garcia et al. 2011; Sciolino et al. 2011) or the pharmacologic blockade of the anandamide-degrading enzyme FAAH, led to reduced anxiety-related behavior. This effect

was antagonized by the CB1 antagonist rimonabant, demonstrating an involvement of the CB1 receptor (Moreira et al. 2008). Consistently, a mild anxiety- or stress-related phenotype in *Dagla*^{-/-} mice in the open-field and light-dark box tests was observed in the present study. The mice spent less time exploring the center of the open-field box, which is correlated with anxiety-like behavior. However, the phenotype is rather mild and only significant for some time points. A similar mild anxiety-related phenotype was detected in the light/dark box test. In this test, the main measure for anxiety is the activity and time spent in the two areas of the light/dark box, based on the innate aversion of rodents to brightly illuminated areas. The number of transitions between the light and dark area and number of rearings were markedly reduced in mice lacking *Dagla*, indicating that reduced levels of 2-AG caused a decreased exploratory behavior. Furthermore, a reduced number of transitions, without decreased spontaneous locomotion, are related to an increased anxiety (Bourin & Hascoet 2003). Previous studies showed that the deletion of CB1 caused a comparable, but more pronounced phenotype with decreased time spent in the light area and reduced number of transitions (Martin et al. 2002). It was suggested that the CB1 anxiety phenotype largely depends on the basal anxiety level of the animals in the test situation (Haller et al. 2002, 2004). Locomotion (distance travelled) was not affected in neither of the two test paradigms. However, there was no genotype effect in the open arm time of the zero-maze, but an increased distance travelled. *Dagla*^{-/-} mice thus also showed a behavioral change in the more aversive zero-maze test, but these changes cannot be readily related to anxiety.

Furthermore, it is possible that the increased anxiety- or stress-related behavior in *Dagla*^{-/-} mice also contributed to the altered maternal behavior in the pup retrieval test. *Dagla*^{-/-} mice needed much more time to retrieve a pup back into the nest, but the nursing behavior was unaffected and the body weight of *Dagla*^{-/-} pups did not differ from WT controls. It thus appears that *Dagla*^{-/-} dams have no general deficit in maternal behavior, but rather behaved different from WT dams because of the stressful test situation. This hypothesis is supported by the unchanged behavior of *Dagla*^{-/-} mice in the social preference test, which indicates that the altered maternal behavior is not due to a generally impaired social interest of the knockout animals. This hypothesis is also in line with previous studies showing that treatment with rimonabant or deletion of the CB1 resulted in slower pup retrieval (Schechter et al. 2012, 2013), whereas nursing behavior was not affected. Schechter et al. (2013) have also suggested that the increased stress sensitivity of CB1^{-/-} mice (Martin et al. 2002; Haller et al. 2004) contributed to the deficit in maternal care. Nevertheless, it cannot be ruled out that vice versa a dysfunctional maternal behavior contributed to the anxiety, fear and stress-related behavioral phenotypes.

The anxiety- and stress-related behavioral phenotypes of *Dagla*^{-/-} mice are entirely consistent with the observed reduction in endocannabinoid levels in the amygdala and

hippocampus, two brain regions essential for normal fear and anxiety behaviors. To determine more precisely how endocannabinoid signaling modulates the neuronal circuits associated with affective behaviors, cell type-specific *Dagla* knockout mice were analyzed in the same behavioral paradigms. Neuronal- and microglia-specific deletion of *Dagla* did not affect anxiety-like behavior in the open-field, zero-maze or light/dark box test. Together with the finding that both mouse lines had unaltered 2-AG levels, the mild anxiety-like phenotype of *Dagla*^{-/-} is most likely dependent on the tremendous reduction of 2-AG. However, it cannot be ruled out that the reduced anandamide levels also contribute to the observed phenotype.

Previous studies revealed a distinct fear extinction deficit in *Dagla*^{-/-} mice and an increased freezing response, indicative of an altered stress-response (Ternes 2013; Jenniches et al. 2015). To determine the impact of DAGL α expressed in neurons and microglia, both conditional mouse lines were subjected to a fear conditioning paradigm. A distinct deficit in fear extinction and increased freezing responses were detected in *Syn-Dagla*^{-/-} similar to that seen in *Dagla*^{-/-} animals. While *Dagla*^{fl/fl} controls displayed progressive fear extinction from day E1 to E3, the freezing response of *Syn-Dagla*^{-/-} increased over time. The mild unexpected increase of freezing time observed in *Dagla*^{fl/fl} mice on day E6 is most likely due to fear-inducing disturbances, such as disruptive noise during the behavioral test or previous cage changes. In addition, *LysM-Dagla*^{-/-} showed a mildly increased freezing responses on day E6, but no deficits in the extinction of fear.

The levels of 2-AG and anandamide increased after the first extinction training in the basolateral amygdala, a brain region critically involved in the acquisition and expression of conditioned fear (Marsicano et al. 2002; Myers & Davis 2007). Genetic ablation of CB1 receptors or pharmacological blockage, systemically or within the amygdala, prevents the extinction of conditioned fear responses. Fear extinction involves safety learning, which refers to the formation of a new association between the conditioned stimulus with the non-appearance of the punishment. The second process involves a non-associative component of extinction, namely the habituation to the conditioned stimulus (Kamprath & Wotjak 2004). *CB1*^{-/-} mice showed distinct deficits in both processes. In particular, *CB1*^{-/-} mice showed delayed between-session extinction, also termed long-term extinction, and inability in achieving within-session extinction (short-term extinction) (Marsicano et al. 2002; Ruehle et al. 2012; Kamprath et al. 2006). It is not entirely clear if and how both of these processes are modulated by the ECS. Studies focusing on repeated homotypic stress showed that 2-AG levels in cortical brain regions were elevated after a repeated stress exposure, whereas glutamate release declined gradually (Rademacher et al. 2008; Patel & Hillard 2008). This mechanism of stress adaptation is supposedly mediated through an increased synthesis of 2-AG (Patel & Hillard 2008). Therefore, the impaired fear extinction seen in *Dagla*^{-/-} and *Syn-*

Dagla^{-/-} mice could be due to a deficit in habituation, which was also shown in CB1^{-/-} mice (Kamprath et al. 2006). This stress-induced increase of 2-AG, which mediates stress adaptation, is very likely reliant on the activity of neuronal DAGL α . This hypothesis is consistent with the finding that Syn-Dagla^{-/-} mice have a distinct fear extinction deficit similar to that seen in Dagla^{-/-} animals, although total brain 2-AG levels are not reduced in these animals. In addition, chronic social defeat stress caused significantly increased 2-AG levels in the amygdala of Dagla^{fl/fl}, but not Syn-Dagla^{-/-} mice. Accordingly, neuronal deletion of Dagla negatively affected the habituation to stress.

In addition, contrary to Dagla^{-/-} mice, Syn-Dagla^{-/-} mice almost completely lacked between-session fear extinction, representing a strong deficit in safety learning. Thus, neuronal 2-AG at least partially mediates this learning paradigm in auditory fear conditioning. The different behaviors observed in Dagla^{-/-} and Syn-Dagla^{-/-} mice might be due to compensatory mechanisms in consequence to the continually reduced 2-AG levels in the amygdala and other brain regions critically involved in fear extinction. On the other hand, reduced anandamide levels in the amygdala and hippocampus of Dagla^{-/-} mice might alter fear conditioning and subsequent fear extinction. Treatment with the FAAH inhibitor URB597, thus increased anandamide levels, enhanced extinction in several paradigms (reviewed in Gunduz-Cinar et al. 2013). However, the consequence of short- or long-term reductions of anandamide levels is still uncertain. Furthermore, microglia-specific deletion of Dagla, causing decreased cortical anandamide levels, did not produce general deficits in fear extinction, but mildly increased the fear response. Since control animals displayed only limited fear extinction in this particular test, it needs to be repeated to allow a firm conclusion. In addition, LysM-Cre only generated a 30-40 % knockout, and more potent microglia-specific Dagla knockout mouse lines are needed to confirm these results. Together with CB1 knockout and pharmacological studies, using either systemic or brain-region-specific blockade of endocannabinoid signaling, the present findings show that the ECS is crucial for efficient extinction learning.

The deletion of Dagla also induced depression-like behaviors. Thus, Dagla^{-/-} mice displayed an enhanced behavioral despair in the forced swim test, anhedonia in the sucrose preference test, and reduced hippocampal neurogenesis (Jenniches et al. 2015), but a normal sleep/wake cycle. It is not clear if these behavioral phenotypes can be entirely attributed to the reduced levels of 2-AG, or if the reduced anandamide levels also had a contribution. However, neither JZL184 nor URB597 treatment, which both increased anandamide concentrations, affected the immobility time in the forced swim test. In addition, deletion of neuronal Dagla also caused behavioral despair and anhedonia similar to that seen in Dagla^{-/-} mice. Therefore, not the generally decreased brain 2-AG levels, but rather

the lack of neuronal 2-AG caused the observed phenotype. It is most likely that neuronal and synaptic plasticity and/or cell-cell communication are limited due to the loss of 2-AG produced by DAGL α in neurons, contributing to the observed behavioral changes. Reduced neuroplasticity is directly connected with depression and other stress-related mood disorders (for review see Pittenger & Duman 2008). In addition, the lack of CB1 receptors impaired neuronal plasticity (for review see Valverde et al. 2012). More importantly, synaptic plasticity is at least partially mediated by 2-AG, produced by DAGL α (Chevalleyre et al. 2003; Hashimoto et al. 2008; Gao et al. 2010).

Another hallmark of animal models of depression is a reduced adult neurogenesis. Nevertheless, neuronal proliferation and survival was not affected by the deletion of neuronal Dagla, indicating that 2-AG produced by non-neuronal cells caused the significant reduction of neuronal proliferation and survival observed in Dagla^{-/-} mice (Gao et al. 2010; Jenniches et al. 2015). Previous studies showed that microglia and astrocytes are critically involved in adult neurogenesis (Morrens et al. 2012). Thus, future studies should analyze the neuronal proliferation and survival in LysM-Dagla^{-/-} mice and further in astrocyte-specific knockout animals.

ECS signaling, in particular the activity of the CB1 receptor, is known to modulate depression-related behavior in rodents and depression in humans. Thus, CB1^{-/-} mice are more sensitive in developing a depressive-like phenotype after chronic stress (Martin et al. 2002, Schechter et al. 2013) and the CB1 receptor antagonist rimonabant increased depressive symptoms in humans. Increase of 2-AG via the blockade of MAGL also produced antidepressant- and anxiolytic effects, and enhanced adult hippocampal neurogenesis (Zhong et al. 2014; Zhang et al. 2014). Furthermore, chronic treatment with antidepressants led to a significant increase in 2-AG levels in various brain areas, indicating that 2-AG could be important for the antidepressant effect of these drugs (Smaga et al. 2014). Previous studies showed a significant reduction in serum 2-AG levels of female patients with major depressive disorders (Hill et al. 2008a; Hill et al. 2009). In contrast, a recent study indicated that mice lacking MAGL display an anxiety and depressive-like phenotype similar to that observed in mice with reduced 2-AG levels (Imperatore et al. 2015). The authors claim that desensitization of CB1 receptors caused an excitatory/inhibitory imbalance, which leads to an excitatory drive in the PFC and an inhibitory drive in the amygdala and hippocampus. Together with the present study these results indicate that alterations in the eCB composition and CB1 signaling severely affect the emotional state.

The analysis of CB1^{-/-} mice showed that the CB1 receptor is essential for normal brain development. It is thus difficult to tell whether the behavioral phenotypes are direct effects of the disrupted 2-AG biosynthesis, or rather an indirect consequence of developmental effects.

This uncertainty, which concerns all studies with genetic mouse models, may be addressed with the help of an inducible Cre recombinase (Lewandowski 2001; Feil et al. 2009).

In conclusion, the results of this study indicate an important role of 2-AG, in particular produced by neurons, in the modulation of emotion and stress-responses. In addition, the activity of microglial Dagla also partially contributes to the processing of fear responses and anhedonic-like behavior. These findings are consistent with the idea that a disrupted endocannabinoid signaling contributes to the development of affective disorders, which is supported by clinical data.

4.2 Chronic social defeat stress

A further aim of this study was to analyze the sensitivity of constitutive and neuronal-specific Dagla knockout animals to chronic stress. Chronic stress models, such as chronic social defeat stress, are known to induce behavioral and molecular changes resembling signs and symptoms of humans with affective disorders (for review see Hammels et al. 2015). Thus, this model mimics cardinal features of a multitude of psychiatric disorders including depression, anxiety and post-traumatic stress disorders.

The ECS plays an important role in stress adaptation. The genetic or pharmacological blockade of CB1 receptors was shown to cause an anxiety- and depressive-like phenotype and increased the sensitivity to chronic stress (Haller et al. 2002; Martin et al. 2002; Beyer et al. 2010). In this study, an increased stress sensitivity was also observed in mice constitutively lacking Dagla. The mortality rate of Dagla^{-/-} mice exposed to chronic social defeat stress exceeded 30 %, whereas only 2 out of 30 tested Dagla^{fl/fl} controls and 1 out of 10 Syn-Dagla^{-/-} mice died in consequence to the stress exposure. None of the deceased animals had severe wounding, thus physiological changes, such as cardiovascular affections, were most likely the leading cause of death. In line with this, social defeat was shown to induce a higher degree of cardiac arrhythmias compared to other chronic stress models (Sgoifo et al. 1999; Sgoifo et al. 2005). Furthermore, the individual susceptibility to chronic stress varies greatly among individuals (for review see Krishnan 2014). As a consequence, the most susceptible mice, which died during the stress paradigm, could not be included in the subsequent behavioral and molecular analysis.

The deletion of Dagla, thus the lack of 2-AG, tremendously increased the sensitivity to chronic stress. Chronic social defeat stress caused a robust long-lasting increase of 2-AG levels in the amygdala of Dagla^{fl/fl} and slightly increased quantities in the PFC. Both brain parts belong to the limbic circuit, which is critically involved in the formation and regulation of emotional processes and stress-related behaviors. In contrast, 2-AG levels of Dagla^{-/-} mice

were not affected, indicating that stress-induced increase of 2-AG is dependent on DAGL α and not the second DAGL isoform DAGL β . Likewise, 2-AG levels of Syn-Dagla $^{-/-}$ were not altered after CSDS, showing that the stress-dependent increase of 2-AG is dependent on the activity of neuronal DAGL α .

Habituation to homotypic stress is at least partially mediated by an increase of amygdalar 2-AG (Patel & Hillard 2008; Hill et al. 2010b). Accordingly, Dagla $^{-/-}$ mice might have a distinct deficit in stress adaptation and habituation, which possibly contributed to the high mortality rate. In contrast to 2-AG, anandamide levels were shown to decrease in the amygdala, PFC, hypothalamus and hippocampus following chronic homotypic and unpredictable stress (Hill et al. 2010b; Hill et al. 2008b). However, CSDS did not affect anandamide levels in wild type animals (Dagla $^{fl/fl}$). These discrepancies are most likely due to the use of different stressors and the time point of eCB measurements. In this study, endocannabinoid levels were determined 12 days after the last day of CSDS and not immediately following the last stress exposure. Thus, it cannot be excluded that anandamide quantities normalized during this time delay. Interestingly, chronic stress lastingly increased anandamide levels in the PFC of Syn-Dagla $^{-/-}$ mice. The same tendency was seen in the amygdala. This effect presumably represents a compensatory mechanism. Due to the lack of a stress-dependent increase in 2-AG levels, the second most common eCB, anandamide, increased to mediate stress adaptation (see also below).

Furthermore, CSDS caused a mild downregulation of several genes related to the ECS. Reduced levels of Magl, Faah and Dagla expression were observed in the amygdala of chronically stressed mice. Accordingly, increased 2-AG levels in the amygdala of Dagla $^{fl/fl}$ mice were most likely caused by the increased activity of the DAGL α protein, irrespective of gene expression, and a decreased metabolism via MAGL. Furthermore, mRNA levels of Nape-Pld and CB1 were not affected. In contrast, previous studies showed that chronic stress caused significant changes in CB1 gene expression and binding site density in a brain region-specific manner. Chronic unpredictable stress increased gene expression (Hillard et al. 2006) and binding site densities of CB1 in the PFC (Hill et al. 2008b), while both parameters were decreased in the hippocampus and hypothalamus (Hill et al. 2008b). Furthermore, FAAH gene expression was upregulated after chronic stress (Patel 2005; Hill & McEwan 2010c), most likely responsible for the reduced anandamide levels described in previous studies (Hill et al. 2010b). The different types of stressors might explain the differences observed in ECS gene expression. Social defeat belongs rather to the homotypic than to the unpredictable stress models. In line with this, CSDS caused significantly increased brain 2-AG levels - an effect being more consistent following repeated homotypic stress exposures compared to unpredictable stressors. Increased 2-AG levels following chronic homotypic stress have been described in the amygdala, hippocampus, PFC and

hypothalamus (Dubreucq et al. 2012; Rademacher et al. 2008; Patel & Hillard 2008).

Responses to acute and chronic stress are predominantly manifested in an activation of the HPA axis, leading to increased stress hormone levels. Glucocorticoid hormones, in rodents mainly corticosterone, are the body's stress hormones and generally increased after exposure to acute or chronic stress. In contrast to plasma corticosterone levels, which show great fluctuation in response to stress, fecal corticosterone levels enable the analysis of long-term effects (cumulative levels of secreted corticosterone). Chronic social defeat stress induced a significant increase of fecal corticosterone levels in group-housed intruder mice regardless of the genotype. However, this effect was not observed in single-housed mice. In this group, baseline corticosterone levels of unstressed mice were already as high as the corticosterone levels of stressed group-housed animals. Even though housing itself was shown not to influence fecal corticosterone levels (Toth et al. 2015), it leads to a sensitization of the HPA axis. Previous studies showed that single-caged mice had higher plasma corticosterone levels after acute stress (Ros-Simó & Valverde 2012). During the ten days of CSDS control animals were housed with unknown C57BL/6 mice, separated by a perforated Plexiglas wall and handled daily for body weight measurements. Thus, the single-housed intruder mice were most likely more sensitive to these stressful testing conditions, leading to higher baseline corticosterone levels in unstressed animals. Nevertheless, a significant increase of fecal corticosterone was detected in stressed single-caged *Dagla*^{-/-} mice, but not in *Dagla*^{fl/fl} or *Syn-Dagla*^{-/-} mice. Thus, the stress-dependent release of corticosterone was most pronounced in mice constitutively lacking *Dagla*, indicative of higher stress sensitivity and altered HPA axis regulation. In line with these findings, previous studies showed that the lack of CB1 receptors increased the release of corticosterone in response to stress (Urigüen et al. 2002, Zoppi et al. 2011). Furthermore, CB1 receptor antagonism prevented HPA axis habituation (Hill et al. 2010b) and CB1 receptors within the PVN mediated glucocorticoid feedback inhibition (Evanson et al. 2007). In addition, 2-AG and anandamide have been shown to be involved in HPA axis regulation. A multitude of studies indicated that 2-AG signaling contributed to the termination and adaptation of the HPA axis, while a stress-dependent decrease in anandamide levels appeared to contribute to the manifestation of the stress response, including an activation of the HPA axis (for review see Morena et al. 2016). Moreover, 2-AG synthesis in the PFC after acute stress was controlled by a corticosterone-mediated activation of GR (Hill et al. 2011). Hill and colleagues showed that this effect was CB1-dependent, since the blockade of CB1 receptors in the PFC prolonged corticosterone secretion. Thus, 2-AG-CB1 signaling in the PFC critically contributed to the feedback inhibition of the HPA axis (Hill et al. 2011). This is in line with the present findings showing that mice constitutively lacking *Dagla* displayed higher corticosterone levels after exposure to

CSDS compared to *Dagla^{fl/fl}* and *Syn-Dagla^{-/-}* mice, indicative of a disrupted HPA axis feedback inhibition in *Dagla^{-/-}* mice. In addition, these finding supports the hypothesis that increased anandamide levels in the PFC of *Syn-Dagla^{-/-}* took on the role of 2-AG in reaction to chronic stress. More precisely, anandamide seemed to mediate the termination of the HPA axis response to stress, leading to lower corticosterone levels in *Syn-Dagla^{-/-}* mice compared to *Dagla^{-/-}* animals. Since both eCBs act through the same receptors, share common functions, and have somehow interconnected biosyntheses, a cell-specific compensatory role of anandamide in case of 2-AG deficiency is reasonable. However, this compensatory role seemed to be restricted to a reaction to chronic stress, since under baseline conditions neuronal deletion of *Dagla* caused similar behavioral alterations as observed in *Dagla^{-/-}* mice. In addition, a comparable compensatory effect of anandamide was missing in *Dagla^{-/-}* mice, substantiated by significantly reduced anandamide levels in several brain areas, possibly caused by a disruption in the anandamide biosynthesis.

Corticosterone is produced and released from the adrenal glands, representing the end effectors of the HPA axis. As a result of long-term corticosterone production, for instance due to chronic stress, adrenal weights can increase. Indeed, CSDS caused significantly increased adrenal weights in *Dagla^{-/-}* mice, but not *Dagla^{fl/fl}* mice. However, this effect was not seen in the single-caged intruder animals. In this case, the unstressed *Dagla^{-/-}* animals had higher adrenal weights compared to unstressed control mice. Discrepancies between increased corticosterone levels and adrenal weights might be due to the time period of approximately two weeks between both measurements. However, the results further support that mice constitutively lacking *Dagla* inhibited strong alterations in HPA axis activity, leading to an increased corticosterone release in response to chronic stress.

Conclusively, the present study offers additional support for the overarching hypothesis that endocannabinoid signaling is fundamental to the intrinsic regulation of the HPA axis. In addition, this study shows for the first time that neuronal DAGL α -dependent 2-AG release in the amygdala and PFC contributed to the regulation of HPA axis responses to stress (Fig. 55). Furthermore, in case of neuronal deletion of *Dagla*, presumably anandamide took over this task and compensated the lack of neuronal 2-AG.

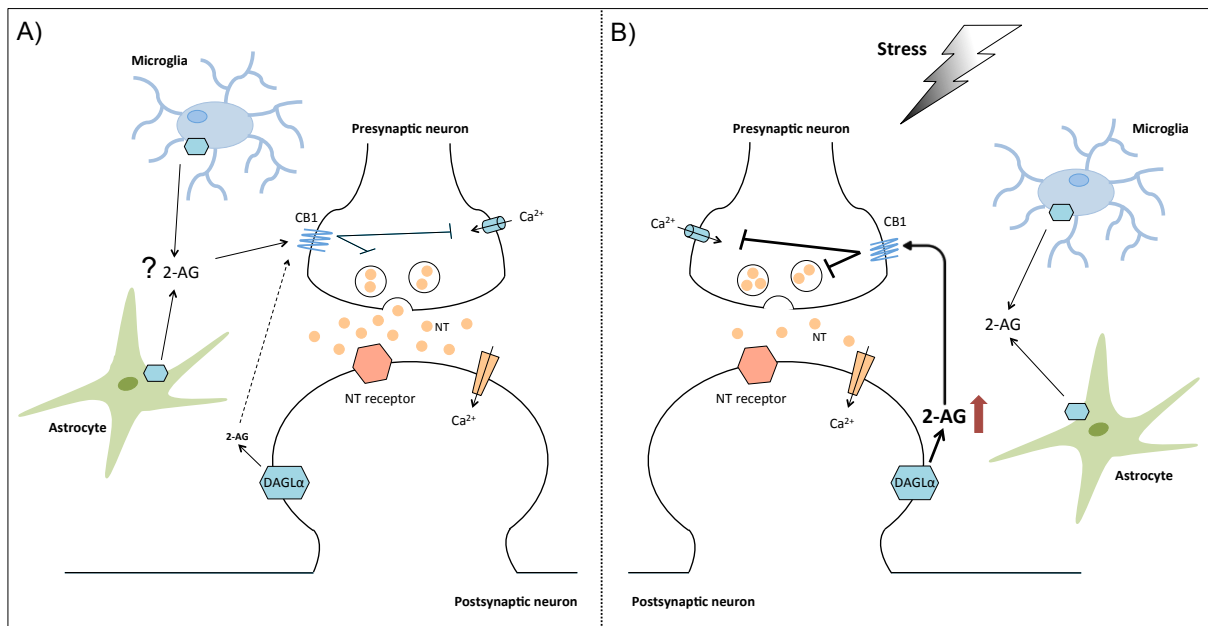


Figure 55: Source of 2-AG under baseline conditions and in response to chronic stress. (A) In the healthy brain neurons produce only a minor part of 2-AG. Since astrocytes and microglia produce more 2-AG compared to neurons *in vitro*, glia cells might be responsible for the main 2-AG content in the unstressed brain. (B) However, in response to chronic stress neurons in the amygdala and PFC release high amounts of 2-AG mediating stress habituation. Abbreviations: 2-AG: 2- arachidonoylglycerol, CB1: cannabinoid receptor 1, DAGL: diacylglycerol lipase, NT: neurotransmitter.

The role of glucocorticoids in the brain is not only dependent on the hormonal levels, but also on the expression profiles of the glucocorticoid (GR) and mineralocorticoid receptors (MR) (Hermann 1993). Due to the low binding affinity of glucocorticoids to GR in comparison to MR, the second adrenal steroid receptor, GR is only activated during periods of high circulating glucocorticoid levels, as experienced during stress. As a result of this binding profile, GR mediates the majority of glucocorticoid negative feedback mechanisms (for review see Myers et al. 2012). The constitutive deletion of *Dagla* caused significantly reduced GR gene expression in the amygdala, hippocampus and PVN, brain parts critically involved in the regulation of the HPA axis. In line with this, previous studies showed that the constitutive deletion of CB1 caused a significant downregulation of GR in the hippocampus, but not the PVN (Cota et al. 2007). However, gene expression of the corticotropin-releasing hormone (CRH) and its main receptor CRHR1 were unchanged following chronic stress. In contrast, Cota et al. (2007) found a significant upregulation of CRH in the PVN of CB1^{-/-} mice. Since gene expression analysis of CRH mRNA levels displayed high variances, further studies are required to confirm these results.

In conclusion, the lack of *Dagla* at least partially altered HPA axis activity and gene expression, leading to a reduced GR expression and most likely a reduced GR-mediated feedback inhibition. In contrast, neuronal-specific deletion of *Dagla* did not affect the expression of GR in the brain. With respect to previous studies, reduced GR mRNA levels

were possibly caused by the persistently decreased 2-AG levels in the brain of *Dagla^{-/-}* mice and the lack of 2-AG-CB1 signaling.

Glucocorticoids were shown to rapidly modulate glutamatergic (Karst et al. 2005; Karst et al. 2010) and GABAergic (Verkuyl et al. 2005) transmission in stress-sensitive brain regions through alterations of neurotransmitter release. Recent studies supported the hypothesis that glucocorticoids modulated the release of glutamate and GABA as a result of enhanced endocannabinoid signaling (for review see Hillard 2014). In line with this, previous studies showed that corticosterone increased 2-AG production in the PFC via activating GR (Hill et al. 2011). This would mean that corticosterone increases 2-AG release and in turn 2-AG inhibits the release of corticosterone. In line with this, mice constitutively lacking *Dagla*, thus 2-AG, had higher corticosterone levels. However, the direct link between *DAGLα*, thus 2-AG, and GR gene expression remains elusive and further experiments are needed to clarify the possible role of the endocannabinoid system in the modulation of brain GR function. Taken together, these results show that the connection between the ECS and the HPA axis is multifaceted and an appropriate interplay between both signaling systems is necessary to maintain homeostasis.

A severe threat to the body's homeostasis is chronic stress. It is known to cause an overactivity of the HPA axis and significant reductions of GR gene expression. More than 50 % of depressed patients show hyperactivity of the HPA axis and impaired GR-mediated negative feedback (Anacker et al. 2011). Indeed, CSDS significantly decreased GR mRNA levels in the amygdala and at least partially in the hippocampus of *Dagla^{fl/fl}*, *Dagla^{-/-}* and *Syn-Dagla^{-/-}* mice. However, this effect was only observed in single-caged intruder mice, again indicative of an increased stress-sensitivity due to housing conditions prior to the stress exposure. Stress-dependent changes in GR gene expression were independent of 2-AG and not directly related to increased corticosterone levels. Thus, 2-AG seems to influence GR expression under baseline conditions, but not in response to chronic stress.

A further housing effect was detected in the stress-dependent regulation of the body weight. CSDS significantly decreased the body weight of single-caged, but not group-housed intruder mice regardless of the genotype. However, since the single-caged CSDS was performed only with one cohort of animals, individual susceptibility of the mice might have contributed to the observed differences. The effects of stress on the body weight were shown to vary greatly depending on the type and duration of the stressor. In rodents, chronic stressors usually decreased chow intake and body weight (Dallmann 2001), while intake of palatable food was specifically increased (Dallmann et al. 2003). Krishnan and colleagues described reduced body weights in susceptible, but not unsusceptible mice after CSDS (Krishnan et al. 2007). In humans, individual differences in food intake responses to acute

stress were also noted. Approximately 40 % increased and 40 % decreased their caloric intake, while 20 % did not change their eating behaviors at all. Similar differences have been observed in response to chronic stress (for review see Yau & Potenza 2013). In addition, depression, which can often be triggered by chronic exposure to stressful events, was frequently associated with a reduced appetite (Nestler et al. 2002). Taken together, these findings suggest that stress promotes irregularities in eating patterns. Several studies indicated that these effects are substantially mediated by glucocorticoids, which act on the hypothalamus to modulate food intake (for review see Dallmann et al. 2004). However, the activity of DAGL α , thus the amount of 2-AG, did not contribute to stress-dependent changes in body weight. This differs clearly from basal conditions, in which both neuronal and constitutive deletion of *Dagla* significantly reduced the body weight of adult mice.

Besides the molecular alterations, chronic stress is known to modulate behavior, leading to increased anxiety and depressive-like phenotypes. In the following, behavioral alterations due to chronic stress are discussed in detail. CSDS produced a robust social avoidance phenotype in all animals. Housing conditions prior to the stress exposure and the deletion of *Dagla* did not affect the stress-induced avoidance behavior. However, even unstressed *Dagla*^{-/-} mice inhibited an increased anxiety phenotype in this behavioral test, reflected by a decreased interaction time with the foreign CD1 mouse. Since mice constitutively lacking *Dagla* inhibited a distinct social preference for a conspecific, the increased avoidance was most likely due to increased anxiety towards an older male animal of a different strain. This is in line with the anxiety-like phenotype of *Dagla*^{-/-} observed in other behavioral tests, such as the open-field or the light/dark box test.

Stress-dependent social avoidance towards animals of the same species/strain, like the former aggressor animal, was also described in previous studies (Berton et al. 2006; Dadomo et al. 2011). However, social avoidance was not detected using conspecific C57BL/6 mice (Desbonnet et al. 2012; data not shown). In conclusion, social avoidance against a former aggressor animal is a reliable measure of the successful performance of the stress paradigm and has been used to distinguish between susceptible and resilient animals (Krishnan et al. 2007). Krishnan and colleagues correlated the susceptibility to increased nucleus accumbens (NAc) BDNF protein levels, not accompanied by BDNF mRNA changes, and upregulated firing-rates in ventral-tegmental area (VTA) dopamine neurons (Krishnan et al. 2007). The nucleus accumbens has a major role in the cognitive processing of aversion, motivation, and reward and gets major inputs from the PFC, the amygdala and the hippocampus. The VTA is the origin of dopaminergic neurons of the mesocorticolimbic system and is mainly involved in the reward circuitry. In the present study no differences in the manifestation of social avoidance between the stressed animals could be detected, thus

all animals were susceptible. Furthermore, BDNF gene expression in different brain areas remained constant. However, protein levels might be altered and are still to be analyzed. Increased dopamine release in animals susceptible to social defeat was also shown to disturb other neurotransmitter systems, such as GABAergic and glutamatergic signaling (for review see Hammels et al. 2015), which might contribute to the stress susceptibility. Endocannabinoids critically contribute to the control of neurotransmitter release, thus altered neurotransmitter release and composition due to the lack of *Dagla* most likely contributed to the increased stress-sensitivity of *Dagla*^{-/-} mice.

Besides the induction of social avoidance, chronic stress is known to increase anxiety in rodents. Accordingly, anxiety-like behavior was assessed in the open-field and zero-maze test. CSDS mildly increased anxiety in the open-field test, but did not elicit anxiety-like phenotypes of *Dagla*^{fl/fl} or *Syn-Dagla*^{-/-} mice in the zero-maze test. However, *Dagla*^{-/-} mice showed significantly increased anxiety-like behavior in the zero-maze test after exposure to chronic stress, representing a further evidence for the augmented stress sensitivity of mice lacking *Dagla*. In contrast, *CB1*^{-/-} mice did not show higher anxiety-like behavior in the zero-maze test after CSDS (Dubreucq et al. 2012). These divergent observations can most likely be ascribed to different social defeat protocols, because other chronic stress models, such as chronic mild stress, significantly increased the anxiety-like behavior of *CB1*^{-/-} mice compared to wild type controls (Martin et al. 2002). Increased corticosterone levels of *Dagla*^{-/-} mice might have contributed to the enhanced stress sensitivity, emerging in increased anxiety. In line with this, previous studies showed that corticosterone administration caused significantly increased anxiety-like behavior in rodents (Demuyser et al. 2015).

Chronic stress is a main risk factor for the development of depression. In laboratory animals depressive-like behavior is assessed by measuring signs of anhedonia, behavioral despair, decreased general activity, and altered circadian rhythm. Anhedonia is the inability to experience pleasure from activities usually considered enjoyable, and represents one of the core symptoms of major depression in humans. CSDS did not induce anhedonic behavior, manifested in reduced sucrose preference. However, the generally decreased sucrose preference observed in *Syn-Dagla*^{-/-} and *Dagla*^{-/-} mice impede the detection of a stress-dependent anhedonic phenotype in these animals. Contradictory studies have been published concerning anhedonia after CSDS. Croft and colleagues (Croft et al. 2005) and von Frijtag and colleagues (von Frijtag et al. 2002) found no difference in sucrose preference after 5 days of CSDS, while other studies reported anhedonia after 10 days of CSDS (Covington et al. 2009; Yu et al. 2011). In contrast, Dubreucq and colleagues detected increased sucrose preference in wild type and *CB1*^{-/-} mice after 7 days of CSDS (Dubreucq et al. 2012). Different social defeat protocols and handling procedures might explain the

different stress-dependent alterations in preference for sweet solutions.

Furthermore, behavioral despair was analyzed in the forced swim test. A mild depressive-like phenotype was observed in single-caged, but not group-housed *Dagla^{fl/fl}* mice. These results indicate that caging influenced the reactivity to CSDS. Again, the strong baseline depressive-like phenotype of *Syn-Dagla^{-/-}* and *Dagla^{-/-}* mice exacerbated the detection of potential stress effects in these animals. However, several studies reported no significant effects of social defeat exposure on the forced swim test (Kinsey et al. 2007; Krishnan et al. 2007). Thus, it is difficult to draw a final conclusion regarding the effect of social defeat on depressive-like behaviors.

A further core symptom of depression in humans is fatigue or loss in energy (DSM-V, American Psychiatric Association 2013), in rodents mirrored by reduced activity in the home cage. However, CSDS caused increased locomotor activity especially during the dark phase, an effect being most pronounced in *Dagla^{-/-}* and *Syn-Dagla^{-/-}* mice. In contrast, Bartolomucci and colleagues detected reduced home cage motor activity of defeated mice, using radiotelemetry recordings (Bartolomucci et al. 2003). However, these authors (Bartolomucci et al. 2003) applied a longer social defeat protocol (15 days) and used a different method for the activity measurements. Other studies also showed increased home cage activity and altered day/night pattern in chronically stressed mice, marked by a similar increased activity during the active phase (dark phase) of the animals as observed in the present study (for review see Strekalova et al. 2011). These authors (Strekalova et al. 2011) suggest that the long lasting increase in locomotion may be due to elevated sympathetic activation and are directly related to the increased stress response of those animals. Thus, the obtained results gives further evidence for the importance of 2-AG in stress response and reactivity.

Finally, it can be stated that a disrupted ECS signaling increase the sensitivity to chronic social defeat stress. In particular, brain 2-AG levels critically modulate the susceptibility to stress. This is the first study showing that augmented 2-AG levels in the amygdala and PFC after chronic homotypic stress are released by neurons. In case of a neuron-specific deletion of *Dagla*, anandamide contributes to this stress adaptation and compensates the lack of 2-AG. Furthermore, the housing of the animals prior to the stress exposure might influence the reactivity to chronic stress. Considering all the stress-dependent behavioral alterations observed in the present study, CSDS represents a valid model for anxiety- and stress-related rather than depressive-like disorders.

4.3 *In vitro* approaches to characterize DAGL α and identify potential interaction partners

Besides the behavioral and molecular characterization of mice lacking *Dagla*, this thesis aimed to establish a method to identify novel interaction partners of DAGL α and to analyze the activity of DAGL α *in vitro*. Both approaches are of high importance, because up to now very little is known about the regulation of DAGL α and its direct interaction with other proteins. A few studies described possible regulatory mechanisms based on posttranslational modifications or protein bindings. Proteomic studies indicated that both DAGL isoforms, DAGL α and DAGL β , can be palmitoylated (Kang et al. 2008; Martin & Cravatt 2009), but the exact mechanisms still remain unclear. Besides palmitoylation, phosphorylation is an important posttranslational modification used to control the activation of a variety of different proteins. Phosphorylation plays critical roles in many cellular processes including cell cycle, apoptosis and signal transduction pathways. DAGL purified from brain microsomes was shown to be positively regulated with direct phosphorylation by protein kinase A (Rosenberger et al. 2007). In line with this, protein kinase A (PKA) and C (PKC) were able to increase 2-AG production in neuronal culture, most likely through DAGL-dependent mechanisms (Vellani et al. 2008). In 2013, Shonesy and colleagues uncovered that the calcium/calmodulin dependent protein kinase II α (CaMKII α) interacts with the C-terminal domain of DAGL α , phosphorylates two serine residues and thereby inhibits DAGL α activity (Shonesy et al. 2013). These results suggest that DAGL α interacts with different protein kinases, which regulates the lipase activity via phosphorylation. Moreover, interaction of DAGL α with CC-Homer proteins (Homer-1, Homer-2) was shown to be required for the membrane localization of this lipase, but most likely not for its activity (Jung et al. 2007). Thus far, CC-Homer proteins, PKC and CamKII α are the only clearly identified interaction partners and regulators of DAGL α . Other proteins that may modulate the subcellular targeting or enzyme activity are poorly understood. Besides protein-protein interactions and posttranslational modifications, co-factors like metal ions or small organic molecules are important regulators of enzyme activity. Previous studies showed that the activity of DAGL α seemed to be dependent on glutathione and Ca²⁺, even though the exact mechanisms are unknown (Bisogno et al. 2003).

To discover further potential regulators of DAGL α , this thesis aimed to establish a method for the identification of protein-protein interactions of DAGL α . Therefore, C-terminal tagged DAGL α was successfully overexpressed and purified from the mouse neuroblastoma cell line Neuro-2a. Subsequent analysis of co-purified proteins via MALDI-TOF/TOF mass spectrometry revealed several potential interaction partners of DAGL α . Two of the identified proteins are of special interest, namely NCAM and dynamin-1, because of their impact on neuronal growth and function. NCAM is involved in a variety of contact-mediated interactions

among neurons, astrocytes and oligodendrocytes. Furthermore, NCAM influences axonal growth during development and synapse formation in the adult brain (for review see Weledji & Assob 2014). DAGL α is also critically involved in these processes. Previous studies showed that activity of DAGL α enhanced axonal growth in the developing brain (Williams et al. 2003; Oudin et al. 2011) and that the deletion of DAGL α caused a reduced adult neurogenesis (Gao et al. 2010; Jenniches et al. 2015). In addition, fibroblast growth factor (FGF) in coordination with NCAM was shown to increase 2-AG levels via DAGL activation in cerebellar neurons to promote axonal growth (Williams et al. 2003). Thus, a direct interaction between DAGL α and NCAM as shown in this study is feasible and further analysis of this protein-protein interaction is promising.

The second interesting candidate protein is dynamin-1. This neuron-specific GTP-binding protein was shown to be involved in synaptic vesicle endocytosis and especially needed during strong neuronal activity (Ferguson et al. 2007). In addition, previous studies showed that dynamin-1 mediated the internalization of CB1 receptors (McDonald et al. 2006) and a knockdown of dynamin-2, the ubiquitously expressed isoform, reduced the uptake of anandamide in neuronal cells *in vitro* (McFarland et al. 2008). Up to now, connections between 2-AG and dynamins are not reported. However, this study showed that constitutive deletion of Dagla also led to significantly decreased anandamide levels. Thus, biosynthetic pathways of both endocannabinoids are somehow linked and uptake of 2-AG might also be dependent on dynamin activity. Consequently, dynamins might play an important role in regulating the ECS by controlling the uptake of eCBs.

Finally, mitogen-activated protein kinase 8 (MAPK8) was co-purified with DAGL α . MAPK8, also known as c-Jun N-terminal kinase 1 (JNK1), belongs to the superfamily of MAP-kinases, mediating a variety of cellular processes. The JNK family consists of ten isoforms coded by three different genes, Jnk1, Jnk2 and Jnk3, all found in the mammalian brain (Gupta et al. 1996). JNK proteins are generally activated by cytokines and environmental stress and control the expression of genes essential for many cellular responses, including cell growth and apoptosis (Marshall 1995). Activation of cannabinoid receptors leads to the activation of MAPK pathways (Howlett et al. 2010). Previous studies showed that cannabinoid receptors activated JNK1 through a pathway that includes phosphatidylinositide 3-kinase (PI3K) and Ras (Rueda et al. 2000). In line with this, CB1 receptor antagonists blocked the THC-dependent activation of JNK1 and 2 in cortical neurons (Downer et al. 2003). In addition, DAGs might promote JNK1 activation via different pathways. Previous studies proposed that IL-1 β -induced DAG generation might contribute to the phosphorylation and activation of JNK1 *in vitro* (Welsh 1996). Among others, DAGLs metabolize DAGs and thereby control their cellular concentration and as a consequence the DAG-dependent activation of JNK1.

The main function of the protein kinase JNK1 is the regulatory phosphorylation of various proteins. Consequently, a feedback inhibition might be a possible link between DAGL α and JNK1. JNK1, as a downstream mediator of CB1 signaling, might phosphorylate and thereby inhibit DAGL α , as a consequence of enhanced CB1 signaling due to high 2-AG levels. Accordingly, this cascade would represent a novel inhibitory feedback mechanism of 2-AG-CB1 signaling. However, further studies are needed to verify this hypothesis and to characterize the protein-protein interaction in detail, for instance via protein complex immunoprecipitation.

CamKII α , PKA, PKC and CC-Homer proteins were already shown to interact with DAGL α . However, none of these proteins were detected and identified in the bulk of co-purified proteins. This might be due to the usage of different tissues, cell lines and methods of measurement. For instance, interaction of DAGL α and CamKII α was detected in mouse striatal extracts using a shotgun proteomics approach, in which DAGL α was immunoprecipitated from solubilized adult mouse striatum (Shonesy et al. 2013). In contrast, phosphorylation of DAGL α by PKA and PKC was shown using either cultured sensory neurons (Vellani et al. 2008) or *in vitro* assays with DAGL α purified from bovine brain microsomes (Rosenberger et al. 2007). In none of the described studies, DAGL α was tag-purified from Neuro-2a cells as in the present study. In addition, the amount of purified DAGL α was quite low, thus some potential interaction partners might had concentrations below the effective detection limit of MALDI-TOF/TOF-MS and were therefore not identified.

In conclusion, DAGL α was successfully overexpressed and purified from Neuro-2a cells followed by identification via MALDI-TOF/TOF-MS. In addition, several proteins representing potential interaction partners of DAGL α were identified. Further studies are needed to confirm possible protein-protein interactions. Nevertheless, the described method is a prospective technique for the identification of novel regulatory mechanisms of DAGL α .

Furthermore, to analyze the activity of DAGL α *in vitro*, a novel enzyme activity assay using click chemistry was performed. Click chemistry has become recognized as a flexible tool to label biomolecules, such as nucleic acids, proteins and lipids (Thirumurugan et al. 2013). In this study, click chemistry was used to detect either free or glycerol bound labeled fatty acids. The labeling consists of a terminal alkyne (C-C triple bond), which neither alters the fatty acid metabolism nor occurs naturally in biomolecules (Thiele et al. 2012). In addition, alkynes do not react with any other molecule present in cells or tissue. Among the various click chemistry reactions, the applied azide-alkyne cycloaddition is the most widely employed reaction in biological studies (Horisawa 2014). This method allows among others the comprehensive non-radioactive tracing and characterization of lipid metabolism (Thiele et al.

2012).

Only a limited number of DAGL α activity assays are currently available. One group of assays is using fluorogenic and chromogenic surrogate substrates (Pedicord et al. 2011; Johnston et al. 2012; Appiah et al. 2014). Nevertheless, surrogate substrates have limited structural similarity to natural ones and might alter the measurable enzyme activity. Up to now, three assays have been reported that utilize DAG, the natural substrate of DAGL α , to determine the lipase activity. For one, radiometric assays mainly using 1-stearoyl-2-[14 C]arachidonoyl-*sn*-glycerol as a substrate have been frequently described (Bisogno et al. 2003, 2013; Jung et al. 2011). However, the synthesis of this substrate is quite expensive and requires handling of radioactive material. Moreover, previously described assays were performed with either membrane preparations or cell lysates of DAGL α overexpressing COS-7 (Bisogno et al. 2003, 2013), HEK293T (Johnston et al. 2012) or Neuro-2a cells (Jung et al. 2011). This is the first study using a click chemistry-based assay and Dagla $^{-/-}$ cell lysates.

In the present study, two different click-labeled DAGs were applied as substrates for the enzyme activity assays. Metabolic activity of wild type and Dagla $^{-/-}$ cells were detected via thin-layer chromatography. In fact, a time-dependent product synthesis was noticeable. However, none of the tested DAGs showed substrate specificity for DAGL α . Substrate conversion was similar in primary wild type and Dagla $^{-/-}$ macrophages. In addition, the unspecific lipase inhibitor orlistat entirely blocked DAG conversion. These results imply that labeled DAGs were metabolized by lipases, although not exclusively by DAGL α . Detected metabolic activity was possibly dependent on, the second DAGL isoform, which is normally expressed in Dagla $^{-/-}$ mice. In addition, a recent study showed that DAGL β might be the predominant DAGL isoform in macrophages, since treatment with selective DAGL β inhibitors significantly reduced 2-AG levels in peritoneal macrophages (Hsu et al. 2012). Remarkably, previous studies never determined the substrate specificity of applied DAGs by using Dagla $^{-/-}$ or Daglb $^{-/-}$ cell lysates.

Although the tested DAGs were not appropriate to analyze DAGL α activity in cell lysates of bone marrow-derived macrophages, they might be suitable for *in vitro* assays using membrane fractions or cell lysates of DAGL α overexpressing cells. Further studies are needed to establish a robust click chemistry based activity assay. Nevertheless, click chemistry is a promising tool for the *in vitro* characterization of lipases such as DAGL α .

4.4 Conclusion and Outlook

Growing evidence supports the notion that the ECS is an integral regulator of emotional processes and critically contributes to the regulation of stress responses. Several psychiatric disorders are associated with altered release of endogenous cannabinoids, mainly 2-AG and anandamide, and altered CB1 receptor expression and viability. The present study gives further support for the involvement of disrupted ECS signaling to the development and manifestation of anxiety and depressive-like behaviors. The neuronal and constitutive deletion of *Dagla* negatively influenced the emotional state of rodents, leading to an enhanced anxiety, depressive-like behavior and impaired extinction of conditioned fear. This is the first study showing that 2-AG especially released by neurons importantly contributed to the body's homeostasis and prevented the formation of depressive-related phenotypes. Even though the main cerebral 2-AG is most likely not produced by neurons, the stress-dependent increase of 2-AG in the amygdala and PFC is depended on the activity of neuronal DAGL α mediating stress habituation and adaptation. In addition, the deletion of *Dagla* in microglia affected fear responses in mice, but did not result in 2-AG content changes. However, the use of LysM-Cre mouse line only led to a 30-40 % knockout of *Dagla* in microglia. Astrocytes and microglia were shown to produce higher amounts of 2-AG compared to neurons *in vitro*. Thus, future studies need to confirm which exact cell-type is responsible for the main production of 2-AG in the brain. Therefore, more potent microglia-specific and astrocyte-specific *Dagla* knockout mouse lines are inevitable. Additionally, both the constitutive and microglia-specific deletion of *Dagla* caused a markedly decreased anandamide level in specific brain regions. Up to now, the connection between the biosynthesis of both cannabinoids remains elusive. This aspect should be emphasized in future studies, to allow a discriminability of the observed behavioral and molecular alterations to one of the eCBs.

Chronic stress is a key risk factor for the development of mood disorders, such as PTSD and depression. Therefore, the stress reactivity of mice lacking *Dagla* to chronic social defeat stress was analyzed. The deletion of *Dagla* increased the sensitivity to chronic stress, manifested in increased anxiety and augmented corticosterone release. However, the neuron-specific deletion of *Dagla* did not affect the susceptibility towards chronic stress. Most likely the stress-dependent increase of anandamide in the amygdala and PFC compensated the lack of neuronal 2-AG and mediated stress habituation. In summary, the current discoveries highlight an essential role of 2-AG in the neuroendocrine network that regulates the HPA axis and the development of affective behaviors. Thus, alterations of the central endogenous cannabinoid tone might be involved in the pathophysiology of stress-related diseases. The effects of stress on the ECS are apparently quite multifaceted, brain region-

specific and dependent on the type and chronicity of stress exposure. The social defeat paradigm produced specific behaviors and physiological changes resembling signs and symptoms of humans with affective disorders. However, it contains both a physical and a social component, which restricts the comparison to human social stress or exclusion. To ensure the impact of 2-AG to stress-sensitivity, constitutive and conditional Dagla knockout mice need to be examined in further chronic stress models, such as chronic mild stress.

Mood and anxiety disorders represent one of the largest health burdens in Western society, yet only little novel therapeutics have emerged in the past two decades. Thus, the specific targeting of the ECS or the development of new drugs indirectly increasing eCB levels represents a promising tool to develop new antidepressants and anxiolytic agents.

Bibliography

- Allen AC, Gammon CM, Ousley AH, McCarthy KD, Morell P (1992): Bradykinin stimulates arachidonic acid release through the sequential actions of an sn-1 diacylglycerol lipase and a monoacylglycerol lipase. *J Neurochem.* 58, 1130–1139.
- Alhouayek M & Muccioli GG (2014): COX-2-derived endocannabinoid metabolites as novel inflammatory mediators. *Trends Pharmacol Sci.* 2014, 35, 284–292.
- American Psychiatric Association (2013). Diagnostic and statistical manual of mental disorders. 5th ed. Arlington: American Psychiatric Association
- Anacker C, Zunszain PA, Carvalho LA, Pariante CM (2011): The glucocorticoid receptor: pivot of depression and of antidepressant treatment? *Psychoneuroendocrinology.* 36(3):415-25.
- Appiah KK, Blat Y, Robertson BJ, Pearce BC, Pedicord DL, Gentles RG, Yu XC, Mseeh F, Nguyen N, Swaffield JC, Harden DG, Westphal RS, Banks MN, O'Connell JC (2014): Identification of small molecules that selectively inhibit diacylglycerol lipase- α activity. *J Biomol Screen.* 19(4):595-605
- Argente-Arizón P, Freire-Regatillo A, Argente J, Chowen JA (2015): Role of non-neuronal cells in body weight and appetite control. *Front Endocrinol (Lausanne).* 26;6:42.
- Ashton JC, Friberg D, Darlington CL, Smith PF (2006): Expression of the cannabinoid CB2 receptor in the rat cerebellum: an immunohistochemical study. *Neurosci Lett.* 396:113–116.
- Atwood BK and Mackie K (2010): CB2: a cannabinoid receptor with an identity crisis. *Br J Pharmacol.* 160(3): 467–479.
- Baldi E, Bucherelli C (2015): Brain sites involved in fear memory reconsolidation and extinction of rodents. *Neurosci Biobehav Rev.* 53:160-90.
- Barden N (2004) Implications of the hypothalamic–pituitary–adrenal axis in the pathophysiology of depression. *J Psychiatry Neurosci* 29:185–193.
- Barlow DH (2002): Anxiety and its Disorders: The Nature and Treatment of Anxiety and Panic. 2nd ed. New York: Guilford Press.
- Bartolomucci A, Palanza P, Costoli T, Savani E, Laviola G, Parmigiani S, Sgoifo A (2003): Chronic psychosocial stress persistently alters autonomic function and physical activity in mice. *Physiol Behav.* 80(1):57-67.
- Berton O, McClung CA, Dileone RJ, Krishnan V, Renthal W, Russo SJ, Graham D, Tsankova NM, Bolanos CA, Rios M, Monteggia LM, Self DW, Nestler EJ (2006): Essential role of BDNF in the mesolimbic dopamine pathway in social defeat stress. *Science.* 311:864–

868.

- Beyer CE, Dwyer JM, Piesla MJ, Platt BJ, Shen R, Rahman Z, Chan K, Manners MT, Samad TA, Kennedy JD, Bingham B, Whiteside GT (2010): Depression-like phenotype following chronic CB1 receptor antagonism. *Neurobiol Dis.* 39(2):148-55.
- Bisogno T, Melck D, De Petrocellis L, Di Marzo V (1999): Phosphatidic acid as the biosynthetic precursor of the endocannabinoid 2-arachidonoylglycerol in intact mouse neuroblastoma cells stimulated with ionomycin. *J Neurochem.* 72:2113.
- Bisogno T, Howell F, Williams G, Minassi A, Cascio MG, Ligresti A et al. (2003): Cloning of the first sn1-DAG lipases points to the spatial and temporal regulation of endocannabinoid signaling in the brain. *J Cell Biol.* 163(3), pp.463–468.
- Bisogno T, Mahadevan A, Coccurello R, Chang JW, Allara M, Chen Y, et al. (2013): A novel fluorophosphonate inhibitor of the biosynthesis of the endocannabinoid 2-arachidonoylglycerol with potential anti-obesity effects. *British Journal of Pharmacology.* 169;784-793.
- Björkqvist K (2001): Social defeat as a stressor in humans. *Physiol Behav.* 73(3):435-42.
- Blankman JL, Simon GM, Cravatt BF (2007): A comprehensive profile of brain enzymes that hydrolyze the endocannabinoid 2-arachidonoylglycerol. *Chemistry & biology,* 14(12), pp.1347–56.
- Bourin M, Hascoët M (2003): The mouse light/dark box test. *Eur J Pharmacol.* 463(1-3):55-65.
- Brusco A, Tagliaferro PA, Saez T, Onaivi ES (2008): Ultrastructural localization of neuronal brain CB2 cannabinoid receptors. *Ann N Y Acad Sci.* 1139:450-7.
- Busquets-Garcia A, Pulghermanal E, Pastor A, de la Torre R, Maldonado R, Ozaita A (2011): Differential role of anandamide and 2-arachidonoylglycerol in memory and anxiety-like responses. *Biol Psychiatry,* 70(5):479-86.
- Can A, Schulze TG, Gould TD (2014): Molecular actions and clinical pharmacogenetics of lithium therapy. *Pharmacol Biochem Behav.* 123:3-16.
- Chen ZY, Jing D, Bath KG, Ieraci A, Khan T, Siao CJ, Herrera DG, Toth M, Yang C, McEwen BS, Hempstead BL, Lee FS (2007): Genetic variant BDNF (Val66Met) polymorphism alters anxiety-related behavior. *Science.* 314, 140–143.
- Chevaleyre V, Castillo PE (2003): Heterosynaptic LTD of hippocampal GABAergic synapses: a novel role of endocannabinoids in regulating excitability. *Neuron.* 38(3):461-72.
- Chiurchiù V, Battistini L, Maccarrone M (2015): Endocannabinoid signaling in innate and adaptive immunity. *Immunology.* doi: 10.1111/imm.12441.
- Christensen R, Kruse Kristensen P, Bartels EM, Bliddal H, Astrup A (2007): Efficacy and safety of the weight-loss drug rimonabant: a meta-analysis of randomised trials. *Lancet,* 370: 1706-13.

- Chrousos GP (2009): Stress and disorders of the stress system. *Nat. Rev. Endocrinol.* 5, 374–381.
- Clausen BE, Burkhardt C, Reith W, Renkawitz R, Forster I (1999): Conditional gene targeting in macrophages and granulocytes using LysMcre mice. *Transgenic Res.* 8, 265–277.
- Covington HE, Maze I, LaPlant QC, Vialou VF, Ohnishi YN, Berton O., et al. (2009): Antidepressant actions of histone deacetylase inhibitors. *Journal of Neuroscience.* 29(37), 11451-11460.
- Coplan JD, Aaronson CJ, Panthangi V, Kim Y (2015): Treating comorbid anxiety and depression: Psychosocial and pharmacological approaches. *World J Psychiatry.* 5(4):366-78.
- Coppen A (1967): The biochemistry of affective disorders. *Br J Psychiatry.* 113, 1237–1264.
- Cota D, Marsicano G, Tschöp M, Grübler Y, Flachskamm C, Schubert M, et al. (2003): The endogenous cannabinoid system affects energy balance via central orexigenic drive and peripheral lipogenesis. *J Clin Invest.* 112:423–31.
- Cota D, Steiner MA, Marsicano G, Cervino C, Herman JP, Grübler Y, Stalla J, Pasquali R, Lutz B, Stalla GK, Pagotto U (2007): Requirement of cannabinoid receptor type 1 for the basal modulation of hypothalamic-pituitary-adrenal axis function. *Endocrinology.* 148(4):1574-81.
- Crawley JN, Skolnick P, Paul SM (1984): Absence of intrinsic antagonist actions of benzodiazepine antagonists on an exploratory model of anxiety in the mouse. *Neuropharmacology.* 23(5):531-7.
- Croft AP, Brooks SP, Cole J, Little HJ.(2005): Social defeat increases alcohol preference of C57BL/10 strain mice; effect prevented by a CCKB antagonist. *Psychopharmacology (Berl).* 183, 163-170.
- Dadomo H1, Sanghez V, Di Cristo L, Lori A, Ceresini G, Malinge I, Parmigiani S, Palanza P, Sheardown M, Bartolomucci A (2011): Vulnerability to chronic subordination stress-induced depression-like disorders in adult 129SvEv male mice. *Prog Neuropsychopharmacol Biol Psychiatry.* (6):1461-71.
- Dallman MF, Bhatnagar S (2001): Chronic stress and energy balance: role of the hypothalamo-pituitary-adrenal axis. Vol IV, section 7. Coping with the environment. Chap 10. *New York: Oxford University Press*; 179–210
- Dallman MF, la Fleur SE, Pecoraro NC, Gomez F, Houshyar H, Akana SF (2004): Minireview: glucocorticoids--food intake, abdominal obesity, and wealthy nations in 2004. *Endocrinology.* 145(6):2633-8.
- Dedic N, Walser SM, Deussing JM (2011): Mouse Models of Depression, *Psychiatric Disorders - Trends and Developments*, Dr. Toru Uehara (Ed.), ISBN: 978-953-307-745-1, InTech, doi: 10.5772/27498.

- Demuyser T, Deneyer L, Bentea E, Albertini G, Van Liefferinge J, Merckx E, De Prins A, De Bundel D, Massie A, Smolders I (2015): In-depth behavioral characterization of the corticosterone mouse model and the critical involvement of housing conditions. *Physiol Behav.* 2015 Dec 18. pii: S0031-9384(15)30215-8.
- Deppermann S, Storchak H, Fallgatter AJ, Ehlis AC (2014): Stress-induced neuroplasticity: (mal)adaptation to adverse life events in patients with PTSD--a critical overview. *Neuroscience.* 283:166-77.
- Desbonnet L1, O'Tuathaigh C, Clarke G, O'Leary C, Petit E, Clarke N, Tighe O, Lai D, Harvey R, Cryan JF, Dinan TG, Waddington JL (2012): Phenotypic effects of repeated psychosocial stress during adolescence in mice mutant for the schizophrenia risk gene neuregulin-1: a putative model of gene × environment interaction. *Brain Behav Immun.* 26(4):660-71.
- Desmedt A, Marighetto A2, Piazza PV (2015): Abnormal Fear Memory as a Model for Posttraumatic Stress Disorder. *Biol Psychiatry.* 78(5):290-7.
- Devane WA, Dysarz FA, Johnson MR, Melvin LS, Howlett AC (1988): Determination and characterization of a cannabinoid receptor in rat brain. *Mol. Pharmacol.* 34, 605–613.
- Devane WA, Hanus L, Breuer A, Pertwee RG, Stevenson LA, et al. (1992): Isolation and structure of a brain constituent that binds to the cannabinoid receptor. *Science.* 258:1946–49
- Di Marzo V and De Petrocellis L (2010) Endocannabinoids as regulators of transient receptor potential (TRP) channels: A further opportunity to develop new endocannabinoidbased therapeutic drugs. *Curr. Med. Chem.* 17, 1430-1449
- Dinh TP, Carpenter D, Leslie FM, Freund TF, Katona I, Sensi SL, Kathuria S, Piomelli D. (2002): Brain monoglyceride lipase participating in endocannabinoid inactivation. *Proceedings of the National Academy of Sciences of the United States of America,* 99(16), pp.10819–24.
- Downer EJ, Fogarty MP, Campbell VA (2003): Tetrahydrocannabinol-induced neurotoxicity depends on CB1 receptor-mediated c-Jun N-terminal kinase activation in cultured cortical neurons. *Br J Pharmacol.* 140(3): 547–557.
- Dubreucq S, Matias I, Cardinal P, Häring M, Lutz B, Marsicano G, Chaouloff F (2012): Genetic Dissection of the Role of Cannabinoid Type-1 Receptors in the Emotional Consequences of Repeated Social Stress in Mice. *Neuropsychopharmacol.* 37(8): 1885–1900
- Dunsmoor JE, Paz R (2015): Fear Generalization and Anxiety: Behavioral and Neural Mechanisms. *Biol Psychiatry.* 78(5):336-43.
- Eisch AJ, Bolaños CA, de Wit J, Simonak RD, Pudiak CM, Barrot M, Verhaagen J, Nestler EJ (2003): Brain-derived neurotrophic factor in the ventral midbrain-nucleus

- accumbens pathway: a role in depression. *Biol Psychiatry*. 54, 994–1005.
- Evanson NK, Ulrich-Lai YM, Furay AR, Tasker JG, Herman JP (2007): Hypothalamic paraventricular cannabinoid receptor signaling in fast feedback inhibition of the hypothalamus-pituitary-adrenal axis response to acute restraint stress. *Soc Neurosci Abs* 197:195.
- Feil S, Valtecheva N, Feil R (2009): Inducible Cre mice. *Methods Mol Biol* 530:343-63
- Fezza F, Bari M, Florio R, Talamonti E, Feole M, Maccarrone M (2014): Endocannabinoids, Related Compounds and Their Metabolic Routes. *Molecules*. 19(11),17078-17106.
- Ferguson SM, Brasnjo G, Hayashi M, Wölfel M, Collesi C, Giovedi S, Raimondi A, Gong LW, Ariel P, Paradise S, O'toole E, Flavell R, Cremona O, Miesenböck G, Ryan TA, De Camilli P (2007): A selective activity-dependent requirement for dynamin 1 in synaptic vesicle endocytosis. *Science*. 316(5824):570-4.
- Fiskerstrand T, H'mida-Ben Brahim D, Johansson S, M'zahem A, Haukanes BI, Drouot N, et al. (2010): Mutations in ABHD12 Cause the Neurodegenerative Disease PHARC: An Inborn Error of Endocannabinoid Metabolism. *The American Journal of Human Genetics*, 87(3), pp.410–417.
- Fluri F, Schuhmann MK, Kleinschnitz C (2015): Animal models of ischemic stroke and their application in clinical research. *Drug Des Devel Ther*. 2; 9:3445-54.
- Galve-Roperh I, Chiurchiù V, Díaz-Alonso J, Bari M, Guzmán M, Maccarrone M (2013): Cannabinoid receptor signaling in progenitor/stem cell proliferation and differentiation. *Prog Lipid Res*. 52(4):633-50.
- Gan Y, Gong Y, Tong X, Sun H, Cong Y, Dong X et al. (2013): Depression and the risk of coronary heart disease: a meta-analysis of prospective cohort studies. *BMC Psychiatry*. 24;14:371.
- Gao Y, Vasilyev DV, Goncalves MB, Howell FV, Hobbs C, Reisenberg M, et al. (2010): Loss of retrograde endocannabinoid signaling and reduced adult neurogenesis in diacylglycerol lipase knock-out mice. *J Neurosci*, 30(6): 2017–24.
- Gao Y, Ottaway N, Schriever SC, Legutko B, García-Cáceres C, de la Fuente E et al. (2014): Hormones and diet, but not body weight, control hypothalamic microglial activity. *Glia*. 62(1):17-25.
- Gaoni Y, Mechoulam R (1964): Isolation, Structure, and Partial Synthesis of an Active Constituent of Hashish. *J. Am. Chem. Soc.* 86 (8):1646–1647
- Golden SA, Convington III HE, Berton O, Russo SJ (2011): A standardized protocol for repeated social defeat stress in mice. *Nat Protoc*. 6(8):1183-1191.
- Gonsiorek W, Lunn C, Fan X, Narula S, Lundell D, Hipkin RW (2000) Endocannabinoid 2-arachidonyl glycerol is a full agonist through human type 2 cannabinoid receptor: antagonism by anandamide. *Mol Pharmacol* 57:1045–1050.

- Gould TD, Dao DT, Kovacsics CE (2009): Mood and Anxiety Related Phenotypes in Mice. *Neuromethods* 42, Chapter 1 (The Open Field Test).
- Grone BP, Baraban SC (2015): Animal models in epilepsy research: legacies and new directions. *Nat Neurosci.* 18(3):339-43.
- Gunduz-Cinar O, Hill MN, McEwen BS, Holmes A (2013): Amygdala FAAH and anandamide: mediating protection and recovery from stress. *Trends Pharmacol Sci.* 34(11):637-44.
- Gupta S., Barrett T., Whitmarsh A.J., Cavanagh J., Sluss H.K., Derijard B., Davis R.J. (1996): Selective interaction of JNK protein kinase isoforms with transcription factors. *EMBO J.* 15:2760–2770
- Haller J, Bakos N, Szirmay M, Ledent C, Freund TF (2002): The effects of genetic and pharmacological blockade of the CB1 cannabinoid receptor on anxiety. *Eur J Neurosci.* 16(7):1395-8.
- Haller J, Varga B, Ledent C, Barna I, Freund TF (2004): Context-dependent effects of CB1 cannabinoid gene disruption on anxiety-like and social behaviour in mice. *Eur J Neuroscience*, 19(7):1906-1912.
- Hammels C, Pishva E, De Vry J, van den Hove DL, Prickaerts J, van Winkel R et al. (2015): Defeat stress in rodents: From behavior to molecules. *Neurosci Biobehav Rev.* 59:111-40.
- Hashimoto Y, Ohno-Shosaku T, Maejima T, Fukami K, Kano M (2008): Pharmacological evidence for the involvement of diacylglycerol lipase in depolarization-induced endocannabinoid release. *Neuropharmacology.* 54(1):58-67.
- Herman, J. P. (1993): Regulation of adrenocorticosteroid receptor mRNA expression in the central nervous system. *Cell. Mol. Neurobiol.* 13, 349–72.
- Herman JP, Figueiredo H, Mueller NK, et al. (2003): Central mechanisms of stress integration: hierarchical circuitry controlling hypothalamo-pituitary-adrenocortical responsiveness. *Front Neuroendocrinol.* 24:151–180
- Hill MN, Miller GE, Ho WS, Gorzalka BB, Hillard CJ (2008a): Serum endocannabinoid content is altered in females with depressive disorders: a preliminary report. *Pharmacopsychiatry.* 2008;41:48–53.
- Hill MN, Carrier EJ, McLaughlin RJ, Morrish AC, Meier SE, Hillard CJ, Gorzalka BB (2008b): Regional alterations in the endocannabinoid system in an animal model of depression: effects of concurrent antidepressant treatment. *J Neurochem.* 106(6):2322-36.
- Hill MN, Miller GE, Carrier EJ, Gorzalka BB, Hillard CJ (2009): Circulating endocannabinoids and N-acyl ethanolamines are differentially regulated in major depression and following exposure to social stress. *Psychoneuroendocrinology*, 34:1257-1262.
- Hill MN, Patel S, Campolongo P, Tasker JG, Wotjak CT, Bains JS (2010a): Functional interactions between stress and the endocannabinoid system: from synaptic signaling to behavioral output. *J Neurosci.* 2010 Nov 10;30(45).

- Hill MN, McLaughlin RJ, Bingham B, Shrestha L, Lee TT, Gray JM, Hillard CJ, Gorzalka BB, Viau V (2010b): Endogenous cannabinoid signaling is essential for stress adaptation. *Proc Natl Acad Sci U S A*. 18;107(20):9406-11
- Hill MN, McEwen BS (2010c): Involvement of the endocannabinoid system in the neurobehavioural effects of stress and glucocorticoids. *Prog Neuropsychopharmacol Biol Psychiatry*. 34(5):791-7.
- Hill MN, McLaughlin RJ, Pan B, Fitzgerald ML, Roberts CJ, Lee TT, Karatsoreos IN, Mackie K, Viau V, Pickel VM, McEwen BS, Liu QS, Gorzalka BB, Hillard CJ (2011): Recruitment of prefrontal cortical endocannabinoid signaling by glucocorticoids contributes to termination of the stress response. *J Neurosci*. 31(29):10506-15.
- Hillard CJ, Hill MN, Carrier EJ, Shi LW, Gorzalka BB (2006): Regulation of cannabinoid receptor expression by chronic unpredictable stress in rats and mice. *Soc. Neurosci. Abstr.* 746, 19.
- Hillard CJ (2014): Stress regulates endocannabinoid-CB1 receptor signaling. *Semin Immunol*. 26(5):380-8.
- Holma KM, Melartin TK, Haukka J, Holma IA, Sokero TP, Isometsä ET (2010): Incidence and predictors of suicide attempts in DSM-IV major depressive disorder: a five-year prospective study. *Am J Psychiatry*. 167(7):801-8.
- Hoess RH, Ziese M, Sternberg N (1984): P1 site-specific recombination: nucleotide sequence of the recombining sites. *PNAS*. 79(11):3398–3402
- Horisawa K (2014): Specific and quantitative labeling of biomolecules using click chemistry. *Front Physiol*. 5:457.
- Howlett AC, Blume LC, Dalton GD (2010): CB(1) cannabinoid receptors and their associated proteins. *Curr Med Chem*. 17(14):1382-93.
- Hu SS, Bradshaw HB, Chen JS, Tan B, Walker JM (2008): Prostaglandin E2 glycerol ester, an endogenous COX-2 metabolite of 2-arachidonoylglycerol, induces hyperalgesia and modulates NFkappaB activity. *Br. J. Pharmacol*. 153;1538–1549.
- Hungund BL, Vinod KY, Kassir SA, Basavarajappa BS, Yalamanchili R, Cooper TB, Mann JJ, Arango V (2004): Upregulation of CB1 receptors and agonist-stimulated [35S]GTPgammaS binding in the prefrontal cortex of depressed suicide victims. *Mol Psychiatry*. 9(2):184-90.
- Hsu KL, Tsuboi K, Adibekian A, Pugh H, Masuda K, Cravatt BF (2012): DAGLβ inhibition perturbs a lipid network involved in macrophage inflammatory responses. *Nat Chem Biol*. 8(12):999-1007.
- Idris A. and Ralsto SH (2012): Role of cannabinoids in the regulation of bone remodeling. *Fron. Endocrinol*. 3, 136
- Imperatore R, Morello G, Luongo L, Taschler U, Romano R, De Gregorio D, Belardo C,

- Maione S, Di Marzo V, Cristino L (2015): Genetic deletion of monoacylglycerol lipase leads to impaired cannabinoid receptor CB1 R signaling and anxiety-like behavior. *J Neurochem.* 135(4):799-813.
- Izzo AA and Sharkey KA (2010): Cannabinoids and the gut: new developments and emerging concepts. *Pharmacol Ther.* 126, 21-38
- Jehle J, Hoyer FF, Schöne B, Pfeifer P, Schild K, Jenniches I, Bindila L, Lutz B, Lütjohann D, Zimmer A, Nickenig G (2016): Myeloid-specific deletion of diacylglycerol lipase alpha inhibits atherogenesis in ApoE-deficient mice. *PLoS One.* 11(1): e0146267.
- Jenniches I, Ternes S, Albayram O, Otte DM, Bach K, Bindila L, Michel K, Lutz B, Bilkei-Gorzo A, Zimmer A. (2015): Anxiety, Stress, and Fear Response in Mice with Reduced Endocannabinoid Levels. *Biol Psychiatry.* pii: S0006-3223(15)00314-5. doi: 10.1016/j.biopsych.2015.03.033.
- Jenniches I, Zimmer A. (2015): Reply To: The Anxiolytic Actions of 2-Arachidonoylglycerol: Converging Evidence from Two Recent Genetic Endocannabinoid Deficiency Models. *Biol Psychiatry.* pii: S0006-3223(15)00531-4. doi: 10.1016/j.biopsych.2015.06.024.
- Johnston M, Bhatt SR, Sikka S, Mercier RW, West JM, Makriyannis A, Gatley SJ, Duclos RI Jr (2012): Assay and inhibition of diacylglycerol lipase activity. *Bioorg Med Chem Lett.* 15;22(14):4585-92.
- Junttila MR, Saarinen S, Schmidt T, Kast J, Westermarck J (2005): Single-step Strep-tag purification for the isolation and identification of protein complexes from mammalian cells. *Proteomics.* 5(5):1199-203.
- Jung KM, Astarita G, Zhu C, Wallace M, Mackie K, Piomelli D (2007): A Key Role for Diacylglycerol Lipase- α in Metabotropic Glutamate Receptor-Dependent Endocannabinoid Mobilization. *Mol Pharmacol.* 2007 Sep;72(3):612-21.
- Jung KM, Astarita G, Thongkham D, Piomelli D (2011): Diacylglycerol lipase-alpha and -beta control neurite outgrowth in neuro-2a cells through distinct molecular mechanisms. *Mol Pharmacol.* 80(1):60-7.
- Kamprath K, Wotjak CT (2004): Nonassociative learning processes determine expression and extinction of conditioned fear in mice. *Learn Mem* 11:770-786.
- Kamprath K, Marsicano G, Tang J, Monory K, Bisogno T, Di Marzo V, et al. (2006): Cannabinoid CB1 receptor mediates fear extinction via habituation-like processes. *J Neurosci,* 26(25), pp.6677–86.
- Kang, R., Wan J, Arstikaitis P, Takahashi H, Huang K, Bailey AO (2008): Neural palmitoyl-proteomics reveals dynamic synaptic palmitoylation. *Nature* 456, 904–909
- Kano M, Ohno-Shosaku T, Hashimoto-dani Y, Uchigashima M, Watanabe M (2009): Endocannabinoid-mediated control of synaptic transmission. *Physiol Rev.* 89(1):309-80.
- Karst H, Berger S, Turiault M, Tronche F, Schutz G, Joels M (2005): Mineralocorticoid

- receptors are indispensable for nongenomic modulation of hippocampal glutamate transmission by corticosterone. *PNAS*. 102:19204–19207.
- Karst H, Berger S, Erdmann G, Schutz G, Joels M (2010): Metaplasticity of amygdalar responses to the stress hormone corticosterone. *PNAS*. 107:14449–14454.
- Kato T, Kubota M, Kasahara T (2015): Animal models of bipolar disorder. *Neurosci Biobehav Rev*. 31(6):832-42.
- Katona I, Sperlagh B, Sik A, Kafalvi A, Vizi ES, et al. (1999): Presynaptically located CB1 cannabinoid receptor regulate GABA release from axon terminals of specific hippocampal interneurons. *J. Neurosci*. 19:4544–58
- Katona I, Urban GM, Wallace M, Ledent C, KM, et al. (2006): Molecular composition of the endocannabinoid system at glutamatergic synapses. *J. Neurosci*. 26:5628–37
- Katona I & Freund TF (2008): Endocannabinoid signaling as a synaptic circuit breaker in neurological disease. *Nature medicine*, 14(9), pp.923–30.
- Katz RJ (1981): Animal models and human depressive disorders. *Neurosci Biobehav Rev*. 5(2):231-46.
- Kinsey SG, Bailey MT, Sheridan JF, Padgett DA, Avitsur R (2007): Repeated social defeat causes increased anxiety-like behavior and alters splenocyte function in C57BL/6 and CD-1 mice. *Brain, behavior, and immunity*. 21, 458-466.
- Kitazawa M, Medeiros R, Laferla FM (2012): Transgenic mouse models of Alzheimer disease: developing a better model as a tool for therapeutic interventions. *Curr Pharm Des*. 18(8):1131-47.
- Kendler KS, Gardner CO, Prescott CA (2002): Toward a comprehensive developmental model for major depression in women. *Am J Psychiatry*. 159(7):1133-45.
- Kendler KS, Gardner CO, Prescott CA (2006): Toward a comprehensive developmental model for major depression in men. *Am J Psychiatry*. 163(1):115-24.
- Kessler RC, Berglund P, Demler O, Jin R, Merikangas KR, Walters EE (2005): Lifetime prevalence and age-of-onset distributions of DSM-IV disorders in the National Comorbidity Survey Replication. *Arch Gen Psychiatry*. 62(6):593-602.
- De Kloet ER, Joels M, Holsboer F (2005): Stress and the brain: from adaptation to disease. *Nat Rev Neurosci*. 6(6):462-75.
- Kessler RC, Aguilar-Gaxiola S, Alonso J, Chatterji S, Lee S, Ormel J, Ustün TB, Wang PS (2009): The global burden of mental disorders: an update from the WHO World Mental Health (WMH) surveys. *Epidemiol Psychiatr Soc* 2009.18(1):23–33.
- Kreitzer AC, Regehr WG (2001): Retrograde inhibition of presynaptic calcium influx by endogenous cannabinoids at excitatory synapses onto Purkinje cells. *Neuron* 29:717–27
- Krishnan V, Han MH, Graham DL, Berton O, Renthal W, Russo SJ, Laplant Q, et al. (2007): Molecular adaptations underlying susceptibility and resistance to social defeat in brain

- reward regions. *Cell*. 131(2):391-404.
- Krishnan V, Nestler EJ (2008): The molecular neurobiology of depression. *Nature*. 455(7215):894-902.
- Krishnan V (2014): Defeating the fear: new insights into the neurobiology of stress susceptibility. *Exp Neurol*. 261:412-6.
- Lallemand Y, Luria V, Haffner-Krausz R, Lonai P. (1998): Maternally expressed PGK-Cre transgene as a tool for early and uniform activation of the Cre site-specific recombinase. *Transgenic Res*. 7:105–112
- Lee CY, Cantle JP, Yang XW (2013): Genetic manipulations of mutant huntingtin in mice: new insights into Huntington's disease pathogenesis. *FEBS J*. 280(18):4382-94.
- Lee MM, Reif A, Schmitt AG (2013): Major depression: a role for hippocampal neurogenesis? *Curr Top Behav Neurosci*. 14:153-79.
- Lee Y, Dawson VL, Dawson TM (2012): Animal models of Parkinson's disease: vertebrate genetics. *Cold Spring Harb Perspect Med*. Oct 1; 2(10).
- Lesch KP, Bengel D, Heils A, et al. (1996): Association of anxiety-related traits with a polymorphism in the serotonin transporter gene regulatory region. *Science*. 274:1527–1531.
- Levinson DF (2006): The genetics of depression: a review. *Biol Psychiatry*. 60:84–92.
- Lewandoski M (2001): Conditional control of gene expression. *Nature Reviews Genetics* 2, 743-755
- Li Y, Kim J (2015): Neuronal expression of CB2 cannabinoid receptor mRNAs in the mouse hippocampus. *Neuroscience* pii: S0306-4522(15)00960-4. doi: 10.1016/j.neuroscience.2015.10.041.
- Little PJ, Compton DR, Johnson MR, Melvin LS, Martin BR (1988): Pharmacology and stereoselectivity of structurally novel cannabinoids in mice. *J Pharmacol Exp Ther*. 247(3):1046-51.
- Livak KJ, Schmittgen TD (2001): Analysis of relative gene expression data using real-time quantitative PCR and the 2(-Delta Delta C(T)) Method. *Methods*, 25(4):402-8.
- Lomazzo E, Bindila L, Remmers F, Lerner R, Schwitter C, Hoheisel U, Lutz B (2014): Therapeutic potential of inhibitors of endocannabinoid degradation for the treatment of stress-related hyperalgesia in an animal model of chronic pain. *Neuropsychopharmacology*. 40: 488–501.
- Lupien SJ, McEwen BS, Gunnar MR, Heim C (2009): Effects of stress throughout the lifespan on the brain, behaviour and cognition. *Nat Rev Neurosci*. 10(6):434-45.
- Mackie K, Devane WA, Hille B (1993) Anandamide, an endogenous cannabinoid, inhibits calcium currents as a partial agonist in N18 neuroblastoma cells. *Mol Pharmacol* 44:498–503.

- Mackie K (2005): Distribution of cannabinoid receptors in the central and peripheral nervous system. *Handb Exp Pharmacologist*. 299–325.
- Marklund N, Hillered L (2011): Animal modelling of traumatic brain injury in preclinical drug development: where do we go from here? *Br J Pharmacol*. 164(4):1207-29.
- Marques AH, Silverman MN, Sternberg EM (2009): Glucocorticoid dysregulations and their clinical correlates. From receptors to therapeutics. *Ann N Y Acad Sci*. 1179:1-18.
- Marshall C.J. (1995): Specificity of receptor protein kinase signaling: transient versus sustained extracellular signal-regulated kinase activation. *Cell*. 80:179–185.
- Marsicano G, Wotjak CT, Azad SC, Bisogno T, Rammes G, Cascio MG (2002): The endogenous cannabinoid system controls extinction of aversive memories. *Nature*, 418: 530-534.
- Martin BR & Cravatt BF (2009): Large-scale profiling of protein palmitoylation in mammalian cells. *Nat. Methods*. 6, 135–138.
- Martin M, Ledent C, Parmentier M, Maldonado R, Valverde O (2002): Involvement of CB1 cannabinoid receptors in emotional behaviour. *Psychopharmacology*, 159(4):379-87.
- Matsuda L.A., Lolait SJ, Brownstein MJ, Young AC, Bonner TI (1990). Structure of a cannabinoid receptor and functional expression of the cloned cDNA. *Nature*, 346(6284), 561–564.
- McDonald NA, Henstridge CM, Connolly CN, Irving AJ (2007): An essential role for constitutive endocytosis, but not activity, in the axonal targeting of the CB1 cannabinoid receptor. *Mol Pharmacol*. 71(4):976-84.
- McFarland MJ, Bardell TK, Yates ML, Placzek EA, Barker EL (2008): RNA interference-mediated knockdown of dynamin 2 reduces endocannabinoid uptake into neuronal dCAD cells. *Mol Pharmacol*. 74(1):101-8.
- McHugh D, Page J, Dunn E, Bradshaw HB (2012): $\Delta(9)$ -Tetrahydrocannabinol and N-arachidonyl glycine are full agonists at GPR18 receptors and induce migration in human endometrial HEC-1B cells. *Br J Pharmacol*. 165(8):2414-24.
- McKinney WT Jr, Bunney WE Jr (1969): Animal model of depression. I. Review of evidence: implications for research. *Arch Gen Psychiatry*. 21(2):240-8.
- Mechoulam R, Ben-Shabat S, Hanus L, Ligumsky M, Kaminski NE, Schatz AR, Gopher A, Almog S, Martin BR, Compton DR, et al. (1995): Identification of an endogenous 2-monoglyceride, present in canine gut, that binds to cannabinoid receptors. *Biochem. Pharmacol*. 50, 83–90.
- Ménard C, Hodes GE, Russo SJ (2015): Pathogenesis of depression: Insights from human and rodent studies. *Neuroscience*. pii: S0306-4522(15)00495-9. doi: 10.1016/j.neuroscience.2015.05.053.
- Meccariello R, Battista N, Bradshaw HB, Wang H (2014): Update in reproduction coming

- from the endocannabinoid system. *Int J Endocrinol*. 2014,412354.
- Montecucco F, Di Marzo V (2012): At the heart of the matter: the endocannabinoid system in cardiovascular function and dysfunction. *Trends Pharmacol Sci*. 33(6):331-40
- Moreira FA, Kaiser N, Monory K, Lutz B (2008): Reduced anxiety-like behaviour induced by genetic and pharmacological inhibition of the endocannabinoid-degrading enzyme fatty acid amide hydrolase (FAAH) is mediated by CB1 receptors. *Neuropharmacology*. 54(1):141-50.
- Morena M, Patel S, Bains JS, Hill MN (2016): Neurobiological Interactions Between Stress and the Endocannabinoid System. *Neuropsychopharmacology*. 41(1):80-102.
- Morrens J, Van Den Broeck W, Kempermann G (2012): Glial cells in adult neurogenesis. *Glia*. 60(2):159-74.
- Mrazek DA, Hornberger JC, Altar CA, Degtiar I (2014): A review of the clinical, economic, and societal burden of treatment-resistant depression: 1996–2013. *Psychiatric Services*. 65(8):977–987.
- Mueller BR, Bale TL (2008) Sex-specific programming of offspring emotionality after stress early in pregnancy. *J Neurosci*. 28:9055–9065.
- Munro S, Thomas KL & Abu-Shaar M (1993): Molecular characterization of a peripheral receptor for cannabinoids. *Nature*. 365, 61–65.
- Murray RM, Morrison PD, Henquet C, Di Forti M (2007): Cannabis, the mind and society: the hash realities. *Nat Rev Neurosci*. 8(11):885-95.
- Myers KM & Davis M (2007): Mechanisms of fear extinction. *Mol psychiatry*, 12(2): 120–50.
- Myers B, McKlveen JM, Herman JP (2012): Neural Regulation of the Stress Response: The Many Faces of Feedback. *Cell Mol Neurobiol*. 2012 Feb 1. [Epub ahead of print]
- Neumeister A, Normandin MD, Pietrzak RH, Piomelli D, Zheng MQ, Gujarró-Anton A, Potenza MN, Bailey CR, Lin SF, Najafzadeh S, Ropchan J, Henry S, Corsi-Travali S, Carson RE, Huang Y (2014): Elevated brain cannabinoid CB1 receptor availability in post-traumatic stress disorder: a positron emission tomography study. *Mol Psychiatry*. 18(9):1034-40.
- Nestler EJ, Barrot M, DiLeone RJ, Eisch AJ, Gold SJ, Monteggia LM (2002): Neurobiology of depression. *Neuron*. 34(1):13-25.
- Nestler EJ & Hyman SE (2010): Animal models of neuropsychiatric disorders. *Nat Neurosci*. 13(10):1161-9
- Nishi M, Horii-Hayashi N, Sasagawa T (2014): Effects of early life adverse experiences on the brain: implications from maternal separation models in rodents. *Front Neurosci*. 17;8:166

- Nomura DK, Morrison BE, Blankman JL, Long JZ, Kinsey SG, Marcondes MCG, et al. (2011): Endocannabinoid hydrolysis generates brain prostaglandins that promote neuroinflammation. *Science* 334, 809–813
- Ohno-Shosaku T, Maejima T, Kano M (2001): Endogenous cannabinoids mediate retrograde signals from depolarized postsynaptic neurons to presynaptic terminals. *Neuron* 29:729–38
- Onaivi ES, Ishiguro H, Gu S, Liu Q-R (2012): CNS effects of CB2 cannabinoid receptors: beyond neuro-immuno-cannabinoid activity. *J Psychopharmacol.* 26(1): 92–103.
- Oudin MJ, Hobbs C, Doherty P (2011): DAGL-dependent endocannabinoid signalling: roles in axonal pathfinding, synaptic plasticity and adult neurogenesis. *Eur J Neuroscience.* 34:1634–1646.
- Pacher P, Mechoulam R (2011): Is lipid signaling through cannabinoid 2 receptors part of a protective system? *Prog Lipid Res.* 50(2):193-211.
- Patel S, Roelke CT, Rademacher DJ, Hillard CJ (2005): Inhibition of restraint stress-induced neural and behavioural activation by endogenous cannabinoid signalling. *Eur J Neurosci.* 21(4):1057-69.
- Patel S, Hillard CJ (2006): Pharmacological evaluation of cannabinoid receptor ligands in a mouse model of anxiety: further evidence for an anxiolytic role for endogenous cannabinoid signaling. *J Pharmacol Exp Ther.* 2006;318:304–11.
- Patel S & Hillard CJ (2008): Adaptations in endocannabinoid signaling in response to repeated homotypic stress: a novel mechanism for stress habituation. *Europ J Neurosci,* 27(11):2821-2829.
- Patel S, Kingsley PJ, Mackie K, Marnett LJ, Winder DG (2009): Repeated homotypic stress elevates 2-arachidonoylglycerol levels and enhances short-term endocannabinoid signaling at inhibitory synapses in basolateral amygdala. *Neuropsychopharmacol.* 34(13):2699-709
- Park H, Poo MM (2013): Neurotrophin regulation of neural circuit development and function. *Nat Rev Neurosci.* 14(1):7-23.
- Pedicord DL, Flynn MJ, Fanslau C, Miranda M, Hunihan L, Robertson BJ, Pearce BC, Yu XC, Westphal RS, Blat Y (2011): Molecular characterization and identification of surrogate substrates for diacylglycerol lipase α . *Biochem Biophys Res Commun.* 12;411(4):809-14.
- Peña CJ, Bagot RC, Labonté B, Nestler EJ (2014): Epigenetic signaling in psychiatric disorders. *J Mol Biol.* 426(20):3389-412.
- Pistis M, Melis M (2019): From surface to nuclear receptors: the endocannabinoid family extends its assets. *Curr Med Chem.* 17(14):1450-67.
- Pittenger C, Duman RS (2008): Stress, depression, and neuroplasticity: a convergence of mechanisms. *Neuropsychopharmacology.* 33(1):88-109.

- Porsolt RD, Bertin A, Jalfre M (1977): Behavioral despair in mice: a primary screening test for antidepressants. *Arch Int Pharmacodyn Ther.*229(2):327-36.
- Pothion S, Bizot J-C, Trovero F, Belzung C (2004): Strain differences in sucrose preference and in the consequences of unpredictable chronic mild stress. *Behavioural Brain Research* 155:135-146
- Powell DR, Gay JP, Wilganowski N, Doree D, Savelieva KV, Lanthorn TH, Read R, Vogel P, Hansen GM, Brommage R, Ding ZM, Desai U, Zambrowicz B (2015): Diacylglycerol Lipase α Knockout Mice Demonstrate Metabolic and Behavioral Phenotypes Similar to Those of Cannabinoid Receptor 1 Knockout Mice. *Front Endocrinol (Lausanne)*. 6:86.
- Prescott SM & Majerus PW (1983): Characterization of 1,2-diacylglycerol hydrolysis in human platelets. Demonstration of an arachidonoyl-monoacylglycerol intermediate. *J. Biol. Chem.* 258, 764–769.
- Rademacher DJ, Meier SE, Shi L, Ho WS, Jarrahian A, Hillard CJ (2008): Effects of acute and repeated restraint stress on endocannabinoid content in the amygdala, ventral striatum, and medial prefrontal cortex in mice. *Neuropsychopharmacology*, 54(1):108-116.
- Rahman IA, Tsuboi K, Uyama T, Ueda N (2014): New players in the fatty acyl ethanolamide metabolism. *Pharmacol. Res.* 86, 1-10
- Ranganathan M, Cortes-Briones J, Radhakrishnan R, Thurnauer H, Planeta B, Skosnik P et al. (2015): Reduced Brain Cannabinoid Receptor Availability In Schizophrenia. *Biol Psychiatry*. pii: S0006-3223(15)00686-1. doi: 10.1016/j.biopsych.2015.08.021.
- Rosenberger TA; Farooqui AA, Horrocks LA (2007): Bovine Brain Diacylglycerol Lipase: Substrate Specificity and Activation by Cyclic AMP-dependent Protein Kinase. *Lipids*. 42:3;187-195.
- Ross, R.A. (2009) The enigmatic pharmacology of GPR55. *Trends Pharmacol. Sci.* 30, 156-163
- Ros-Simó C, Valverde O (2012): Early-life social experiences in mice affect emotional behaviour and hypothalamic-pituitary-adrenal axis function. *Pharmacol Biochem Behav.* 102(3):434-41.
- Rotella F & Mannucci E (2013): Depression as a risk factor for diabetes: a meta-analysis of longitudinal studies. *J Clin Psych.* 74(1):31–37
- Rouzer CA & Marnett LJ (2011): Endocannabinoid oxygenation by cyclooxygenases, lipoxygenases, and cytochromes P450: Cross-talk between the eicosanoid and endocannabinoid signaling pathways. *Chem. Rev.*111, 5899–5921.
- Rubino T, Parolaro D (2008): Long lasting consequences of cannabis exposure in adolescence. *Mol Cell Endocrinol.* 286:S108–13
- Rueda D., Galve-Roperh I., Haro A., Guzman M (2000): The CB1 cannabinoid receptor is coupled to the activation of c-Jun N-terminal kinase. *Mol. Pharmacol.* 58:814–820.

- Ruehle S, Rey AA, Remmers F, Lutz B (2012): The endocannabinoid system in anxiety, fear memory and habituation. *J Psychopharmacology*, 26(1):23-39.
- Ruscio AM, Chiu WT, Roy-Byrne P, Stang PE, Stein DJ, Wittchen HU, Kessler RC (2007): Broadening the definition of generalized anxiety disorder: effects on prevalence and associations with other disorders in the National Comorbidity Survey Replication. *J Anxiety Disord*. 21(5):662-76.
- Sareen J1 (2014): Posttraumatic stress disorder in adults: impact, comorbidity, risk factors, and treatment. *Can J Psychiatry*. 59(9):460-7.
- Sansom JN, Wong AH (2015): Schizophrenia and Depression Co-Morbidity: What We have Learned from Animal Models. *Front Psychiatry*. 2015 Feb 18;6:13.
- Savinainen JR, Järvinen T, Laine K, Laitinen JT (2001): Despite substantial degradation, 2-arachidonoylglycerol is a potent full efficacy agonist mediating CB(1) receptor-dependent G-protein activation in rat cerebellar membranes. *Br J Pharmacol* 134:664–672
- Schechter M, Pinhasov A, Weller A, Fride E (2012): Blocking postpartum mouse dam's CB1 receptors impairs maternal behavior as well as offspring development and their adult social-emotional behavior. *Behav Brain Res*, 226:481-492.
- Schechter M, Weller A, Zittel P, Gross M, Zimmer A, Pinhasov A (2013): Endocannabinoid receptor deficiency affects maternal care and alters the dam's hippocampal oxytocin receptor and brain-derived neurotrophic factor expression. *J Neuroendocrinology*, 25:898-909.
- Scheuing L, Chiu CT, Liao HM, Chuang DM (2015): Antidepressant mechanism of ketamine: perspective from preclinical studies. *Front Neurosci*. 9:249.
- Schildkraut JJ (1965): The catecholamine hypothesis of affective disorders: a review of supporting evidence. *Am J Psychiatry*. 122(5):509-22.
- Schlosburg JE, Blankman JL, Long JZ, Nomura DK, Pan B, Kinsey SG, et al. (2010): Chronic monoacylglycerol lipase blockade causes functional antagonism of the endocannabinoid system. *Nat Neurosci* .13, 1113–1119
- Sciolino NR, Zhou W, Hohmann AG (2011): Enhancement of endocannabinoid signaling with JZL184, an inhibitor of the 2-arachidonoylglycerol hydrolyzing enzyme monoacylglycerol lipase, produces anxiolytic effects under conditions of high environmental aversiveness in rats. *Pharmacol Res*, 64(3):226-34.
- Sgoifo A, Koolhaas J, De Boer S, Musso E, Stilli D, Buwalda B, Meerlo P (1999): Social stress, autonomic neural activation, and cardiac activity in rats. *Neurosci Biobehav Rev*.23(7):915-23.
- Sgoifo A, Costoli T, Meerlo P, Buwalda B, Pico'-Alfonso MA, De Boer S, Musso E, Koolhaas J (2005): Individual differences in cardiovascular response to social challenge. *Neurosci Biobehav Rev*. 29(1):59-66. Epub 2004 Dec 1.

- Sheline YI, Gado MH, Kraemer HC (2003): Untreated depression and hippocampal volume loss. *Am J Psychiatry*. 160(8):1516-8.
- Shepherd JK, Grewal SS, Fletcher A, Bill DJ, Dourish CT (1994): Behavioural and pharmacological characterisation of the elevated "zero-maze" as an animal model of anxiety. *Psychopharmacology (Berl)*. 116(1):56-64.
- Shonesy BC, Wang X, Rose KL, Ramikie TS, Cavener VS, Rentz T, Baucum AJ, Jalan-Sakrikar N, Mackie K, Winder DG, Patel S, Colbran RJ (2013): CaMKII regulates diacylglycerol lipase- α and striatal endocannabinoid signaling. *Nat Neurosci*. 16(4):456-63
- Smaga I, Bystrowska B, Gawlinski D, Pomierny B, Stankowicz P, Filip M (2014): Antidepressants and changes in concentration of endocannabinoids and N-acylethanolamines in rat brain structures. *Neurotox Res*, 26:190-206.
- Smith SM, Vale WW (2006): The role of the hypothalamic-pituitary-adrenal axis in neuroendocrine responses to stress. *Dialogues Clin Neurosci*. 8(4):383-95.
- Steiner MA, Wanisch K, Monory K, Marsicano G, Borroni E, Bächli H, et al. (2008): Impaired cannabinoid receptor type 1 signaling interferes with stress-coping behavior in mice. *Pharmacogenomics J*. 8:196–208.
- Strekalova T, Couch Y, Kholod N, Boyks M, Malin D, Leprince P, Steinbusch HM (2011): Update in the methodology of the chronic stress paradigm: internal control matters. *Behav Brain Funct*. 7:9.
- Sugiura T, Kondo S, Sukagawa A, Nakane S, Shinoda A, Itoh K, Yamashita A, Waku K. (1995): 2-Arachidonoylglycerol: a possible endogenous cannabinoid receptor ligand in brain. *Biochem. Biophys. Res. Commun*. 215, 89–97.
- Sugiura T, Kishimoto S, Oka S, Gokoh M (2006): Biochemistry, pharmacology and physiology of 2-arachidonoylglycerol, an endogenous cannabinoid receptor ligand. *Prog Lipid Res* 45:405–446.
- Tanimura A, Yamazaki M, Hashimotodani Y, Uchigashima M, Kawata S, Abe M, Kita Y, Hashimoto K, Shimizu T, Watanabe M, Sakimura K, Kano M (2010): The endocannabinoid 2-arachidonoylglycerol produced by diacylglycerol lipase alpha mediates retrograde suppression of synaptic transmission. *Neuron* 65:320–327
- Ternes S. (2013): *Investigation of the endocannabinoid system using in vivo and in vitro models* [Dissertation]. Bonn: Rheinische Friedrich-Wilhelms University
- Thiele C, Papan C, Hoelper D, Kusserow K, Gaebler A, Schoene M et al. (2012): Tracing Fatty Acid Metabolism by Click Chemistry. *ACS Chem Biol*. 7(12):2004-11
- Thirumurugan P, Matosiuk D, Jozwiak K (2013): Click chemistry for drug development and diverse chemical-biology applications. *Chem Rev*. 113(7):4905-79.
- Toth LA, Trammell RA, Ilsley-Woods M (2015): Interactions Between Housing Density and Ambient Temperature in the Cage Environment: Effects on Mouse Physiology and

- Behavior. *J Am Assoc Lab Anim Sci.* 54(6):708-17.
- Ueda Y, Ishitsuka R, Hullin-Matsuda F, Kobayashi T (2014): Regulation of the transbilayer movement of diacylglycerol in the plasma membrane. *Biochimie.*107 Pt A:43-50.
- Uher R, McGuffin P. The moderation by the serotonin transporter gene of environmental adversity in the etiology of depression: 2009 update. *Mol Psychiatry.* 2010;15:18–22.
- Urigüen L, Fernández B, Romero EM, De Pedro N, Delgado MJ, Guaza C, Schmidhammer H, Viveros MP (2002): Effects of 14-methoxymetopon, a potent opioid agonist, on the responses to the tail electric stimulation test and plus-maze activity in male rats: neuroendocrine correlates. *Brain Res Bull.* 57(5):661-6.
- Urigüen L, Pérez-Rial S, Ledent C, Palomo T, Manzanares J (2004): Impaired action of anxiolytic drugs in mice deficient in cannabinoid CB1 receptors. *Neuropharmacology,* 46(7):966-73.
- Urquhart P, Nicolaou A, Woodward DF (2015): Endocannabinoids and their oxygenation by cyclo-oxygenases, lipoxygenases and other oxygenases. *Biochim Biophys Acta.* 1851(4):366-76
- Valverde O, Karsak M, Zimmer A (2005): Analysis of the endocannabinoid system by using CB1 cannabinoid receptor knockout mice. *Handb Exp Pharmacol* 168, 117–142.
- Valverde O. & Torrens M. (2012): CB1 receptor-deficient mice as a model for depression. *Neuroscience,* 204: 193-206.
- Van Sickle MD, Duncan M, Kingsley PJ, Mouihate A, Urbani P, Mackie K, Stella N, Makriyannis A, Piomelli D, Davison JS, Marnett LJ, Di Marzo V, Pittman QJ, Patel KD, Sharkey KA (2005): Identification and functional characterization of brainstem cannabinoid CB2 receptors. *Science.* 310(5746):329-32
- Vellani V, Petrosino S, De Petrocellis L, Valenti M, Prandini M, Magherini PC, McNaughton PA, Di Marzo V (2008): Functional lipidomics. Calcium-independent activation of endocannabinoid/ endovanilloid lipid signalling in sensory neurons by protein kinases C and A and thrombin. *Neuropharmacology.* 55(8):1274-9.
- Verkuyl JM, Karst H, Joëls M (2005): GABAergic transmission in the rat paraventricular nucleus of the hypothalamus is suppressed by corticosterone and stress. *Eur J Neurosci.* 21(1):113-21.
- Von Frijtag J C, Van den Bos R, Spruijt BM (2002): Imipramine restores the longterm impairment of appetitive behavior in socially stressed rats. *Psychopharmacology.* 162(3), 232-238. doi: 10.1007/s00213-002-1093-3
- Walter L, Franklin A, Witting A, Moller T, Stella N (2002): Astrocytes in culture produce anandamide and other acylethanolamides. *J Biol Chem.* 277, 20869–20876.
- Walter L, Franklin A, Witting A, Wade C, Xie Y, Kunos G, Mackie K, Stella N (2003): Non-psychotropic cannabinoid receptors regulate microglial cell migration. *J Neurosci.*

- 23,1398–1405.
- Walter L, Stella N (2003): Endothelin-1 increases 2-arachidonoyl glycerol (2-AG) production in astrocytes. *Glia*.44(1):85-90.
- Warden D, Rush AJ, Trivedi MH, Fava M, Wisniewski SR (2007): The STAR*D Project results: a comprehensive review of findings. *Curr Psychiatry Rep* 9:449–459.
- Weledji EP, Assob JC (2014): The ubiquitous neural cell adhesion molecule (N-CAM). *Ann Med Surg (Lond)*. 3(3):77-81.
- Welsh N (1996): Interleukin-1 beta-induced ceramide and diacylglycerol generation may lead to activation of the c-Jun NH2-terminal kinase and the transcription factor ATF2 in the insulin-producing cell line RINm5F. *J Biol Chem*. 271(14):8307-12.
- WHO (World Health Organization): Fact sheet N°369, Oktober 2015.
- Williams EJ, Walsh FS, Doherty P (2003): The FGF receptor uses the endocannabinoid signaling system to couple to an axonal growth response. *J Cell Biol*. 17;160(4):481-6.
- Williamson EM, Evans FJ (2000): Cannabinoids in clinical practice. *Drugs*. 60:1303–14.
- Willner P (2005) Chronic mild stress (CMS) revisited: consistency and behavioural-neurobiological concordance in the effects of CMS. *Neuropsychobiology* 52:90–110.
- Wittchen HU & Jacobi F (2005): Size and burden of mental disorders in Europe—A critical review and appraisal of 27 studies. *Eur Neuropsychopharmacol*, 15, 357–376.
- Yau YH, Potenza MN (2013): Stress and eating behaviors. *Minerva Endocrinol*. 38(3):255-67.
- Yu T, Guo M, Garza J, Rendon S, Sun XL, Zhang W, Lu XY (2011): Cognitive and neural correlates of depression-like behaviour in socially defeated mice: an animal model of depression with cognitive dysfunction. *Journal of Neuropsychopharmacology*.14(3), 303-317.
- Zhang Z, Wang W, Zhong P, Liu SJ, Long JZ, Zhao L, Gao HQ, Cravatt BF, Liu QS (2014): Blockade of 2-arachidonoylglycerol hydrolysis produces antidepressant-like effects and enhances adult hippocampal neurogenesis and synaptic plasticity. *Hippocampus*, 25(1):16-26.
- Zhong P, Wang W, Pan B, Liu X, Zhang Z, Long JZ, et al. (2014): Monoacylglycerol lipase inhibition blocks chronic stress-induced depressive-like behaviors via activation of mTOR signaling. *Neuropsychopharmacology*, 39(7):1763-76.
- Zhu Y, Romero MI, Ghosh P, Ye Z, Charnay P, Rushing EJ, Marth JD, Parada LF (2001): Ablation of NF1 function in neurons induces abnormal development of cerebral cortex and reactive gliosis in the brain. *Genes Dev*.15:859–876.
- Zoellner LA, Pruitt LD, Farach FJ, Jun JJ (2014): Understanding heterogeneity in PTSD: fear, dysphoria, and distress. *Depress Anxiety*. 31(2):97-106.
- Zoppi S, Pérez Nievas BG, Madrigal JL, Manzanares J, Leza JC, García-Bueno B (2011):

Regulatory role of cannabinoid receptor 1 in stress-induced excitotoxicity and neuroinflammation. *Neuropsychopharmacology*. 36(4):805-18.

A Appendix

A.1 Protein list

Proteins detected and identified via MALDI-TOF/TOF-MS. The list only contains the 142 proteins, which were solely identified in the sample of transfected Neuro-2a cells (sample B).

Accession	Description	Σ Coverage	Σ # Proteins	A: Area	B: Area	Coverage A	Coverage B	# Peptides A	# PSM A	# Peptides B	# PSM B
Q8K2C9	Very-long-chain (3R)-3-hydroxyacyl- [acyl-carrier protein] dehydratase 3 OS=Mus musculus GN=ptplad1 PE=1 SV=2 - [HACD3_MOUSE]	11,88	1	2,219E7	1,911E6	0,00	11,88			3	3
P08752	Guanine nucleotide- binding protein G(i) subunit alpha-2 OS=Mus musculus GN=Gnai2 PE=1 SV=5 - [GNAI2_MOUSE]	10,14	1	2,019E7	4,365E6	0,00	10,14			3	3
Q52KR3	Protein prune homolog 2 OS=Mus musculus GN=Prune2 PE=2 SV=2 - [PRUN2_MOUSE]	1,88	1	1,461E7	2,200E6	0,00	1,88			3	3
Q9CQ71	Replication protein A 14 kDa subunit OS=Mus musculus GN=Rpa3 PE=2 SV=1 - [RFA3_MOUSE]	45,45	1	1,244E7	2,081E6	0,00	45,45			5	5
Q9D2M8	Ubiquitin- conjugating enzyme E2 variant 2 OS=Mus musculus GN=Ube2v2 PE=2 SV=4 - [UB2V2_MOUSE]	11,72	2	1,229E7	4,368E6	0,00	11,72			2	2
P59708	Pre-mRNA branch site protein p14 OS=Mus musculus GN=Sf3b14 PE=2 SV=1 - [PM14_MOUSE]	32,00	1	1,229E7	1,649E6	0,00	32,00			3	4
P97379	Ras GTPase- activating protein- binding protein 2 OS=Mus musculus GN=G3bp2 PE=1 SV=2 - [G3BP2_MOUSE]	11,83	1	1,209E7	1,300E6	0,00	11,83			3	7
O35381	Acidic leucine-rich nuclear phosphoprotein 32 family member A OS=Mus musculus GN=Anp32a PE=1 SV=1 - [AN32A_MOUSE]	10,93	1	1,165E7	4,012E6	0,00	10,93			2	3

Accession	Description	Σ Coverage	$\Sigma\#$ Proteins	A: Area	B: Area	Coverage A	Coverage B	# Peptides A	# PSM A	# Peptides B	# PSM B
Q80UW8	DNA-directed RNA polymerases I, II, and III subunit RPABC1 OS=Mus musculus GN=Polr2e PE=2 SV=1 - [RPAB1_MOUSE]	14,76	1	1,012E7	2,037E6	0,00	14,76			2	2
Q91V12	Cytosolic acyl coenzyme A thioester hydrolase OS=Mus musculus GN=Acot7 PE=1 SV=2 - [BACH_MOUSE]	5,77	1	9,677E6	4,981E6	0,00	5,77			2	2
Q9CZH3	Proteasome assembly chaperone 3 OS=Mus musculus GN=Psmg3 PE=1 SV=1 - [PSMG3_MOUSE]	22,95	1	9,315E6	1,559E6	0,00	22,95			2	2
P70698	CTP synthase 1 OS=Mus musculus GN=Ctps1 PE=1 SV=2 - [PYRG1_MOUSE]	11,51	1	9,256E6	2,226E6	0,00	11,51			5	6
P45878	Peptidyl-prolyl cis-trans isomerase FKBP2 OS=Mus musculus GN=Fkbp2 PE=1 SV=1 - [FKBP2_MOUSE]	39,29	1	9,117E6	7,352E5	0,00	39,29			3	3
O35658	Complement component 1 Q subcomponent-binding protein, mitochondrial OS=Mus musculus GN=C1qbp PE=1 SV=1 - [C1QBP_MOUSE]	19,42	1	8,779E6	4,054E6	0,00	19,42			4	5
Q8BGJ9	Splicing factor U2AF 26 kDa subunit OS=Mus musculus GN=U2af114 PE=1 SV=1 - [U2AF4_MOUSE]	10,00	2	8,204E6	4,520E6	0,00	10,00			3	5
P56959	RNA-binding protein FUS OS=Mus musculus GN=Fus PE=2 SV=1 - [FUS_MOUSE]	7,72	1	7,874E6	1,664E6	0,00	7,72			2	8
Q923D5	WW domain-binding protein 11 OS=Mus musculus GN=Wbp11 PE=1 SV=2 - [WBP11_MOUSE]	4,06	1	7,835E6	7,170E5	0,00	4,06			2	2
P00405	Cytochrome c oxidase subunit 2 OS=Mus musculus GN=Mtco2 PE=1 SV=1 - [COX2_MOUSE]	11,45	1	6,829E6	1,675E6	0,00	11,45			2	3
Q61584	Fragile X mental retardation syndrome-related protein 1 OS=Mus musculus GN=Fxr1 PE=1 SV=2 - [FXR1_MOUSE]	5,91	1	6,555E6	9,556E5	0,00	5,91			3	4
P06837	Neuromodulin OS=Mus musculus GN=Gap43 PE=1 SV=1[NEUM MOU]	31,72	1	5,869E6	2,954E6	0,00	31,72			4	5

Accession	Description	Σ Coverage	$\Sigma\#$ Proteins	A: Area	B: Area	Coverage A	Coverage B	# Peptides A	# PSM A	# Peptides B	# PSM B
O88653	Ragulator complex protein LAMTOR3 OS=Mus musculus GN=Lamtor3 PE=1 SV=1 - [LTOR3_MOUSE]	27,42	1	5,381E6	1,220E6	0,00	27,42			3	3
P60898	DNA-directed RNA polymerase II subunit RPB9 OS=Mus musculus GN=Polr2i PE=2 SV=1 - [RPB9_MOUSE]	27,20	1	5,366E6	6,288E5	0,00	27,20			2	2
P42125	Enoyl-CoA delta isomerase 1, mitochondrial OS=Mus musculus GN=Eci1 PE=2 SV=2 - [ECI1_MOUSE]	9,69	1	4,971E6	0,000E0	0,00	9,69			2	2
P28740	Kinesin-like protein KIF2A OS=Mus musculus GN=Kif2a PE=1 SV=2 - [KIF2A_MOUSE]	6,52	1	4,816E6	2,923E6	0,00	6,52			4	4
Q8BTW3	Exosome complex component MTR3 OS=Mus musculus GN=Exosc6 PE=1 SV=1 - [EXOS6_MOUSE]	15,38	1	4,801E6	1,873E6	0,00	15,38			3	3
P51807	Dynein light chain Tctex-type 1 OS=Mus musculus GN=Dynlt1 PE=1 SV=1 - [DYLT1_MOUSE]	23,01	1	4,677E6	1,613E6	0,00	23,01			2	2
Q9CQC6	Basic leucine zipper and W2 domain-containing protein 1 OS=Mus musculus GN=Bzw1 PE=1 SV=1 - [BZW1_MOUSE]	11,93	1	4,612E6	0,000E0	0,00	11,93			2	2
Q9JKY0	Cell differentiation protein RCD1 homolog OS=Mus musculus GN=Rqcd1 PE=1 SV=1 - [RCD1_MOUSE]	10,37	1	4,610E6	1,392E6	0,00	10,37			2	2
P26041	Moesin OS=Mus musculus GN=Msn PE=1 SV=3 - [MOES_MOUSE]	15,08	1	4,568E6	3,874E6	0,00	15,08			7	7
Q8R349	Cell division cycle protein 16 homolog OS=Mus musculus GN=Cdc16 PE=2 SV=1 - [CDC16_MOUSE]	3,23	1	4,386E6	1,799E6	0,00	3,23			2	2
P62897	Cytochrome c, somatic OS=Mus musculus GN=Cycc PE=1 SV=2 - [CYC_MOUSE]	32,38	2	4,147E6	1,216E6	0,00	32,38			4	5
P97496	SWI/SNF complex subunit SMARCC1 OS=Mus musculus GN=Smarcc1 PE=1 SV=2 - [SMRC1_MOUSE]	10,51	1	3,977E6	2,519E6	0,00	9,51			7	8

Accession	Description	Σ Coverage	$\Sigma\#$ Proteins	A: Area	B: Area	Coverage A	Coverage B	# Peptides A	# PSM A	# Peptides B	# PSM B
Q8CGC6	RNA-binding protein 28 OS=Mus musculus GN=Rbm28 PE=1 SV=4 - [RBM28_MOUSE]	3,33	1	3,646E6	8,301E5	0,00	3,33			2	3
Q9R190	Metastasis-associated protein MTA2 OS=Mus musculus GN=Mta2 PE=1 SV=1 - [MTA2_MOUSE]	8,08	1	3,424E6	9,315E5	0,00	8,08			4	4
Q61191	Host cell factor 1 OS=Mus musculus GN=Hcfc1 PE=1 SV=2 - [HCFC1_MOUSE]	1,61	1	3,364E6	1,871E6	0,00	1,61			2	3
Q9CQV5	28S ribosomal protein S24, mitochondrial OS=Mus musculus GN=Mrps24 PE=2 SV=1 [RT24_MOUSE]	12,57	1	3,260E6	3,092E5	0,00	12,57			2	2
P83870	PHD finger-like domain-containing protein 5A OS=Mus musculus GN=Phf5a PE=1 SV=1 - [PHF5A_MOUSE]	40,00	1	3,204E6	1,446E6	0,00	40,00			4	4
Q9JIX0	Enhancer of yellow 2 transcription factor homolog OS=Mus musculus GN=Eny2 PE=2 SV=1 - [ENY2_MOUSE]	25,74	1	3,189E6	8,512E5	0,00	25,74			2	3
Q9WU78	Programmed cell death 6-interacting protein OS=Mus musculus GN=Pcdc6ip PE=1 SV=3 - [PDC6I_MOUSE]	6,90	1	3,143E6	8,741E5	0,00	6,90			4	4
Q3UEB3	Poly(U)-binding-splicing factor PUF60 OS=Mus musculus GN=Puf60 PE=2 SV=2 - [PUF60_MOUSE]	25,89	1	2,932E6	5,525E6	0,00	25,89			8	11
Q9JHU9	Inositol-3-phosphate synthase 1 OS=Mus musculus GN=Isynal PE=2 SV=1 - [INO1_MOUSE]	5,21	1	2,894E6	1,654E6	0,00	5,21			2	2
Q99KG3	RNA-binding protein 10 OS=Mus musculus GN=Rbm10 PE=1 SV=1 - [RBM10_MOUSE]	2,69	1	2,848E6	1,212E6	0,00	2,69			2	2
Q3U0V1	Far upstream element-binding protein 2 OS=Mus musculus GN=Khsrp PE=1 SV=2 - [FUBP2_MOUSE]	11,10	1	2,731E6	9,296E5	0,00	11,10			5	6
Q91VD9	NADH-ubiquinone oxidoreductase 75 kDa subunit, mitochondrial OS=Mus musculus GN=Ndufs1 PE=1 SV=2 - [NDUS1_MOUSE]	9,35	1	2,620E6	1,392E6	0,00	9,35			4	4

Accession	Description	Σ Coverage	$\Sigma\#$ Proteins	A: Area	B: Area	Coverage A	Coverage B	# Peptides A	# PSM A	# Peptides B	# PSM B
P47856	Glutamine-- fructose-6-phosphate aminotransferase [isomerizing] 1 OS=Mus musculus GN=Gfpt1 PE=1 SV=3 - [GFPT1_MOUSE]	6,74	1	2,539E6	8,801E5	0,00	6,74			3	3
Q91W50	Cold shock domain- containing protein E1 OS=Mus musculus GN=Csde1 PE=2 SV=1 - [CSDE1_MOUSE]	5,89	1	2,413E6	8,716E5	0,00	5,89			3	4
Q61205	Platelet-activating factor acetylhydrolase IB subunit gamma OS=Mus musculus GN=Pafah1b3 PE=1 SV=1 - [PA1B3_MOUSE]	13,36	1	2,328E6	7,487E5	0,00	13,36			2	2
O54774	AP-3 complex subunit delta-1 OS=Mus musculus GN=Ap3d1 PE=1 SV=1 - [AP3D1_MOUSE]	3,42	1	2,319E6	1,746E6	0,00	3,42			3	3
Q6PD26	GPI transamidase component PIG-S OS=Mus musculus GN=Pigs PE=1 SV=3 - [PIGS_MOUSE]	12,61	1	2,168E6	9,287E5	0,00	12,61			4	4
O08992	Syntenin-1 OS=Mus musculus GN=Sdcbp PE=2 SV=1 - [SDCB1_MOUSE]	12,04	1	2,146E6	4,041E5	0,00	12,04			2	2
Q60790	Ras GTPase- activating protein 3 OS=Mus musculus GN=Rasa3 PE=1 SV=2 - [RASA3_MOUSE]	10,07	1	2,102E6	9,804E5	0,00	10,07			6	6
P56960	Exosome component 10 OS=Mus musculus GN=Exosc10 PE=1 SV=2 - [EXOSX_MOUSE]	3,83	1	1,996E6	1,219E6	0,00	3,83			2	2
Q9QXK7	Cleavage and polyadenylation specificity factor subunit 3 OS=Mus musculus GN=Cpsf3 PE=1 SV=2 - [CPSF3_MOUSE]	4,97	1	1,914E6	1,323E6	0,00	4,97			2	2
Q91Y86	Mitogen-activated protein kinase 8 OS=Mus musculus GN=Mapk8 PE=1 SV=1 - [MK08_MOUSE]	5,73	3	1,911E6	9,947E4	0,00	5,73			2	2
Q8CCP0	Nuclear export mediator factor Nemf OS=Mus musculus GN=Nemf PE=1 SV=2 - [NEMF_MOUSE]	3,38	1	1,904E6	7,387E5	0,00	3,38			3	3
Q61495	Desmoglein-1- alpha OS=Mus musculus GN=Dsg1a PE=2 SV=2 - [DSG1A_MOUSE]	2,27	2	1,904E6	6,053E5	0,00	2,27			2	3

Accession	Description	Σ Coverage	Σ # Proteins	A: Area	B: Area	Coverage A	Coverage B	# Peptides A	# PSM A	# Peptides B	# PSM B
P52479	Ubiquitin carboxyl-terminal hydrolase 10 OS=Mus musculus GN=Usp10 PE=1 SV=3 - [UBP10_MOUSE]	4,29	1	1,746E6	6,238E5	0,00	4,29			3	3
Q9R0P6	Signal peptidase complex catalytic subunit SEC11A OS=Mus musculus GN=Sec11a PE=2 SV=1 - [SC11A_MOUSE]	15,64	1	1,738E6	6,566E5	0,00	15,64			3	3
Q8R050	Eukaryotic peptide chain release factor GTP-binding subunit ERF3A OS=Mus musculus GN=Gsp11 PE=1 SV=2 - [ERF3A_MOUSE]	9,28	1	1,721E6	2,235E6	0,00	9,28			4	4
Q8CJG0	Protein argonaute-2 OS=Mus musculus GN=Eif2c2 PE=1 SV=3 - [AGO2_MOUSE]	3,95	1	1,645E6	7,501E7	0,00	3,95			2	2
P23780	Beta-galactosidase OS=Mus musculus GN=Glb1 PE=2 SV=1 - [BGAL_MOUSE]	3,55	1	1,590E6	8,945E5	0,00	3,55			2	2
Q9ESV0	ATP-dependent RNA helicase DDX24 OS=Mus musculus GN=Ddx24 PE=1 SV=2 - [DDX24_MOUSE]	4,55	1	1,564E6	9,572E5	0,00	4,55			3	3
Q11011	Puromycin-sensitive aminopeptidase OS=Mus musculus GN=Npepps PE=1 SV=2 - [PSA_MOUSE]	6,74	1	1,532E6	5,664E5	0,00	6,74			5	5
Q9CWX9	Biogenesis of lysosome-related organelles complex 1 subunit 2 OS=Mus musculus GN=Bloc1s2 PE=1 SV=1 - [BL1S2_MOUSE]	25,17	1	1,478E6	1,613E6	0,00	25,17			2	2
Q8C111	Guanine nucleotide-binding protein-like 3 OS=Mus musculus GN=Gnl3 PE=1 SV=2 - [GNL3_MOUSE]	9,67	1	1,416E6	7,133E5	0,00	9,67			3	5
Q8BUN5	Mothers against decapentaplegic homolog 3 OS=Mus musculus GN=Smad3 PE=1 SV=2 - [SMAD3_MOUSE]	5,65	3	1,304E6	2,817E6	0,00	5,65			2	2
Q9CQZ5	NADH dehydrogenase [ubiquinone] 1 alpha subcomplex subunit 6 OS=Mus musculus GN=Ndufa6 PE=1 SV=1 - [NDUA6_MOUSE]	14,50	1	1,241E6	2,918E5	0,00	14,50			2	2

Accession	Description	Σ Coverage	$\Sigma\#$ Proteins	A: Area	B: Area	Coverage A	Coverage B	# Peptides A	# PSM A	# Peptides B	# PSM B
Q9D706	RNA polymerase II-associated protein 3 OS=Mus musculus GN=Rpap3 PE=1 SV=1 - [RPAP3_MOUSE]	9,39	1	1,180E6	7,470E5	0,00	9,39			3	3
O08740	DNA-directed RNA polymerase II subunit RPB11 OS=Mus musculus GN=Polr2j PE=2 SV=1 - [RPB11_MOUSE]	15,38	1	1,161E6	4,434E5	0,00	15,38			2	2
Q9JMA1	Ubiquitin carboxyl-terminal hydrolase 14 OS=Mus musculus GN=Usp14 PE=1 SV=3 - [UBP14_MOUSE]	8,92	1	1,129E6	1,139E6	0,00	8,92			3	3
O35343	Importin subunit alpha-4 OS=Mus musculus GN=Kpna4 PE=2 SV=1 - [IMA4_MOUSE]	5,95	1	1,107E6	1,635E6	0,00	5,95			2	3
Q99KK7	Dipeptidyl peptidase 3 OS=Mus musculus GN=Dpp3 PE=2 SV=2 - [DPP3_MOUSE]	5,56	1	1,045E6	9,731E5	0,00	5,56			2	2
Q9ES00	Ubiquitin conjugation factor E4 B OS=Mus musculus GN=Ube4b PE=1 SV=3 - [UBE4B_MOUSE]	2,90	1	1,031E6	4,459E5	0,00	2,90			2	2
Q7TT50	Serine/threonine-protein kinase MRCK beta OS=Mus musculus GN=Cdc42bpb PE=1 SV=2 - [MRCKB_MOUSE]	1,81	1	9,817E5	1,763E5	0,00	1,81			2	2
Q8BIJ6	Isoleucine--tRNA ligase, mitochondrial OS=Mus musculus GN=lars2 PE=2 SV=1 - [SYIM_MOUSE]	5,24	1	9,600E5	5,403E5	0,00	5,24			3	3
Q3TIV5	Zinc finger CCCH domain-containing protein 15 OS=Mus musculus GN=Zc3h15 PE=1 SV=2 - [ZC3HF_MOUSE]	12,21	1	8,853E5	3,980E6	0,00	12,21			3	3
O88379	Bromodomain adjacent to zinc finger domain protein 1A OS=Mus musculus GN=Baz1a PE=1 SV=3 - [BAZ1A_MOUSE]	1,61	1	7,883E5	2,824E5	0,00	1,61			2	2
Q01405	Protein transport protein Sec23A OS=Mus musculus GN=Sec23a PE=1 SV=2 - [SC23A_MOUSE]	11,37	1	7,751E5	2,116E6	0,00	11,37			6	7
D3YXK2	Scaffold attachment factor B1 OS=Mus musculus GN=Safb PE=1 SV=2 - [SAFB1_MOUSE]	5,66	1	6,170E5	1,105E6	0,00	5,66			3	3

Accession	Description	Σ Coverage	$\Sigma\#$ Proteins	A: Area	B: Area	Coverage A	Coverage B	# Peptides A	# PSM A	# Peptides B	# PSM B
P70399	Tumor suppressor p53-binding protein 1 OS=Mus musculus GN=Tp53bp1 PE=1 SV=2 - [TP53B_MOUSE]	3,47	1	5,838E5	7,391E5	0,00	3,47			4	4
P37913	DNA ligase 1 OS=Mus musculus GN=Lig1 PE=1 SV=2 - [DNL1_MOUSE]	5,13	1	2,861E5	4,498E5	0,00	5,13			3	3
Q6PGG6	Guanine nucleotide- binding protein-like 3-like protein OS=Mus musculus GN=Gnl3l PE=1 SV=1 - [GNL3L_MOUSE]	6,24	1	2,548E5	2,802E5	0,00	6,24			2	2
Q70FJ1	A-kinase anchor protein 9 OS=Mus musculus GN=Akap9 PE=2 SV=2 - [AKAP9_MOUSE]	0,66	1	0,000E0	7,145E4	0,00	0,66			2	2
P39053	Dynamamin-1 OS=Mus musculus GN=Dnm1 PE=1 SV=2 - [DYN1_MOUSE]	1,96	1	0,000E0	4,471E5	0,00	1,96			2	2
Q60902	Epidermal growth factor receptor substrate 15-like 1 OS=Mus musculus GN=Eps15l1 PE=1 SV=3 - [EP15R_MOUSE]	2,98	1	0,000E0	4,826E5	0,00	2,98			2	2
Q8CHG3	GRIP and coiled- coil domain- containing protein 2 OS=Mus musculus GN=Gcc2 PE=1 SV=2 - [GCC2_MOUSE]	1,61	1	0,000E0	4,051E5	0,00	1,61			2	2
Q9CQQ8	U6 snRNA- associated Sm-like protein LSm7 OS=Mus musculus GN=Lsm7 PE=3 SV=1 - [LSM7_MOUSE]	25,24	1	0,000E0	6,622E5	0,00	25,24			2	2
Q8K224	N-acetyltransferase 10 OS=Mus musculus GN=Nat10 PE=2 SV=1 - [NAT10_MOUSE]	11,72	1	0,000E0	9,199E5	0,00	11,72			9	9
Q9CSH3	Exosome complex exonuclease RRP44 OS=Mus musculus GN=Dis3 PE=2 SV=4 - [RRP44_MOUSE]	2,92	1	0,000E0	5,435E5	0,00	2,92			2	2
Q8CH25	SAFB-like transcription modulator OS=Mus musculus GN=Sltm PE=1 SV=1 - [SLTM_MOUSE]	5,63	1	0,000E0	9,269E5	0,00	5,63			4	4
Q8BLY2	Probable threonine- -tRNA ligase 2, cytoplasmic OS=Mus musculus GN=Tarsl2 PE=2 SV=1 - [SYTC2_MOUSE]	2,91	1	0,000E0	3,957E5	0,00	2,91			2	2

Accession	Description	Σ Coverage	$\Sigma\#$ Proteins	A: Area	B: Area	Coverage A	Coverage B	# Peptides A	# PSM A	# Peptides B	# PSM B
Q6PFR5	Transformer-2 protein homolog alpha OS=Mus musculus GN=Tra2a PE=1 SV=1 - [TRA2A_MOUSE]	15,66	1	0,000E0	2,427E6	0,00	15,66			3	3
Q8C7V3	U3 small nucleolar RNA-associated protein 15 homolog OS=Mus musculus GN=Utp15 PE=2 SV=1 - [UTP15_MOUSE]	3,79	1	0,000E0	3,560E5	0,00	3,79			2	2
Q99KQ4	Nicotinamide phosphoribosyltransf erase OS=Mus musculus GN=Nampt PE=1 SV=1 - [NAMPT_MOUSE]	5,09	1	0,000E0	2,495E6	0,00	5,09			2	2
Q6P542	ATP-binding cassette sub-family F member 1 OS=Mus musculus GN=Abcf1 PE=1 SV=1 - [ABCF1_MOUSE]	7,29	1	0,000E0	7,370E5	0,00	7,29			4	4
Q9EST5	Acidic leucine-rich nuclear phosphoprotein 32 family member B OS=Mus musculus GN=Anp32b PE=1 SV=1 - [AN32B_MOUSE]	11,40	1	0,000E0	5,485E6	0,00	11,40			2	2
Q99LI7	Cleavage stimulation factor subunit 3 OS=Mus musculus GN=Cstf3 PE=1 SV=1 - [CSTF3_MOUSE]	3,91	1	0,000E0	9,368E5	0,00	3,91			2	2
Q8C175	DIS3-like exonuclease 2 OS=Mus musculus GN=Dis3l2 PE=1 SV=1 - [DI3L2_MOUSE]	3,68	1	0,000E0	0,000E0	0,00	3,68			2	2
Q5U458	DnaJ homolog subfamily C member 11 OS=Mus musc GN=Dnajc11 PE=2 SV=2 - [DJC11_MOUSE]	4,83	1	0,000E0	5,401E5	0,00	4,83			2	2
Q91WJ8	Far upstream element-binding protein 1 OS=Mus musculus GN=Fubp1 PE=1 SV=1 - [FUBP1_MOUSE]	3,99	1	0,000E0	1,258E6	0,00	3,99			2	2
P07310	Creatine kinase M- type OS=Mus musculus GN=Ckm PE=1 SV=1 - [KCRM_MOUSE]	11,81	1	0,000E0	4,678E6	0,00	11,81			4	4
Q9QWT9	Kinesin-like protein KIFC1 OS=Mus musculus GN=Kifc1 PE=1 SV=2 - [KIFC1_MOUSE]	7,72	1	0,000E0	1,250E6	0,00	7,72			3	4
Q99KE1	NAD-dependent malic enzyme, mitochondrial OS=Mus musculus GN=Me2 PE=2 SV=1 - [MAOM_MOUSE]	4,24	1	0,000E0	9,576E5	0,00	4,24			2	2

Accession	Description	Σ Coverage	$\Sigma\#$ Proteins	A: Area	B: Area	Coverage A	Coverage B	# Peptides A	# PSM A	# Peptides B	# PSM B
Q91YP2	Neurolysin, mitochondrial OS=Mus musculus GN=Nln PE=2 SV=1 - [NEUL_MOUSE]	4,12	1	0,000E0	8,037E5	0,00	4,12			2	2
Q9R0B9	Procollagen- lysine,2-oxoglutarate 5-dioxygenase 2 OS=Mus musculus GN=Plod2 PE=2 SV=2 - [PLOD2_MOUSE]	4,48	1	0,000E0	3,010E5	0,00	4,48			3	3
Q99LL5	Periodic tryptophan protein 1 homolog OS=Mus musculus GN=Pwp1 PE=1 SV=1 - [PWP1_MOUSE]	17,96	1	0,000E0	4,030E6	0,00	17,96			5	5
Q9D1H8	39S ribosomal protein L53, mitochondrial OS=Mus musculus GN=Mrpl53 PE=2 SV=1 [RM53_MOU]	25,42	1	0,000E0	1,415E6	0,00	25,42			2	2
Q6NZC7	SEC23-interacting protein OS=Mus musculus GN = Sec23ip PE=1 SV=2 - [S23IP_MOUSE]	3,21	1	0,000E0	1,276E6	0,00	3,21			3	4
Q60520	Paired amphipathic helix protein Sin3a OS=Mus musculus GN=Sin3a PE=1 SV=3 - [SIN3A_MOUSE]	4,71	1	0,000E0	6,654E5	0,00	4,71			5	5
Q9CZW5	Mitochondrial import receptor subunit TOM70 OS=Mus musculus GN=Tomm70a PE=1 SV=2 - [TOM70_MOUSE]	5,73	1	0,000E0	1,816E6	0,00	5,73			2	2
Q8CE96	tRNA (adenine(58)- N(1))- methyltransferase non-catalytic subunit TRM6 OS=Mus musculus GN=Trmt6 PE=1 SV=1 - [TRM6_MOUSE]	3,82	1	0,000E0	9,263E5	0,00	3,82			2	2
Q6PAM1	Alpha-taxilin OS=Mus musculus GN=Txlna PE=2 SV=1 - [TXLNA_MOUSE]	5,05	1	0,000E0	1,020E6	0,00	5,05			2	2
Q9D1C1	Ubiquitin- conjugating enzyme E2 C OS=Mus musculus GN=Ube2c PE=2 SV=1 - [UBE2C_MOUSE]	18,44	1	0,000E0	1,651E6	0,00	18,44			2	2
Q9JKC8	AP-3 complex subunit mu-1 OS=Mus musculus GN=Ap3m1 PE=1 SV=1 - [AP3M1_MOUSE]	6,70	1	0,000E0	2,043E6		6,70			2	2
Q91XV3	Brain acid soluble protein 1 OS=Mus musculus GN=Basp1 PE=1 SV=3 - [BASP1_MOUSE]	30,09	1	0,000E0	3,936E6		30,09			2	2

Accession	Description	Σ Coverage	$\Sigma\#$ Proteins	A: Area	B: Area	Coverage A	Coverage B	# Peptides A	# PSM A	# Peptides B	# PSM B
P67871	Casein kinase II subunit beta OS=Mus musculus GN=Csnk2b PE=1 SV=1 - [CSK2B_MOUSE]	12,56	1	0,000E0	2,860E6		12,56			2	2
Q9JIQ3	Diablo homolog, mitochondrial OS=Mus musculus GN=Diablo PE=1 SV=2 - [DBLOH_MOUSE]	12,66	1	0,000E0	3,534E5		12,66			2	2
Q6WQJ1	Sn1-specific diacylglycerol lipase alpha OS=Mus musculus GN=Dagla PE=1 SV=2 - [DGLA_MOUSE]	3,93	1	0,000E0	1,138E6		3,93			3	4
O70378	ER membrane protein complex subunit 8 OS=Mus musculus GN=Emc8 PE=1 SV=1 - [EMC8_MOUSE]	12,08	1	0,000E0	6,897E5		12,08			2	2
O08579	Emerin OS=Mus musculus GN=Emd PE=1 SV=1 - [EMD_MOUSE]	12,36	1	0,000E0	4,238E5		12,36			2	2
Q8BFZ9	Erlin-2 OS=Mus musculus GN=Erlin2 PE=1 SV=1 - [ERLN2_MOUSE]	8,53	1	0,000E0	2,383E6		8,53			2	2
P51859	Hepatoma-derived growth factor OS=Mus musculus GN=Hdgf PE=1 SV=2 - [HDGF_MOUSE]	27,00	1	0,000E0	3,010E6		27,00			3	3
Q9CQZ1	Heat shock factor-binding protein 1 OS=Mus musculus GN=Hsbp1 PE=2 SV=1 - [HSBP1_MOUSE]	39,47	1	0,000E0	2,545E5		39,47			2	2
Q8BWW4	La-related protein 4 OS=Mus musculus GN=Larp4 PE=1 SV=2 - [LARP4_MOUSE]	4,03	1	0,000E0	2,977E5		4,03			2	2
P53986	Monocarboxylate transporter 1 OS=Mus musculus GN=Slc16a1 PE=1 SV=1 - [MOT1_MOUSE]	6,09	1	0,000E0	2,397E6		6,09			2	2
Q9DCJ5	NADH dehydrogenase [ubiquinone] 1 alpha subcomplex subunit 8 OS=Mus musculus GN=Ndufa8 PE=1 SV=3 - [NDUA8_MOUSE]	18,60	1	0,000E0	1,046E6		18,60			2	2
P52503	NADH dehydrogenase [ubiquinone] iron-sulfur protein 6, mitochondrial OS=Mus musculus GN=Ndufs6 PE=1 SV=2 - [NDUS6_MOUSE]	25,00	1	0,000E0	1,958E5		25,00			2	3

Accession	Description	Σ Coverage	Σ # Proteins	A: Area	B: Area	Coverage A	Coverage B	# Peptides A	# PSM A	# Peptides B	# PSM B
Q99N92	39S ribosomal protein L27, mitochondrial OS=Mus musculus GN=Mrpl27 PE=2 SV=1 - [RM27_MOUSE]	17,57	1	0,000E0	5,434E5		17,57			2	2
Q9CZ83	39S ribosomal protein L55, mitochondrial OS=Mus musculus GN=Mrpl55 PE=2 SV=1 - [RM55_MOUSE]	30,71	1	0,000E0	1,295E6		30,71			4	4
Q791N7	DNA-directed RNA polymerase I subunit RPA12 OS=Mus musculus GN=Znrd1 PE=2 SV=1 - [RPA12_MOUSE]	30,89	1	0,000E0	6,175E5		30,89			2	2
Q60710	SAM domain and HD domain-containing protein 1 OS=Mus musculus GN=Samhd1 PE=1 SV=2 - [SAMH1_MOUSE]	6,38	1	0,000E0	6,807E5		6,38			2	2
Q8CAY6	Acetyl-CoA acetyltransferase, cytosolic OS=Mus musculus GN=Acat2 PE=1 SV=2 - [THIC_MOUSE]	9,07	1	0,000E0	2,793E6		9,07			2	2

A.2 Publications

Parts of this work have been published:

1. Jenniches I, Ternes S, Albayram O, Otte DM, Bach K, Bindila L, Michel K, Lutz B, Bilkei-Gorzo A, Zimmer A. (2016): Anxiety, Stress, and Fear Response in Mice with Reduced Endocannabinoid Levels. *Biol Psychiatry*. 79(10):858-68.
2. Jenniches I, Zimmer A. (2016): Reply To: The Anxiolytic Actions of 2-Arachidonoylglycerol: Converging Evidence from Two Recent Genetic Endocannabinoid Deficiency Models. *Biol Psychiatry*. 79(10):e80-1.

A.3 Declaration

I hereby solely declare that I prepared this thesis entitled “Importance of endogenous cannabinoids in stress and depression” entirely by myself except otherwise stated. All text passages that are literally or correspondingly taken from published or unpublished papers/writings are indicated as such. All materials or services provided by other persons are equally indicated.

Bonn, April 2016

Imke Jenniches

Acknowledgement

Mein besonderer Dank gilt Herrn Prof. Dr. Andreas Zimmer für die Überlassung des Themas, seinen fachlichen Rat und seine konstante Unterstützung während der gesamten Zeit meiner Doktorarbeit. Besonders bedanken will ich mich auch für die Freiheit, die er mir während des gesamten Forschungsprojektes gewährte.

Herrn Prof. Dr. Michael Hoch danke ich recht herzlich für die bereitwillige Übernahme der Funktion als Zweitgutachter meiner Arbeit.

Bei PD Dr. Andras Bilkei-Gorzo bedanke ich mich für seinen wissenschaftlichen Rat und ein offenes Ohr für alle Fragen und Probleme, die mich u.a. bei der Durchführung der Verhaltensexperimenten beschäftigt haben.

Ebenfalls bedanken möchte ich mich bei allen Kooperationspartnern für eine sehr gute Zusammenarbeit und die Bereitstellung von Zeit, Material und Expertise. Im Besonderen danke ich Dr. Laura Bindila, Dr. Marc Sylvester und Prof. Dr. Christian Thiele.

Bei Dr. Irene Melo de Carvalho und Dr. Onder Albayram möchte ich mich für zahlreiche wissenschaftliche Diskussionen und ihre Unterstützung bei der Planung der Verhaltensexperimente bedanken.

Vielen Dank an Hanna Schrage und Kirsten Krengel für die tatkräftige Unterstützung im Labor und die Hilfe bei unzähligen Genotypisierungen. Außerdem möchte ich mich im Besonderen bei Kerstin Michel bedanken ohne die ich unzählige Male verzweifelt wäre und deren Hilfsbereitschaft ich nicht genug würdigen kann. Du bist einfach unbezahlbar!

Bei allen Mitarbeitern des Instituts für Molekulare Psychiatrie möchte ich mich für die angenehme Arbeitsatmosphäre und die allseitige Hilfsbereitschaft bedanken. Danke für die wunderschöne und erlebnisreiche Zeit. Besonders erwähnen möchte ich hierbei Kerstin, Hanna, Eva und Ramona die neben der Arbeit auch gute Freunde für mich geworden sind.

Ein außerordentlicher Dank gilt meiner Familie, die stets hinter mir steht und mich mein ganzes Leben lang unterstützt hat. Danke für alles!

Zu guter Letzt danke ich dem Menschen, der seit vielen Jahren bedingungslos an meiner Seite steht und auf dessen Verständnis und Rückhalt ich stets zählen kann. Nersi...du bist das Beste was mir je passiert ist!